AN INVESTIGATION OF COMPUTERISED PREDICTION MODELS FOR MOBILE RADIO PROPAGATION OVER IRREGULAR TERRAIN

by

S.A.A. Fouladpouri, B.Eng.

Thesis submitted in accordance with the regulations of The University of Liverpool for the award of the degree of Ph.D.

October, 1988.

SYNOPSIS

A number of signal-strength prediction techniques have been examined and a comparative study has been undertaken to assess their accuracy under various propagation conditions. The experimental data used for comparison was collected principally in rural areas of Cheshire at a frequency of 139 MHz and at ranges of up to 40 Km. The area concerned represents the irregular terrain situation in which the major problem is to estimate the diffraction losses caused by obstacles along the path. Several well-known techniques used for estimating diffraction losses along obstructed paths have been investigated in order to assess their accuracy.

The investigation has led to a proposal for a new computerised prediction technique which uses a digitised terrain data map to derive the required path profile and/or terrain parameters. When compared with the measured data from the Cheshire experiment the new technique proved to be more accurate than the other models considered in the comparative study. However the addition of an urban loss factor enabled the model to be compared with experimental data that had been independently collected in urban areas of Ipswich at 160 and 900 MHz; the predictions and measurements were in close agreement.

The use of a computer-based prediction technique provides a fast and accurate method of calculating propagation losses and is an invaluable aid in radio system planning.

ACKNOWLEDGEMENTS

I would like to express my deep gratitude to my supervisor, Professor J.D. Parsons, for his advice, guidance and continuous encouragement during the course of this research. The work was financially supported by the Science and Engineering Research Council through the Departmental Users' Radio Propagation Programme.

The author is very appreciative of the useful discussions which took place with representatives from RAL, BBC and the DTI.

I wish also to express my gratitude to my colleagues in the mobile radio research group at Liverpool. Finally, I wish to thank Mrs. B. Lussey for typing the thesis.

LIST OF PRINCIPAL SYMBOLS

a	The actual earth radius (approximately 6370 Km)
d	A distance variable
f	Frequency in MHz
g_r	Gain of receiving antenna
g_t	Gain of transmitting antenna
h	A height variable
h_r	Height of receiving antenna
h_t	Height of transmitting antenna
n	Refractive index
r_1	Radius of first Fresnel zone
v	Fresnel v-parameter
x_o	Mean power
A	Surface wave attenuation factor
D	Divergence factor
E_o	Free-space field strength
K	Ratio of the earth's effective radius to its actual radius
L_D	Diffraction loss (dB)
L_F	Free-space loss (dB)
L_p	Plane-earth loss (dB)
P_L	Median path loss (dB)
P_r	Received power (W)
P_t	Transmitted power (W)
R	Reflection coefficient
UL	Urban loss factor
V	Speed of the mobile
β	The diffraction angle
ε_c	Permittivity of the ground

λ	Wavelength
θ	Angle of incidence
σ	Conductivity of the ground
ψ	The grazing angle of reflection
Δ	Phase difference between the reflected and the direct paths
Δd	Path length difference
Δh	Terrain irregularity factor
ρ	Curvature parameter
ω_n	Doppler shift (rads/sec)

CONTENTS

CHAPTER 1

INTRODUCTION

Radio communication benefits society in many ways and its application is vital for security purposes and public safety. Industrial organisations and businesses make use of radio services to operate more efficiently, while individuals rely on them for their various communication needs.

Since their early days, radio systems, as a major part of the telecommunication network, have been under constant development to keep pace with the advances in electronic technology and increasing demand. One major area of rapid expansion has been in the development of mobile radio communication systems, since the potential for communicating with non-fixed points at a distance has been increasingly recognised. In particular, mobile radio services have attracted much attention in recent years and this has led to the emergence of new systems which provide the user with more freedom and a better quality of service.

An essential factor in the consideration of any communication system is the efficient use of frequency spectrum. Radio frequency spectrum can be looked upon as a scarce national resource and therefore its utilisation requires Governmental regulation and licensing, and international co-operation, so that different users can operate with a minimum of mutual interference. The question of how the spectrum should be allocated among the various possible uses and users is partially an engineering one and partially an economic and political question. The allocation of frequency bands should take into account what is feasible and practical technically, and the design features of practical systems are influenced strongly by the frequency allocations that have been

made. To utilise an available frequency band for a given application in an efficient manner, a knowledge of several technical parameters is required. These parameters depend partly on equipment performance considerations and partly on effects introduced by the propagation medium. The VHF and UHF bands between 30 MHz and 3 GHz are used for broadcasting and two-way communications which consist mainly of communications between fixed base stations and several mobile units located on vehicles, ships, or aircraft. Typical applications are in control-tower-to-aircraft communication at airports, fire departments, ship control within harbours, police departments, armed-forces field operations, pipeline and transmission line maintenance, highway maintenance, taxi and delivery vehicle dispatch, paging systems and personal mobile radio phones.

Propagation in the VHF and UHF bands is mainly through the earth's atmosphere, and reflection and refraction of radio waves in the ionosphere which gives rise to long-range communications at the lower frequencies does not occur. Also, ground-wave propagation is limited because of absorption losses at high frequencies. Therefore, in the VHF and UHF range, the signal is transmitted by space waves directly to the receiving antenna and since the waves follow a straight line, the range of operation is generally limited to within the line-of-sight horizon of the transmitter or that much further again if a repeater station is used. Hence, the height of the base station antenna is very important for good reception and usually the antenna is located on top of a high hill or building to gain additional height.

As demand for radio services rises, existing frequency allocations need to be updated and revised as some frequency bands are under-used and others, like mobile services and CB bands, are very crowded.

Frequencies need to be shared by a number of users, rather than assigned exclusively on a nationwide scale. The ability of a user to select from several channels instead of having to rely on one could be expanded. Antenna characteristics can be improved, and higher frequencies can be employed. Low-power transmitters can be used in localised areas and this is the case for the cellular radio systems.

Cellular systems involve dividing the area to be served into a number of cells, each cell with a radio receiver-transmitter at its centre. Cellular radio systems provide a high quality communication to a large number of users by efficient use of spectrum through repeated usage of the available frequency. The United Kingdom has adopted the Total Access Communication System (TACS) for its cellular mobile telephone system. TACS operates in the UHF band at frequencies in the ranges 890-915 MHz and 935-960 MHz, with 25 KHz channel spacing, hence offering 1000 duplex mobile telephone channels, although at present only 600 channels are licensed for use. The size of a cell varies with the number of users expected to operate in that area. In cities, for example, cells may be 2 Km across while in less densely populated rural areas the cells may be as large as 30 Km across.

The radio station within a cell provides two types of radio channel; a control channel to transfer system control messages to and from mobile telephones, and a voice channel which provides a telephone quality link for conversation or data transmission and all in-call supervision activities. The radio stations are connected, via the conventional land-line system or microwave links to a Mobile Switching Centre (MSC), which in turn connects to the Public Switched Telephone Network (PSTN). During conversation, the radio station monitors the level of received signals and messages are sent to the mobile to adjust

its transmitter power as required. If the received level becomes too low, the MSC checks adjacent radio stations to determine which can provide the best reception. The mobile is advised of the new channel to be used and the MSC connection is remade to the new radio station. These "hand-off" events occur without the mobile user's knowledge or intervention and the call continues uninterrupted. To limit co-channel and adjacent-channel interference, adjacent cells use different sets of channels and within the same cell, adjacent channels are not used; however non-adjacent radio stations can use the same frequency simultaneously. The cell area is determined by the anticipated traffic, as there is a limit to the number of channels available per cell, and by the propagation characteristics. Indeed, an examination of the factors which influence the radio wave propagation is an essential part of any radio system planning. For example, for VHF and UHF radio propagation, these factors include the various states of the atmosphere, the intervening hills, buildings and trees, which provide scattering obstacles within sizes of the same order of magnitude as the wavelength.

The ability to predict the propagation losses incurred, given a radio system, is important in determining the useful service area, and with increasing demand for radio services and limited frequency spectrum, prediction work greatly reduces the time consumed and the cost involved in the field trial program for any new proposed system. Accordingly, there is a need for reliable techniques which can predict the median transmission loss due to various terrain and environmental features and its variability. The present thesis outlines the results of an assessment work on some of the available prediction models. The models have been compared in their range of applicability and against measured data which has been obtained as a result of measurement

programmes carried out in rural areas of Cheshire. Three different transmitter sites were used, with the operating frequency of 139 MHz and the received signals were recorded in a mobile unit at distances of up to 40 Km from the base station.

In a typical mobile radio propagation situation, the received field will show fading consisting of very rapid fluctuations around the mean signal level superimposed on relatively slow variations of the mean level itself. Rapid fading is caused by scattering of the waves in the vicinity of the mobile whereas slow fading results from shadowing effects in the radio path. The comparative study is primarily concerned with prediction errors of propagation loss along the transmission path, by using the median signal strength obtained in test squares of side 0.5 Km. The ground profile from the base station to the centre of each test square is reconstructed by using a topographical data base. A computerised prediction method is proposed which produces more accurate results when compared against the measured data. The method is then evaluated by comparing it with data obtained as a result of an independent measurement programme.

REFERENCES

1.1 Flock, W.L.

"Electromagnetics and the Environment: Remote Sensing and Telecommunications", Englewood Cliffs, N.J.: Prentice-Hall, 1979.

1.2 Barsis, A.P.

"Determination of Service Area for VHF/UHF Land Mobile and Broadcast Operations Over Irregular Terrain", IEEE Trans. Veh. Tech., Vol. VT-22, No.2, May 1973.

CHAPTER 2

PRINCIPLES OF RADIO WAVE PROPAGATION

In order to establish the parameters of a communication system, an understanding of the factors which influence the transmitted signal is essential. In general the received field consists of waves which have travelled through many possible propagation paths, but these waves vary in importance depending upon the practical situation.

The following is an examination of the propagation conditions which are most relevant to the communication ranges and frequencies considered in the present work.

2.1 FREE SPACE PROPAGATION

The basic concept in estimating radio transmission loss is the loss expected in free space; that is, in a region free of all objects that might absorb or reflect radio energy.

In this case, the field intensity E_o is given by : [2.1]

$$E_o = \frac{\sqrt{30\ g_t P_t}}{d} \qquad (2.1)$$

The power which is delivered to a matched receiver at a distance d from the transmitter is:

$$P_r = P_t g_t g_r \left(\frac{\lambda}{4\pi d} \right)^2 \qquad (2.2)$$

Therefore the path loss in dB, for isotropic antennas is given by:

$$10 \log \frac{P_t}{P_r} = P_L = 32.45 + 20 \log_{10} f_{MHz} + 20 \log_{10} d_{Km} \qquad (2.3)$$

As (2.3) indicates, the loss increases by 6 dB as either the distance or the frequency is doubled.

2.2 TROPOSPHERIC PROPAGATION

The troposphere is the lowest region of the atmosphere, adjacent to the earth and about 10 Km high, in which the temperature decreases with height. At VHF and UHF, propagation is appreciably affected by atmospheric conditions in this region. Lower frequencies will propagate via the ionosphere at much higher altitudes, but this situation is not considered here. Refraction and scattering are the main mechanism by which radio waves propagate in the troposphere, of which refraction is more important for shorter ranges.

2.2.1 Refraction and Equivalent Earth's Radius

If the state of the atmosphere above the entire surface of the earth is averaged over a long period, it is found that temperature, pressure and humidity decrease with altitude, which causes a variation in the dielectric constant of the atmospheric air and consequently its refractive index. This causes the radio waves to follow a downward curved path due to refraction.

For the study of a radio link, it is particularly useful to draw the radio rays as straight lines, and this is achieved by using an effective earth radius Ka rather than the actual earth radius, a(6370 Km). The coefficient K is given by: [2.2]

$$K = \frac{1}{1 + a\frac{dn}{dh}}$$

A standard atmosphere can be defined as a hypothetical atmosphere in

which the properties are arbitrarily chosen to fit certain average conditions. In the standard atmosphere considered here, the average value of $\frac{dn}{dh}$ (vertical gradient of the index) near the ground is given by:

$$\frac{dn}{dh} = -0.039 \times 10^{-6} \text{ per metre}$$

This results in a value of K of 4/3. The apparent reduction of the earth's curvature, which is greater when the variation in refractive index with height is larger, tends to overcome partially the loss of signal due to curvature of the earth and permits the direct ray to reach points slightly beyond the horizon as determined by the straight-line path.

2.3 PROPAGATION NEAR THE EARTH'S SURFACE

The presence of the ground modifies the propagation of radio waves so that the transmission loss is normally greater than that of free space. The earth's surface is neither a perfect conductor nor a perfect dielectric and the theory of reflection and diffraction by the earth's surface is quite complex. However, by using some approximations, suitable estimates can be obtained for the effects of reflection from the surface of the earth and diffraction of radio waves by the obstructing features on the ground.

2.3.1 Ground Reflection of Radio Waves

When radio waves propagate in the vicinity of the two media separated by a plane boundary, the boundary conditions have to be satisfied for the incident, the reflected and the transmitted waves as illustrated in Fig. 2.1.

The ratio of the incident wave to its associated reflected wave is called the "reflection coefficient". The reflection coefficients for vertically and horizontally polarised waves are given by: [2.3]

$$R_V = \frac{\varepsilon_c \sin\theta - Z}{\varepsilon_c \sin\theta + Z}$$

$$R_H = \frac{\sin\theta - Z}{\sin\theta + Z}$$

where

$$Z = [\varepsilon_c - \cos^2\theta]^{\frac{1}{2}}$$

$$\varepsilon_c = \varepsilon_r - j\ 60\ \sigma\lambda$$

θ is the angle of incidence, ε_r is the relative permittivity and σ is the conductivity of the reflecting ground in Siemens per metre. The reflection coefficient is a complex quantity and for horizontally polarised waves its magnitude is essentially constant at the value of unity for frequencies below about 400 MHz, while for vertically polarised waves, it drops to relatively low values.

The relative permittivity ε_r varies from about 7 for a low condutivity earth to about 30 for a high conductivity earth, so a value of $\varepsilon_r = 15$ is usually assumed for an average ground. Because of the low antenna heights that are used, the incidence angle θ is generally very small for ground reflections in a mobile radio environment.

2.3.2 Plane Earth Propagation

Over a smooth, conducting flat earth, the ratio of field strength to that of free space is given by: [2.1]

$$\frac{E}{E_o} = 1 + R\, e^{j\Delta} + (1 - R)Ae^{j\Delta} + \ldots. \qquad (2.4)$$

where the unity term represents the direct wave, the second term represents the ground-reflected wave and the third term represents the surface wave. There are negligible additional terms due to the induction field and secondary effects of the ground. The surface wave is that part of the radiated wave which travels chiefly along the earth's surface and depends upon the presence of earth for its existence.

The surface wave attenuation factor A, like the ground reflection coefficient R, depends on the angle of incidence, the polarisation of the wave, and the electrical constants of the ground. For nearly grazing paths, R is approximately equal to -1 and the effect of the surface wave can be neglected for antenna heights of more than a wavelength above the ground. Under these conditions (2.4) reduces to:

$$\left| \frac{E}{E_o} \right| = \sqrt{\frac{P_r}{P_o}} = \left| 1 - e^{j\Delta} \right| = 2 \sin \frac{\Delta}{2} \qquad (2.5)$$

where P_o is the received power in free space.

The quantity Δ is the phase difference between the reflected and the direct paths between transmitting and receiving antennas, illustrated in Fig. 2.2.

$$\Delta = \frac{2\pi}{\lambda} (r_R - r_D)$$

For $d \gg h_t, h_r$ $\qquad \Delta \approx \dfrac{4\pi\, h_t h_r}{\lambda d}$

and for mobile radio applications, $\sin \frac{\Delta}{2} \approx \frac{\Delta}{2}$.

Hence using (2.1), (2.5) can be written as:

$$P_r = P_t g_t g_r \left(\frac{\lambda}{4\pi d} \right)^2 \left(\frac{4\pi\ h_t h_r}{\lambda d} \right)^2$$

$$P_r = P_t g_t g_r \left(\frac{h_t h_r}{d^2} \right)^2 \qquad (2.6)$$

This relation is independent of frequency and shows an inverse fourth power relationship of received power with distance from the base station antenna.

2.3.3 Propagation Over a Smooth Spherical Earth

The curvature of the earth causes the ground-reflected wave to diverge at a greater rate than in the case when it is reflected from a flat surface, (Fig. 2.3). The power density and field strength are smaller than for a flat earth by the "divergence factor", D, which depends solely on the shape of the surface and not on its electrical properties. With reference to Fig. 2.4, this factor is given by: [2.4]

$$D = \left[1 + \frac{2d_1 d_2}{ad\ \tan\psi} \right]^{-\frac{1}{2}}$$

where it has been assumed that $\sin\psi = \tan\psi$ for small values of grazing angle. It can also be written as

$$D \approx \left[1 + \frac{2d_1 d_2}{a(h_t + h_r)} \right]^{-\frac{1}{2}}$$

The divergence factor will be smaller when the incident beam is closer to grazing incidence.

2.3.4 Propagation Over Rough Terrain

Smooth earth reflection theory may no longer apply when terrain has substantial surface irregularities. If the surface is not smooth enough to support specular reflection, the radio waves will be scattered by the surface irregularities and diffuse reflection will occur and the greater the irregularities, the smaller will be the reflection coefficient. A roughness criterion may be used to determine whether a given surface will support specular reflection or not and a generally accepted criterion is the "Rayleigh criterion".

Fig. 2.5 illustrates the effects of surface roughness on two rays of an incident wavefront. The path difference between the two rays is Δd and is given by

$$\Delta d = 2H \sin\theta$$

where θ is the grazing angle and H is the height of the terrain undulation. Hence the phase difference between the two rays is

$$\frac{2\pi}{\lambda} \cdot \Delta d = \frac{4\pi H \sin\theta}{\lambda}$$

It has been shown [2.2] that the surface can be considered smooth for phase differences up to $\frac{\pi}{4}$. This gives the value for the maximum height of the obstacles or irregularities of the terrain as:

$$H_{max} = \frac{\lambda}{16\sin\theta}$$

and the criterion for roughness is then $H > H_{max}$. At high frequencies, the magnitude of the reflection coefficient decreases due to multiple reflections from the irregularities on the earth's surface.

2.3.5 Validity of the Reflection Theory

In practical mobile radio systems the two path propagation model depicted in Fig. 2.2 is seldom valid as reflected rays may reach the receiver through many paths. Terrain features such as hills or valleys and absorbing or reflecting objects like buildings and trees modify the propagation picture.

The variation in the value of surface conductivity and dielectric constant of the ground over the longer ranges results in a non-uniform reflection coefficient. Also, the generally complicated nature of the terrain roughness and water surfaces prevent specular reflection. In certain relatively simple cases, the addition of a third or a fourth ray path for the solution of a propagation problem by means of ray theory, may prove satisfactory. However, in many cases this will not be so and the solution has to be a suitable combination of ray theory, wave theory and actual measurement results. In the ray theory of reflection, the grazing angle, Fig. 2.4, is restricted to a minimum value given by [2.2]

$$\psi = \left(\frac{\lambda}{2\pi\ Ka} \right)^{1/3}$$

For any value of grazing angle less than this value, the ray theory becomes invalid and the surface wave may contribute an appreciable part of the total field strength.

Although it was argued that the terrain roughness modifies the ground reflection coefficient, large irregularities cannot be treated in this way and diffraction theory should be incorporated.

2.3.6 Diffraction of Radio Waves

Electromagnetic waves bend around the edges of obstacles which lie in their propagation path. This diffraction property of the radio waves, facilitates the reception of the signal at points which are in the geometrical shadow region of the obstructions, such as hills, in the path.

The classical approach to diffraction problems is to apply Huyghens' principle to the aperture above the obstacle. This principle states that each point on a spherical wavefront can be considered as a secondary source of radiation.

The secondary source does not radiate energy equally in all directions. The amplitude of the secondary wave field strength at any point is proportional to the factor $(1 + \cos\delta)$, where δ is the angle subtended by the point at the secondary source with respect to the line normal to the wavefront (Fig. 2.6).

2.3.7 Diffraction Over a Perfectly Absorbing Knife-edge

When a straight-edged obstructing screen or knife-edge is inserted between a transmitting source T and a receiving location R, as shown in Fig. 2.7, the resultant field at R is obtained by a vector summation of all the fields due to the secondary sources in the half-plane above the knife-edge.

As the edge is moved upwards approaching the line TR and in a plane perpendicular to it, the field strength at R begins to oscillate about its free-space value. At position 0, where the edge is in line with T and R, the field strength is just half of the unobstructed value. As the edge is moved further upwards, the field stops oscillating and decreases steadily to zero.

Following the classical approach, the field behind an absorbing knife-edge relative to that obtained in free space is given in terms of a complementary Fresnel integral by:

$$F(v) = \frac{E}{E_o} = \frac{1-j}{2} \int_v^\infty e^{j\,\pi t^2/2}\, dt$$

where the parameter v is given by: (Fig. 2.8)

$$v = h \sqrt{\frac{2}{\lambda} \left(\frac{1}{d_1} + \frac{1}{d_2} \right)}$$

Fig. 2.9 shows the magnitude of the relative field strength as a function of v, and the loss due to diffraction which is given by:

$$L_D = -20 \log_{10} |F(v)|$$

The computation of the Fresnel integral requires numerical techniques, however, an approximate solution is given by: [2.5]

$$L_D = 0 \text{ dB} \qquad v \leq -1$$

$$L_D = -20 \log_{10}(0.5 - 0.62\, v) \qquad -1 \leq v \leq 0$$

$$L_D = -20 \log_{10}(0.5 e^{-0.95v}) \qquad 0 \leq v \leq 1$$

$$L_D = -20 \log_{10}\left(0.4 - \sqrt{0.1184 - (0.38-0.1\, v)^2}\right) \qquad 1 \leq v \leq 2.4$$

$$L_D = -20 \log_{10}\left(\frac{0.225}{v}\right) \qquad v > 2.4$$

The clearance over a knife-edge obstruction is usually considered in terms of the first Fresnel zone. This is an ellipsoid whose surface is the locus of points, by way of which the total path length from the transmitter to the receiver is $\lambda/2$ greater than the direct line of sight between the terminals.

The radius of the first Fresnel zone at any point in the

path, perpendicular to the direct line of sight is given by:

$$r_1 = \sqrt{\frac{\lambda d_1 d_2}{d_1 + d_2}}$$

The relationship between the Fresnel parameter v, and r_1 is given by:

$$v = \frac{h}{r_1}\sqrt{2}$$

In Fig. 2.10, h has a negative value.

2.3.8 Diffraction Over a Knife-edge with Reflection from the Ground

When a knife-edge is surrounded by two ground planes with good reflection coefficients we must consider not only the direct ray from transmitter to receiver via the knife-edge, but also the rays which are reflected from the ground on either or both sides of the knife-edge [2.6]. In this case there are four paths for the waves to travel from the transmitter to the receiver (Fig. 2.11): one path without reflection by the ground, two paths each with one reflection, and one path with two reflections. The field at the receiver can be calculated by summation of the fields due to diffraction of each of the rays and taking into account their difference in length and therefore their phases.

Bullington [2.7] calculated the field by assuming a reflection coefficient of -1, and by using some approximations showed that the loss is equal to that of the plane-earth loss added to $-20 \log_{10} 2S$, where S is the magnitude of the shadow loss caused by the knife-edge without reflection. A good correlation with the measured results was observed in the 30 to 150 MHz range.

2.3.9 Diffraction Over Rounded Obstacles

Radio wave propagation is more commonly impeded by rounded hills rather than knife-edge obstruction. Rice [2.8] has shown that an obstacle can be considered as a knife-edge when the diffraction angle satisfies the inequality (Fig. 2.12):

$$\beta < \frac{1}{4} \left(\frac{\lambda}{r_c} \right)^{1/3}$$

where r_c is the mean radius of curvature of the hill crest. In terms of the Fresnel parameter v, this limit corresponds approximately to $v < 1$ for gently curved hills and $v < 3$ for the sharper crests [2.9].

At UHF many situations arise where the v parameter lies in the range 3 to 5 and therefore, significant errors can be expected if a knife-edge approximation is used.

The surface of a curved obstacle can support reflections which perturb the field above it and therefore the diffraction loss is higher than the knife-edge loss. However, as the surface becomes rough, the field reducing effect due to specularly reflected components is reduced and the result will be a return towards the knife-edge field [2.9]. The excess loss to be added to the loss obtained if the obstruction were a knife-edge is calculated by adding two terms: $A(\rho)$ and $U(v\rho)$, and given by [2.10]:

$$A(\rho) = 6 + 7.19\,\rho - 2.02\,\rho^2 + 3.63\,\rho^3 - 0.75\,\rho^4 \qquad \text{for } \rho < 1.4$$

$$U(v\rho) = (43.6 + 23.5\,v\rho)\,\log_{10}(1 + v\rho) - 6 - 6.7\,v\rho \qquad \text{for } v\rho < 2$$

$$U(v\rho) = 22\,v\rho - 20\,\log_{10}(v\rho) - 14.13 \qquad \text{for } v\rho \geq 2$$

Where v is the Fresnel parameter for an equivalent knife-edge with the same diffraction angle as the curved surface and ρ is a

dimensionless parameter defined as:

$$\rho = \left(\frac{\lambda}{\pi} \right)^{1/6} r_c^{1/3} \left(\frac{d}{d_1 d_2} \right)^{1/2}$$

2.3.10 Multiple Knife-edge Diffraction

In many cases of radio propagation over terrain obstacles, there is more than one knife-edge diffraction source along a given propagation path. The extension of the theory for more than one knife-edge results in multiple integrals which are difficult to handle.

A solution for the case of two knife edges has been obtained by Millington [2.11] and is expressed in terms of Fresnel surface integrals. Vogler [2.12] has derived an expression for the attenuation caused by diffraction over multiple knife edges. The expression is in the form of a multiple integral which is then developed into a series through the use of repeated integrals of the error function. However, for rapid prediction purposes, the trend has been towards using simple approximate methods to estimate the diffraction loss. The following is an examination of several well known diffraction models.

2.3.10.1 The Bullington Method

In order to calculate the diffraction loss over multiple obstructions, the whole profile is replaced by a single equivalent knife-edge [2.7]. The virtual edge is constructed at the crossing point of the horizon lines from each terminal, as shown in Fig. 2.13.

If a_m denotes the diffraction loss over a knife-edge with Fresnel parameter v which is a function of separation distances of

the edge from the terminals and height of the knife-edge, the loss in dB is then given by:

$$a_m = f(d_1, d_2, h)$$

Although the method is simple to apply, it cannot be considered as accurate and produces optimistic results. This is to be expected since paths with several significant obstructions are oversimplified in that only two of these are ever relevant in the construction of the equivalent knife-edge.

2.3.10.2 The Epstein-Peterson Method

Epstein and Peterson [2.13] proposed that the diffraction loss be evaluated as the sum of attenuations due to each edge in turn. The loss for an edge is obtained by assuming the path is from the previous edge (or transmitter for first edge) to the subsequent edge (or receiver for last edge). Referring to Fig. 2.14, for a double knife-edge situation, this may be expressed as:

$$a_m = a_{m1} + a_{m2} \quad \text{dB}$$

with $a_{m1} = f(d_1, d_2, h_1)$

and $a_{m2} = f(d_2, d_3, h_2)$

The method is reciprocal and physically has some justification in the fact that an illuminated knife-edge behaves approximately like an equivalent source, as was described previously.

Millington [2.11] analysed this method and suggested its use over a wide range of conditions in which neither knife-edge is visible from a terminal over the top of the other. In comparison with the rigorous solution for the double knife-edge situation [2.11], and where individual losses due to each edge are relatively large, a

correction factor was derived to be added to the loss estimated by the method as:

$$20 \log_{10}(\text{cosec}\alpha) \qquad \text{dB}$$

where α is a spacing parameter given by:

$$\text{cosec}\alpha = \sqrt{\frac{(d_1 + d_2)(d_2 + d_3)}{d_2(d_1 + d_2 + d_3)}}$$

2.3.10.3 The Japanese Atlas Method

This method [2.14] is similar to that of Epstein-Peterson except that the contribution of each edge subsequent to the first edge is found by assuming that the previous edge is absent, and the transmitter is raised to the grazing line of the edges. Referring to Fig. 2.15, the diffraction loss due to each edge is given by:

$$a_{m1} = f(d_1, d_2, h_1)$$

$$a_{m2} = f(d_1 + d_2, d_3, h_2')$$

It has been shown [2.15] that the diffraction loss estimated by this method is equivalent to that obtained by the Epstein-Peterson method plus the correction factor derived by Millington.

2.3.10.4 The Deygout Method

The principle of this method [2.16] is that the total loss is evaluated as the sum of the losses over all the obstacles in order of decreasing influence. It consists of obtaining a loss for each diffraction edge in turn as if the remaining edges were absent. The larger of these losses is used initially, and the edge (main edge)

which produced this loss is used to divide the path in two and the process repeated in the two halves as if the edges were a terminal. This process is repeated indefinitely until each of the diffracting edges has been used. This construction is shown in Fig. 2.16 for the case of two edges. If $v_1 > v_2$, then edge 1 is considered as the main edge and the total diffraction loss is obtained by adding the two loss terms given by:

$$a_{m1} = f(d_1, d_2 + d_3, h_1)$$

$$a_{m2} = f(d_2, d_3, h_2)$$

For this situation, where the magnitudes of the v parameters are comparable, the method is found to overestimate the total diffraction loss [2.10]. A correction factor to be added to the estimated loss for this case has been derived as follows:

When $v_1 \geq v_2$ and $v_1, v_2, (v_2 \operatorname{cosec}\alpha - v_1 \cot\alpha) > 1$

$$\text{Correction} = 20 \log_{10}\left(\operatorname{cosec}^2\alpha - \frac{v_2}{v_1} \operatorname{cosec}\alpha \cot\alpha\right) \quad \text{dB}$$

where

$$\operatorname{cosec}\alpha = \sqrt{\frac{(d_1 + d_2)(d_2 + d_3)}{d_2(d_1 + d_2 + d_3)}}$$

and

$$\cot\alpha = \sqrt{\frac{d_1 d_3}{d_2(d_1 + d_2 + d_3)}}$$

This correction factor reaches a minimum of -6 dB for $v_1 = v_2$ and $\alpha = 0^o$.

As the number of edges increases, the application of this model becomes quite difficult and time consuming and the solution will be more pessimistic. Fig. 2.17 illustrates the application of

the method to the multiple knife-edge situation, where edge 3 is the main edge. Edges below the line-of-sight which are not clear of the first Fresnel zone are accounted for.

2.4 MOBILE RADIO PROPAGATION OVER IRREGULAR TERRAIN

In a mobile radio environment, a line-of-sight path between the transmitter and receiver rarely exists and as the mobile moves, the location of the scatterers and shadowing objects changes.

The signal received by the mobile at any point consists of a large number of generally horizontally travelling plane waves whose amplitudes, phases and angles of arrival relative to the direction of vehicle motion are random. These plane waves interfere and produce a varying field strength pattern with minima and maxima occurring approximately every quarter-wavelength, analogous to that obtained from the idealised standing wave pattern set up by summation of the direct and a reflected wave. Therefore at high frequencies, the received signal fades rapidly and deeply as the mobile station moves through the interference pattern. Superimposed on the rapid fading are slow variations in the average field strength, as the mobile station changes its location, since general terrain features in the propagation path vary.

Fig. 2.18 shows an example of received signal strenth, measured at the frequency of 167 MHz [2.18].

2.4.1 Characteristics of the Fast Fading Field

Many studies have shown that the envelope of the mobile radio signal is Rayleigh distributed when measured over distances of a few tens of wavelengths where the mean signal is considered to be

constant [2.19],[2.20].

The vector sum of a large number of sinusoidal plane waves with random amplitudes and phase angles can be shown by using the central limit theorem to be a Gaussian random variable. The envelope of a Gaussian random process can be shown to be Rayleigh distributed. The amplitudes and phases are assumed to be statistically independent and the phases of the waves are uniformly distributed from 0 t 2π. The vehicle motion introduces a Doppler shift in every wave and the received frequency differs from that transmitted by an amount

$$\omega_n = \frac{2\pi}{\lambda} V \cos\alpha_n$$

for an incoming wave with angle α_n to the direction of motion (Fig. 2.19). V is the speed and λ the wavelength of the transmitted carrier frequency.

The electric field component for a vertically polarised signal can be expressed in terms of its in-phase, $T_c(t)$, and quadrature, $T_s(t)$ components as [2.21]:

$$E_z = T_c(t) \cos \omega_c t - T_s(t) \sin \omega_c t$$

where ω_c is the carrier frequency, and

$$T_c(t) = E_o \sum_{n=1}^{N} C_n \cos(\omega_n t + \phi_n)$$

$$T_s(t) = E_o \sum_{n=1}^{N} C_n \sin(\omega_n t + \phi_n)$$

$E_o C_n$ is the amplitude of the nth wave with C_n normalised so that the ensemble average $< \sum_{n=1}^{N} C_n^2 > = 1$, and ϕ_n is the phase angle.

$T_c(t)$ and $T_s(t)$ are independent Gaussian random processes with zero

mean and equal variance.

$$< T_c^2 > = < T_s^2 > = \frac{E_o^2}{2}$$

$$< T_c \, T_s > = 0$$

Both T_c and T_s have a probability density function of the form:

$$P(x) = \frac{1}{\sqrt{2\pi x_o}} \, e^{-x^2/2x_o}$$

where $x = T_c$ or T_s and $x_o = \frac{E_o^2}{2}$ is the mean power.

The envelope r, of E_z is given by:

$$r = (T_c^2 + T_s^2)^{\frac{1}{2}}$$

It can be shown that the probability density function of r is:

$$P(r) = \frac{r}{x_o} \, e^{-r^2/2x_o} \qquad r \geq 0$$

which is a Rayleigh distribution, with only x_o required to completely describe the distribution. The cumulative distribution function of the envelope is then obtained as:

$$P[r \leq R_T] = \int_{-\infty}^{R_T} P(r)dr = 1 - e^{-R_T^2/2x_o}$$

Fig. 2.20 illustrates the Gaussian and Rayleigh density functions.

2.4.2 Variation of Median Signal Strength; Slow Fading

The large scale variation of the received field strength extending over many tens of wavelengths is commonly termed "slow

fading". Experimental results have shown that the median field strength for a small sector (about 20 m) in a sampling interval (1 ~ 1.5 Km) is approximately log-normally distributed [2.22].

If x denotes the small sector median field value, the probability density of x can be expressed [2.5]:

$$P(x) = \frac{1}{\sqrt{2\pi}\, D_1 x} \exp\left[-\frac{(\omega - \mu_1)}{2D_1^2}\right] \qquad x \geq 0$$

where $\omega = \log_e x$ and is assumed to be a random Gaussian process; u_1 is the mean value of ω, and the variance, D_1^2, is given by:

$$D_1^2 = < \omega^2 > - \mu_1^2$$

The mean value and variance of x are given by:

$$< x > = e^{[\mu_1 + D_1^2/2]}$$

$$var(x) = (< x >)^2 [\, e^{D_1^2} - 1 \,]$$

2.4.3 Effect of Environmental Clutter

In addition to terrain features in the propagation path, different structures surrounding the mobile station greatly influence the transmitted signal. In urban areas the reflection from different buildings, and also their shadowing effects, are more important, whereas in suburban and rural areas the effect of foliage is often a significant factor. As the mobile station moves through an urban environment, changes in the surrounding building density cause a significant change in the value of the received median signal strength. A quantitative analysis has been carried out by different authors [2.23], [2.24] to characterise the effect of buildings.

The presence of foliage reduces the received signal strength [2.25], but precise estimates of attenuation are difficult

because tree heights are not uniform, as well as their type, shape, density and distribution. Typical dense and rather extensive woods are opaque to radio signals at UHF and higher frequencies. Based on signal strength measurements along the same suburban streets in both summer and winter, variations of up to 10 dB have been observed.

References

2.1 Bullington, K., "Radio Propagation Fundamentals", Bell System Tech.J. 36, May 1957, p.593.

2.2 Picquenard, A., "Radio Wave Propagation", The Macmillan Press Ltd., 1974.

2.3 Jordan, E.C. and Balmain, K.G., "Electromagnetic Waves and Radiating Systems", Englewood Cliffs, NJ: Prentice-Hall, 1968.

2.4 Reed, H.R. and Russel, C.M., "Ultra High Frequency Propagation", John Wiley and Sons, NY, 1953.

2.5 Lee, W.C.Y., "Mobile Communications Engineering", McGraw-Hill Book Company, 1982.

2.6 Anderson, L.J. and Trolese, L.G., "Simplified Methods for Computing Knife-Edge Diffraction in the Shadow Region", IRE Trans. Ant. and Prop., July 1958.

2.7 Bullington, K., "Radio Propagation at Frequencies above 30 Megacycles", Proc. IRE, Vol.35, No.10, 1947, pp.1122-1136.

2.8 Rice, S.O., "Diffraction of Plane Radio Waves by a Parabolic Cylinder", Bell System Tech.J. 33, March 1954, pp.417-504.

2.9 Hacking, K., "Propagation Over Rounded Hills", BBC Research Report RA-21, 1968.

2.10 Causebrook, J.H. and Davies, B., "Tropospheric Radio Wave Propagation Over Irregular Terrain: The Computation of Field Strength for UHF Broadcasting", BBC Research Report 1971/43, 1971.

2.11 Millington, G., Hewitt, R. and Immirzi, F.S., "Double Knife-Edge Diffraction in Field Strength Predictions", IEE Monograph 1962, No.507E.

2.12 Vogler, L.E., "The Attenuation of Electromagnetic Waves by Multiple Knife-Edge Diffraction", NTIA Rep. 91-86, Natl. Telecommunication and Inf. Admin., Boulder, Colo., October 1981.

2.13 Epstein, J. and Peterson, D.W., "An Experimental Study of Wave Propagation at 850 mc/s", IRE Trans. Ant. and Prop., April 1955.

2.14 "Atlas of Radio Wave Propagation Curves for Frequencies between 30 and 10000 mc/s", The Radio Research Labs., Ministry of Postal Services, Tokyo, Japan, 172-179.

2.15 Hacking, K., "Approximate Methods for Calculating Multiple Diffraction Loss", Electronics Letters, Vol. 2, No. 5, May 1966.

2.16 Deygout, J., "Multiple Knife-Edge Diffraction of Microwaves", IEEE Trans., Vol.AP-14, No.4, July 1966.

2.17 Wilkerson, R.E., "Approximations to the Double Knife-Edge Attenuation Coefficient", Radio Science, Vol. 1, No.12, December 1966.

2.18 Allsebrook, K., "An Investigation of the Propagation of Radio Waves at Frequencies in the VHF and UHF Bands Within Certain British Cities", Ph.D. Thesis, University of Birmingham, 1977.

2.19 Young, W.R.Jr., "Comparison of Mobile Radio Transmission at 150, 900 and 3700 MHz", Bell System Tech.J., Vol.31, pp.1068-1085, November 1952.

2.20 Nyland, H.W., "Characteristics of Small-Area Signal Fading on Mobile Circuits in the 150 MHz Band", IEEE Trans.Veh.Tech., Vol.VT-17, pp.24-30, October 1968.

2.21 Jakes, W.C., "Microwave Mobile Communications", John Wiley and Sons, New York, 1974.

2.22 Okumura, Y., Ohmori, E., Kawano, T. and Fukuda, K., "Field Strength and its Variability in VHF and UHF Land Mobile Service", Rev.Elec.Comm.Lab., 16, Sept-Oct. 1968, pp.825-873.

2.23 Kozano, S. and Watanabe, K., "Influence of Environmental Building on UHF Land Mobile Radio Propagation", IEE Trans. on Communication, Vol.Com-25, No.10, October 1977.

2.24 Ibrahim, M.F.A., "Signal Strength Prediction in Mobile Radio Communication in Built-up Areas", Ph.D. Thesis, University of Birmingham, 1981.

2.25 Reudink, D.O. and Wazawicz, M.F., "Some Propagation Experiments Relating Foliage Loss and Diffraction Loss at X-band at UHF Frequency", Joint IEEE Comm.Soc.Veh. Tech. Group Special Trans. on Mobile Radio Comm., November 1973, pp.1198-1206.

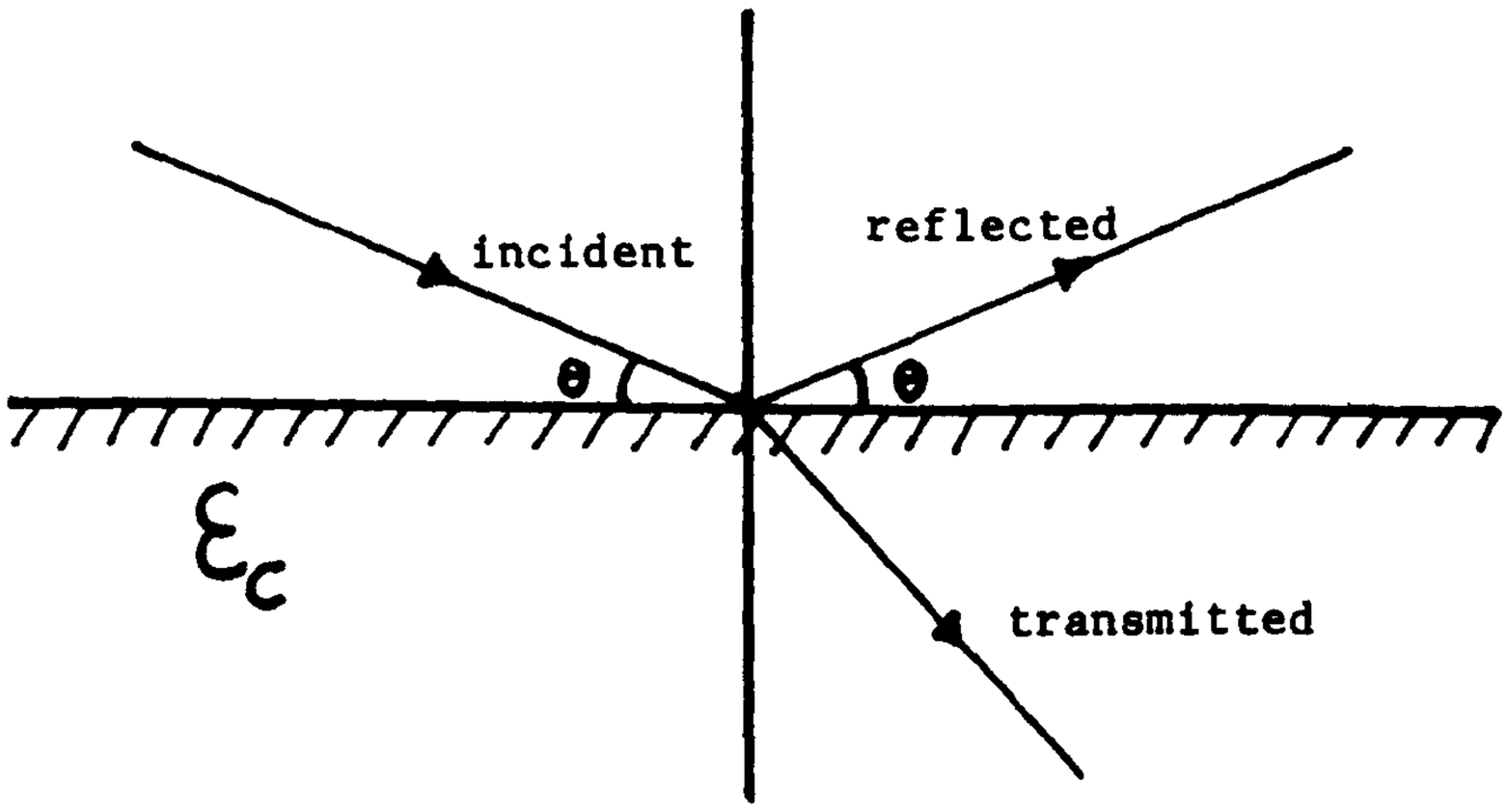

Fig. 2.1 Incident, Reflected and Transmitted Waves Between Two Media

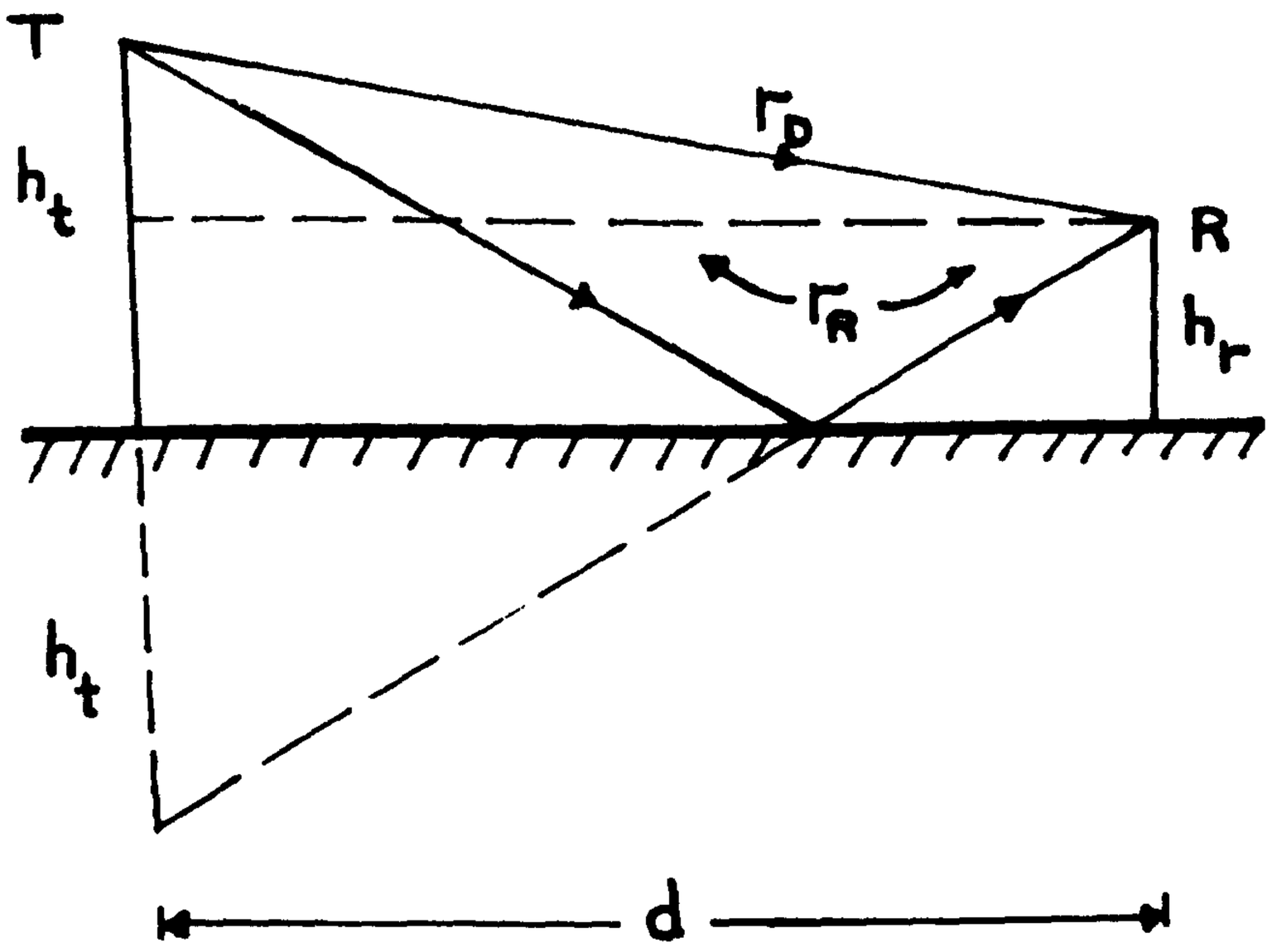

Fig. 2.2 Model for Plane Earth Propagation.

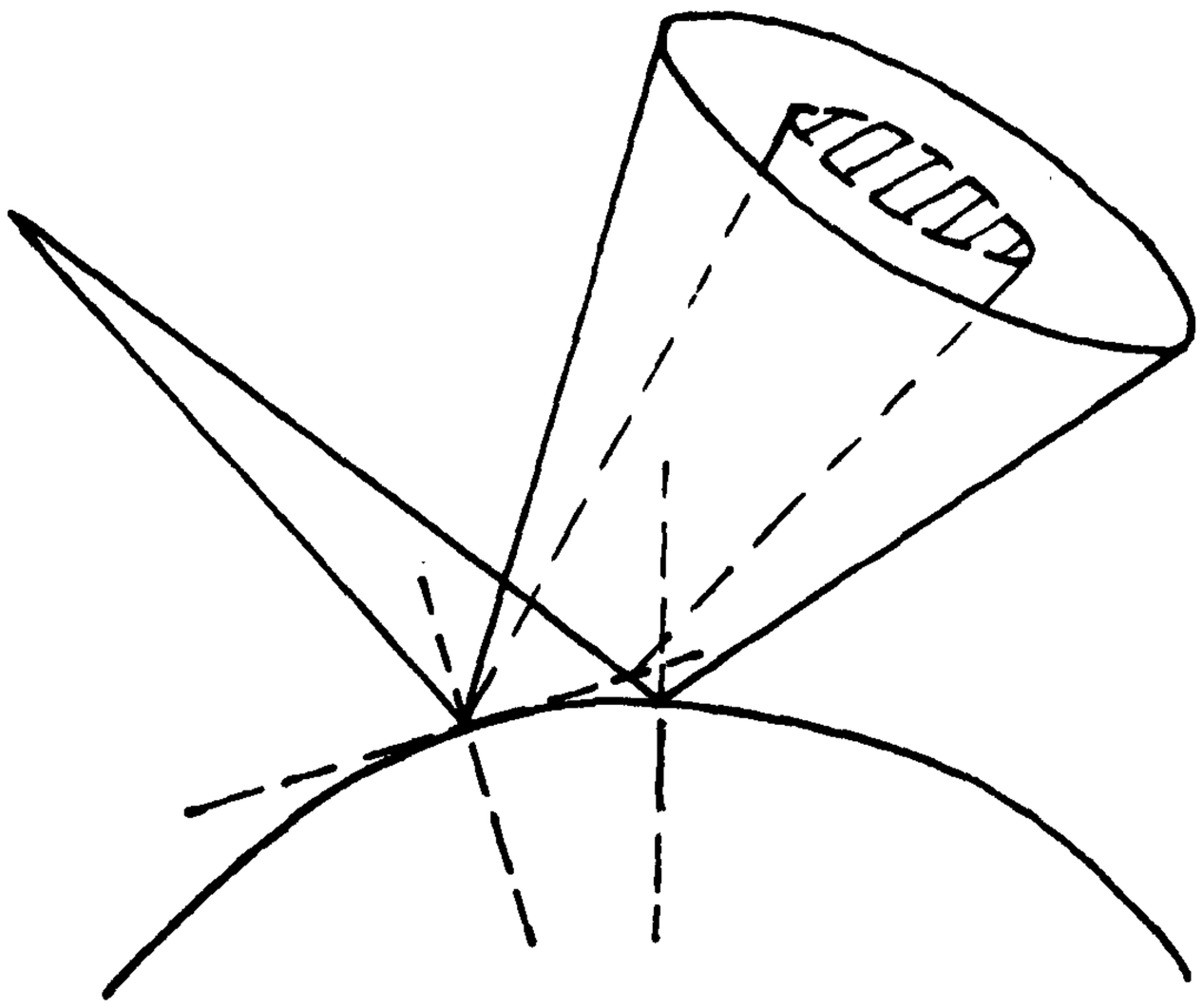

Fig. 2.3 Divergence of Reflected Rays from a Spherical Surface.

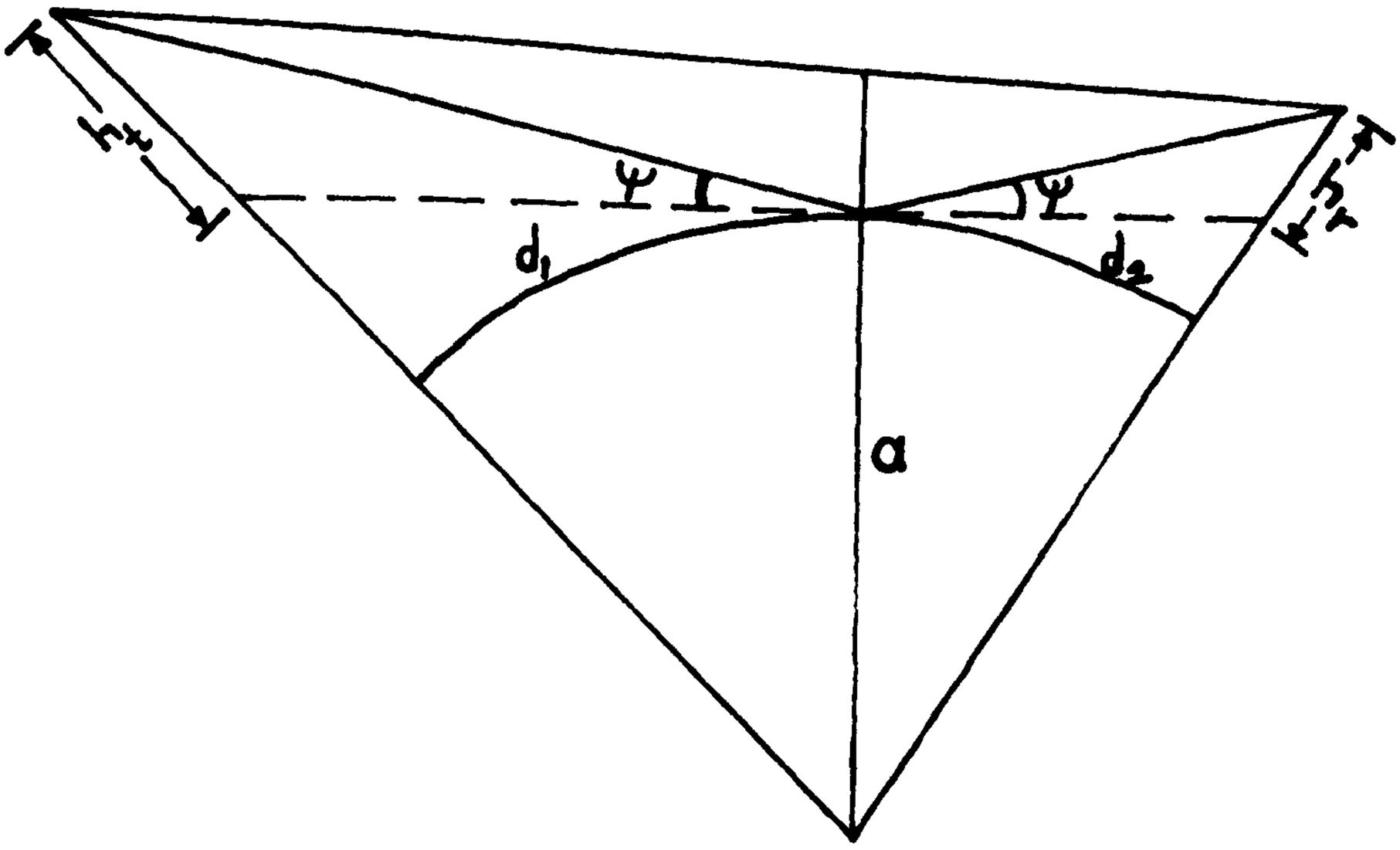

Fig. 2.4 Reflection from a Spherical Ground.

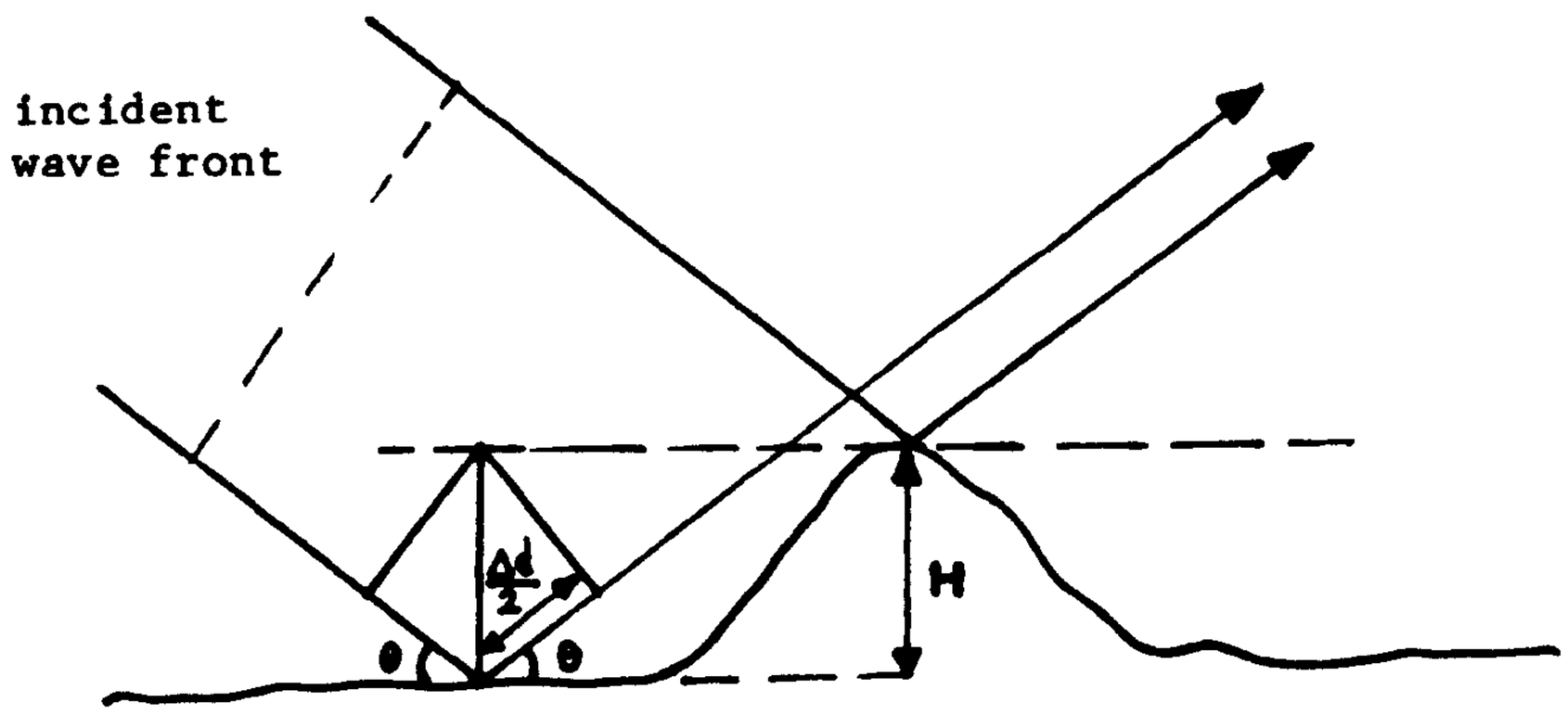

Fig. 2.5 Model for Surface Roughness Criteria.

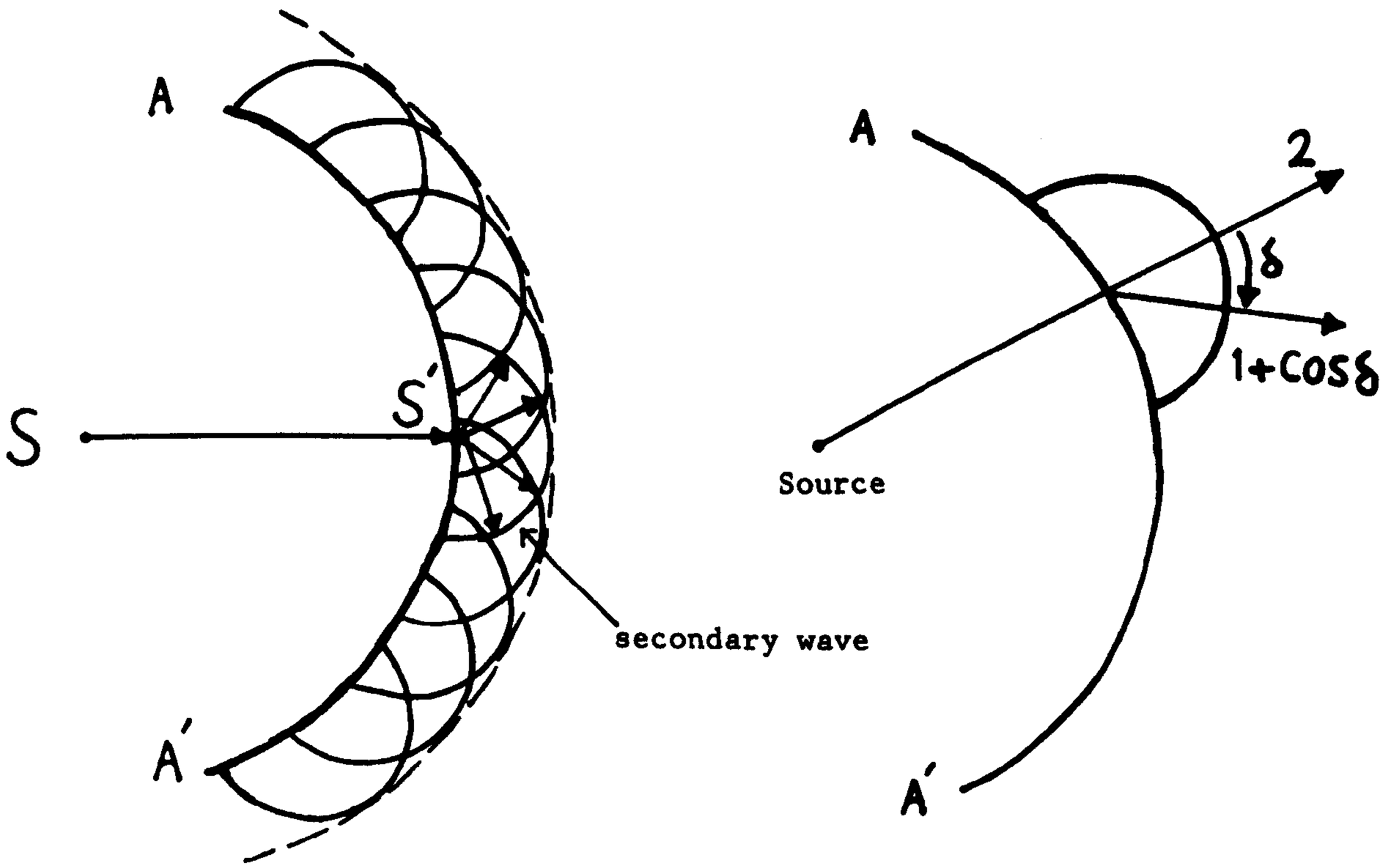

Fig. 2.6 Huyghen's Principle.

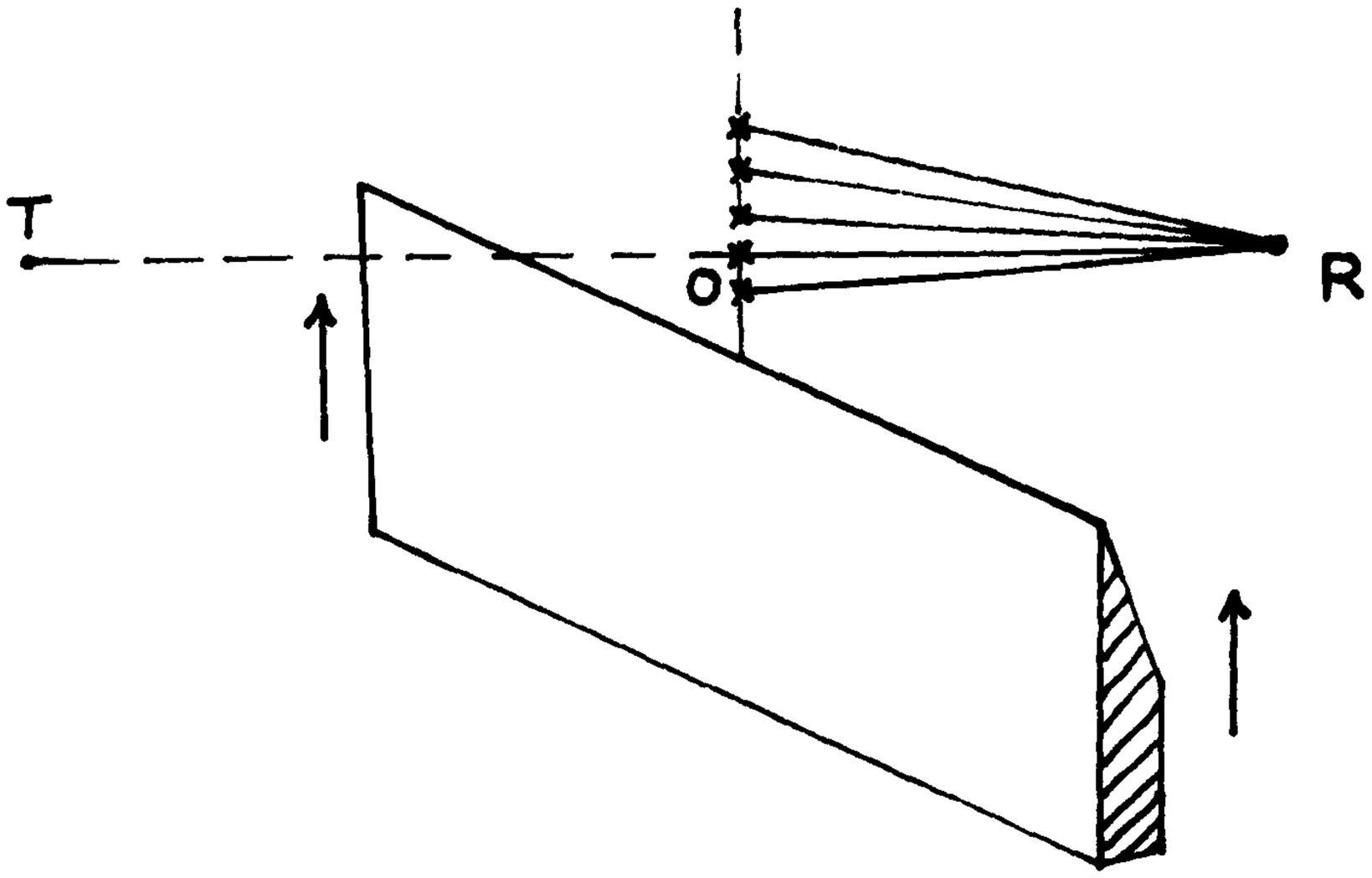

Fig. 2.7 Straight-edge Obstruction and Summation of the Secondary Sources.

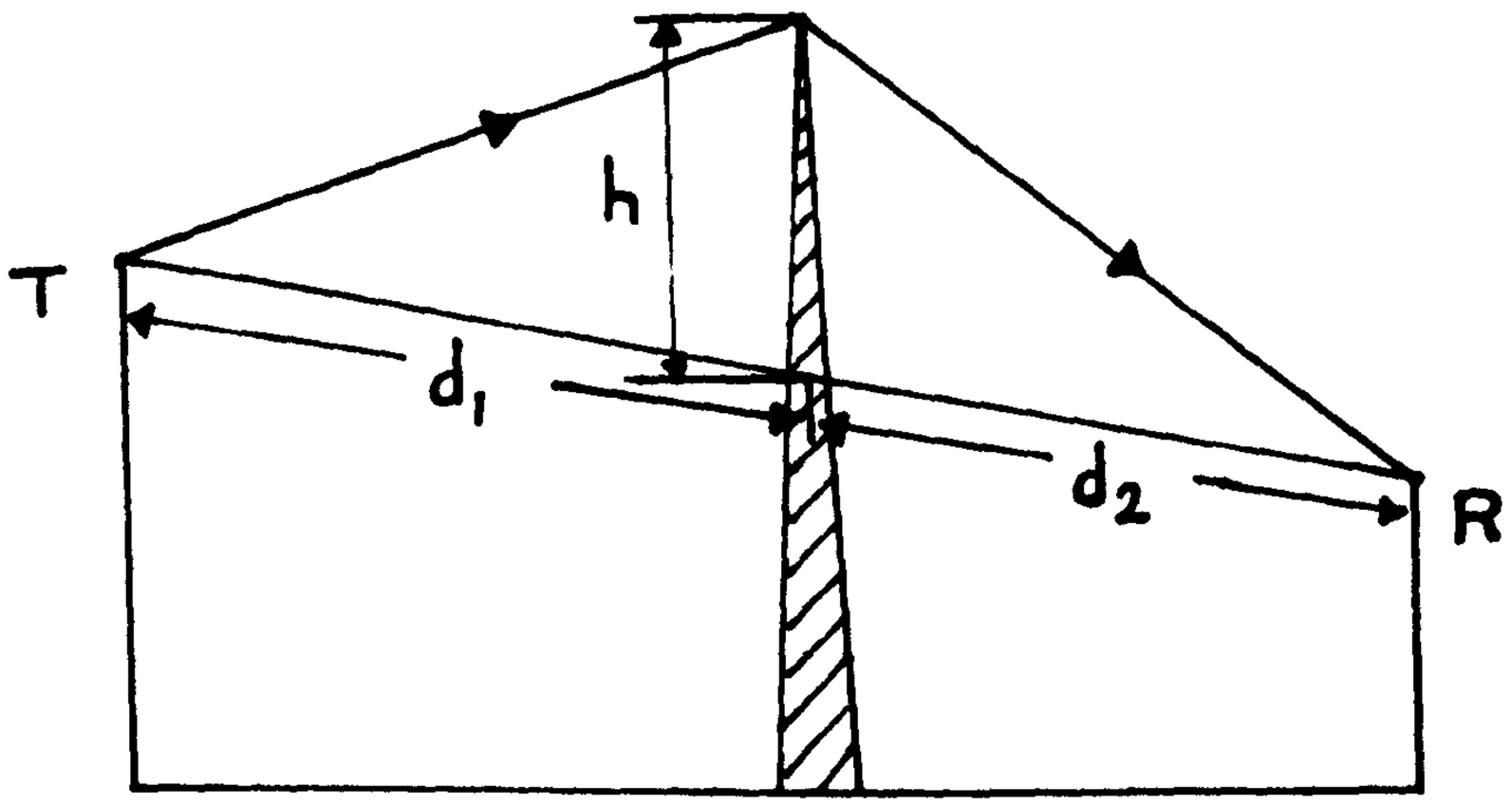

Fig. 2.8 Knife-edge Diffraction.

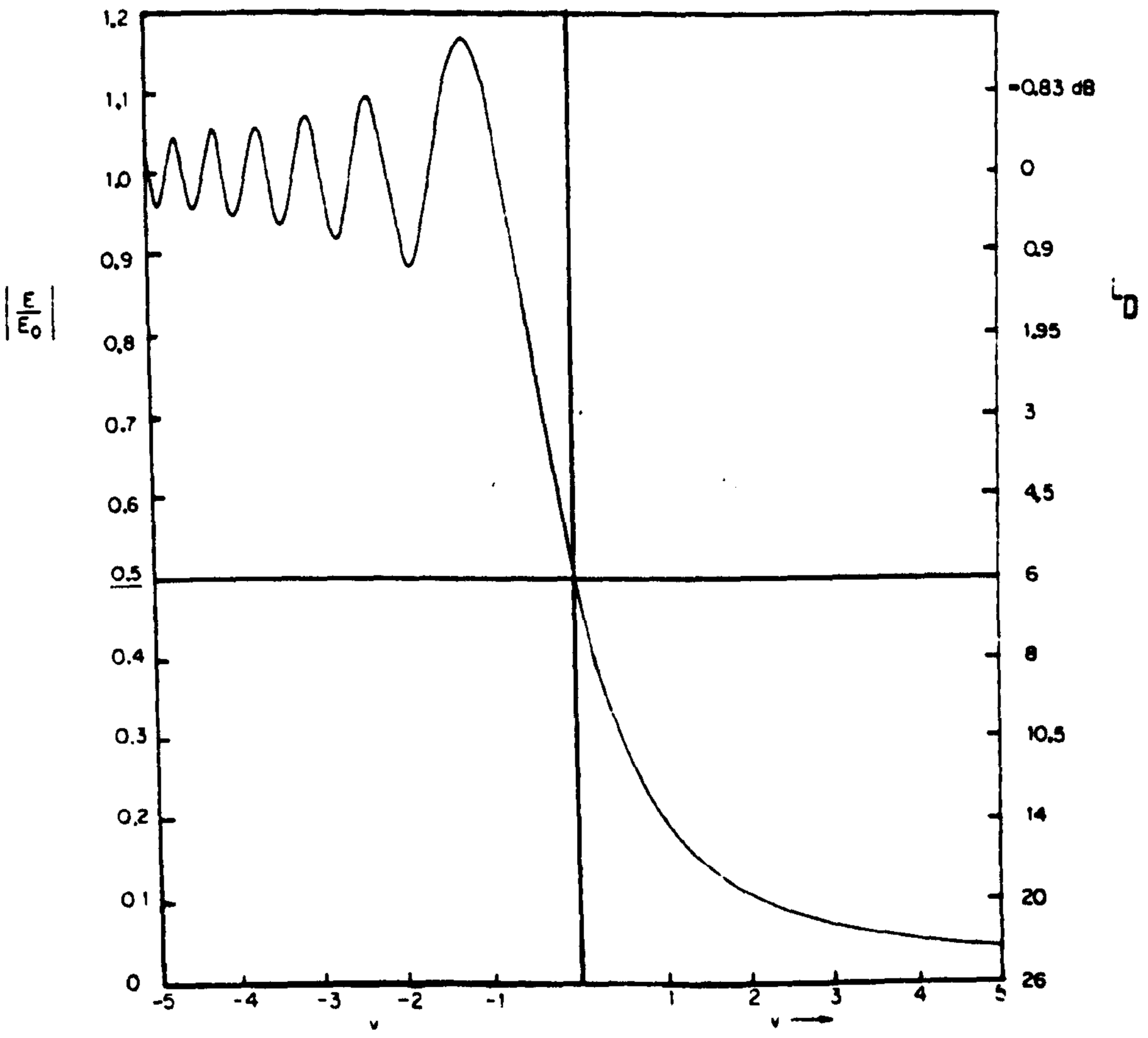

Fig. 2.9 Magnitude of Relative Field Strength and Diffraction Loss due to a Knife-edge.

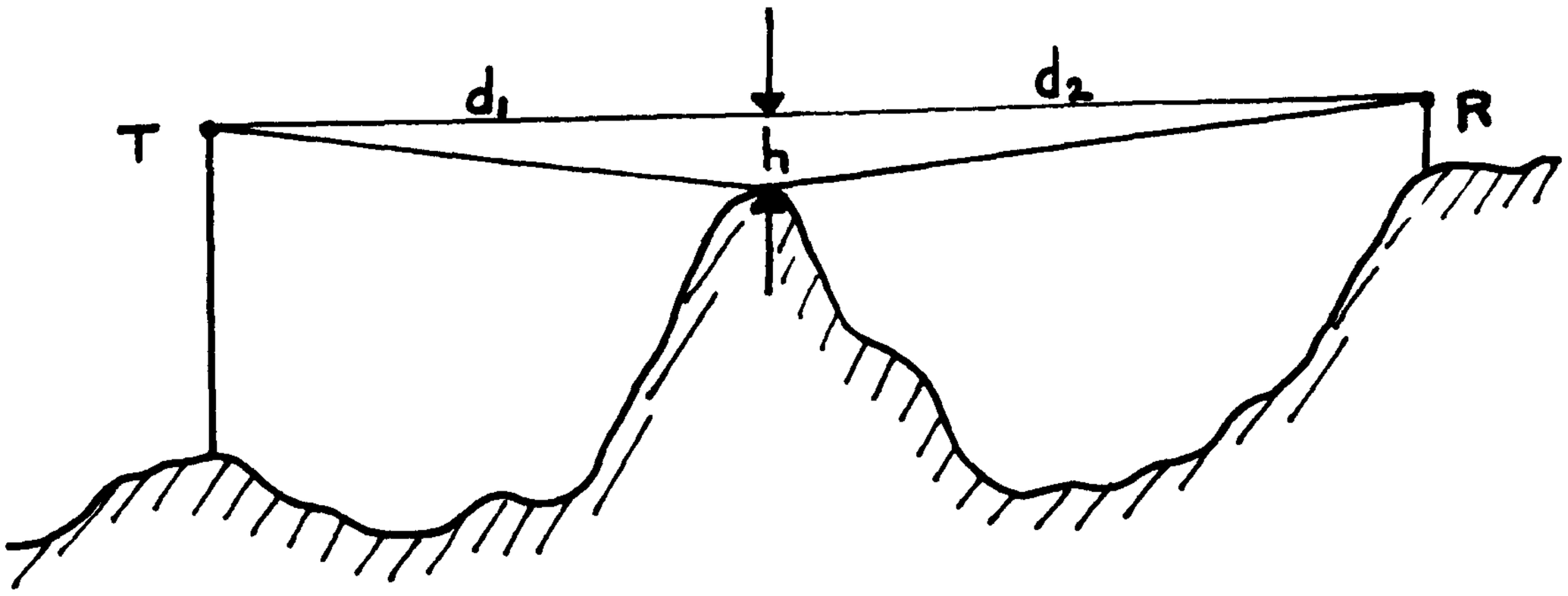

Fig. 2.10 Path Clearance Model of a Knife-edge Obstruction.

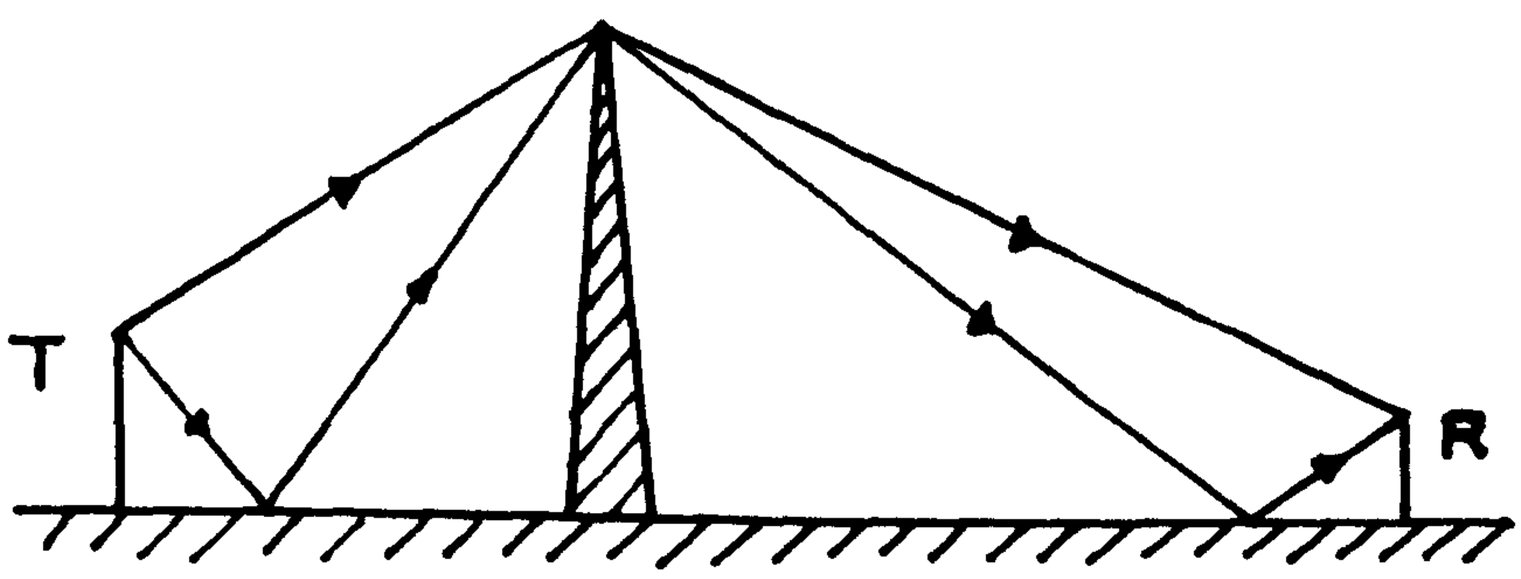

Fig. 2.11 Four Ray Model of Diffraction over a Knife-edge.

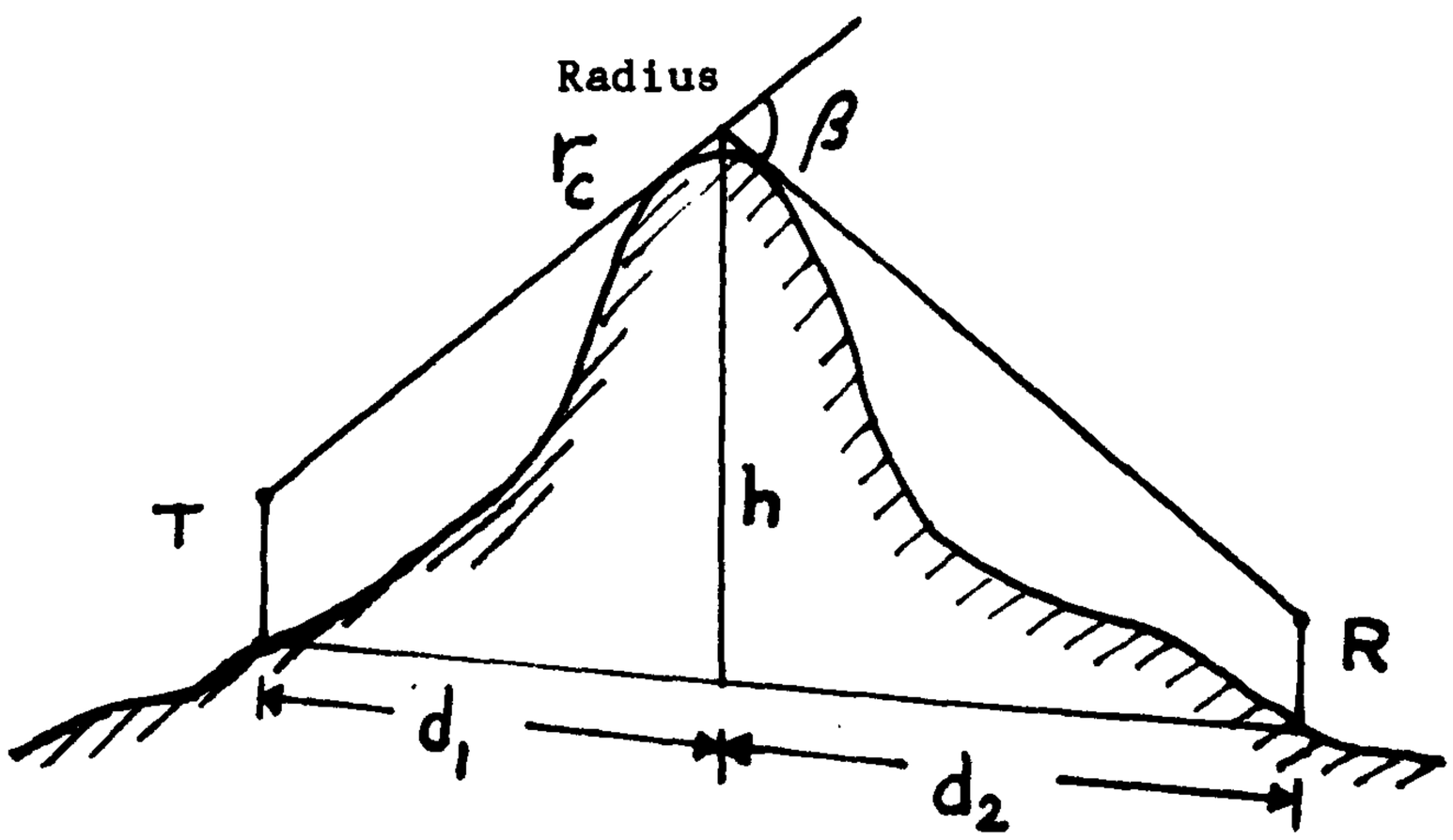

Fig. 2.12 Diffraction over a Rounded Hill.

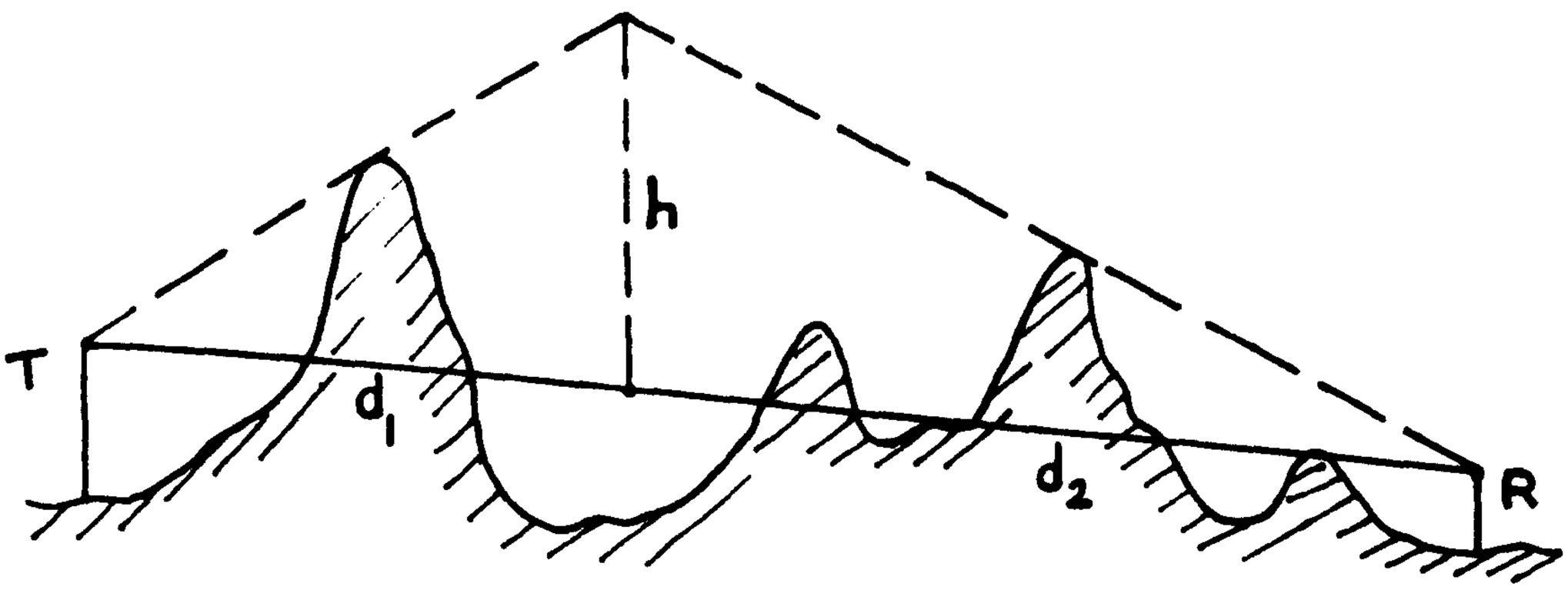

Fig. 2.13 Bullington's Construction of an Equivalent Knife-edge.

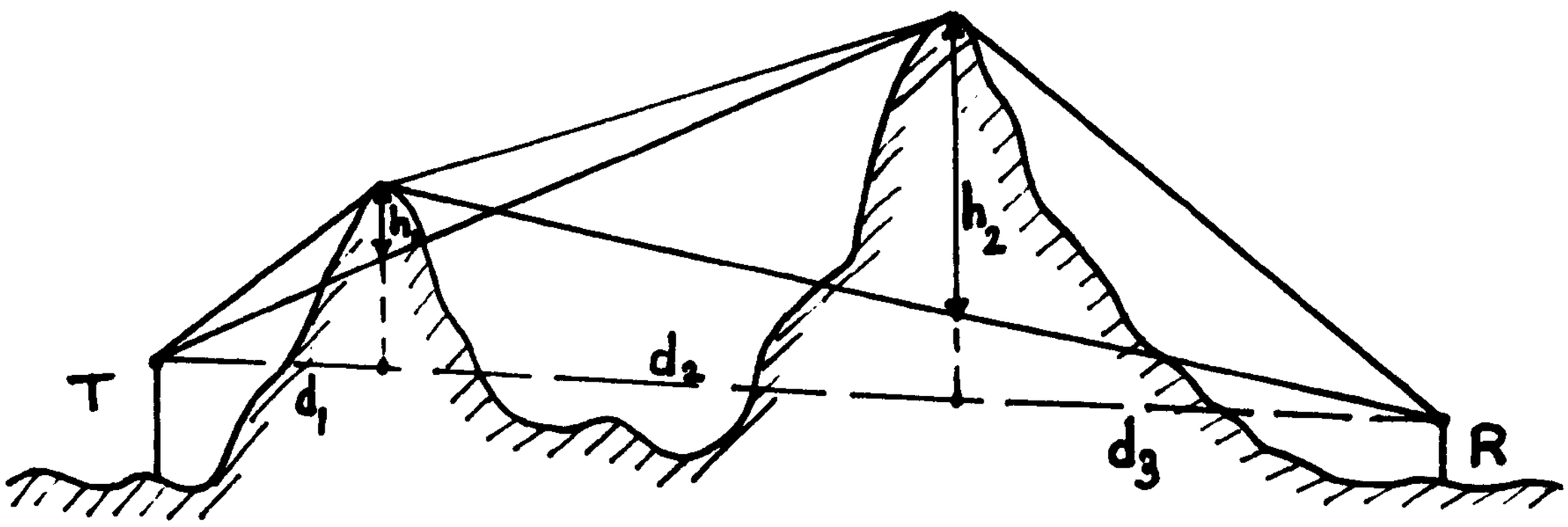

Fig. 2.14 Epstein-Peterson Construction.

Fig. 2.15 Japanese Atlas Construction.

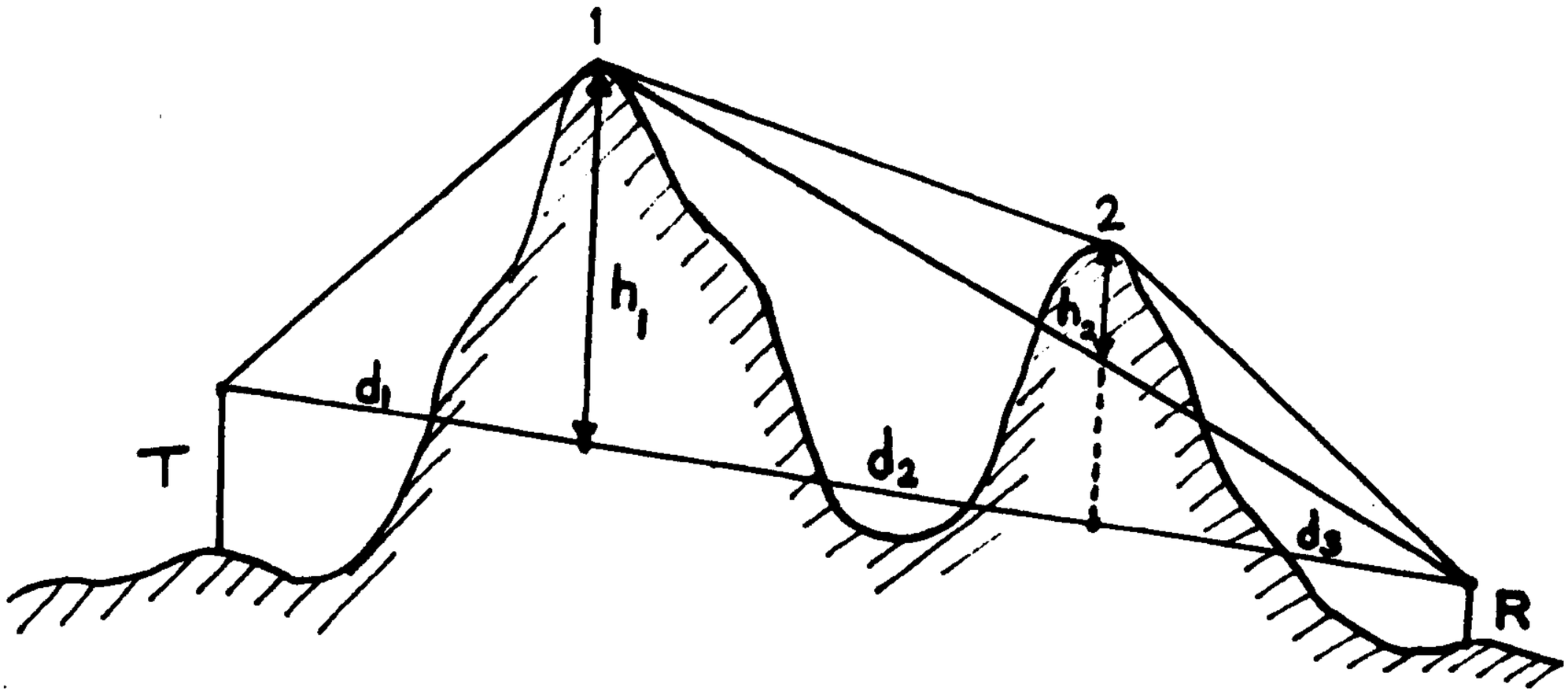

Fig. 2.16 Deygout Construction.

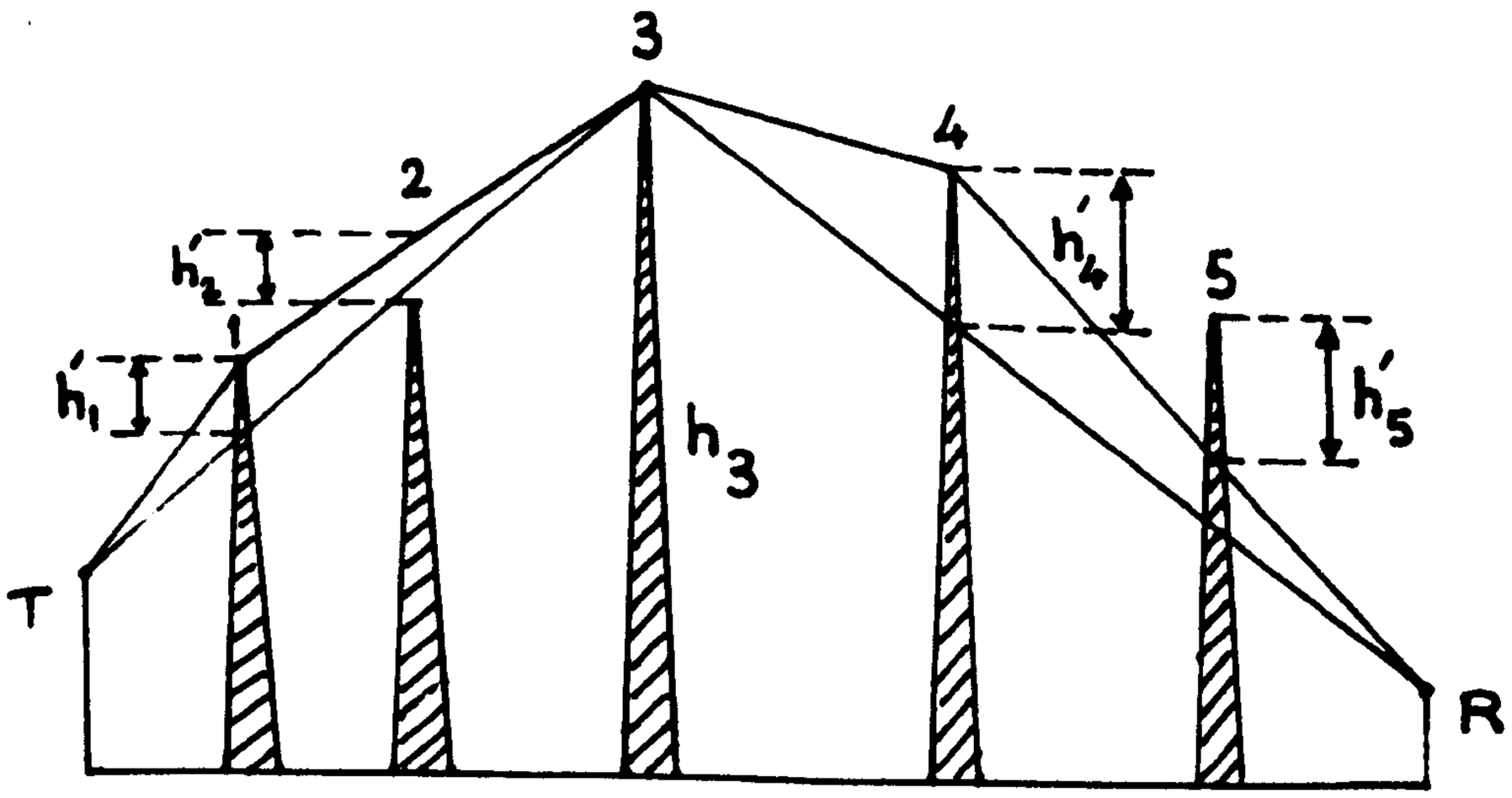

Fig. 2.17 Deygout Multiple Knife-edge Approximation.

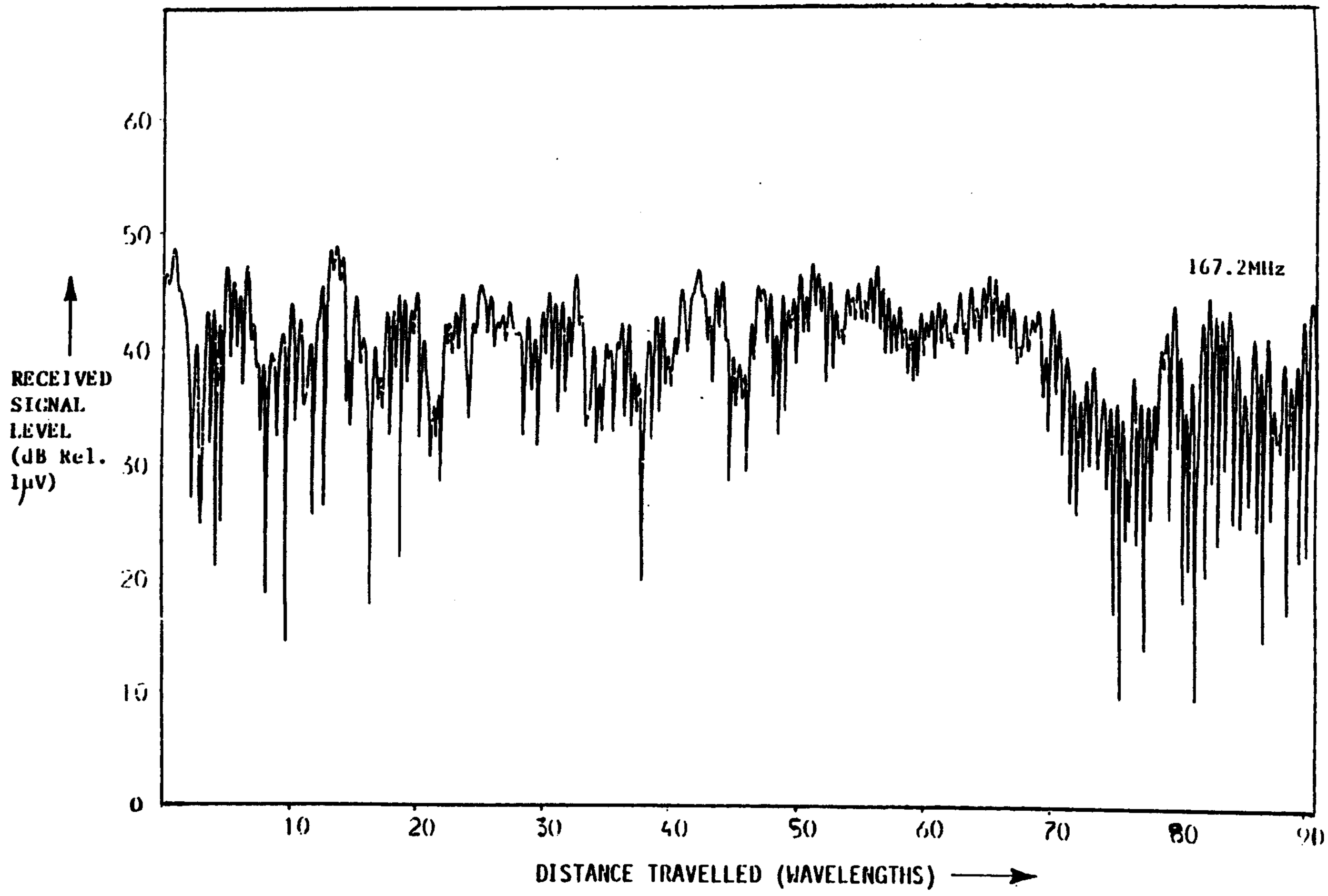

Fig. 2.18 A Measured Signal Envelope.

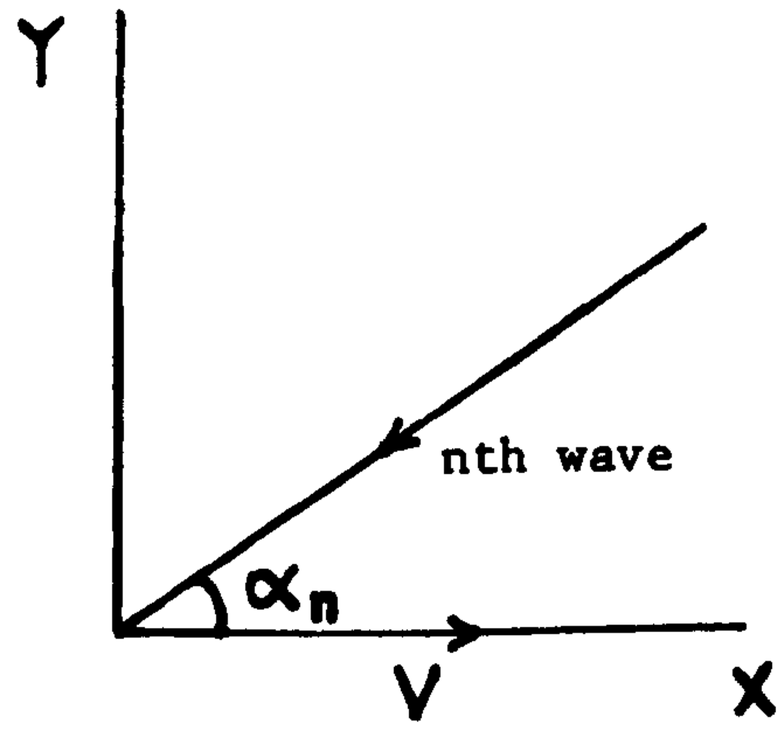

Fig. 2.19 A Typical Wave Received by the Mobile.

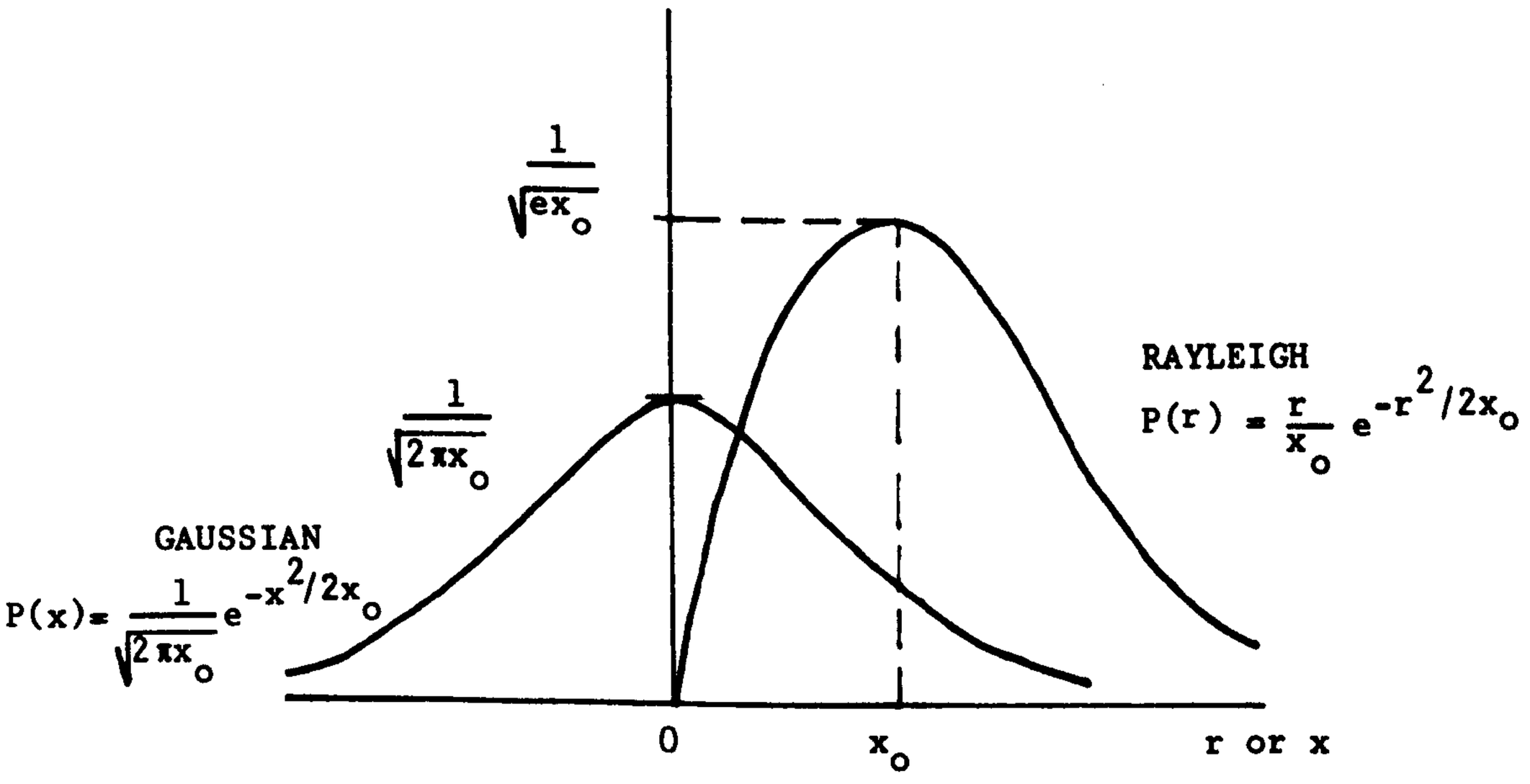

Fig. 2.20 Gaussian and Rayleigh Probability Density Functions.

CHAPTER 3

A REVIEW OF PATH LOSS PREDICTION MODELS

The prediction of propagation loss is an important step in the planning of radio communication services and prediction methods are needed to determine the parameters of a radio system which will provide efficient and reliable coverage of a specified area.

The problem of prediction involves a proper analysis of the influencing factors and most propagation models intended for predicting the transmission loss over irregular terrain rely on a statistical analysis of communication system parameters and terrain related factors.

The existing prediction models differ in their applicability over different terrain and environment; some are more general while others treat more specialised situations. However, there does not appear to be any one model which is ideally suited to all environments and of those available each requires the insertion of one or more parameters in order to be fully applicable to a given radio channel. The purpose of this chapter is to outline some of the more widely used methods for the prediction of radio transmission loss.

3.1 THE EGLI MODEL

By using measured field strength data obtained over irregular terrain situations, Egli [3.1] derived a frequency-dependent correction factor which could be used in conjunction with the theoretically predicted plane-earth received signal strength. The empirical median received power is given by:

$$P_{50} = P_t g_t g_r \left(\frac{h_t h_r}{d^2}\right)^2 \left(\frac{40}{f_{MHz}}\right)^2 \quad \text{Watts} \qquad (3.1)$$

where 40 MHz has been taken as the reference frequency and a square power law variation has been assumed for other frequencies. It is apparent that the median path loss reduces to that of the plane-earth theoretical value at 40 MHz irrespective of the degree of variation in the terrain irregularity, which limits the use of the model.

The median deviation from the theoretical plane-earth attenuation had been found to be log-normally distributed. Therefore, by calculating the standard deviation at different frequencies and using the median value given by (3.1), Egli obtained a graph (Fig. 3.1), which gives the terrain correction factor when the received power to other than 50 percent of locations is required.

Although a terrain factor has been included in the empirical expression, it should be noted that the model does not explicitly take into account diffraction losses caused by propagation over irregular terrain. The Egli model is intended for use in rural areas, since it does not include the effects of environmental factors such as buildings in its prediction procedure.

3.2 THE JRC METHOD

Following the work by Edwards and Durkin [3.2], the Joint Radio Committee of the Nationalised Power Industries of the U.K. have adopted a computer based technique for predicting the area coverage of a radio transmitter [3.3], [3.4].

The computer program executes two main computational operations. First, from stored topographical data, the ground profile

along the radial from the transmitter to a chosen receiver location is reconstructed. Secondly, the path attenuation to be expected along this profile is evaluated. The topographical data base has been extracted from Ordnance Survey maps, where each map is divided into 500 m squares and each square is represented by a single height value. The output from the program is presented in the form of a listing of the predicted field strengths and path losses at 500 m squares over the service area.

Evaluation of the expected attenuation along a given transmission path profile is made by calculating the line-of-sight loss and adding the diffraction loss caused by intervening obstacles. The path profile is therefore first examined and if line-of-sight with adequate first Fresnel-zone clearance exists over the path, the larger of free-space and plane-earth loss is selected. If, however, this is not the case, additional losses are calculated due to inadequate Fresnel-zone clearance or diffraction over the obstacles, according to the given profile.

The diffraction loss is estimated using the method of Epstein-Peterson (section 2.3.10.2), for up to three diffracting edges in the transmission path. If there are more than three edges in the path, a virtual knife-edge between the two outer edges is constructed in the manner suggested by Bullington (section 2.3.10.1), reducing the number of edges to three, as illustrated in Fig. 3.2.

In its calculation of plane-earth loss, the method considers the antenna heights above a horizontal plane which passes through the foot of the terminal with the lower ground height. The JRC method is one of the most widely used prediction methods in the U.K., and is intended for use in various terrain situations. However,

the main shortcoming of the method is its inability to take into account the effects of buildings or trees.

3.3 THE BLOMQUIST AND LADELL PREDICTION MODEL

Blomquist and Ladell [3.5] have suggested a model in an attempt to describe the propagation path loss over irregular terrain and in rural areas. This is essentially given by:

$$\text{Path Loss} = L_F + ((L_p' - L_F)^2 + L_D^2)^{\frac{1}{2}} \qquad \text{dB}$$

where L_p' consists of the plane-earth loss taking into account the surface wave and the loss due to curvature of the earth's surface and the factor $(L_p' - L_F)$ is given by a simple approximate formula in the model.

The Epstein-Peterson method is used for the estimation of diffraction losses, L_D, over terrain obstacles in the transmission path. It is apparent that the computed path loss will never be lower than the one estimated for free space, L_F, and the path loss over flat land ($L_D = 0$) reduces to the modified plane-earth transmission equation. For highly obstructed link [$L_D >> (L_p' - L_F)$], the total path loss is equal to the sum of the free-space and diffraction losses ($L_F + L_D$).

While the limiting conditions appear intuitively reasonable, it is worth noting that there is no apparent theoretical explanation to the model from the propagation point of view.

3.4 THE OKUMURA PREDICTION MODEL

The Okumura method [3.6] is based on empirical data collected as a result of an extensive series of mobile propagation

measurements over various types of terrain and environmental clutter in the frequency range of 200 to 2000 MHz in Japan.

Essentially Okumura's method is based on determining the free-space path loss between the transmitter and the receiver and then adding or subtracting numerous correction factors to account for the nature of the terrain, the extent of urbanisation, the heights of the antennas, etc. The basic formulation of Okumura's prediction technique can be expressed as:

$$\text{Path Loss} = L_F + A_{mu} - H_{tu} - H_{ru} \qquad \text{dB}$$

where A_{mu} is the median attenuation relative to free space in an urban area over quasi-smooth terrain, where the base station effective antenna height h_{te} = 200 m, mobile station antenna height h_{re} = 3 m, expressed by the curves in Fig. 3.3 as a function of frequency in the range 100 to 3000 MHz, and distance in the range 1 to 100 Km.

H_{tu} is the base station antenna height gain factor in dB and is a function of the base station effective antenna height (20 to 1000 m), and distance, as shown in Fig. 3.4.

H_{ru} is the vehicular station antenna height gain factor in dB and is a function of the mobile antenna height (1 to 10 m) and frequency, as shown in Fig. 3.5.

Further correction factors are provided in graphical form, for transmission in suburban and open areas and over irregular terrain situations. The irregular terrain is divided into: rolling hilly terrain, isolated mountain, general sloping terrain and mixed land sea path.

The terrain related parameters which must be evaluated in

order to determine the various correction factors of the Okumura model are:

(a) The effective base station antenna height (h_{te}):

The height of the base station antenna above the average ground level calculated over the range interval of 3 to 15 Km (or less if the total range is below 15 Km), as illustrated in Fig. 3.6.

(b) The terrain undulation height (Δh):

This parameter classifies surface irregularities and is defined as the difference between the 10% and 90% values of terrain height within a distance of 10 Km of the receiver in a direction towards the transmitter, as illustrated in Fig. 3.7.

(c) Isolated ridge height:

When the propagation path includes a single obstructing mountain, the height of the ridge is measured from the average ground level in the path between the ridge and base station.

(d) Average ground slope (θ_m):

The average ground slope is determined over the 5 to 10 Km of the sloping terrain in the path.

(e) Mixed land-sea path distance parameter:

This is the ratio in percentage of the path covered with water over the total path length.

The Okumura model has been developed for land mobile services in built-up areas and takes account of variations in both terrain and urbanisation. The model is often used for comparison with

other prediction methods and a comparative study of a computerised version of the method with measured data will be reported later.

3.5 HATA MODEL

In an attempt to formulate Okumura's prediction curves, Hata [3.7] has established an empirical formula for path loss prediction. It is limited in its range of applicability and is intended only for quasi-smooth terrain situations. The prediction formulae and their application ranges are as follows:-

Urban area:

$$P_L \simeq 69.55 + 26.16 \log_{10} f - 13.82 \log_{10} h_t - a(h_r) + (44.9 - 6.55 \log_{10} h_t). \log_{10} d$$

where: f lies in the range 150-1500 MHz

h_t lies in the range 30-200 m

d lies in the range 1-20 Km

$a(h_r)$ is the correction factor for the mobile antenna height and is computed as follows:

For a small or medium city:

$$a(h_r) = (1.1 \log_{10} f - 0.7)\, h_r - (1.56 \log_{10} f - 0.8)$$

where h_r lies in the range 1-10 m.

For a large city:

$$a(h_r) = 8.29\, (\log_{10} 1.54\, h_r)^2 - 1.1 \quad ; \quad f \leq 200 \text{ MHz}$$

and $$a(h_r) = 3.2\, (\log_{10} 11.75\, h_r)^2 - 4.97 \quad ; \quad f \geq 400 \text{ MHz}$$

Suburban area :

$$P_{LS} = P_L \text{ [urban area]} - 2[\log_{10}(f/28)]^2 - 5.4$$

Open area:

$$P_{LO} = P_L \text{ [urban area]} - 4.78(\log_{10} f)^2 + 18.33 \log_{10} f - 40.94$$

3.6 THE LONGLEY-RICE PREDICTION MODEL

This is a general purpose semi-empirical model [3.8], in which statistical terrain parameters are used, together with some of the well-known rules of electromagnetic wave propagation. The model can be used even if the actual terrain profile in any given situation is not available since estimates of the various terrain parameters required are given. These have been obtained statistically from a large number of terrain profiles of various types. Table 3.1 lists the input parameters required by the model.

Table 3.1

System parameters	
Frequency	20 MHz to 20 GHz
Distance	1 Km to 2000 Km
Antenna heights	0.5 m to 3000 m
Polarization	vertical or horizontal
Environmental parameters	
Terrain irregularity parameter, Δh	
Electrical ground constants	
Surface refractivity	250 to 400 N-units
Climate	
Deployment parameters	
Siting criteria	random, careful or very careful

The method by which Δh, the interdecile range of terrain elevations, is evaluated differs from that used in the Okumura model and is related to a function $\Delta h(d)$ which varies with the path

distance, d. This function $\Delta h(d)$ is called the interdecile range of terrain heights above and below a straight line fitted to elevations above sea level and for long enough path lengths, the asymptotic behaviour $\Delta h(d)$ is very close to Δh. The relation between $\Delta h(d)$ and Δh is given by:

$$\Delta h(d) = \Delta h[1 - 0.8 \exp(- 0.02\ d)]$$

Table 3.2 shows the suggested values of Δh by the model according to type of terrain, for situations where the actual terrain profiles are not available.

Table 3.2

	Δh (metres)
Flat (or smooth water)	0
Plains	30
Hills	90
Mountains	200
Rugged mountains	500

For an average terrain, use $\Delta h = 90$ m.

The suggested values for the electrical ground constants are shown in table 3.3.

Table 3.3

	Relative Permittivity	Conductivity (Siemens/metre)
Average ground	15	0.005
Poor ground	4	0.001
Good ground	25	0.020
Fresh water	81	0.010
Sea water	81	5.0

Further, the model uses other path related parameters such as, smooth earth horizon distance, d_{LS}, horizon distance, d_L, over irregular terrain and the horizon elevations angle, θ_e, for each terminal. These are shown in Fig. 3.8, and when the terrain profiles are not available, they can be calculated by using the suggested empirical formulae, as a function of Δh and the antenna effective height.

For prediction of transmission loss, the reference attenuation below free space is calculated first as a continuous function of distance, and then converted to basic transmission loss by adding the free-space loss at each distance.

The reference attenuation is computed according to three distance ranges as specified below:

a - for distances less than the smooth-earth horizon distance d_{LS}.

b - for distances just beyond the horizon from d_{LS} to d_x, where d_x is the point where diffraction and scatter losses are equal.

c - for distances greater than d_x.

This model does not provide predictions for distances less than 1 Km. For distances from 1 Km to d_{LS}, the predicted attenuation is based on two-ray reflection theory and extrapolated diffraction theory.

For distances from d_{LS} to d_x, the predicted attenuation is a weighted average of knife-edge and smooth-earth diffraction calculations. The weighting factor in this region is a function of frequency, terrain irregularity and antenna heights. For highly irregular terrain, the horizon obstacles from the terminals are considered as sharp ridges and hence the diffraction loss is

calculated over a double knife-edge path using the Epstein-Peterson approximation.

For distances greater than d_x, the predicted attenuation is calculated by means of a forward scatter formulation. Since the original publication there have been several revisions of the model and some corrections have been made. In particular, there has been the addition of an urban factor, UF, used for predictions in urban areas. This factor has been derived by comparing the original model with the prediction curve of Okumura for urban areas. It is given as [3.10],

$$UF = 16.5 + 15 \log_{10} (f/100) - 0.12\ d$$

where, the frequency f is in MHz and d in Km.

The Longley-Rice model allows for a small adjustment due to each climate to convert the reference attenuation to an all-year median attenuation and further allowances can be made to account for time and location variability.

3.7 THE B.B.C. MODEL

The B.B.C. uses a computer based field strength prediction method [3.11] to assist with the planning and development of its UHF television services. The method assumes that the transmitter sites are well clear of any local obstructions and the receiving antennas are taken to be 10 m high, this being the typical height of a domestic antenna installation.

Topographical data are used to derive the path profile, after which diffraction loss is estimated. For line-of-sight paths with inadequate Fresnel zone clearance and for paths with one

obstruction, the loss is computed for a wedge shaped terrain with the apex positioned at the edge. The problem is treated as a modified Fresnel diffraction problem using a four ray technique, the additional rays arising through ground reflection, being associated with images of the transmitter and receiver [3.12]. For more obstructed paths, diffraction loss is a weighted sum of knife-edge loss and cylindrical surface loss, where the multiple knife-edge loss is calculated with a modified Deygout procedure. Added to diffraction loss is the attenuation caused by buildings and trees which are close to the receiver. This clutter loss is weighted in inverse proportion to its physical distance from the receiver, and clutter further than 2 Km from the receiver is not considered. Free-space loss is then added to obtain the total predicted path loss.

3.8 ALLSEBROOK MODEL

Allsebrook [3.13] proposed a semi-empirical model based on the technique adopted by Blomquist and Ladell, but including correction factors which were found as a result of measured data analysis. The propagation path loss in dB is given by

$$\text{Path Loss} = L_F + [(L_p - L_F)^2 + L_D^2]^{\frac{1}{2}} + L_B + \gamma$$

where L_F is the free-space loss, L_p is the plane-earth loss and L_D is the diffraction loss over terrain obstacles in the transmission path calculated by using the Japanese Atlas diffraction method (section 2.3.10.3).

L_B is the diffraction loss over the building adjacent to the mobile, obstructing the signal path, and γ is the UHF correction factor which ranges from 0 to approximately 15 dB as the frequency

increases from 200 to 500 MHz. Over the smooth terrain where $L_D = 0$ and at VHF, the model calculates the path loss as $L_P + L_B$, which is similar in form to that used by the JRC for propagation over irregular terrain, except that L_B has replaced the diffraction loss due to terrain obstacles.

In order to calculate L_B, the diffraction loss due to buildings, the effective street width, i.e. the distance between the mobile and the building obstructing the line of sight path between the transmitter and receiver, the height of that building and the distance between that building and transmitter, have to be known.

3.9 IBRAHIM'S MODEL

Two models have been proposed by Ibrahim [3.14] for path loss prediction over flat urban areas. The first is an empirical model which gives the median path loss in dB between isotropic antennas as:

$$P_L = 47.7 - 8 \log_{10} h_r - 20 \log_{10} f h_t + \left[40 + 14.15 \log_{10}\left(\frac{f+100}{156}\right)\right] \log_{10} d$$

$$+ 0.265\ L - 0.37\ H + K$$

where $K = 0.087\ U - 5.5$ dB.

The second model which is semi-empirical gives the path loss as:

$$P_L = L_P + 20 + \frac{f}{40} + 0.18\ L - 0.34\ H + K \quad \text{dB}$$

where L_P is the theoretical plane-earth loss and

$$K = 0.0\ 94\ U - 5.9 \quad \text{dB}\ .$$

The factor K as given in the above is used for the highly urbanised part of the city, otherwise $K = 0$.

In the above equations :

f is the frequency in MHz,

L is the building-site area factor, defined as the percentage of the test square area (500 m x 500 m square) that is covered by buildings of any kind.

U is the degree of urbanisation factor, defined as the percentage of the building-site area within a test square, occupied by buildings having 4 or more floors.

H is the mobile relative spot height, defined as the magnitude of the difference between the spot heights of the base and the mobile test squares.

The application of this model requires the creation of an urban environment data base to provide the values of L and U.

References

3.1 Egli, J. "Radio Propagation above 40 MC over Irregular Terrain", Proc. IRE, Vol.45, 1957, pp.1383-1391.

3.2 Edwards, R. and Durkin, J. "Computer Prediction of Service Areas for VHF Mobile Radio Networks", Proc. IEEE, Vol.116, No.9, September 1969.

3.3 Dadson, C.E., Durkin, J. and Martin, J. "Computer Predictions of Field Strength in the Planning of Radio Systems", IEEE Trans. Veh.Tech., Vol.VT-24, 1975.

3.4 Dadson, C.E. "Radio Network and Radio link Surveys Derived by Computer from a Terrain Data Base", NATO AGARD Conf.Pub., CPP 269, 1979.

3.5 Blomquist, A. and Ladell, L. "Prediction and Calculation of Transmission Loss in Different Types of Terrain", NATO AGARD Conf. Pub., CP144, 1974, Res.Inst.Nat.Defence, Dept.3, S-104 50 Stockholm 80, Sweden.

3.6 Okumura, Y., Ohmori, E., Kawano, T. and Fukuda, K. "Field Strength and Its Variability in VHF and UHF Land Mobile Service", Rev.Elec.Comm.Lab., 16, Sept-Oct. 1968, pp.825-873.

3.7 Hata, M. "Empirical Formula for Propagation Loss in Land Mobile Radio Services", IEEE Trans.Veh.Tech., Vol. VT-29, No. 3, August 1980, pp.317-325.

3.8 Longley, A.G. and Rice, P.L. "Prediction of Tropospheric Radio Transmission Loss over Irregular Terrain, A Computer Method, 1968", ESSA Tech. Report ERL 79-ITS 67.

3.9 Hufford, G.A., Longley, A.G. and Kissick, W.A. "A Guide to the Use of the ITS Irregular Terrain Model in the Area Prediction Mode", NTIA Report 82-100, 1982.

3.10 Longley, A.G. "Radio Propagation in Urban Areas", OT Report 78-144, Office of Telecommunications, Boulder, Colorado, 1978.

3.11 Causebrook, J.H. "Computer Prediction of UHF Broadcast Service Areas", BBC Research Report RD 1974/4, January 1974.

3.12 Causebrook, J.H. and Davis, B. "Tropospheric Radio Wave Propagation Over Irregular Terrain: The Computation of Field Strength for UHF Broadcasting", BBC Research Report 1971/43, 1971.

3.13 Allsebrook, K. "An Investigation of the Propagation of Radio-Waves at Frequencies in the VHF and UHF Bands Within Certain British Cities", Ph.D. Thesis, University of Birmingham, 1977.

3.14 Ibrahim, M.F.A., "Signal Strength Prediction in Mobile Radio Communication in Built-up Areas", Ph.D. Thesis, University of Birmingham, 1981.

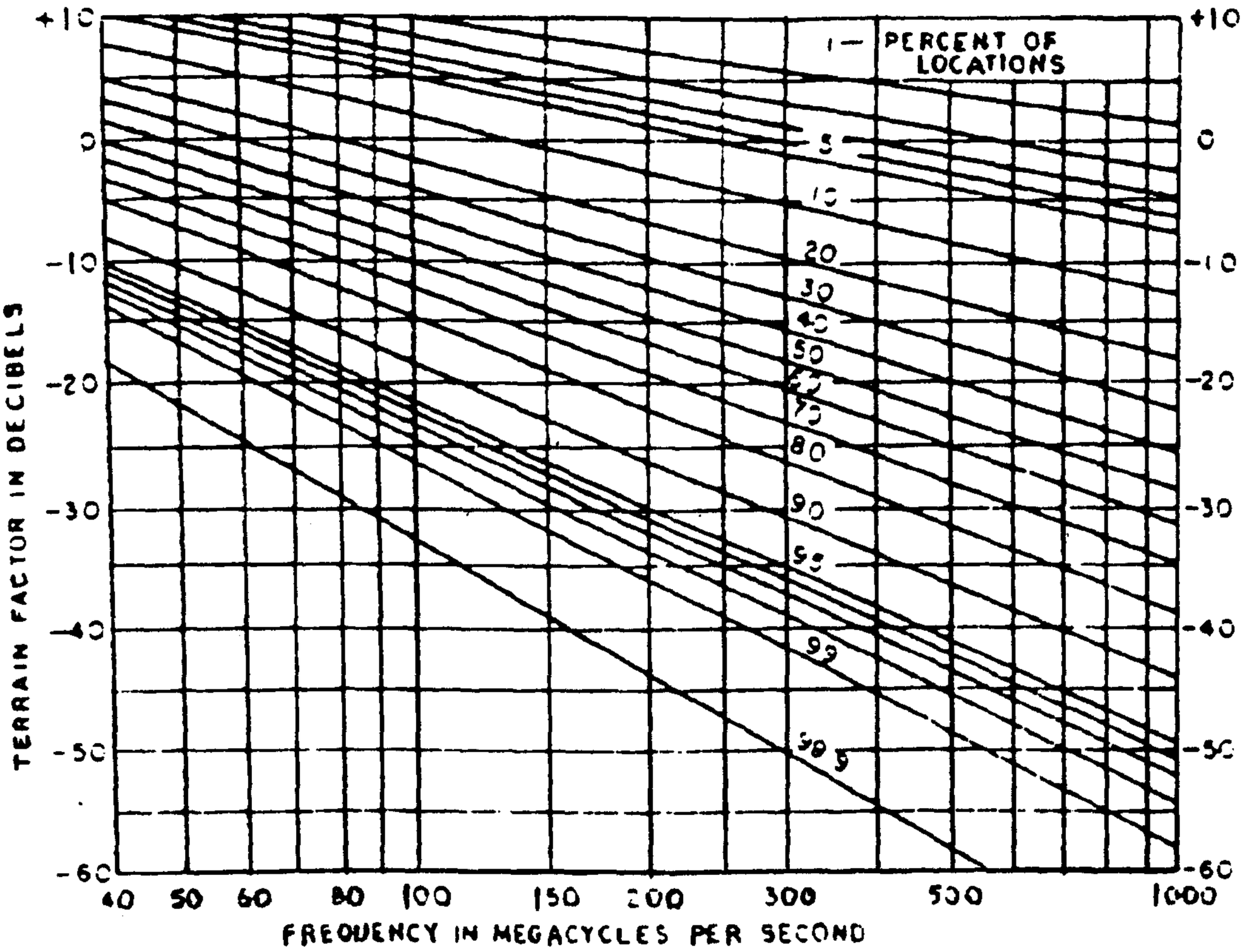

Fig. 3.1 Egli's Method for Calculation of the Terrain Factor.

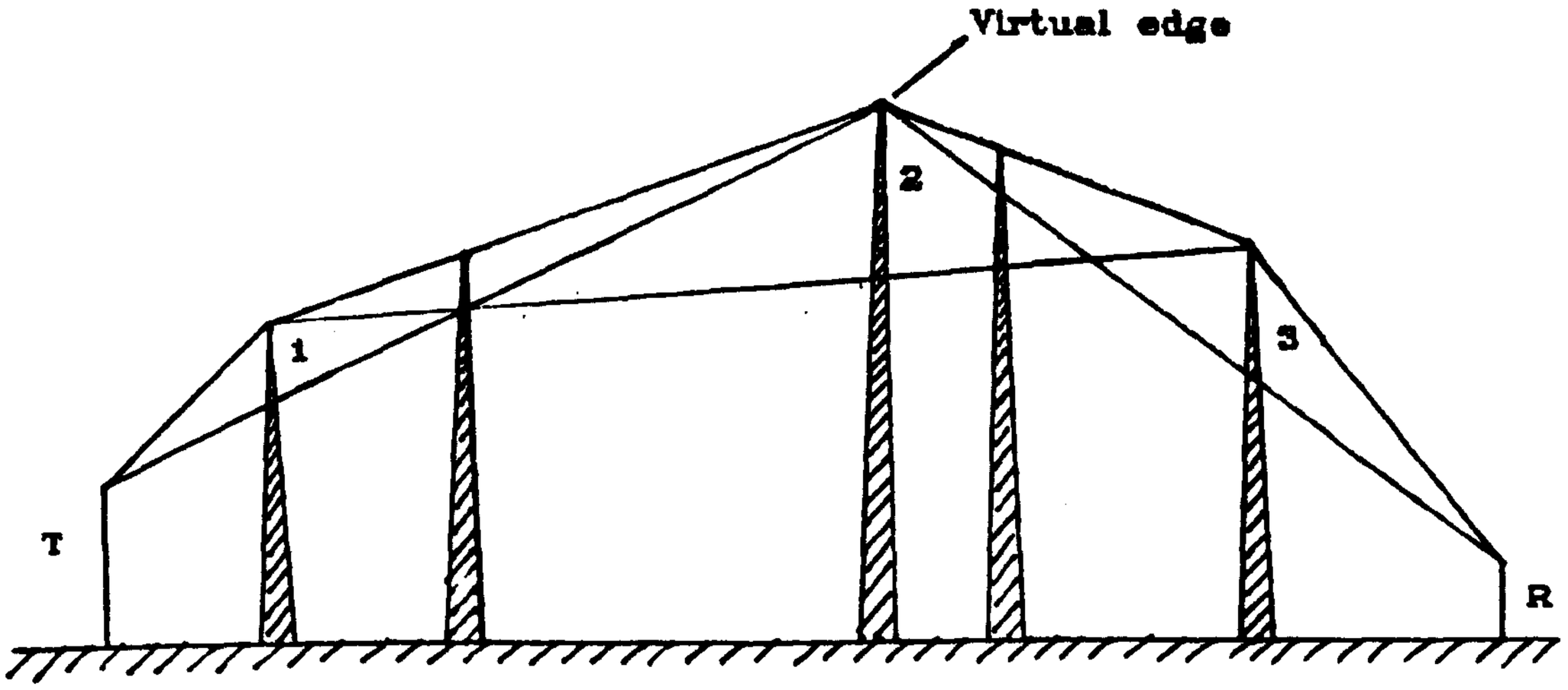

Fig. 3.2 JRC Construction of Virtual Diffraction Edge.

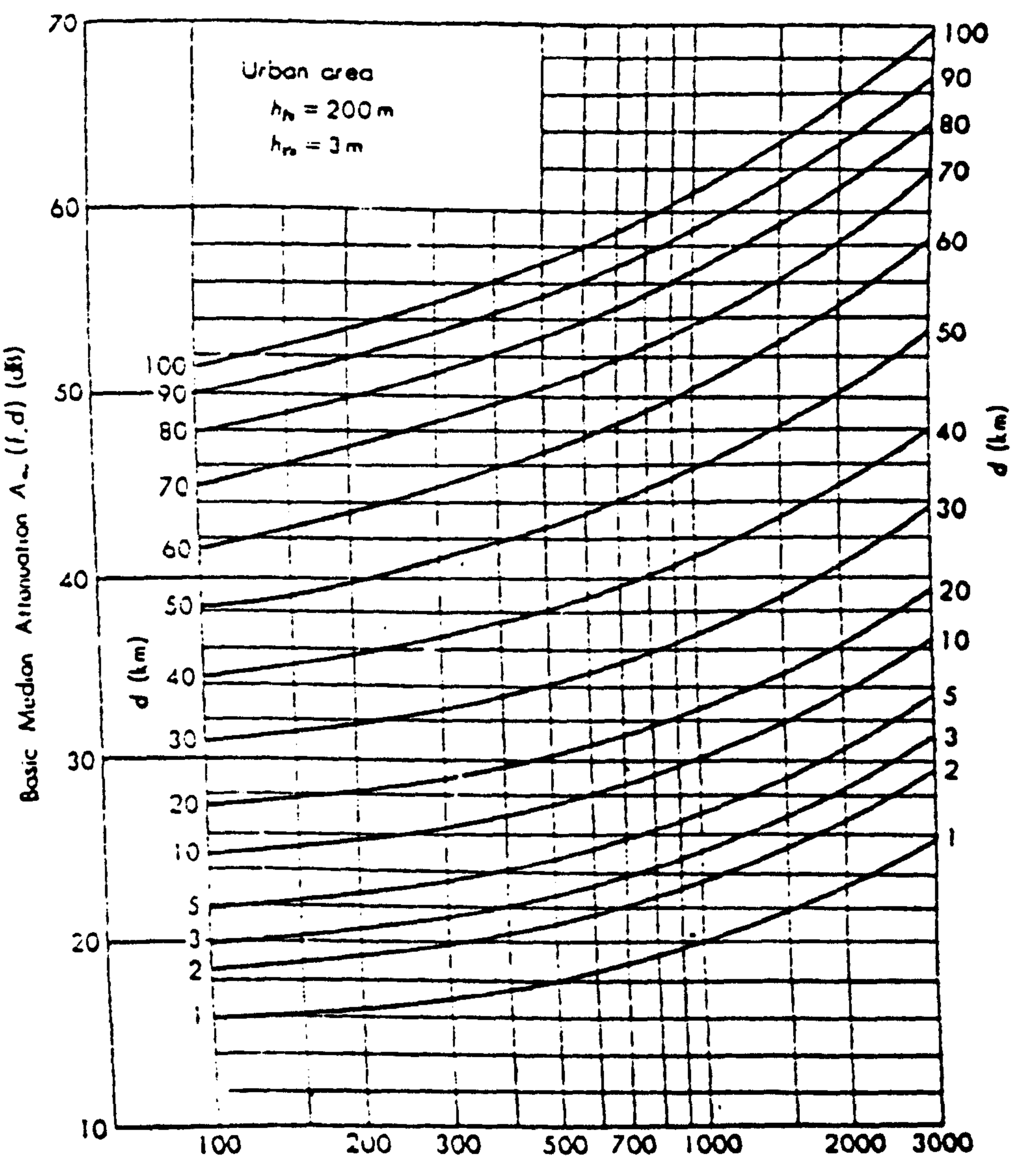

Fig. 3.3 Prediction Curves for Basic Median Attenuation Relative to Free Space in Urban Area over Quasi-smooth Terrain, Referred to h_{te}= 200 m, h_{re} = 3 m.

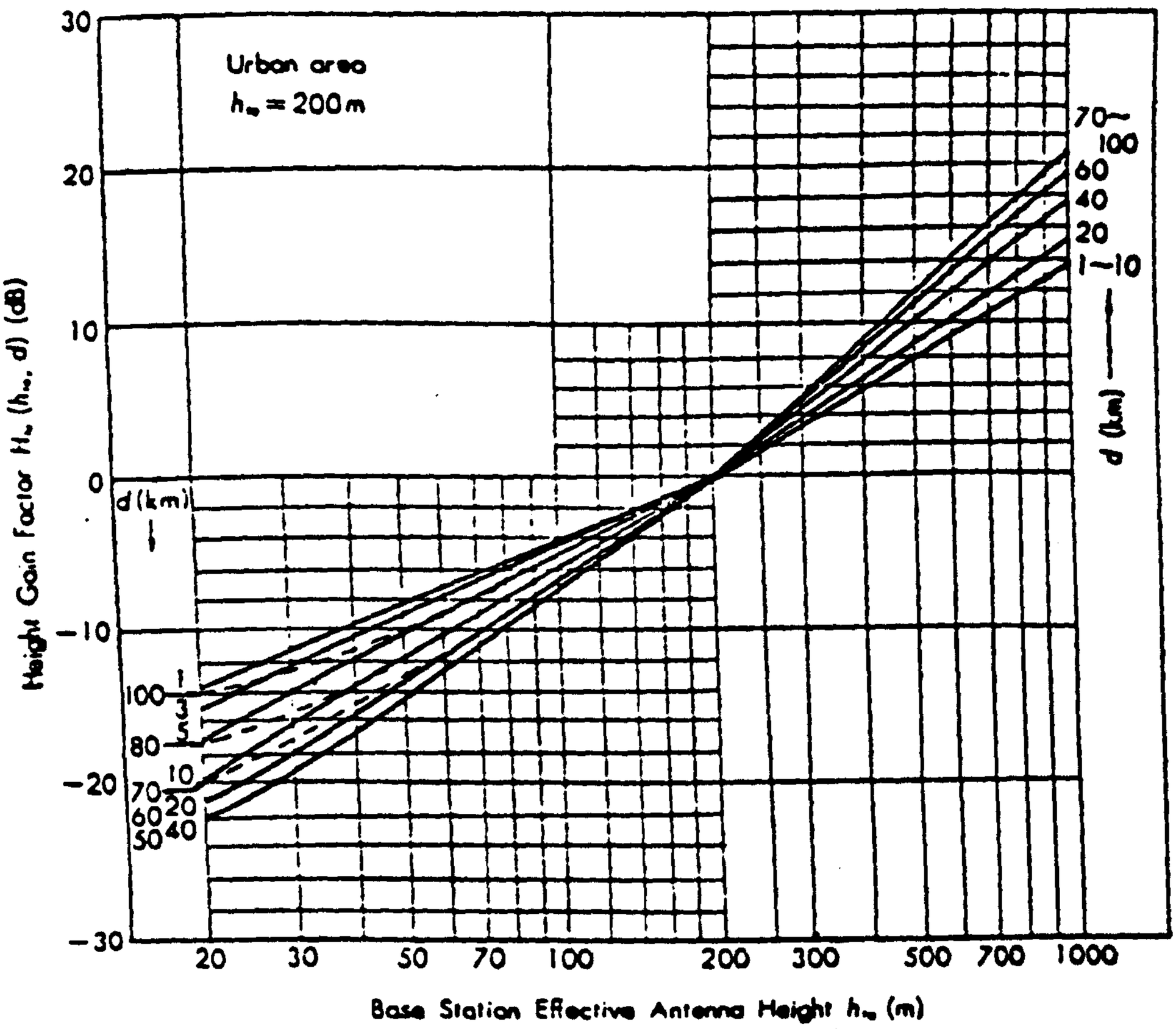

Fig. 3.4 Prediction Curves for Base Station Antenna Height Gain Factor Referred to h_{te} = 200 m, as a Function of Distance.

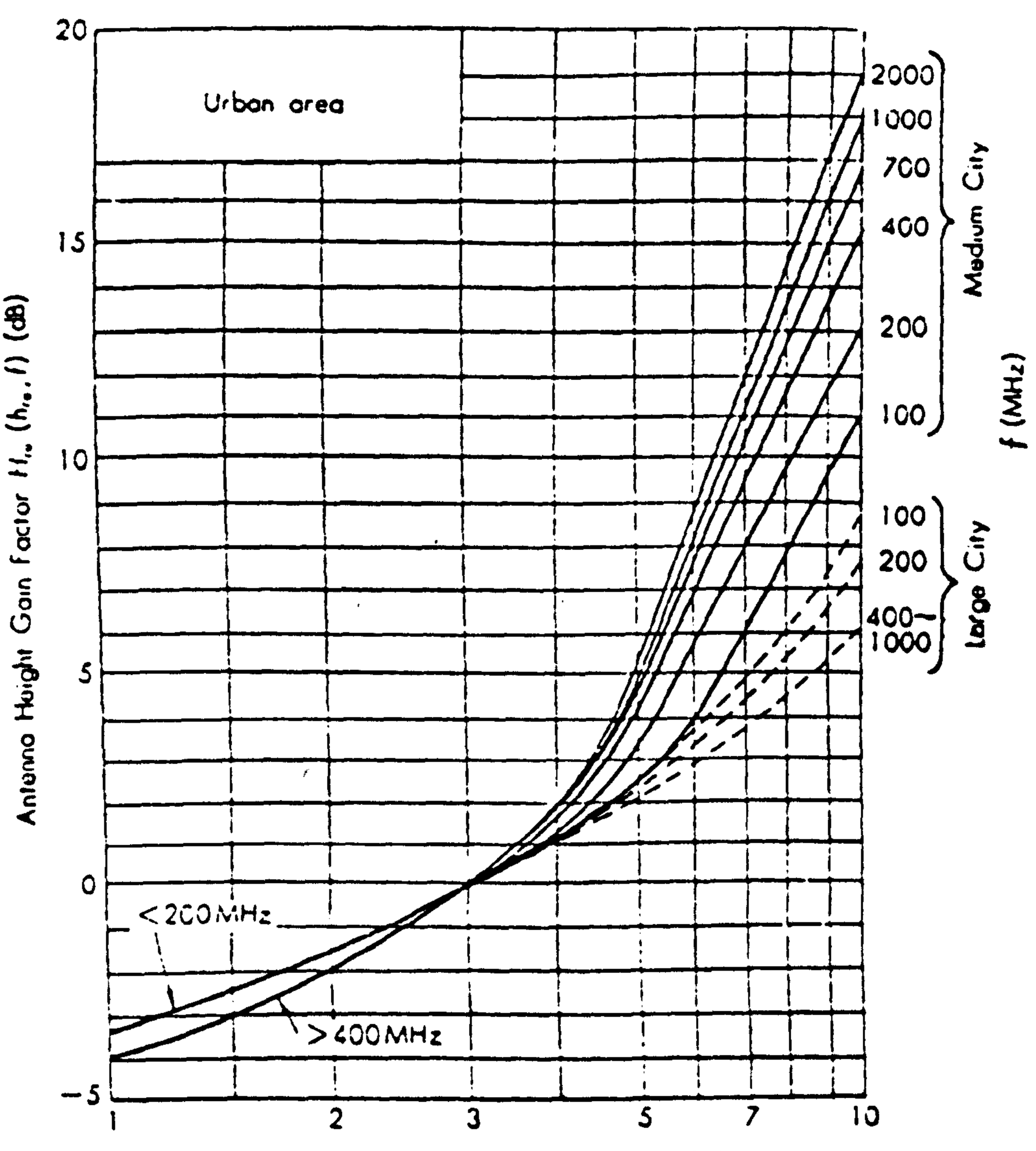

Fig. 3.5 Prediction Curves for Vehicular Antenna Height Gain Factor in Urban Area.

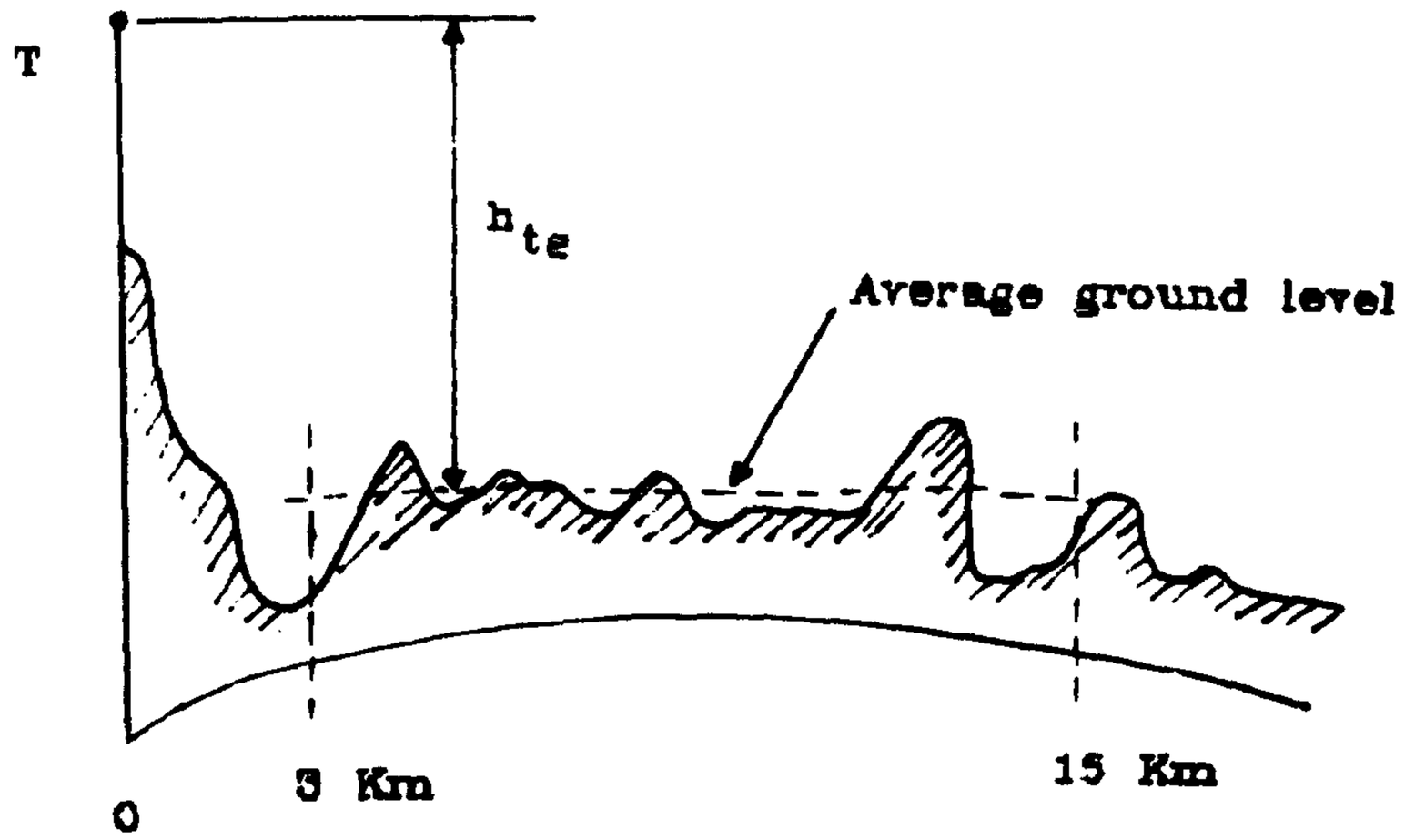

Fig. 3.6 Definition of Effective Transmitting Antenna Height (h_{te}).

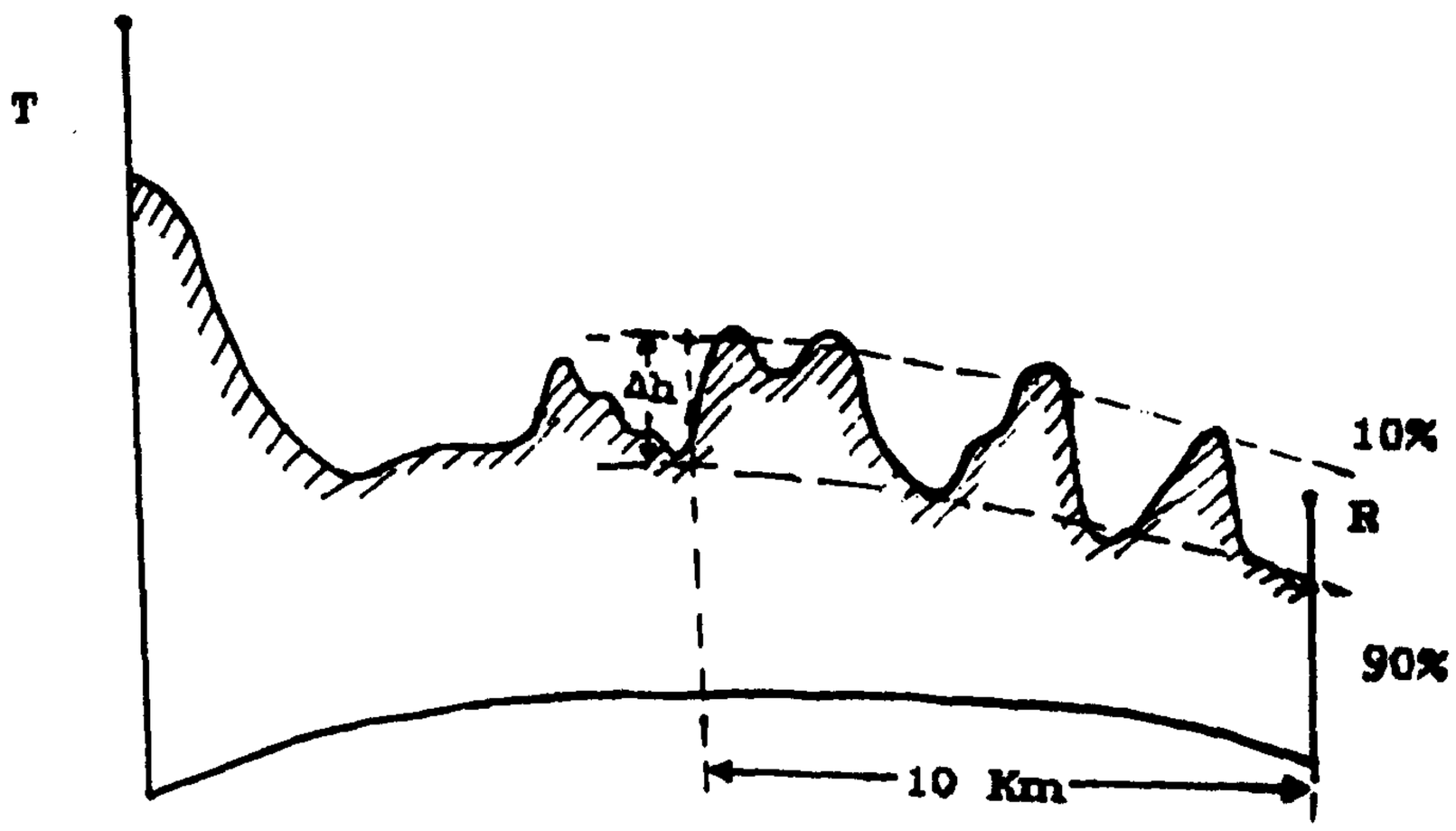

Fig. 3.7 Definition of the Parameter (Δh, "terrain undulation height") for Rolling Hilly Terrain.

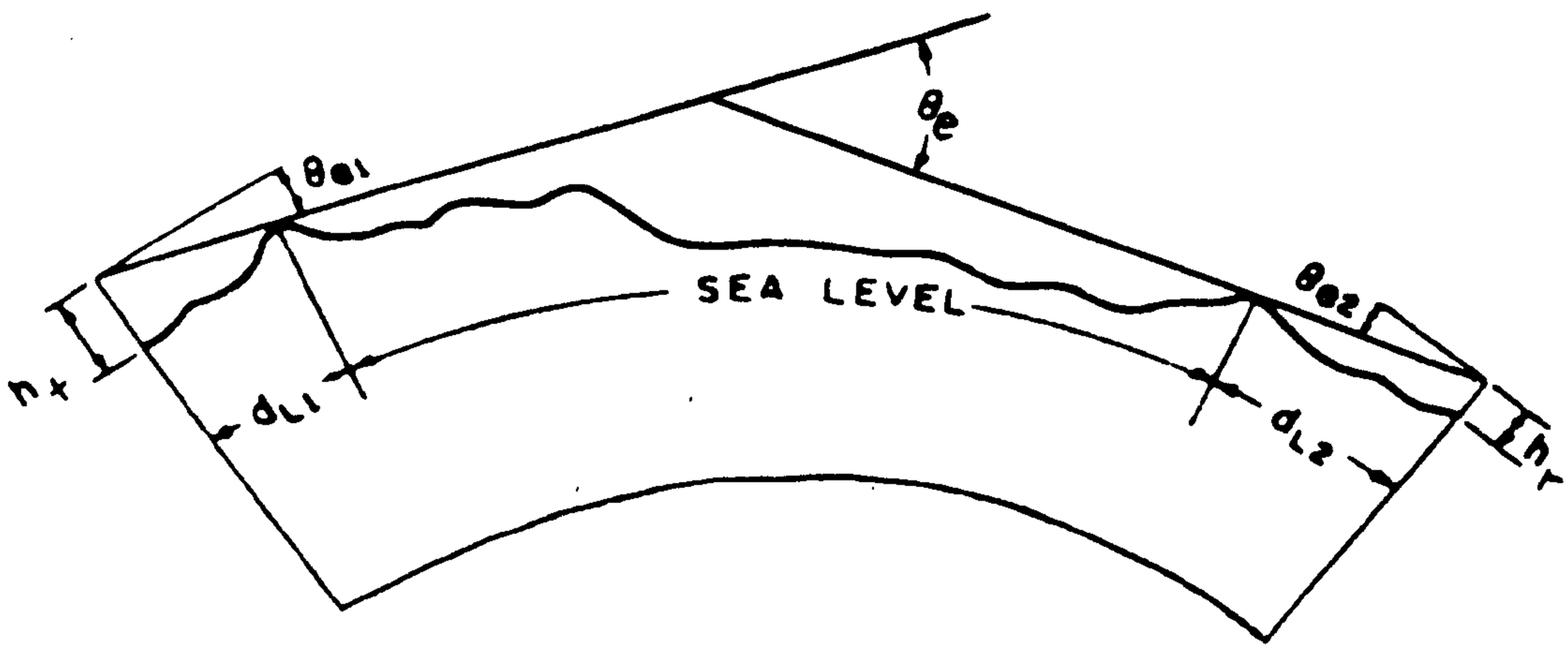

Fig. 3.8 Geometry of a Transhorizon Radio Path.

CHAPTER 4

FIELD TRIALS AND MEASURING EQUIPMENT

4.1 FIELD TRIALS

Generally, the problem of path loss prediction within a service area requires an empirical approach, although theoretical predictions may be made for the propagation losses of certain idealised path profiles. In order to establish a prediction method based on path profiles, the first step is to obtain a data set of measured losses and associated path profiles. To determine the statistical parameters of the spatially distributed field, the received signal envelope should be measured over a large distance of travel, typically many tens of wavelengths.

The parameters used in the propagation measurements should ideally correspond to the situations for which predictions are required and the data base used for the present study is the outcome of an extensive series of field trials which had been conducted in rural areas of Cheshire at 139.01 MHz.

4.1.1 The Transmitting Station

Three transmitter sites were used in the measurement programme, each being located in a different type of environment. The Newton Firs transmitter site is situated in a completely rural area with clear foreground, the Altrincham and Wavertree transmitter sites were surrounded by a number of buildings which could have a major influence on the transmitted signal. Table 4.1 lists the details of the transmitting sites.

Table 4.1

Base Station	Effective radiated power (w)	Antenna height (m)	Height of local ground (m)	Type of surrounding area	O.S. grid reference
Newton Firs	18	44	150	rural	SJ 527749
Altrincham	24	56	31	suburban	SJ 776876
Wavertree	11	63	50	urban	SJ 376898

4.1.2 The Receiving Station

The receiver was housed in a mobile vehicle which measured the signal strength as the vehicle travelled through a number of preplanned routes. A quarter-wave whip antenna was used, being mounted in the centre of the vehicle roof and 2 m above the ground.

The measured antenna azimuth pattern with the antenna mounted on the vehicle, is shown in Fig. 4.1, where 0^{o} bearing corresponds to the case where the front of the mobile is facing the base station. Although there are small deviations about the constant line, the azimuth pattern can be considered as omnidirectional. The antenna was calibrated against a reference Yagi antenna placed at the same height, in the absence of the vehicle[1]. The relative gain in dB in Fig. 4.1 is below that of a Yagi antenna which has a gain of 4.5 dB with respect to $\lambda/2$ dipole antenna. This results in the gain of the whip antenna being approximately -2 dB with respect to $\lambda/2$ dipole antenna.

1 The calibration was undertaken at the BBC Research Department, Kingswood Warren, with the vehicle placed on a turntable.

4.1.3 Terrain Characteristics and Measurement Routes

The measurements were carried out in rural areas of Cheshire over generally irregular terrain situations, although for some parts, the ground was substantially flat. A computerised data map which covers an area of size 50 Km x 70 Km was provided by the JRC. Over the whole area the terrain varies in height from zero metre at sea level to heights of 450 m in very hilly parts. A view of the terrain is shown in Fig. 4.2, which was generated by a computer using the height information from the terrain data map.

The terrain data for the U.K. has been extracted from Ordnance Survey maps (1:25000) and is held in blocks of 400 units comprising squares of 10 Km side. Each unit corresponds to a square of ½ Km side and its representative height is either the height of a definable feature such as a peak or valley, or otherwise the mean height in the square.

A 1:25000 map was used to plan the routes to be covered. The method of data collection was to select routes within a 500 x 500 metre square to provide reasonable coverage of that square. Figs. 4.3 to 4.5 show the location of the transmitting base station and the test squares for the three tests, with reference to the Ordnance Survey grid system. In the Newton Firs test, 198 squares of 500 x 500 m were covered. In the Altrincham test 196 squares, and in the Wavertree test 165 squares were covered. The signal strength was sampled every 1.8 cm of linear travel by the mobile unit and Figs. 4.6 to 4.8 show the value of median signal strength which was measured in each of the test squares. The test squares lie in the range 8 Km to 43 Km from the base station.

4.1.4 Ground Profile Reconstruction

For a specified transmitter site and each chosen receiver, it is necessary to reconstruct the intervening ground profile from the stored geographical data so that the path loss can be predicted.

A computer routine was implemented on the University's IBM mainframe 3083 computer system which accesses the information from the data base to reconstruct a close approximation to the radio path profile by using a linear interpolation technique. The terrain data map used for the construction of terrain profiles provides the terrain heights above sea level for an area, in matrix form, with elements 500 m apart. The areas covered with water were identified by examining the Ordnance Survey map of the whole area on a 500 x 500 m square basis and the locational codes of the relevant squares were inserted into a data file.

By identifying the locations of the transmitter and the receiver initially, the program determines the squares which surround the radial line joining the terminals, (Fig. 4.9). By joining the centres of two such squares, the location of the interception point on the profile is derived and then the height of the point is determined. Three methods of row, column and diagonal interpolation are used to derive as many points as possible along the radial path. The generated terrain profile is stored in the form of the n x 2 matrix

$$\begin{bmatrix} d_1 & h_1 \\ d_2 & h_2 \\ \cdot & \cdot \\ \cdot & \cdot \\ \cdot & \cdot \\ d_n & h_n \end{bmatrix}$$

where the first column includes the distances measured from the

transmitter ($d_1 = 0$, $d_n = d$), and the second column provides the corresponding heights above sea level. A generated path profile is shown in Fig. 4.10, where the vertical lines along the path are the interpolated height values and the plot also shows the position of the path in the test area.

In order to evaluate the accuracy of the terrain profile generation routine, a number of paths were chosen and information about the terrain profile was extracted directly from the Ordnance Survey maps. A comparison shows that the computer routine was found to be reasonably accurate in retaining the essential features along the path. Fig. 4.11 shows the terrain profile of one typical transmission path. The effect of earth curvature can be introduced to the path profile by choosing an appropriate value for K, which in our study was assumed to be equal to 4/3. A copy of the computer program is included in Appendix A.

The computer generation of path profiles provides a better way for close examination of terrain features in the transmission path and can eliminate expensive field surveys or path testing, dependent upon the precision of the topographical data base. It can be used for diffraction loss calculation and reflection analysis in the transmission path and antenna height selection, given a set of communication system parameters. By calculating the expected path attenuation for an appropriate number of radials from a certain base station, a field strength contour can be deduced for area coverage purposes.

4.2 DATA LOGGING SYSTEM

Field trials were carried out using a vehicle (a Rover 2600) which was equipped with a digital data logging system to collect and store a large amount of data [4.1].

The system samples the received analog data, digitizes, formats and stores it onto computer compatible magnetic tapes which can be used directly on any computer installation for the analysis of data. A block diagram of the system is shown in Fig 4.12. It consists of a Singer NM37/57 receiver, a 380Z microcomputer and a SE 8800 buffered tape unit.

The receiver NM37/57 measures the field strength within the frequency range 30 MHz to 1 GHz with a dynamic range of approximately 70 dB. The characteristic of the receiver is shown in Fig. 4.13, where the output from the log-video terminal of the receiver is drawn versus the input signal strength. An interfacing circuit converts the output of the receiver into a level in the range 0-2.55 V to be suitable as input to an ADC.

The 380Z microcomputer uses an ADC to digitize the receiver output with sampling initiated by the pulses from a distance transducer. The interrupt pulses are generated every 1.8 cm and the digitized output is written into a FIFO buffer within the 380Z. The microcomputer system includes two disc drives, a keyboard and a visual display unit for various system controls and analysis of data.

The tape unit consists of a buffered interface board which can store the data before it is formatted and recorded on a 9-track magnetic tape. This board also controls the writing and recording of data, tape motion and status signals and interprets the various commands between the computer and formatter.

4.2.1 System Aspects and the Measurement Procedure

In order to meet the system requirements and conduct a reliable operation, it is necessary to take into account limitations imposed by different system components. The average data transfer rate is mainly determined by considering the time taken by different operations in the tape unit to record the data. However, allowance must be made for error routines, i.e. backspace-erase-rewrite sequences.

A number of software programs had been written [4.1] on the 380Z, for the control of data transfers and manipulation and statistical analysis of the data. The system's ability to do some on-line analysis allows useful tests to be carried out on the collected data away from a mainframe computer.

The system is powered by a vehicle-mounted sine wave invertor which is fed from two 12 V heavy duty batteries connected in series. The batteries are charged by an alternator driven by an extra pulley available on the engine.

To start the data collection, the receiver is tuned onto the unmodulated transmitted carrier signal and the 380Z is loaded with the appropriate disc. The disc contains the program which accepts the interrupt pulses from the speed transducer to sample the signal, digitize it and write it in the FIFO buffer. It also sends the data from the FIFO buffer to the tape unit buffer. After loading the program and preparing the tape, the data collection is initiated by entering K on the keyboard and moving the vehicle. As the mobile is travelling, data are written on tape in blocks of 2 K bytes, and required file marks can be put on tape by pressing an appropriate key on the keyboard. The recorded data can be read back onto a disc for performing the required data analysis.

References

4.1 Atefi, A. "An Investigation of Radio Wave Propagation in Mobile Radio Frequency Bands", Ph.D. Thesis, University of Liverpool, 1985.

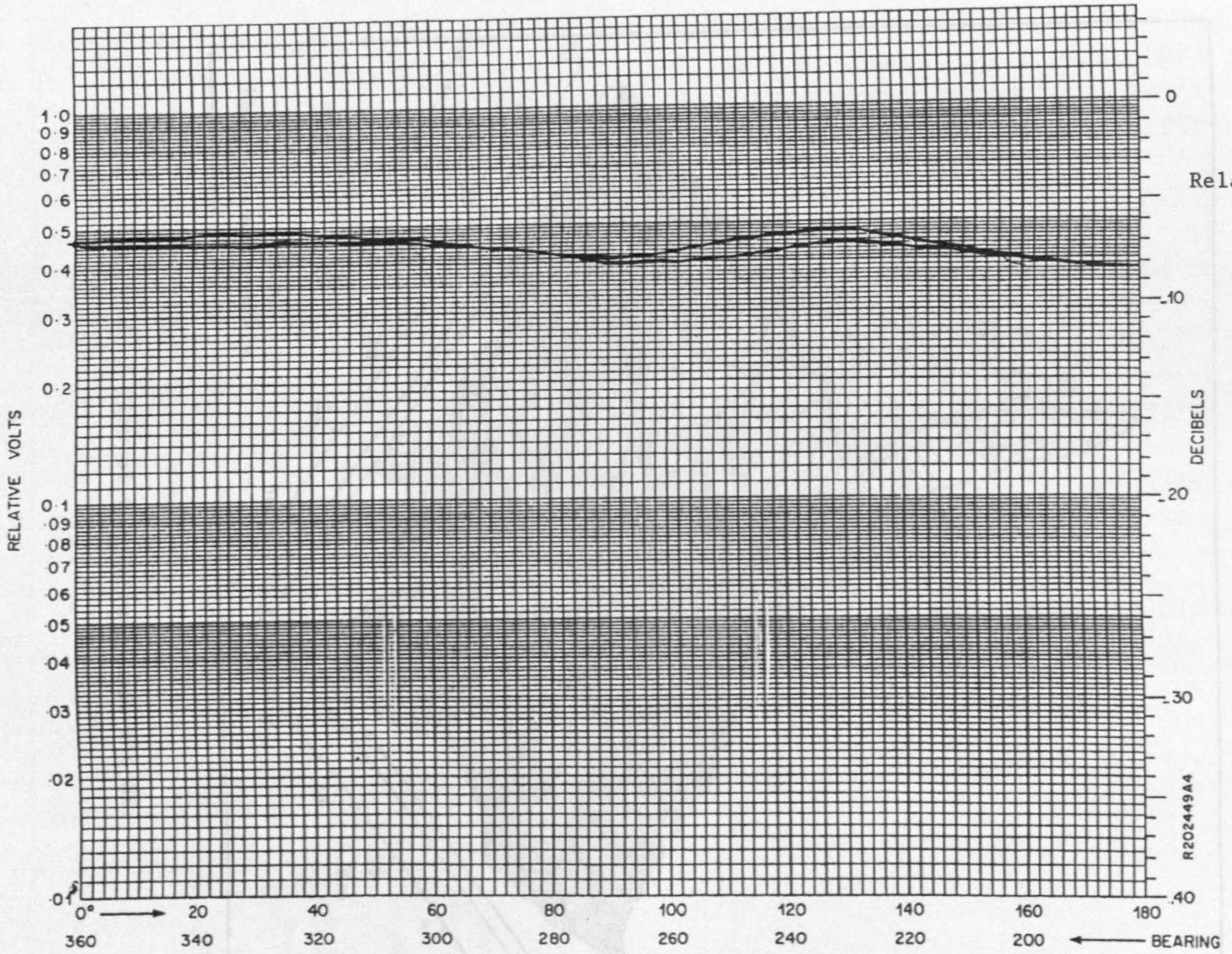

Fig. 4.1 Mobile Antenna Azimuth Pattern.

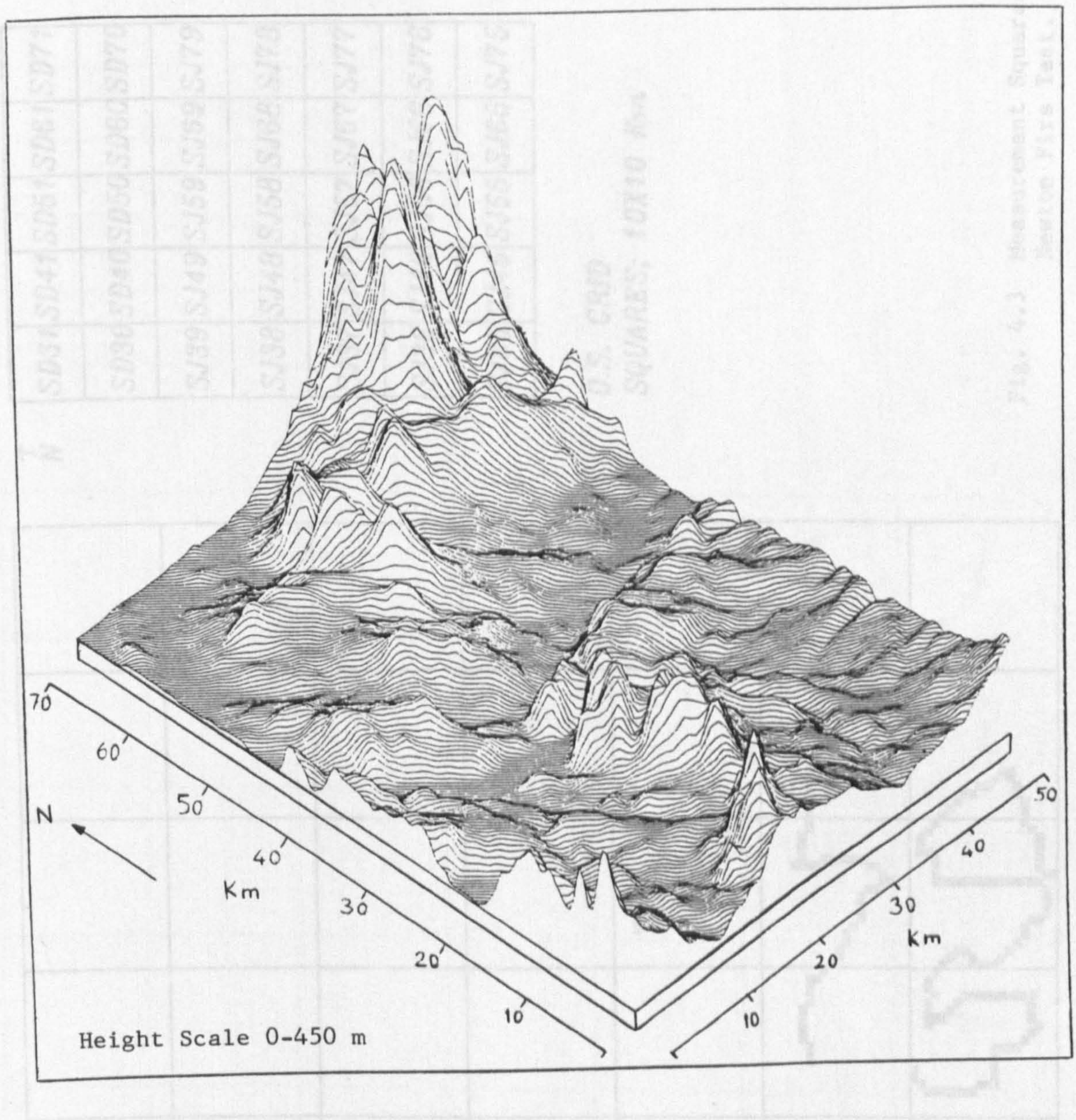

Fig. 4.2 A View of the Terrain from the SW.

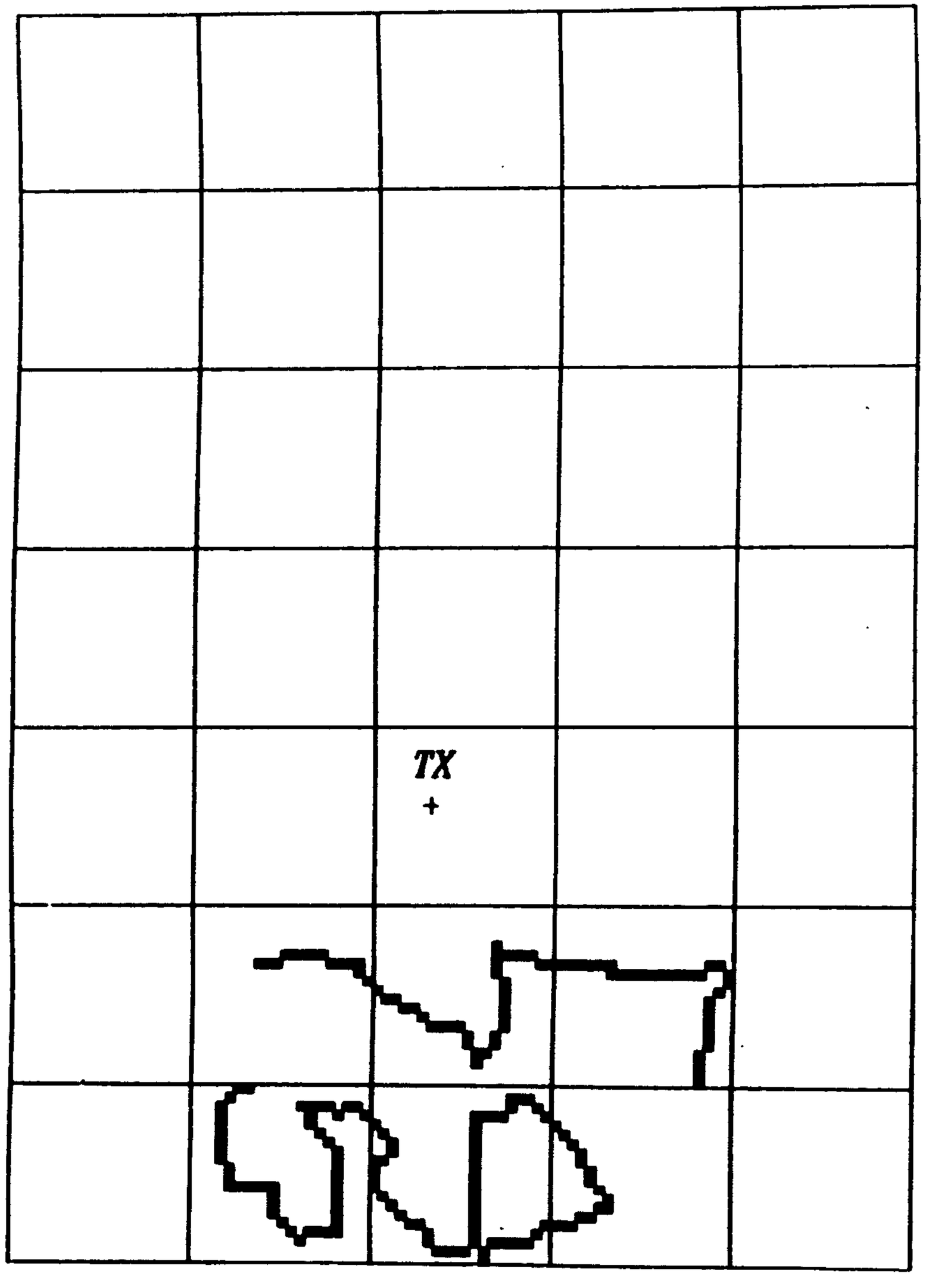

N

SD31	SD41	SD51	SD61	SD71
SD30	SD40	SD50	SD60	SD70
SJ39	SJ49	SJ59	SJ69	SJ79
SJ38	SJ48	SJ58	SJ68	SJ78
SJ37	SJ47	SJ57	SJ67	SJ77
SJ36	SJ46	SJ56	SJ66	SJ76
SJ35	SJ45	SJ55	SJ65	SJ75

O.S. GRID
SQUARES; 10X10 Km

Fig. 4.3 Measurement Squares in the Newton Firs Test.

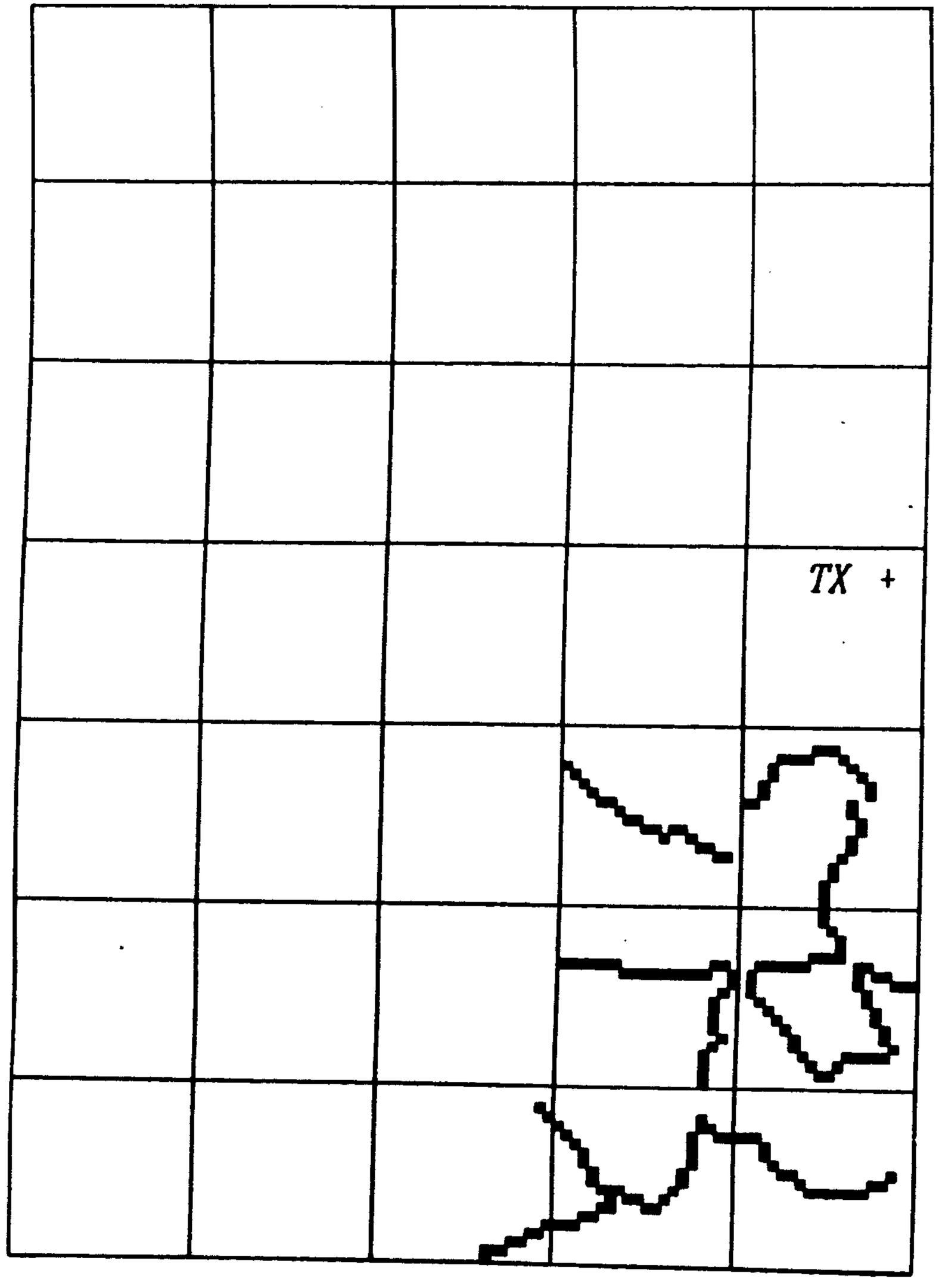

N

SD31	SD41	SD51	SD61	SD71
SD30	SD40	SD50	SD60	SD70
SJ39	SJ49	SJ59	SJ69	SJ79
SJ38	SJ48	SJ58	SJ68	SJ78
SJ37	SJ47	SJ57	SJ67	SJ77
SJ36	SJ46	SJ56	SJ66	SJ76
SJ35	SJ45	SJ55	SJ65	SJ75

O.S. GRID
SQUARES; 10X10 Km

Fig. 4.4 Measurement Squares in the Altrincham Test.

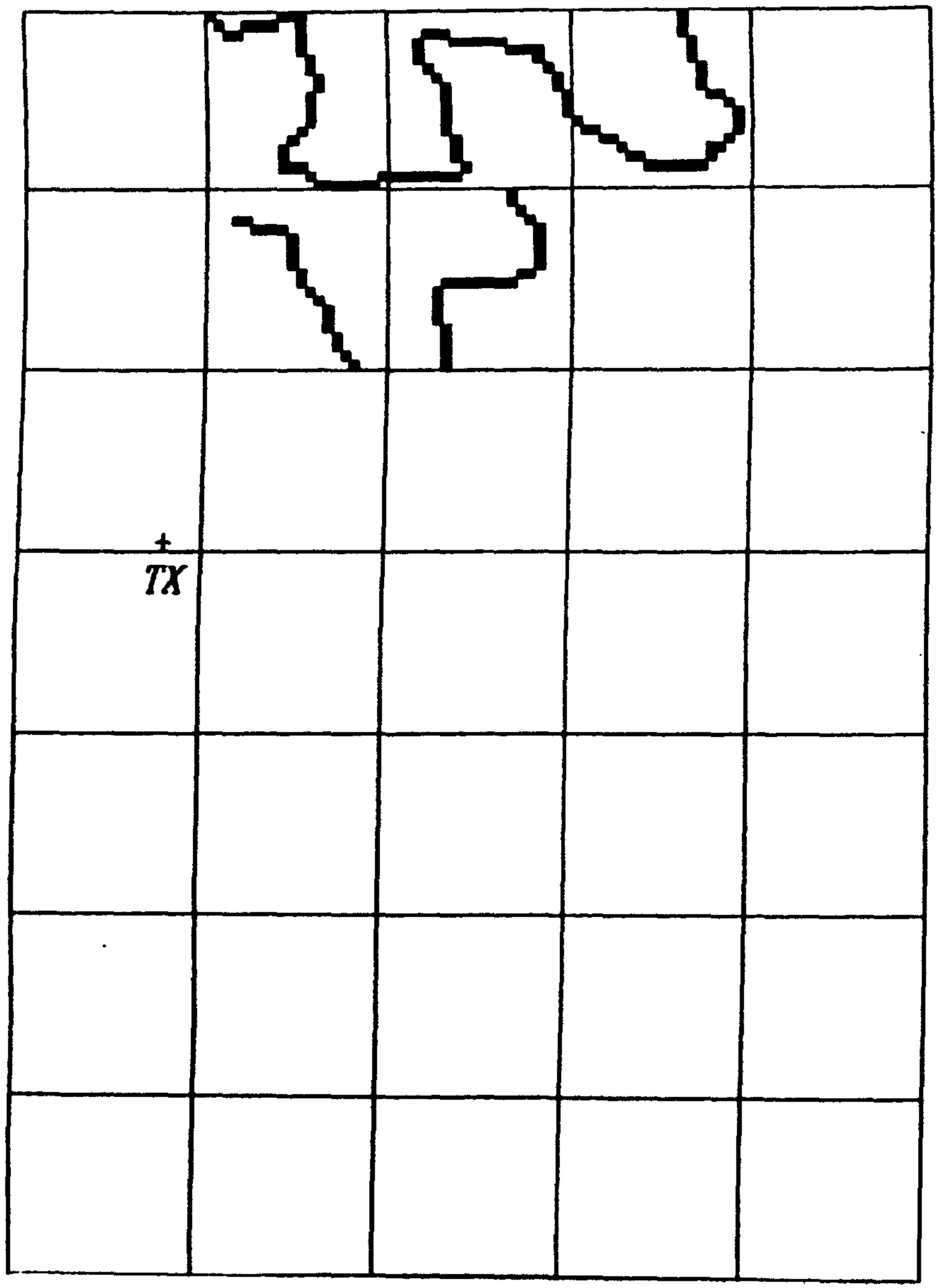

N

SD31	SD41	SD51	SD61	SD71
SD30	SD40	SD50	SD60	SD70
SJ39	SJ49	SJ59	SJ69	SJ79
SJ38	SJ48	SJ58	SJ68	SJ78
SJ37	SJ47	SJ57	SJ67	SJ77
SJ36	SJ46	SJ56	SJ66	SJ76
SJ35	SJ45	SJ55	SJ65	SJ75

O.S. GRID
SQUARES; 10X10 Km

Fig. 4.5 Measurement Squares
in the Wavertree Test.

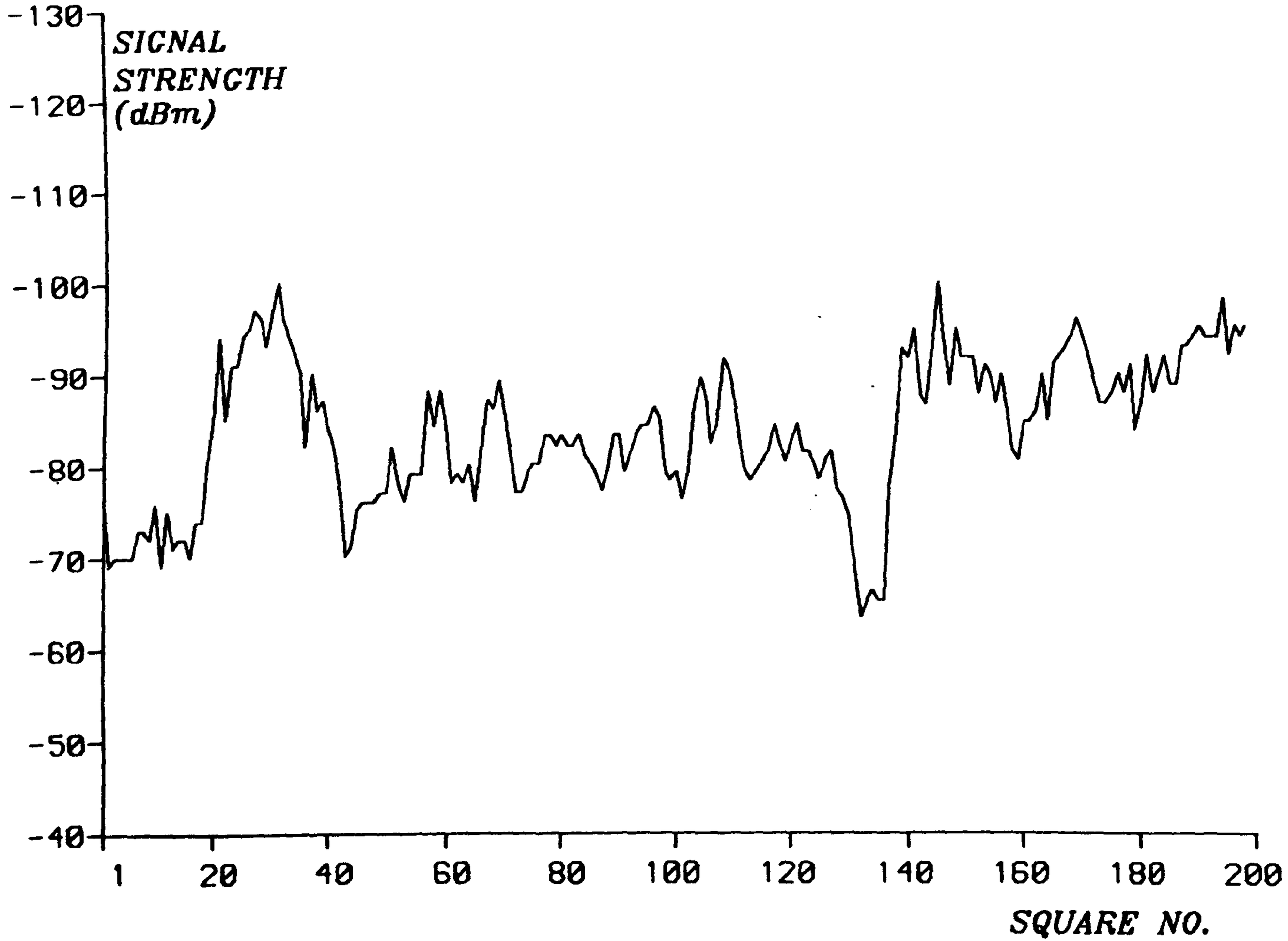

Fig. 4.6 Measured Signal Strength (Newton Firs).

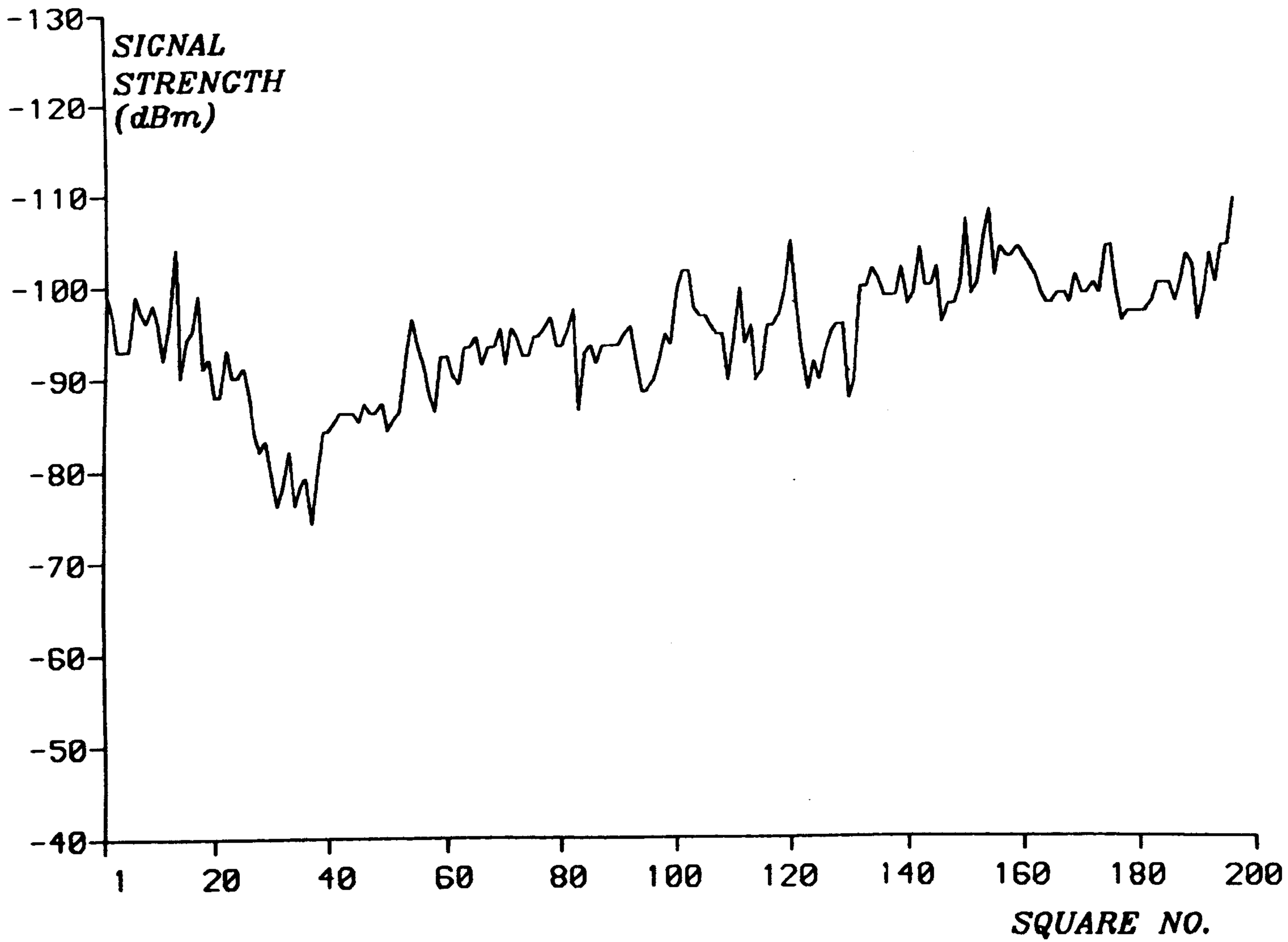

Fig. 4.7 Measured Signal Strength (Altrincham).

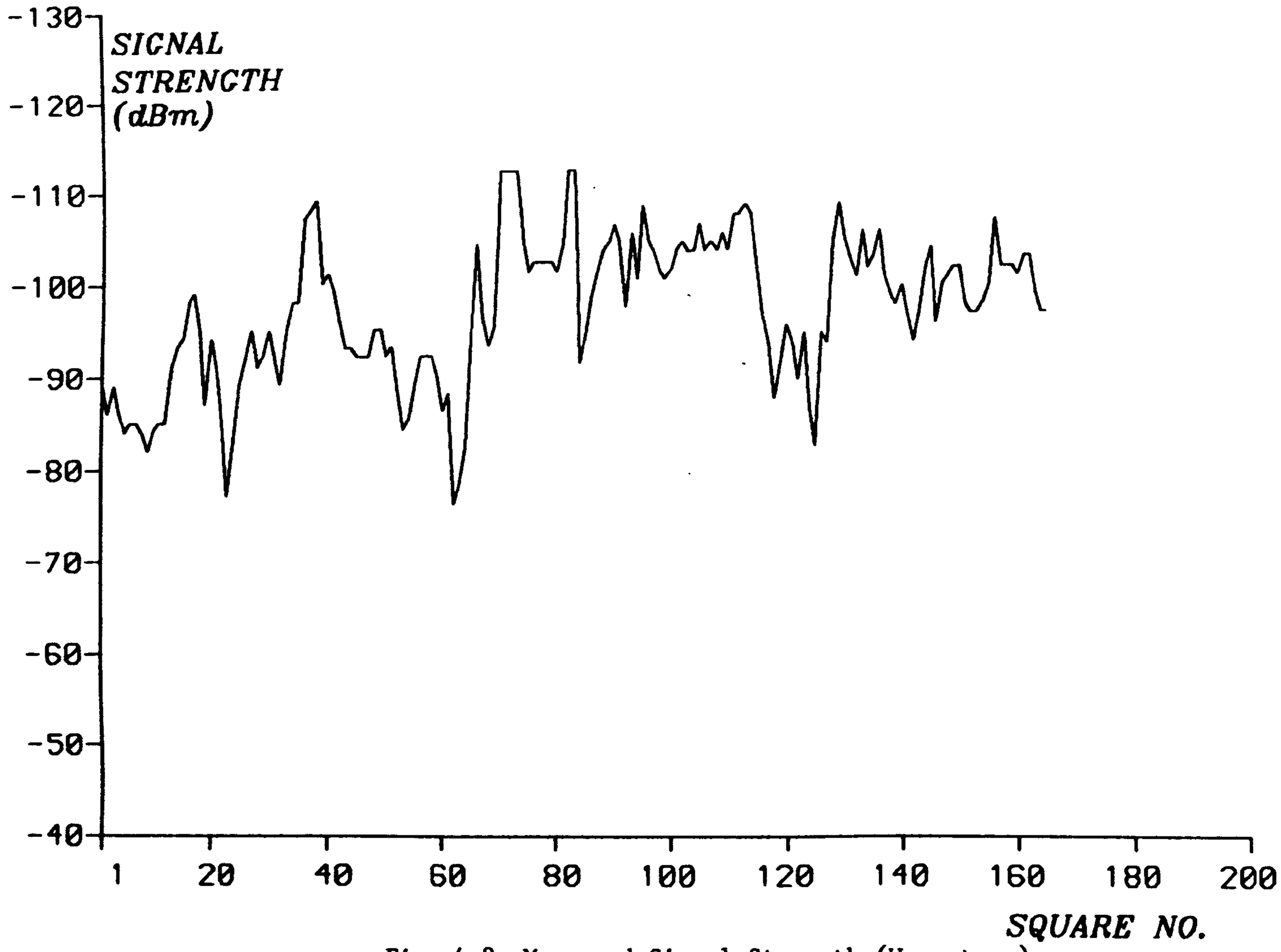

Fig. 4.8 Measured Signal Strength (Wavertree).

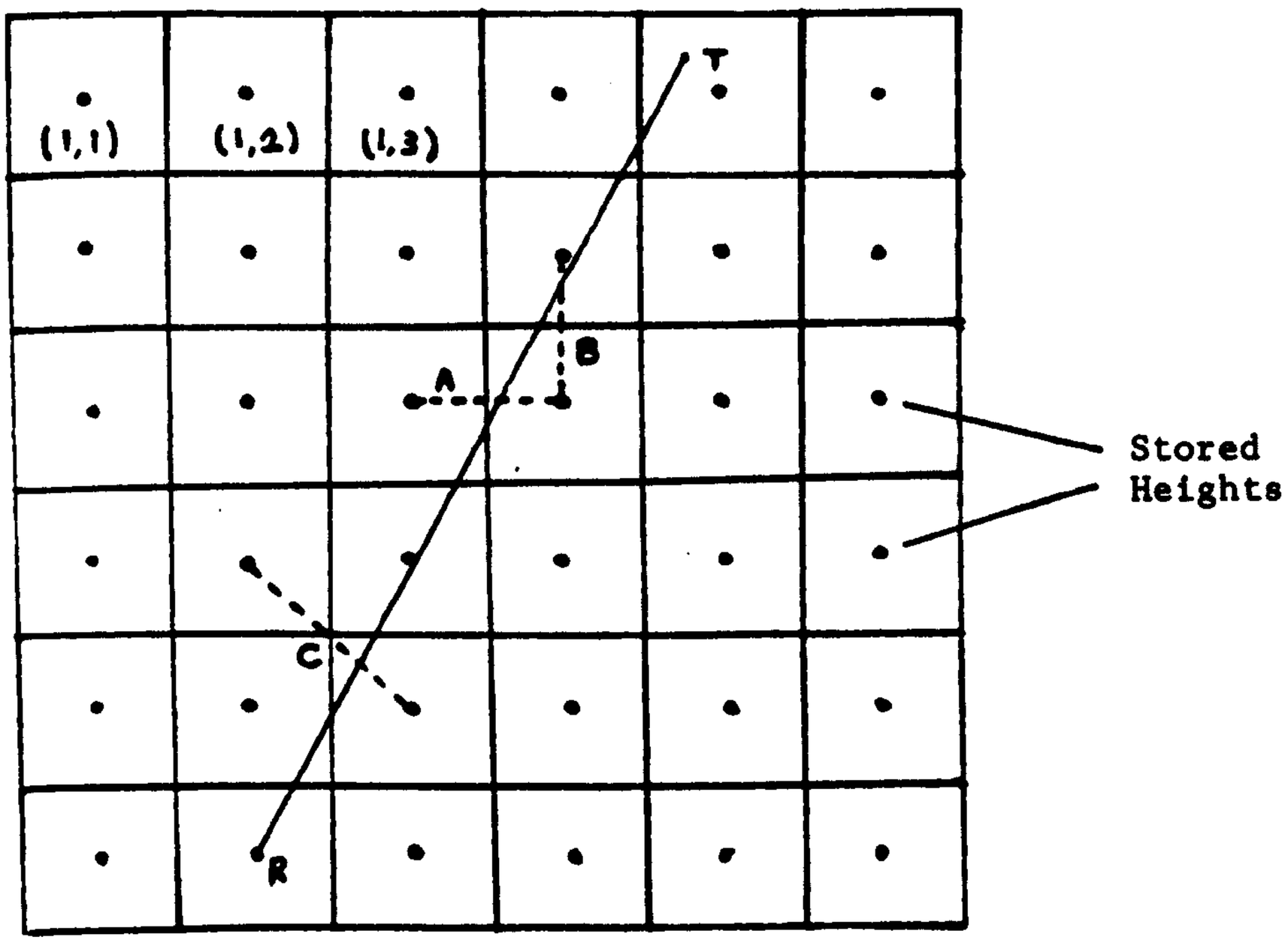

A - Row Interpolation
B - Column Interpolation
C - Diagonal Interpolation

Fig. 4.9 Construction of Ground Profile.

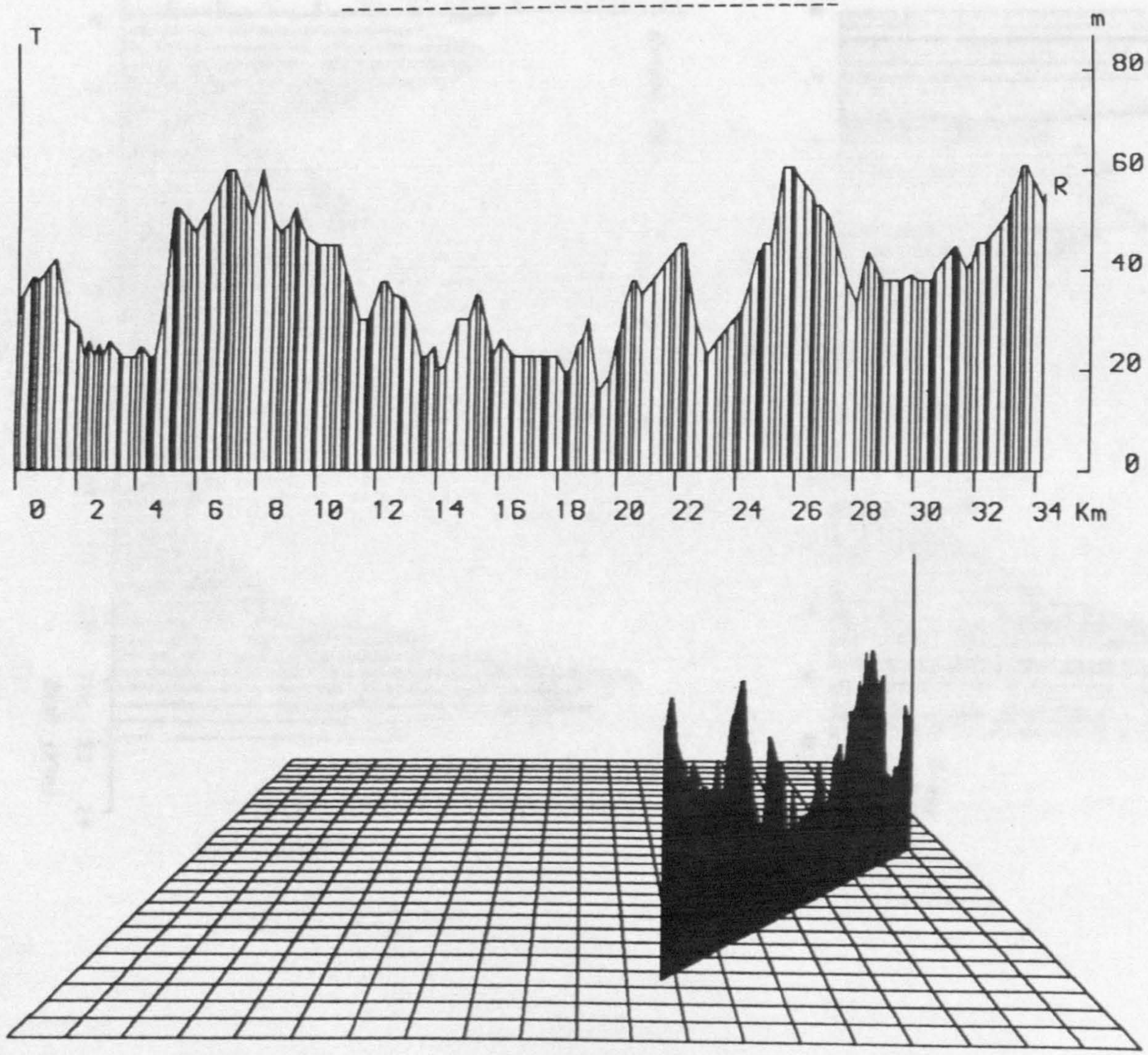

Fig. 4.10 A Typical Path Profile.

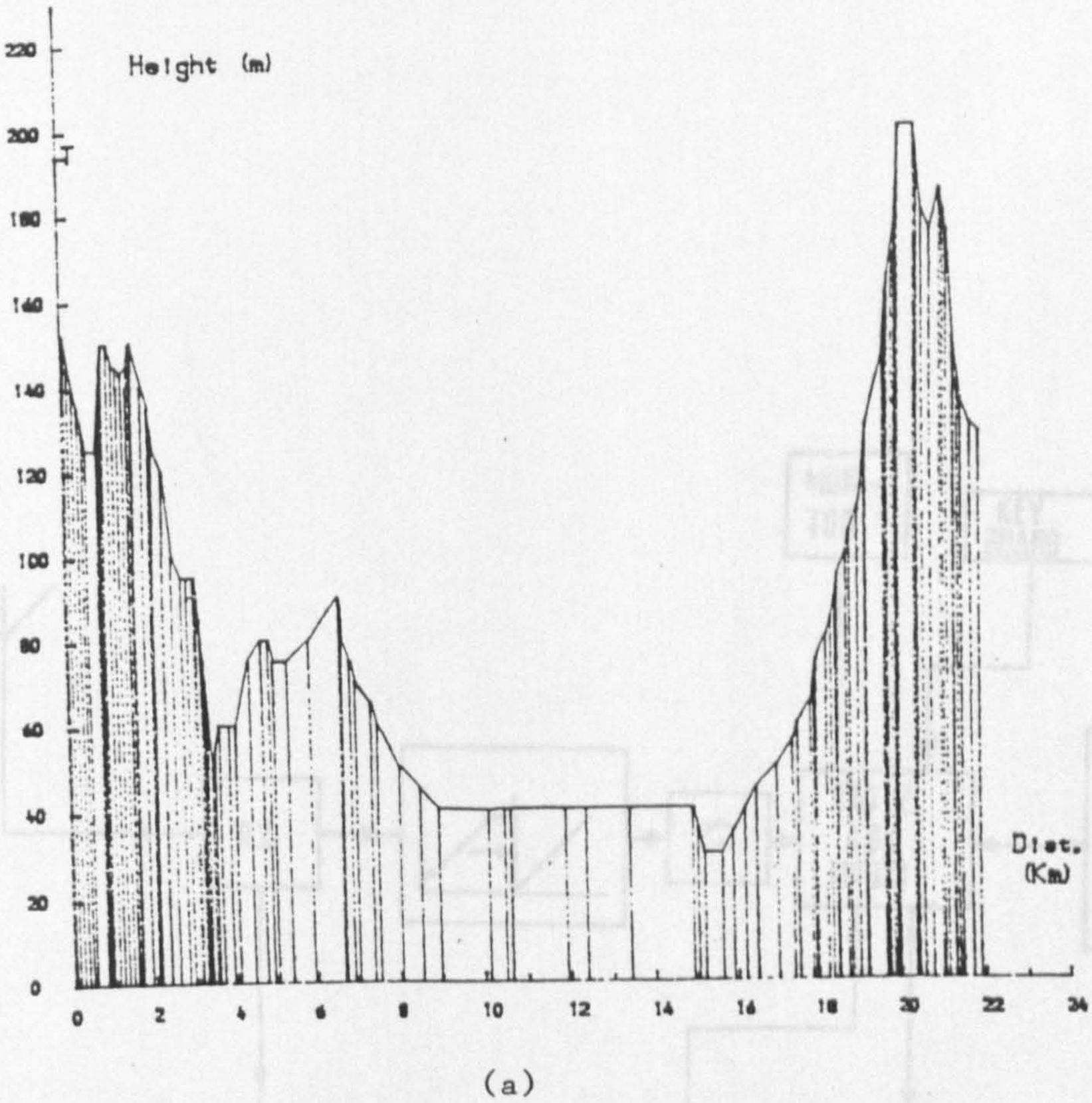

(a)

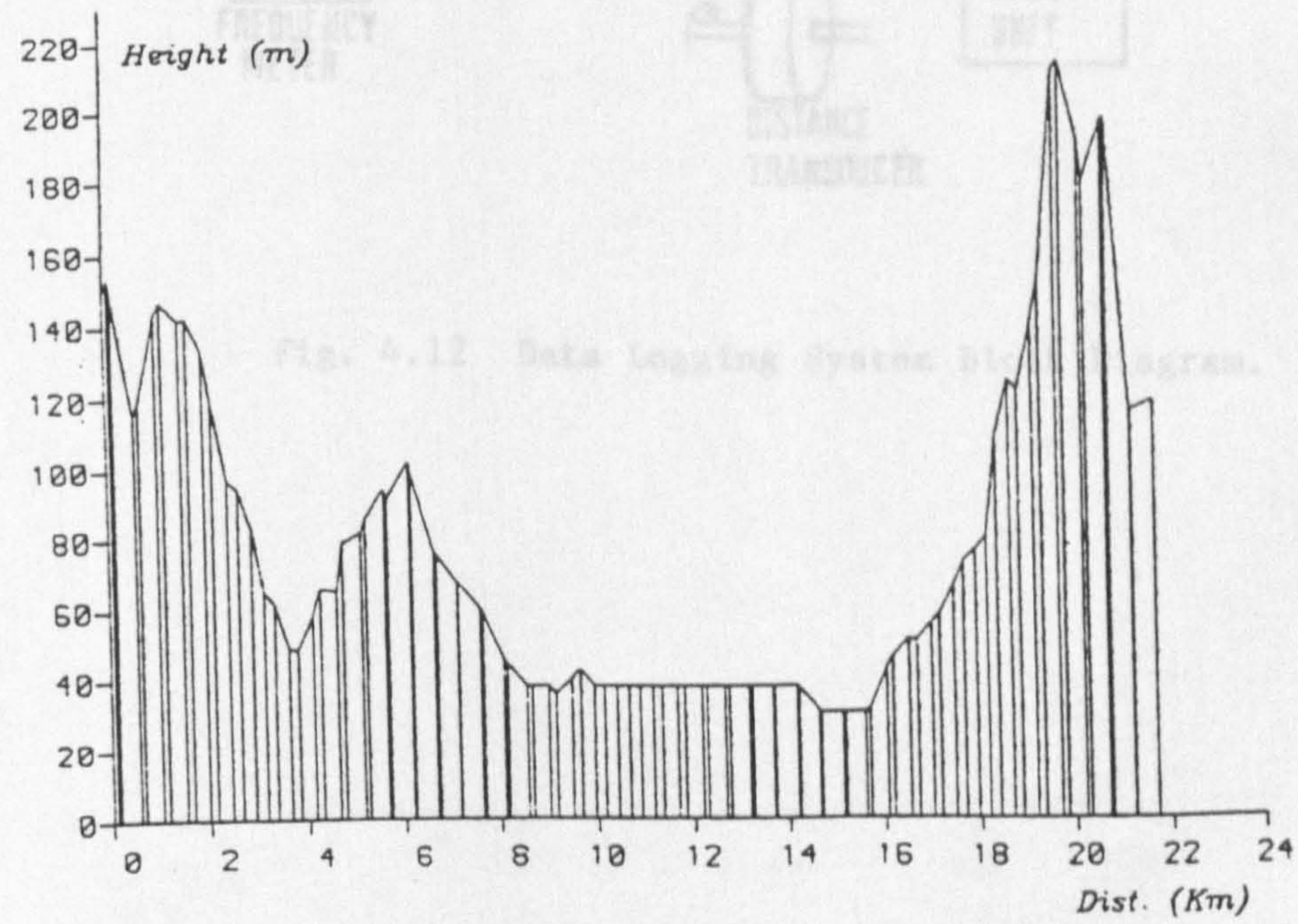

(b)

Fig. 4.11 Terrain Profile

(a) extracted from map,
(b) computer generated.

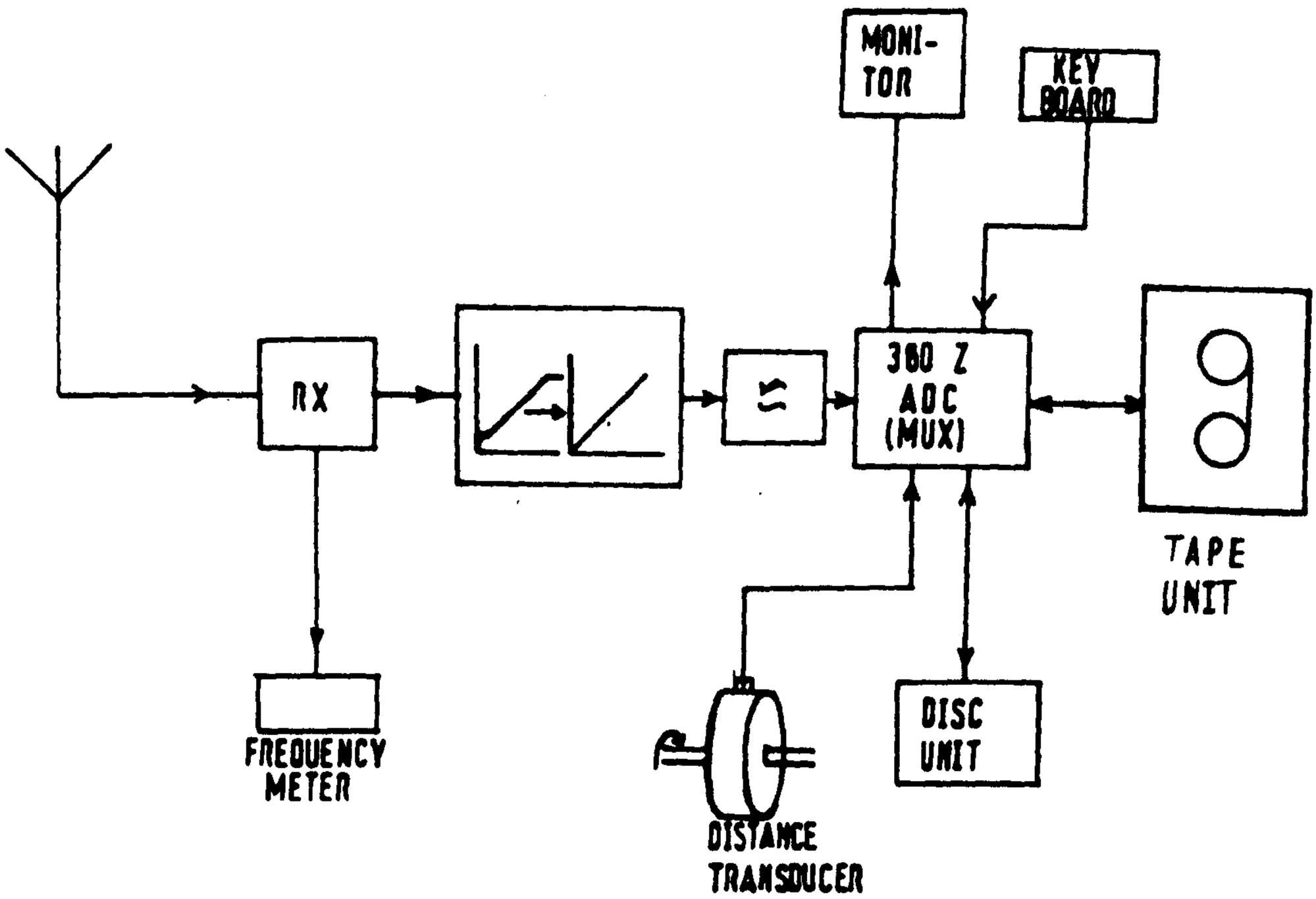

Fig. 4.12 Data Logging System Block Diagram.

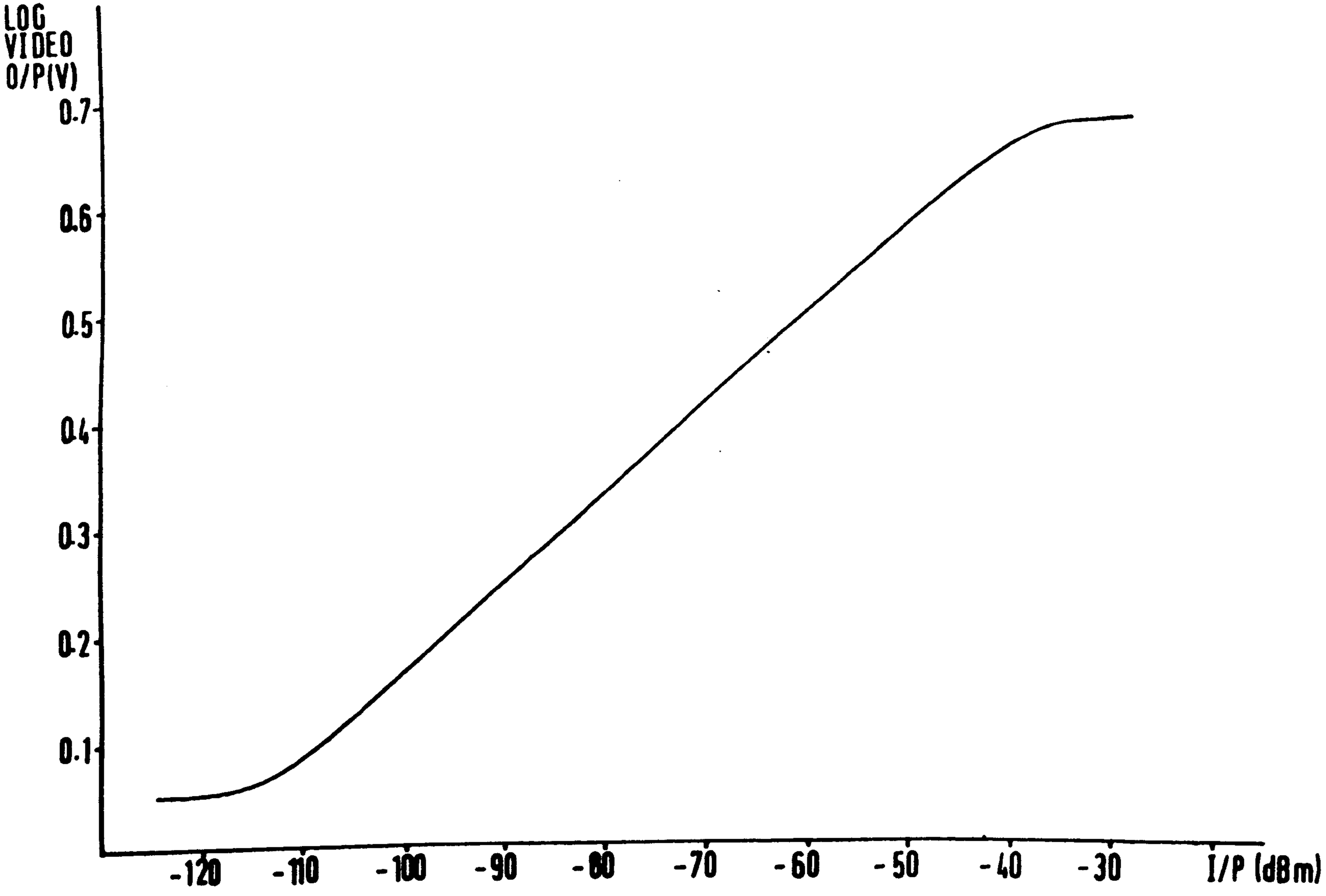

Fig. 4.13 Receiver Characteristic.

CHAPTER 5

A COMPARATIVE STUDY OF THE PREDICTION MODELS

In order to assess the propagation models and verify their applicability under various circumstances, they have been compared with available measured data. The models of interest are those due to Okumura, Hata, JRC and Longley-Rice (Chapter 3). All have been implemented in software, although the values predicted by the JRC model have been provided by the Electricity Council. The advantage of computerised techniques lies in the speed and efficiency with which they can handle a large amount of data and the ease with which the propagation parameters needed for prediction purposes can be calculated.

5.1 IMPLEMENTATION OF THE OKUMURA MODEL

The Okumura prediction model is probably the most commonly used of the available models. It is frequently used as a standard by which to compare other prediction models, since it is intended for the prediction of propagation loss for radio paths over a variety of terrain situations and in different environments at frequencies in the VHF and UHF bands.

In order to computerise the model, an appropriate number of points were read from each prediction curve and by using a suitable interpolation routine, the curves were stored in the computer. In some cases, a correction factor is given versus an input parameter by a number of prediction curves which are intended for certain ranges of another parameter. Therefore two consecutive interpolations were required to derive the appropriate value of the required correction

factor. The prediction curves are contained in sub-programs and a correction factor can be obtained by accessing the appropriate program with the required parameters. To check the accuracy of the interpolations used, the curves were reproduced for a large number of values in the specified parameter ranges, using the computer graphical facilities.

There are basically two modes of operation according to whether the terrain is quasi-smooth or irregular in the propagation medium. For prediction of path loss over quasi-smooth terrain, the required input parameters include frequency, antenna heights above ground and separation distance, also type of area, size of city and the orientation of streets, should be specified. When terrain is irregular, a number of terrain related parameters, in addition to the above parameters, are required as input. A computer routine determines the type of the irregularity, as defined by the model, by examining the terrain profile in the transmission path, and derives the appropriate terrain parameters.

The Okumura model is wholly empirical and therefore the parameters used are limited to specific ranges determined by the measured data on which the model is based. When a certain input parameter is out of range, depending on the smoothness of the corresponding prediction curve and the distance by which the parameter is outside the specified range, an appropriate extrapolation of the curve is carried out. In some cases, the extrapolation produced unrealistic results, and hence other possible approximations were examined for calculation of the required factor. It also became apparent that there were some constraints in the derivation of some of the terrain related parameters and

modifications had to be made to the definition of these parameters, based on reasonable assumptions, making the model more suitable for computerisation.

(a) Base station effective antenna height

This is defined in the same manner as is suggested by the model, except for the following situations where the antenna height above local ground is taken as the effective antenna height:

(1) transmission path distance is less than 3 Km;

(2) the calculated effective antenna height becomes negative due to the height of the base station antenna height being less than the average ground level in the appropriate range;

(3) path profile terrain data is not available, in this case only prediction over quasi-smooth terrain is relevant.

(b) The terrain undulation height

This parameter is required for derivation of the rolling hilly terrain correction factor and is calculated in the 10 Km range, close to the receiver, or in the whole path if the path distance is less than this.

(c) Isolated ridge height

If there is a single obstructing edge in the path, then it is considered as an isolated ridge, otherwise the rolling hilly situation is assumed. This is also the case when the calculated ridge height, according to the model's definition, becomes negative, or the distance from the ridge to the receiver is greater than 10 Km, as this is outside the

specified range and extrapolation would produce erroneous results.

(d) Average angle of general slope

Initially, best fit lines are fitted to terrain heights along the path over the ranges of 5 Km to 10 Km and then the most significant positive and negative slope angles of the lines are taken. If the transmission path is less than 5 Km, the correction factor due to this factor is not considered. When the slope angle is outside the specified range of - 20 mrad to 20 mrad, depending on the sign of the angle, the correction factor at the extreme value of the range is taken.

The computerised version of the Okumura model has been devised to be practical for use with real terrain situations and representative of the original model as much as possible. Fig. 5.1 shows the radial terrain profile to a typical test square, a listing of the terrain parameters and the predicted path loss derived by the computer program for the Okumura method. The computer program also outputs a list of error numbers indicating whether a parameter is out of range as specified by the model.

5.2 IMPLEMENTATION OF THE LONGLEY-RICE MODEL

Although the Longley-Rice model is provided as a set of mathematical relationships, an appropriate computer implementation of the model was needed, due to the compatibility requirement with the comparison study undertaken. The computer implementation allows for the two modes which are supported by the model. These modes are called "area prediction" and the "point-to-point". In the area

prediction mode, terrain parameters are determined by generalised terrain statistics. In the point-to-point mode, the actual terrain profile between the defined radio terminals is considered in the computations. This yields a prediction that is more specific to the propagation environment under investigation.

Using the computer generated path profile matrix, a computer routine derives the required information about the terrain roughness and average terrain heights. The model computes the variability statistics for a given transmission path. These statistics account for the fluctuations in signal level as a function of time and location. In order to produce a prediction of the median signal level, the time variability and prediction confidence are set to 50 percent. Average atmospheric conditions and average ground electrical constants have been assumed in the comparison work.

5.3 COMPARATIVE RESULTS

The main part of the comparison analysis has been to investigate the propagation models by using the measured data obtained from the Cheshire area field trials. However, the availability of some measured data obtained as a result of field measurements conducted in London, also proved useful in assessing the prediction capability of the models in urban areas.

The transmitting and receiving parameters associated with the measurements were taken into account to derive the median path loss between two isotropic antennas.

One criterion which was used as a basis for the comparison was to calculate the value of the standard error of estimate, and is given by

$$\text{Standard error} = \sqrt{\frac{\Sigma(X_{\text{prediction}} - X_{\text{measured}})^2}{N}}$$

where N is the number of samples.

5.3.1 Urban Results

In the London measurement programme, five different locations within and on the outskirts of the city had been chosen for the base stations, transmitting at 940 MHz to the mobile unit with an antenna height of 1.8 m.

The data had been collected as samples of signal strength taken every 1.8 cm of travel along routes within 500 m x 500 m squares. The routes had been selected to provide reasonable coverage of the squares and on average a route length of about 2 Km was covered within each square. The transmission range lies generally between 1 and 7.5 Km. The terrain in the transmission medium is considered to be quasi-smooth with the average height of the ground being approximately 5 m above sea level. Overall about 161 squares had been covered with the five transmitter sites.

For this part, the models of Okumura, Hata and Longley-Rice were compared with measured data. The factor due to orientation of the streets was not considered for the Okumura model, since specific data about this was not available, in some cases the difference between Okumura's "along path" and "across path" corrections may be as large as 12 dB.

The Okumura model and Hata's formulation are expected to compare well within the specified range. The results indicate this fact with a constant small difference in the predicted path loss values by the models. The Longley-Rice model in area prediction mode

is used in conjunction with the suggested urban factor. For flat terrain, the model assumes Δh to be 0. However when the value of 30 m, which is the value suggested for plains, is assumed, the prediction error decreases. Table 5.1 lists some details of the transmitter sites and the standard error of prediction produced by the models.

Table 5.1

Base Station Location	Area	Overall antenna height (m)	Standard Error (dB)				
			Okumura	Hata	Longley-Rice Δh/m 30	20	0
Bunhill Row	Urban	76.4	3.7	4.0	3.9	4.1	4.7
Colombo House	Urban	64.3	5.0	4.4	5.6	6.4	7.9
Ebury Bridge	Suburban	22.0	12.9	10.9	4.0	5.0	8.8
Eltham	Suburban	88.4	12.7	11.8	7.9	8.2	8.4
Westel House	Suburban	85.4	7.9	7.1	7.7	7.2	7.2

The prediction error is higher in suburban areas than in the urban situation, particularly for the Okumura method where the errors are quite large in suburban areas. However, the way a particular area has been classified as urban or suburban may differ to that adopted by the model at the time of analysing the empirical data. The Okumura model suggests the value of 10 dB for the suburban area correction factor at the frequency of 940 MHz. Hata's method produced the best results and it is simple to use, but its application range is limited.

5.3.2 Rural Results

Over the rural areas the measurement vehicle covered a distance of less than 1 Km in many 500 m x 500 m squares, much shorter than those in the squares over the urban areas. The set of

all transmission path profiles for the measurement squares include a variety of terrain situations. In the Newton Firs test, 92 squares were found to have a line-of-sight path between their centre and the transmitter. There were 48 such squares in the Altrincham test and in the Wavertree test 16 squares had an unobstructed transmission path.

In calculating the predicted path loss value for each test square, a computer routine initially determines the ground profile from the transmitter to the centre of the test square under consideration by using the terrain data map stored in the computer. The profile is then processed to derive the terrain-related parameters which are required by the particular prediction model under consideration. The predicted values of path loss were compared against the measured values for the models due to Okumura, JRC and Longley-Rice. Hata's model is only applicable to quasi-smooth terrain situations.

Predictions using the JRC method had previously been provided. However, the need for an independent computer routine to implement the JRC model was justified, since this would allow an investigation of the model's behaviour under various circumstances to be carried out. In relation to the model's choice of free-space loss or plane-earth loss as its basic loss factor, it was found that in the majority of cases the plane-earth loss was taken. The low value of the transmission frequency of 139 MHz used in the free-space equation and the large transmission distance which is more dominant in the plane-earth formula, could explain this fact. However, in some cases even over relatively long paths, free-space loss is chosen, since large values of the terminals' effective antenna height affecting

the term - 20 $\log_{10}$ ($h_{te}h_{re}$) included in the plane-earth equation, cause the predicted plane-earth loss to fall below that of the free-space.

Figs. 5.2 to 5.4 show the relationships between the predicted and measured median path loss values in each test square for the three transmitter sites. The errors were calculated as the difference between the predicted and measured values and one format adopted to show this difference was to plot measured against predicted path loss values, (Figs. 5.5 to 5.7). The correlation and regression parameters of the best fit line are evaluated and compared against the ideal line corresponding to the case when measured and predicted values would be equal. Tables 5.2 and 5.3 list the results of the data analysis for all the prediction models. The same statistical analysis was performed over the entire set of data for all three transmitters, and the results are also listed in the following tables.

Table 5.2

Base Station Location	Correlation Coefficient			Standard Error (dB)		
	Okumura	JRC	L-R	Okumura	JRC	L-R
Newton Firs	0.50	0.73	0.67	9.8	6.4	9.5
Altrincham	0.78	0.81	0.78	11.6	9.9	4.8
Wavertree	0.31	0.62	0.62	12.4	9.8	13.6
All	0.62	0.77	0.68	11.3	8.8	9.7

Table 5.3

Base Station Location	Standard Deviation of Error (dB)			Slope of Regression Line		
	Okumura	JRC	L-R	Okumura	JRC	L-R
Newton Firs	7.0	6.4	6.4	0.64	0.60	0.64
Altrincham	4.2	9.8	4.8	0.75	0.36	0.63
Wavertree	11.4	9.8	10.0	0.21	0.38	0.37
All	8.2	8.8	8.2	0.58	0.52	0.56

The error values indicated in the above tables for the Longley-Rice model have been derived when individual values of Δh appropriate to the path under consideration have been used in the prediction procedure. However, when the median value of Δh is used, the error increases by approximately 1 dB for all three transmitter sites. One interesting aspect is a comparison of the value of Δh as derived according to the Okumura and Longley-Rice definitions. The Longley-Rice definition always produces a lower value even compared to those suggested by the model for the areas of interest.

The Okumura model suggests the use of the rolling hilly terrain fine correction factor to be added to the signal strength, which could be positive or negative depending on whether there are many roads running on tops or bottoms of hills correspondingly. Such classifications were not possible for the squares where measurements had been carried out, therefore the correction factor which amounts to 9 dB for an average value of Δh of 50 m, was not considered for prediction purposes, although it is incorporated in the computerised version of the model. The number of radial profiles with water expanses in the path was not large, however, the correction term for this condition, which is only provided by the Okumura model, has been taken into account.

The error histograms are shown in Figs. 5.8 to 5.10, and they indicate whether the predictions are optimistic or pessimistic for any particular situation. An error analysis of the results obtained over the line-of-sight paths and only for the Newton Firs and Altrincham tests, where the sample size is adequate, showed improved performance of the Okumura model. The values of standard errors obtained in this case were about 3 dB less than the corresponding

values listed in table 5.2.

5.3.2.1 The Newton Firs (Frodsham) Results

In the Frodsham test, the transmitter site was in a strictly rural area, transmitting over mainly flat ground to the test squares and only a few squares included very hilly areas. The transmitter height is greater than either of the other two sites. The models are generally optimistic, predicting a lower value for the path loss than that actually measured, the notable exception being for squares numbered 130-140. Fig. 5.11 shows the path profile of one such square, where it can be seen that the prediction models have not taken into account the increased effective height of the mobile antenna which results in a higher received signal strength.

The JRC model produces the highest correlation coefficient between the predicted and measured values and has the lowest standard error. The statistical analysis of the prediction errors showed that there are no particular relationships between the errors and the transmission range. This further indicates that the dominant factors affecting the propagation are terrain related.

5.3.2.2 The Altrincham Results

Following the data analysis for the Altrincham test, a high value of correlation coefficient was found for each prediction model. This indicates that the predictions follow the trend of the measurements very closely with the exception of a fairly constant difference. However, the Longley-Rice model produces much lower standard error value and the standard deviation of the error due to the JRC model is highest, indicating a large spread in the value of

prediction errors.

The Longley-Rice and JRC models both include a specific calculation of diffraction loss and hence produce lower prediction errors. However, in certain situations the JRC model produces large errors, as can be seen in Fig. 5.3 for the squares numbered 26-40, where the predicted path loss is very much lower than the measured values.

Fig. 5.12 shows the terrain profile for one such square and as can be seen, the effective receiving antenna height h_{re}, as defined by the model and used in the plane-earth formula, is quite large. In this case the prediction is improved when the actual structural heights above the ground are used, thereby indicating the importance of the local ground surrounding the mobile receiver.

5.3.2.3 The Wavertree Results

The transmitter in the Wavertree site is within the City of Liverpool, surrounded by buildings and the transmission ranges are longer. The area chosen for the test is more hilly and the prediction errors were found to be greatest. The correlation coefficients are very low and the value of standard error is high for all three models, also the errors are more widely spread.

A similar statistical analysis of the error in relation to the transmission range was carried out for the Wavertree test and this did not give any useful conclusions. A further error analysis with regards to the number of obstructing edges in the transmission path, also did not produce any viable results.

For some of the test squares, the Longley-Rice model predicts a much higher value for path loss than the corresponding measured

results. Fig. 5.13 shows the terrain profile of one such square and the reason for these large differences can be explained in terms of receiver location with respect to the closest obstructing hill. This is the receiving terminal horizon obstacle and as can be realised from the figure, it will result in a large horizon elevation angle which is defined as the angle between the line joining the top of the obstacle to the antenna and the horizon line. The value of this angle affects the weighting factor used for the calculation of diffraction loss.

One typical situation which emphasises each model's approach to the problem of path loss prediction over irregular terrain, is provided by the path profile shown in Fig. 5.14. The measured value and path loss values predicted by each model are listed in table 5.4.

Table 5.4

Path Profile	Transmission Range (Km)	Measured Path Loss (dB)	Predicted Path Loss (dB)		
			Okumura	JRC	L-R
WAV 63	36.2	118.6	147.8	108.6	137.8

As can be noted, whereas the JRC model predicts a much lower value, the Okumura and Longley-Rice prediction models produce a rather large value for path loss with respect to the measured value. The relatively small value of measured path loss reflects the gain in signal strength resulting from the very large height of the ground level where the mobile lies and the unobstructed transmission path. However, the prediction models fail to take this into account and in the case of the Okumura model, this large value of terrain height near the mobile results in a large value of terrain undulation height, Δh, producing a higher value of predicted terrain loss. The

JRC prediction model calculates the total path loss in this case, as the sum of the free-space loss and the diffraction loss due to the inadequate first Fresnel-zone clearance. The plane-earth loss is calculated to be small due to the large value of the receiving antenna effective height and is 7 dB below the free-space loss.

5.4 CONTOUR TECHNIQUES

During the comparative study, computerised routines have been devised which will allow a contour analysis of the terrain heights, and the predicted signal strength and path loss values, to be carried out in an area over which terrain data map is available. This provides a simpler and more efficient way of determining the coverage area of a particular transmitter.

The contour curves are drawn by using the representative value from all the ½ Km side squares within the area of interest. Fig. 5.15 shows the contour heights of the area of size 30 Km x 30 Km over which the Newton Firs trials had been conducted, the area is shaded to indicate its position within the national Ordnance Survey grid. Fig. 5.16 shows the contour curves of the predicted path loss by the Okumura model over the same area where transmitter site lies in the small dark square. Since the number of measurement squares was not sufficient, a contour plot of measured values of path loss could not be obtained.

5.5 CONCLUDING REMARKS

The prediction models have been compared with each other and against measured data which has been obtained in rural areas over irregular terrain. In order to improve the prediction accuracy, it is

necessary to investigate the factors which can be incorporated into the various models to make them more applicable to the different situations. For example the method of determining the position of the effective reflecting plane for determining the effective antenna height of the terminals and thus the calculation of plane-earth path loss, and the way in which the terrain irregularity factor is defined with respect to the intervening path, plays an important part in the prediction procedure.

Generally the Okumura model produced the largest prediction errors over all the transmitter sites, indicating its weakness for predictions over irregular terrain. Although the Longley-Rice prediction model has been found to compare well with the measured data in general, there is more scope within the JRC model to introduce improvements. This is not the case for the Okumura model since it is wholly dependent on empirical results and only empirical improvements can be added.

It should be considered, however, that the attenuation caused by man-made obstacles or vegetation cannot be computed deterministically because of the non-availability of data about these features in the data bank. The data bank contains no information about the height of buildings, the width of the streets, whether a road is radial or circumferential with respect to the base station or whether in wooded areas, the trees are felled or grown. Thus the use of the topographical data bank in its present form has inherent limitations and it is of interest to speculate on whether the extra effort involved in producing a more accurate data bank would lead to a reasonable increase in the accuracy of path loss prediction. The influence of man-made obstacles and vegetation on the received field

strength is predominantly determined by obstacles in the vicinity of the radio terminals. Thus, these obstacles can be expected to cause similar effects on signal attenuation in hilly or mountainous terrain.

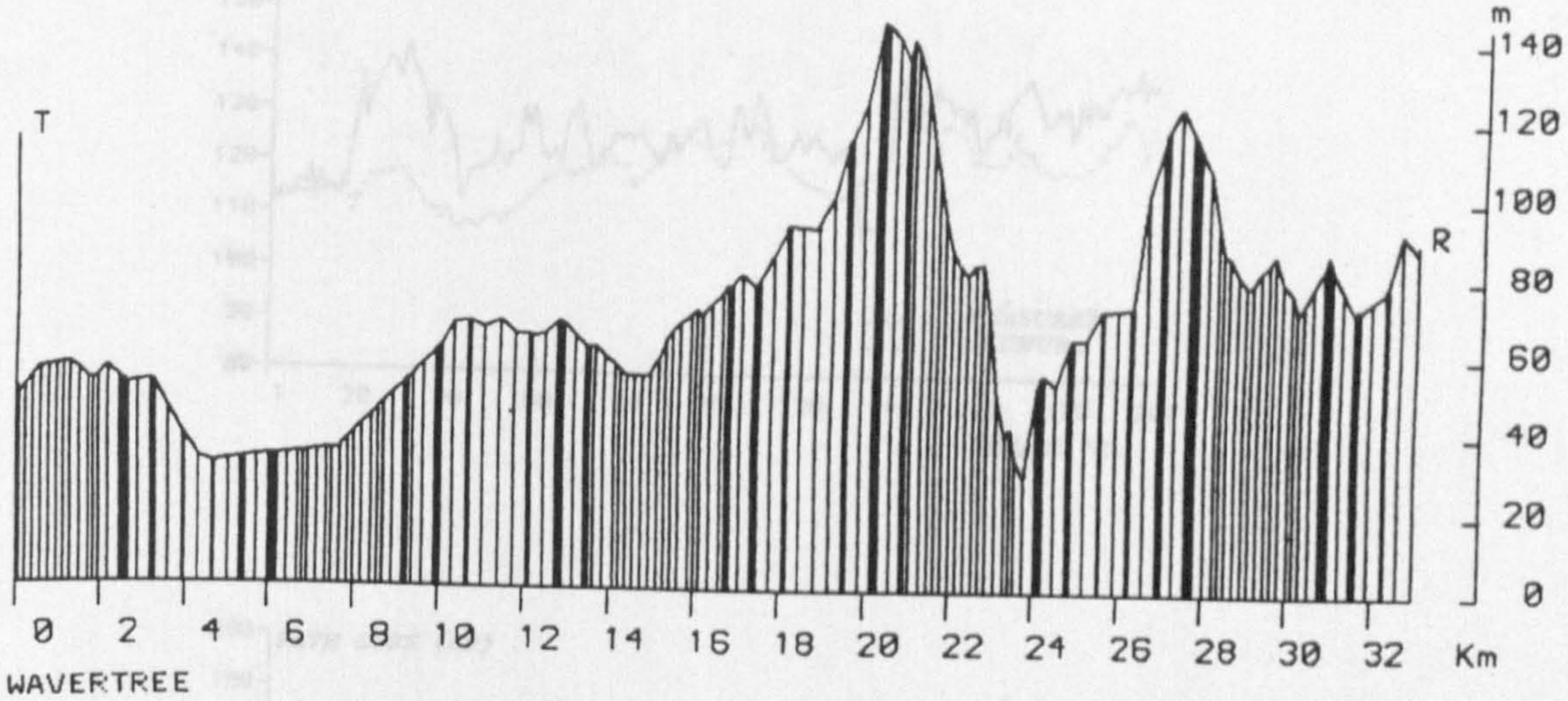

* FREQUENCY = 139.0 MHz
* MOBILE ANTENNA HEIGHT ABOVE THE GROUND = 2.0 m

RANGE = 32.99 Km
BASE STATION EFFECTIVE ANTENNA HEIGHT = 75.9 m

NUMBER OF DATA POINTS 187

TYPE OF IRREGULARITY :

ROLLING HILLY ;
DH = 65.5 m
CORRECTION FACTOR = -6.09 dB

GENERALLY SLOPED ;
TETA IN mRAD :
18.1
-22.4
CORRECTION FACTOR = -10.53 dB

TOTAL TERRAIN LOSS = 16.62 dB

PATH LOSS = 142.28 dB

ERROR NUMBERS :
6 15 16

Fig. 5.1 Computer Output for Okumura Method.

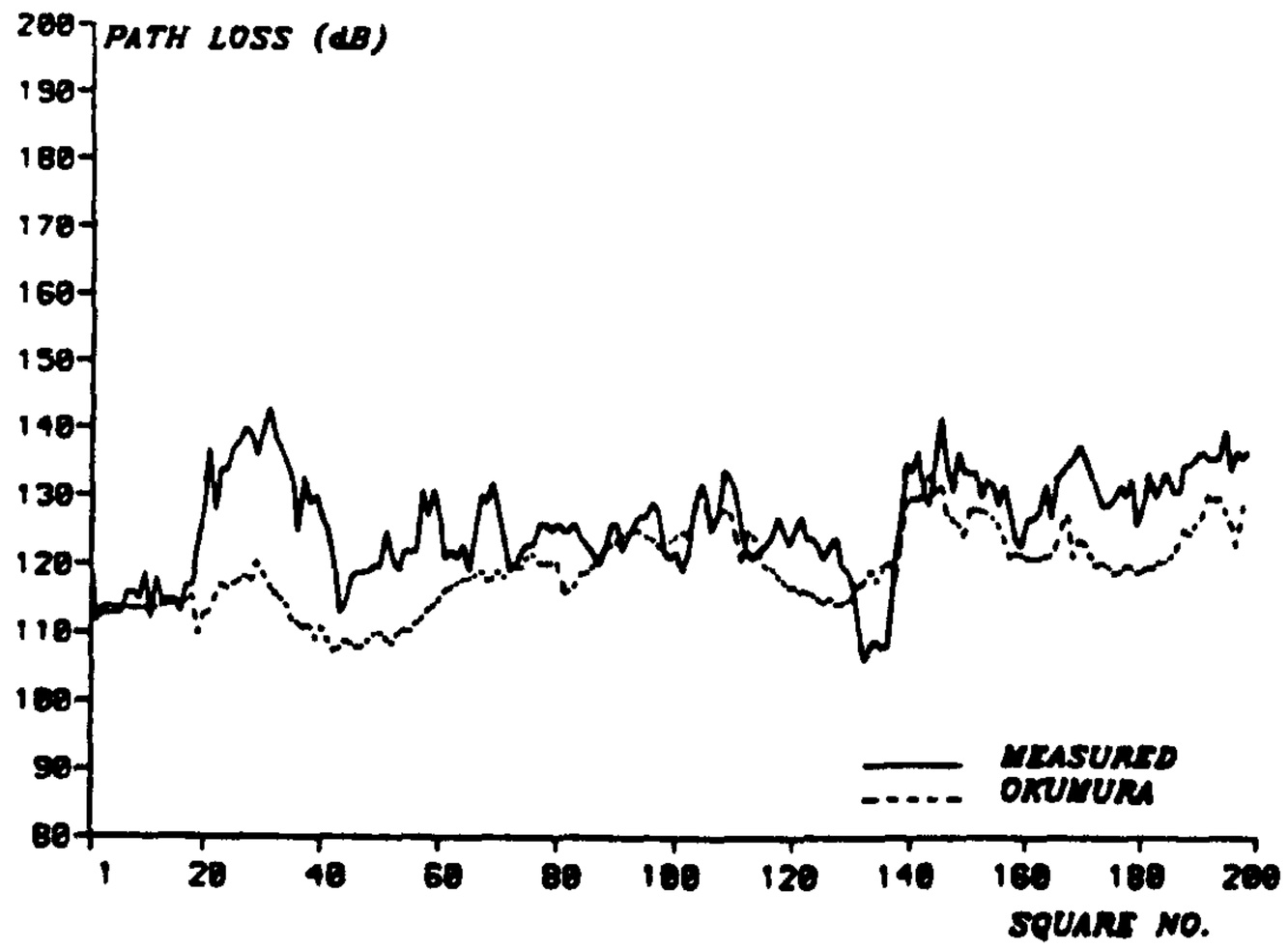

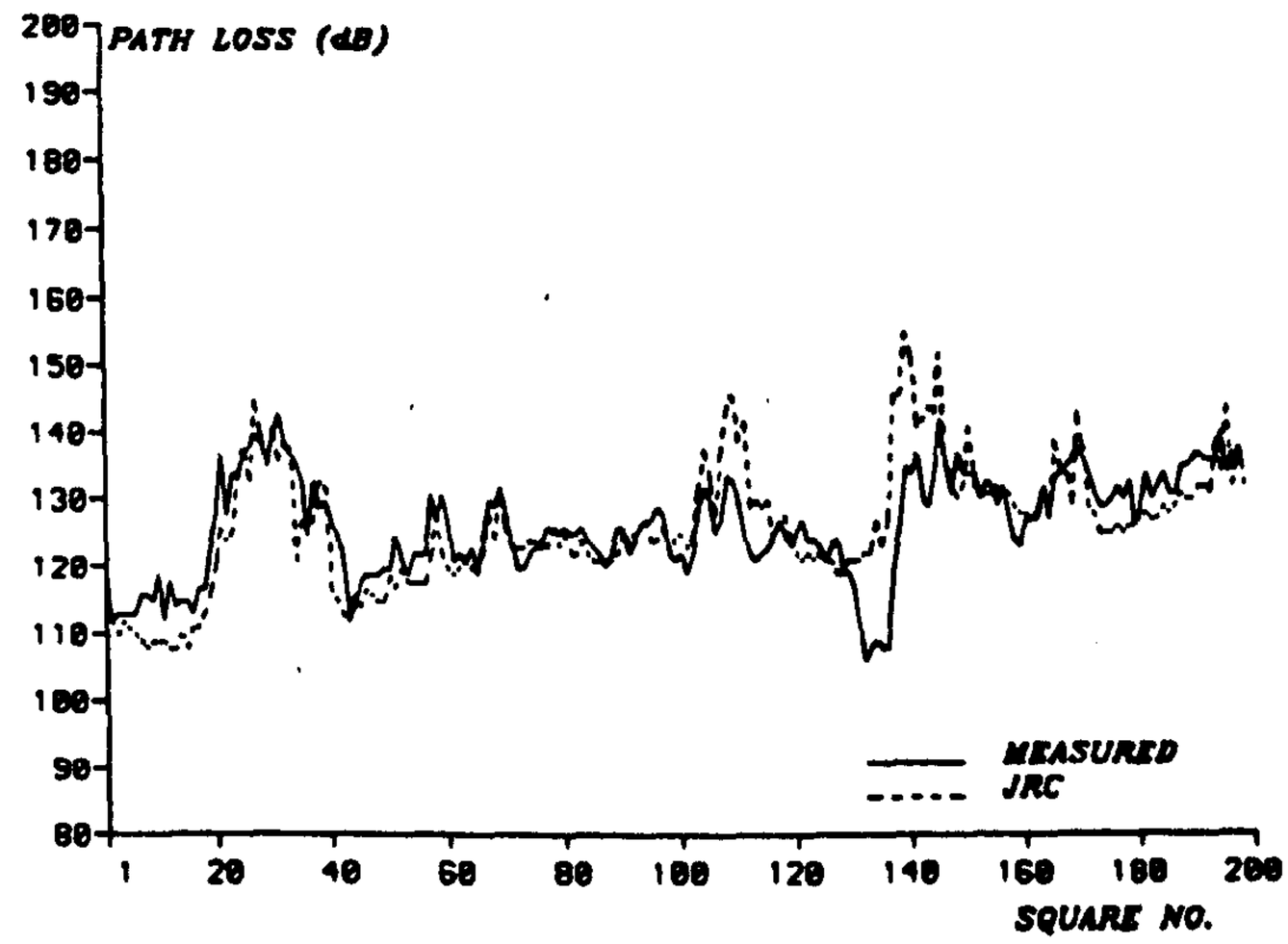

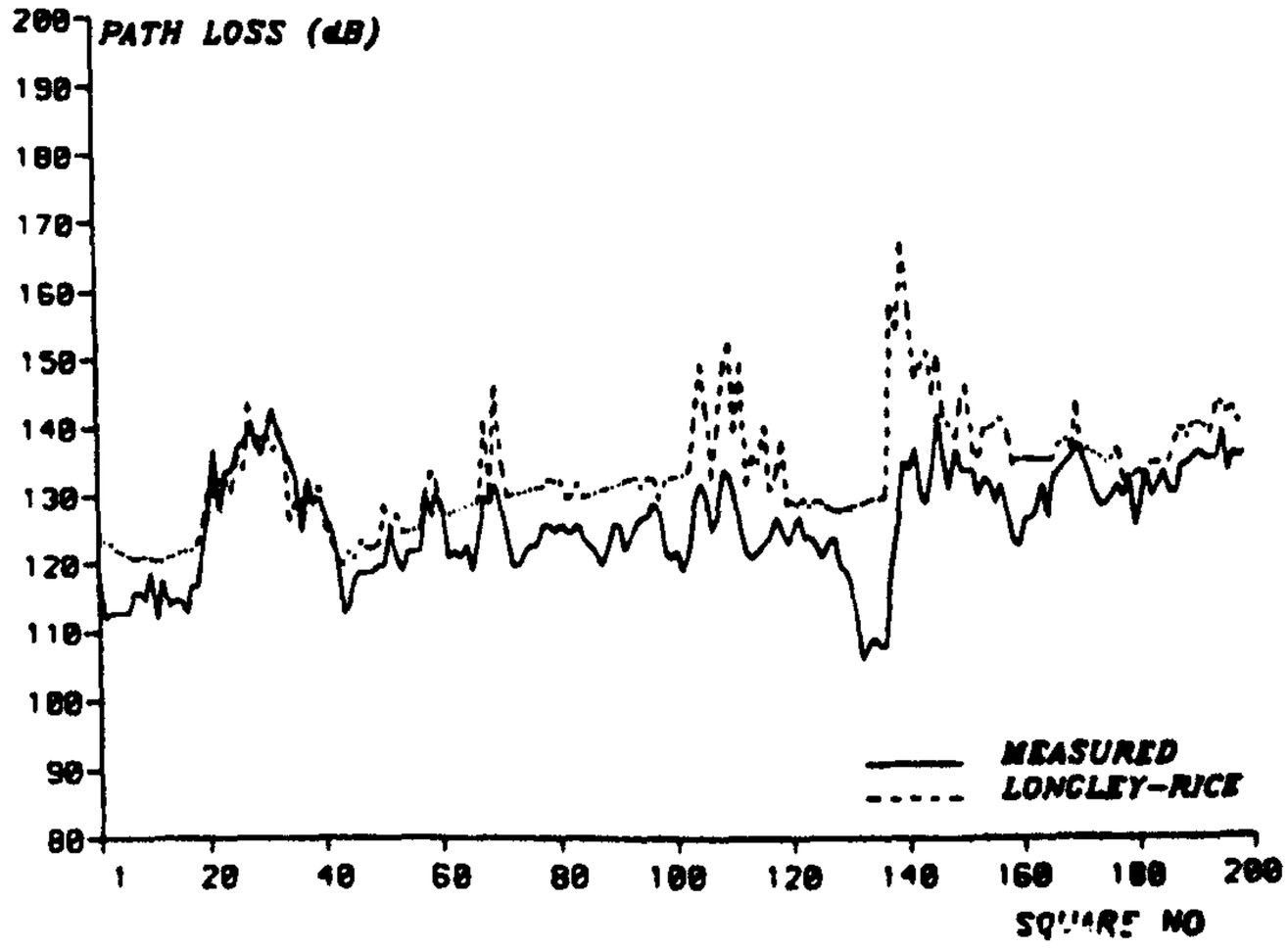

Fig. 5.2 Predicted and Measured Path Loss (Newton Firs).

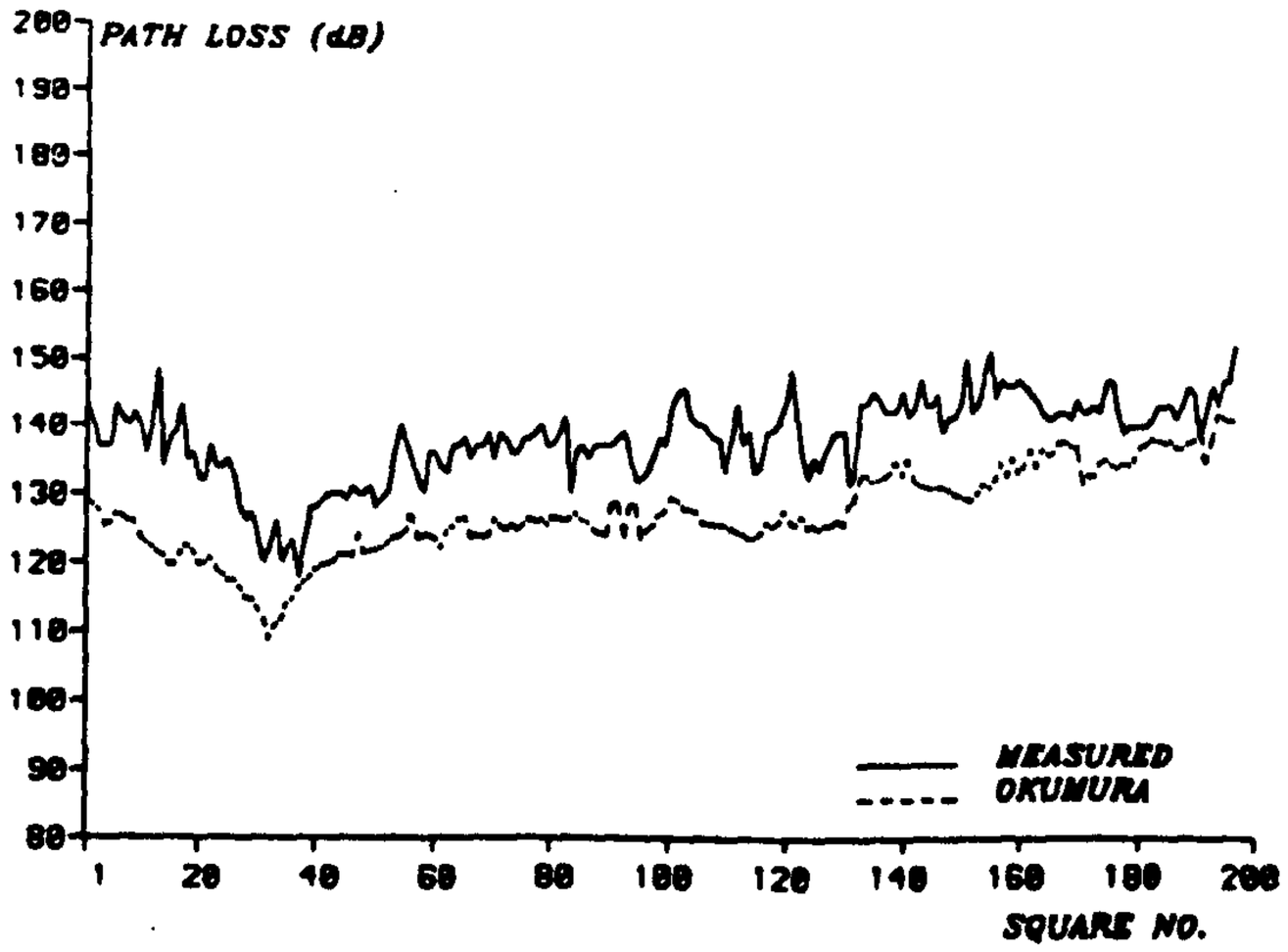

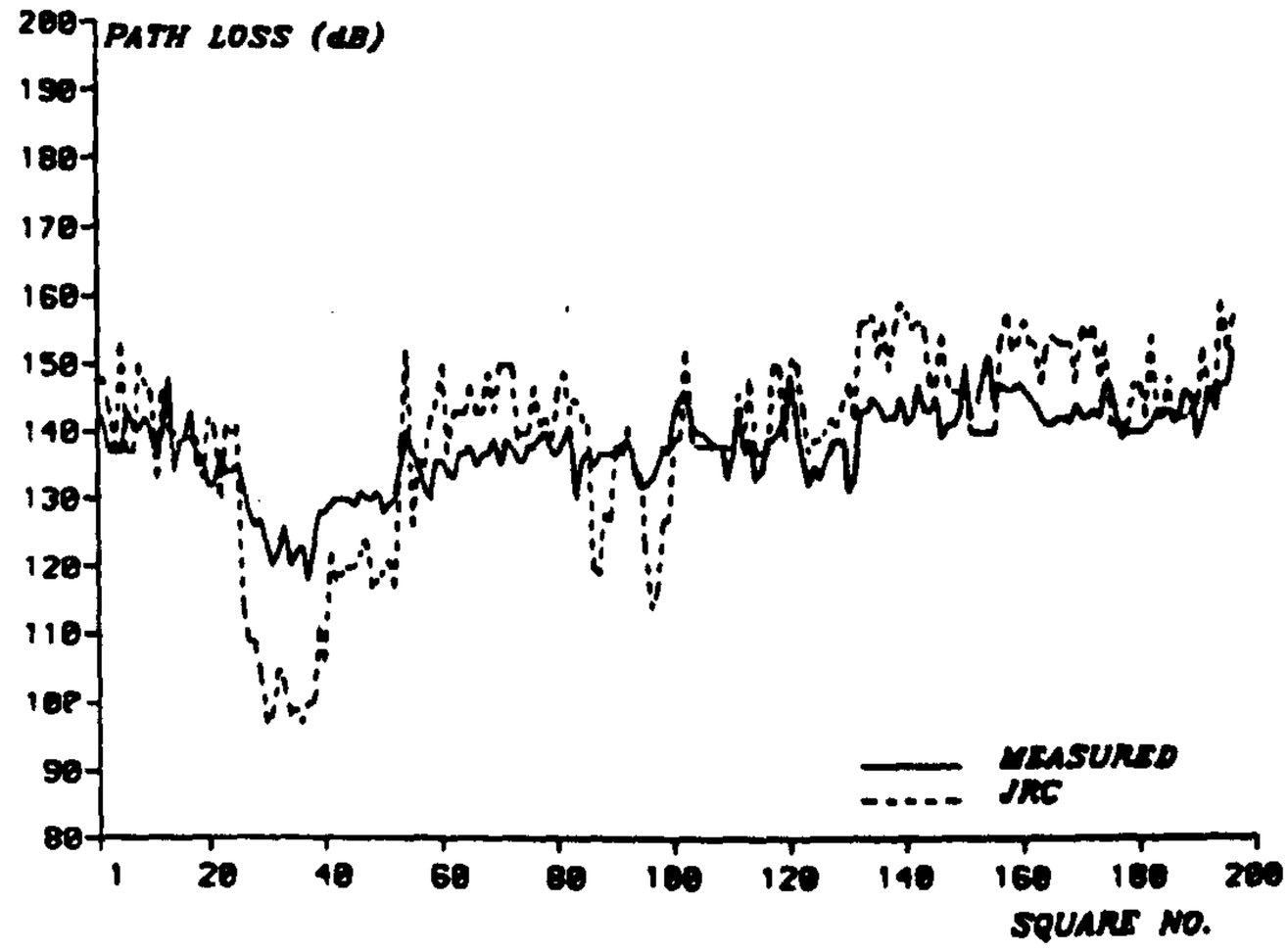

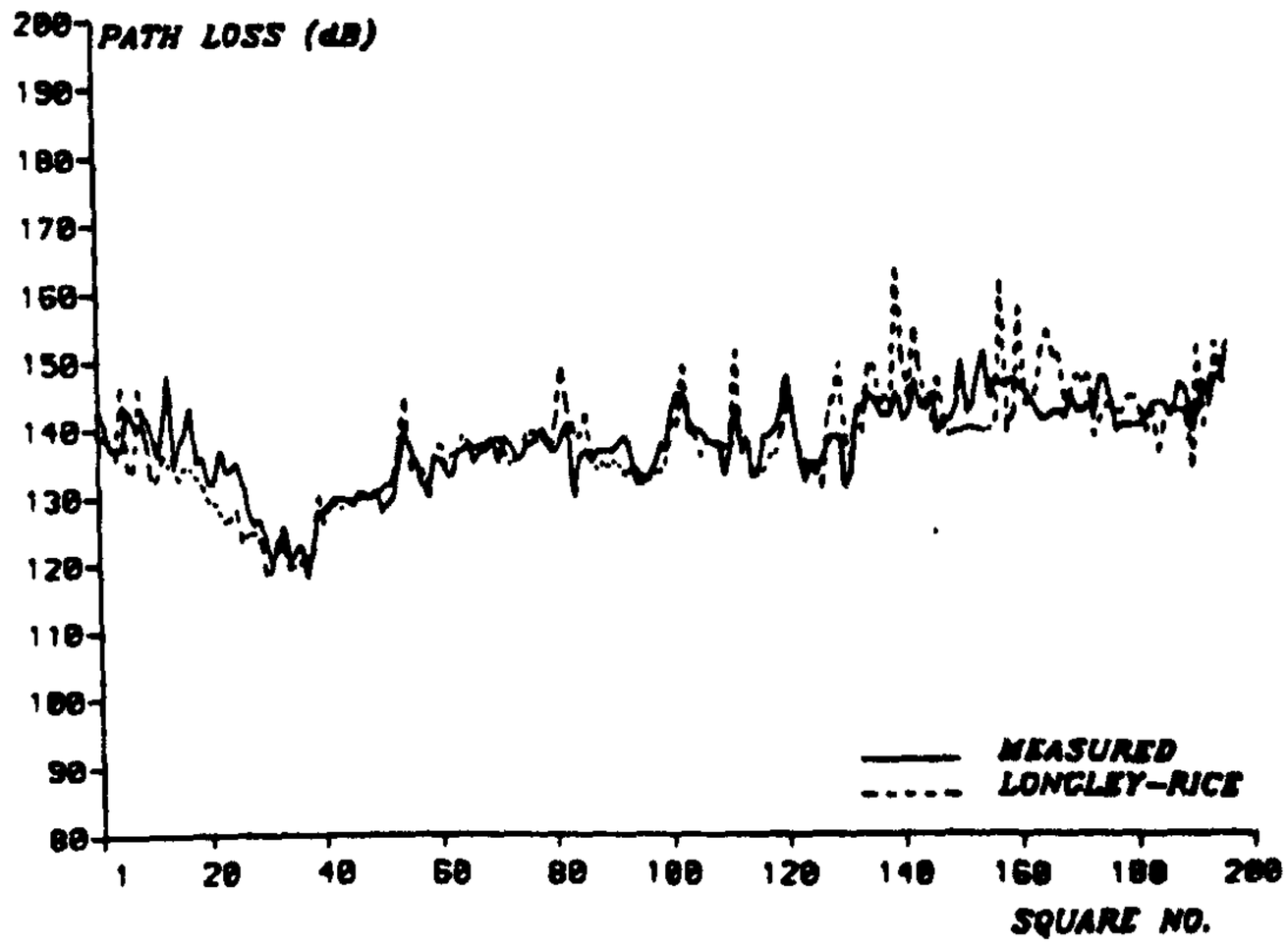

Fig. 5.3 Predicted and Measured Path Loss (Altrincham).

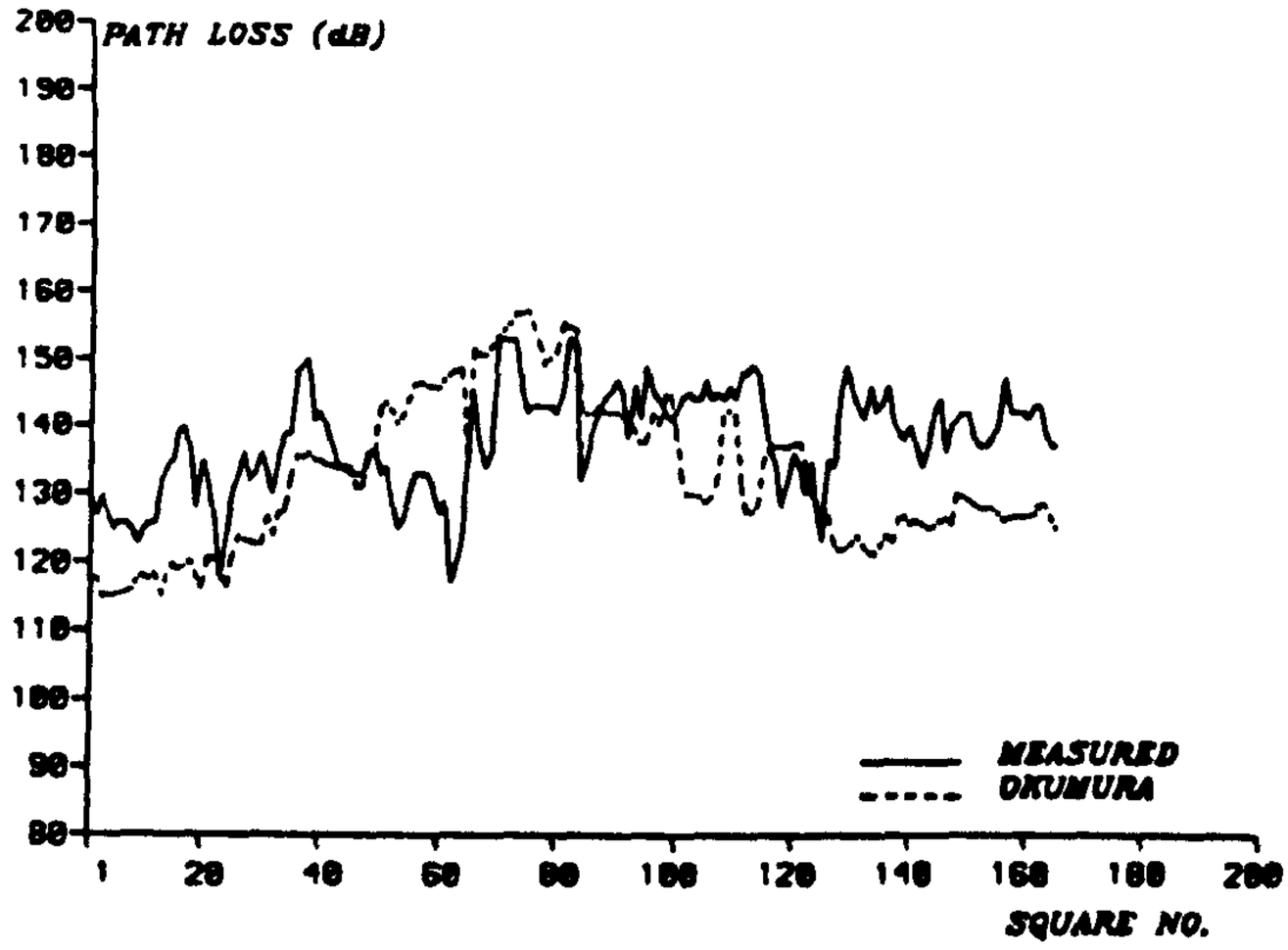

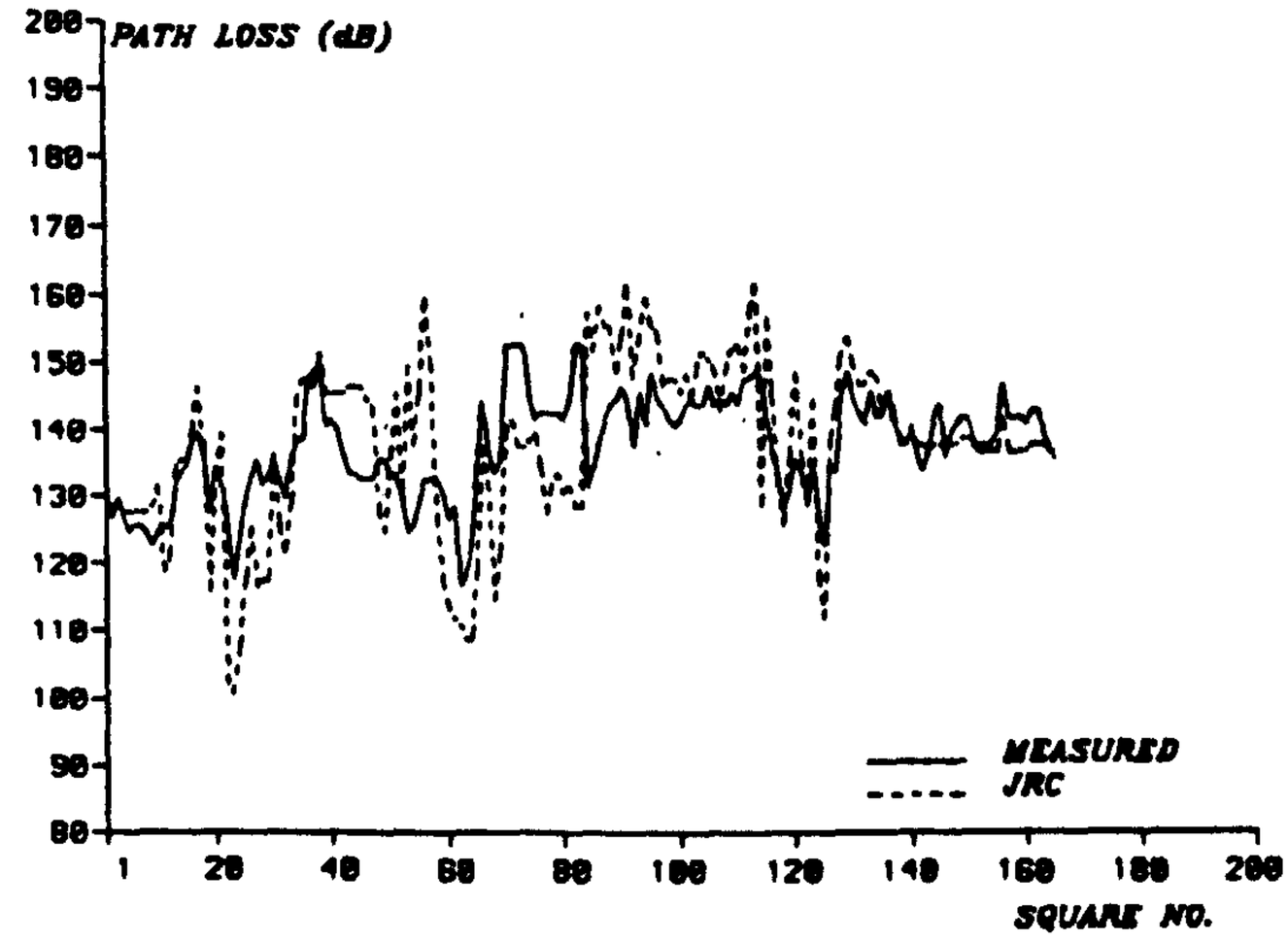

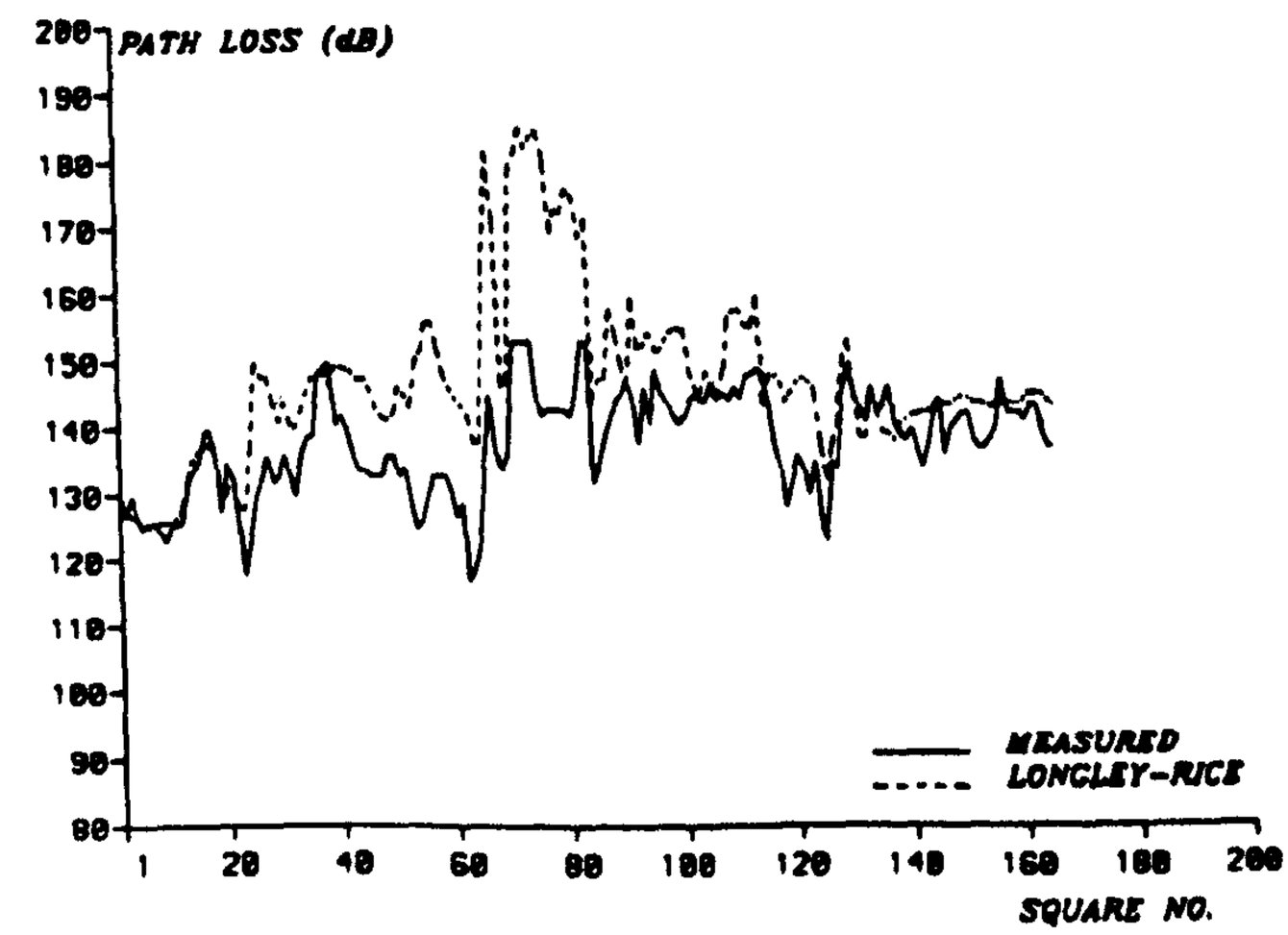

Fig. 5.4 Predicted and Measured Path Loss (Wavertree).

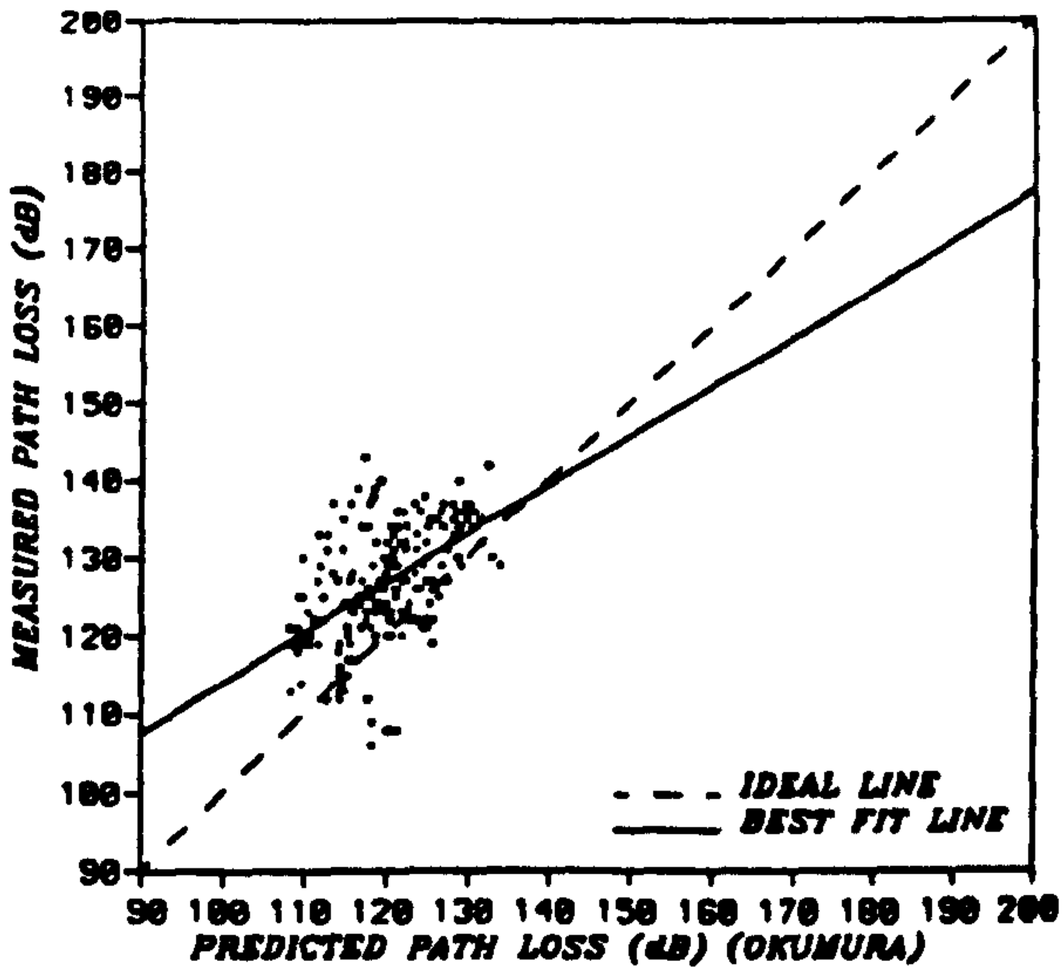

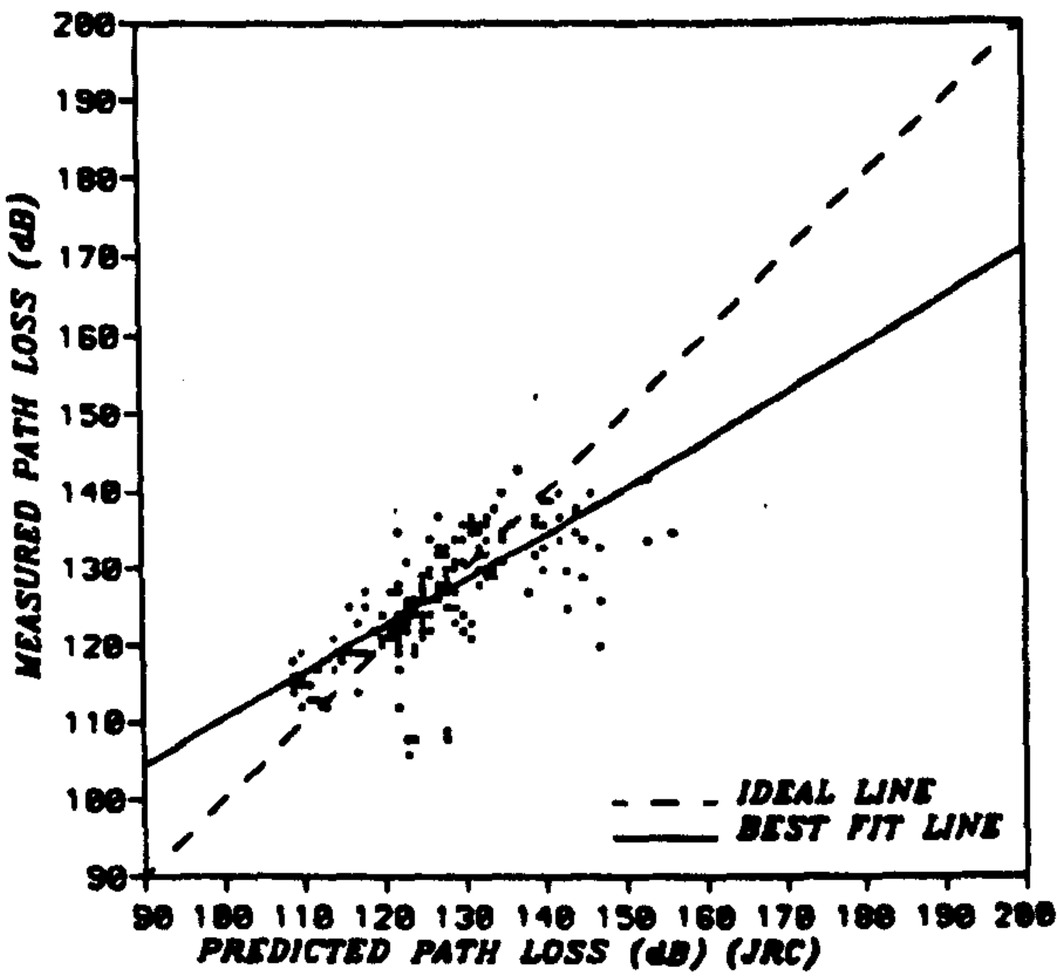

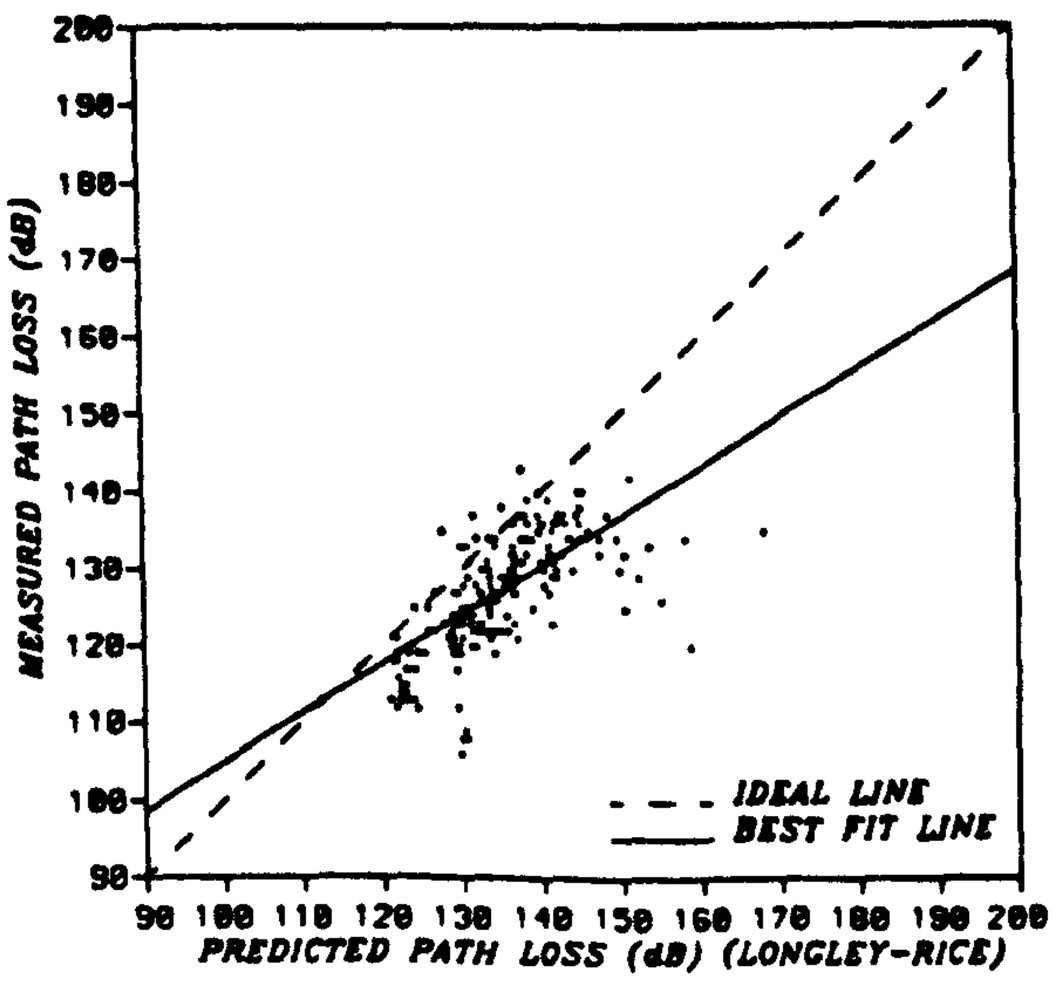

Fig. 5.5 Regression Lines (Newton Firs).

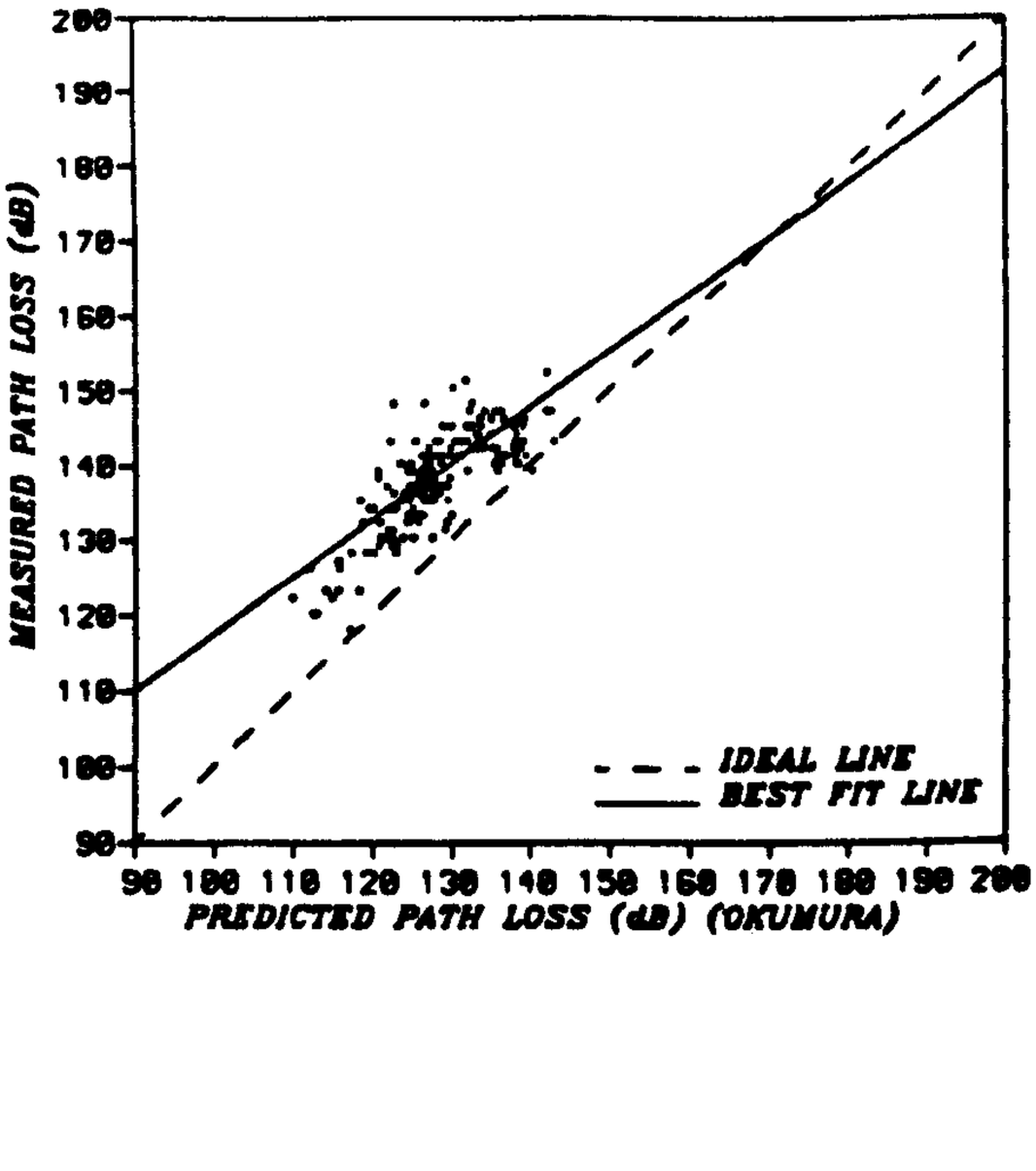

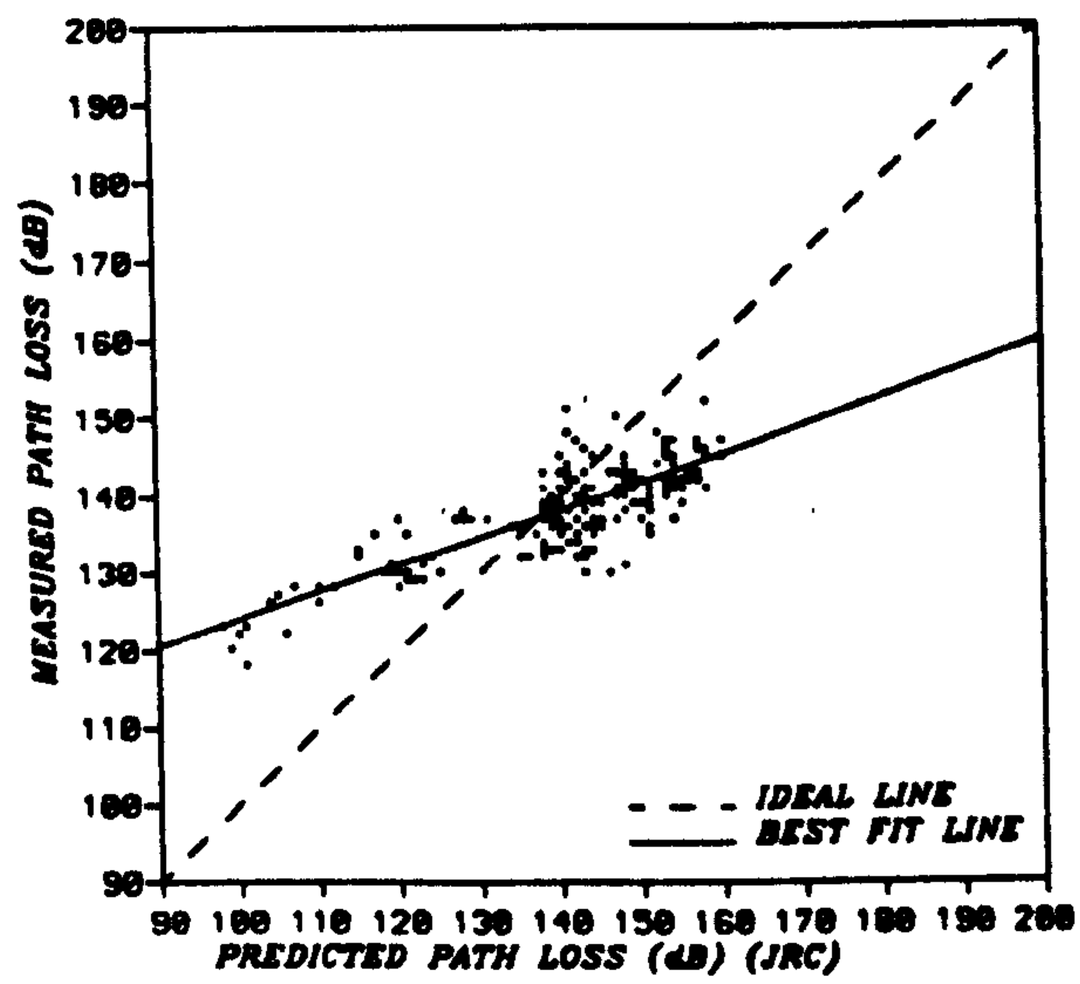

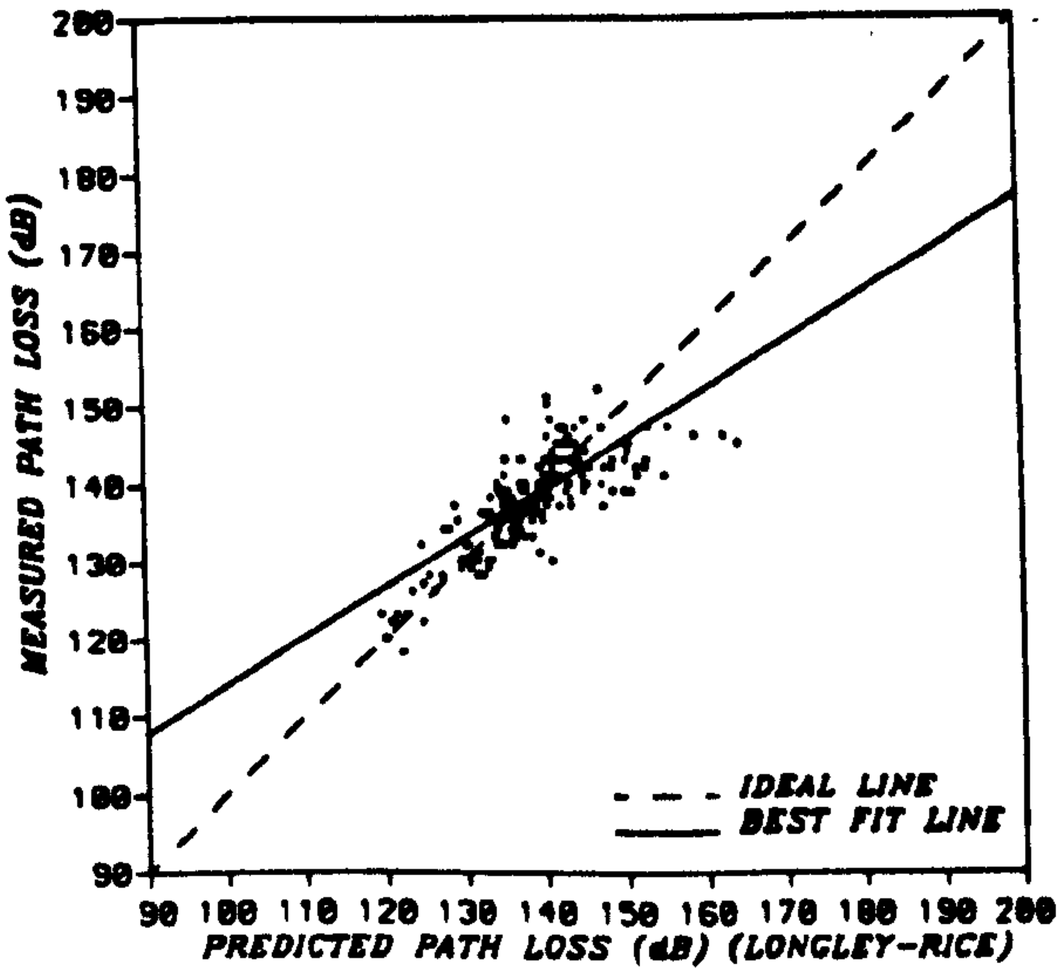

Fig. 5.6 Regression Lines (Altrincham).

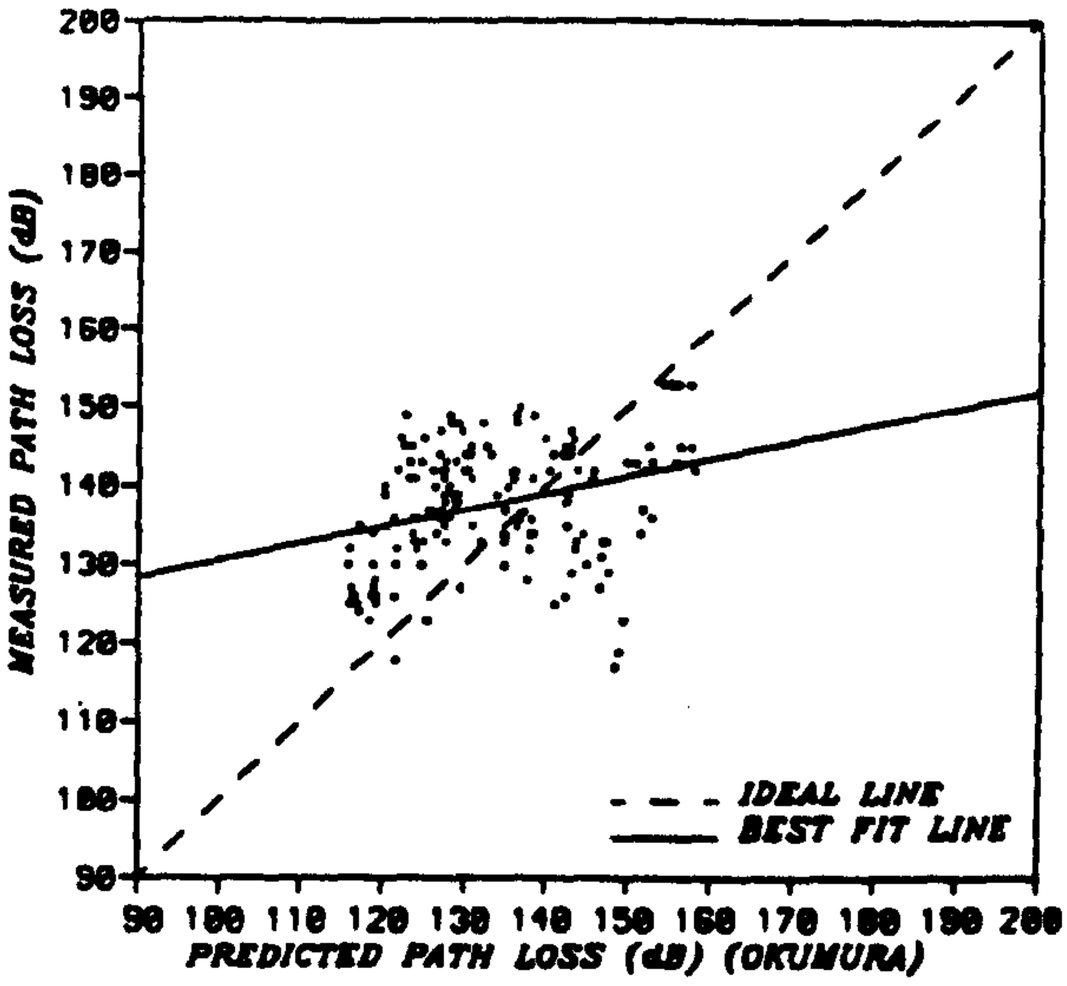

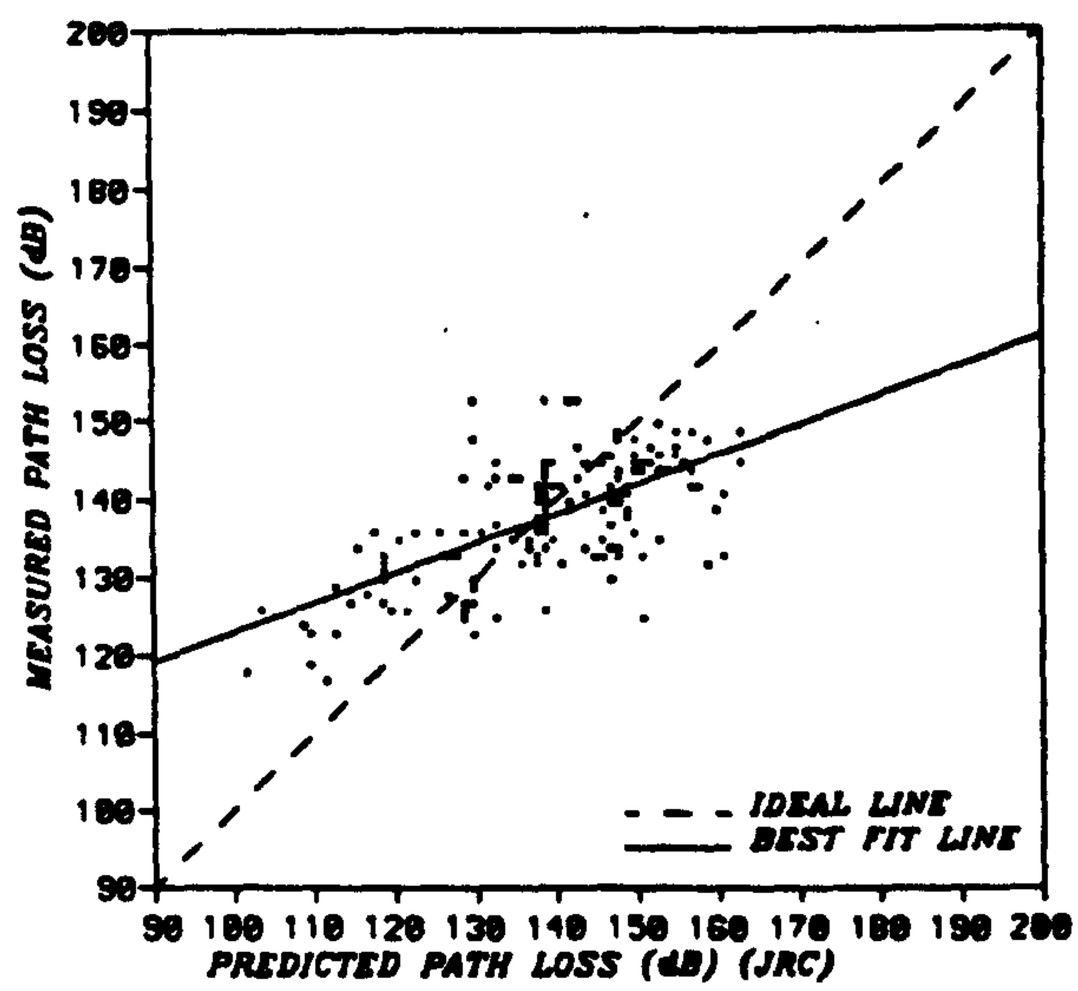

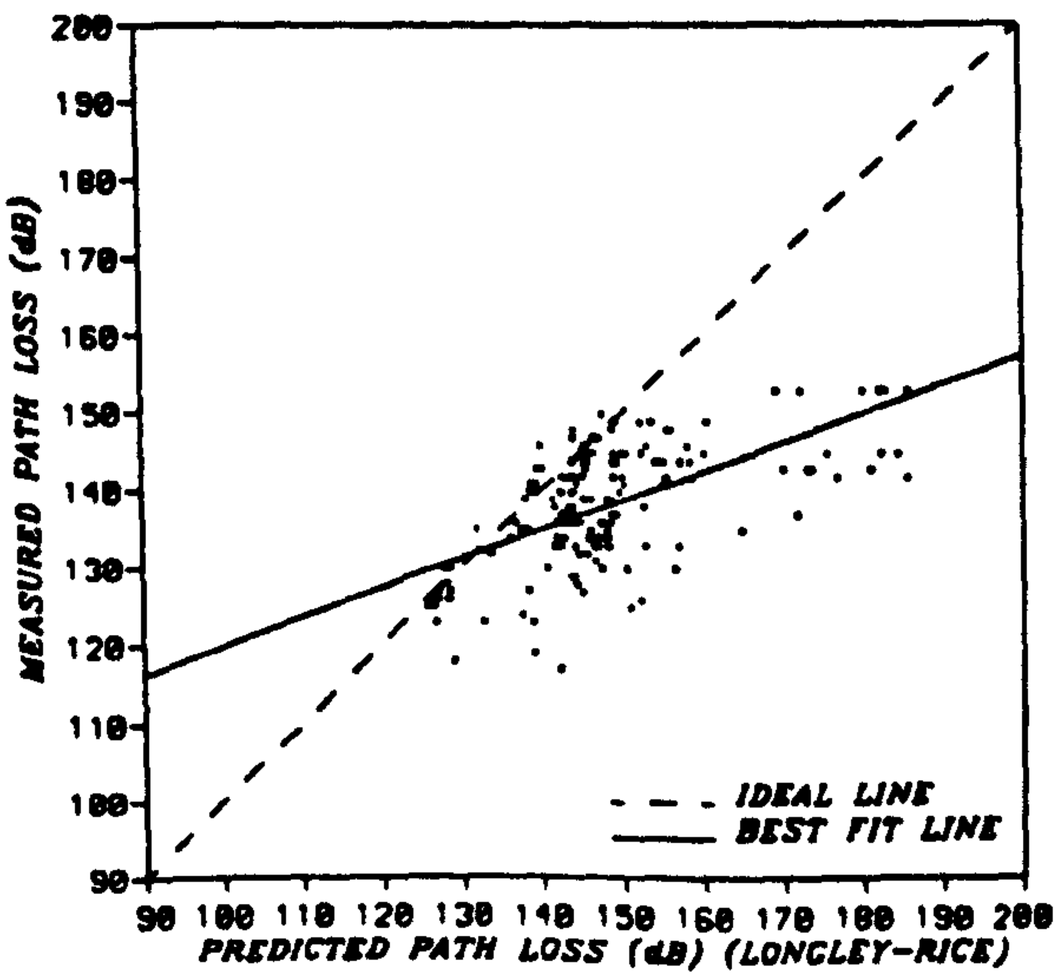

Fig. 5.7 Regression Lines (Wavertree).

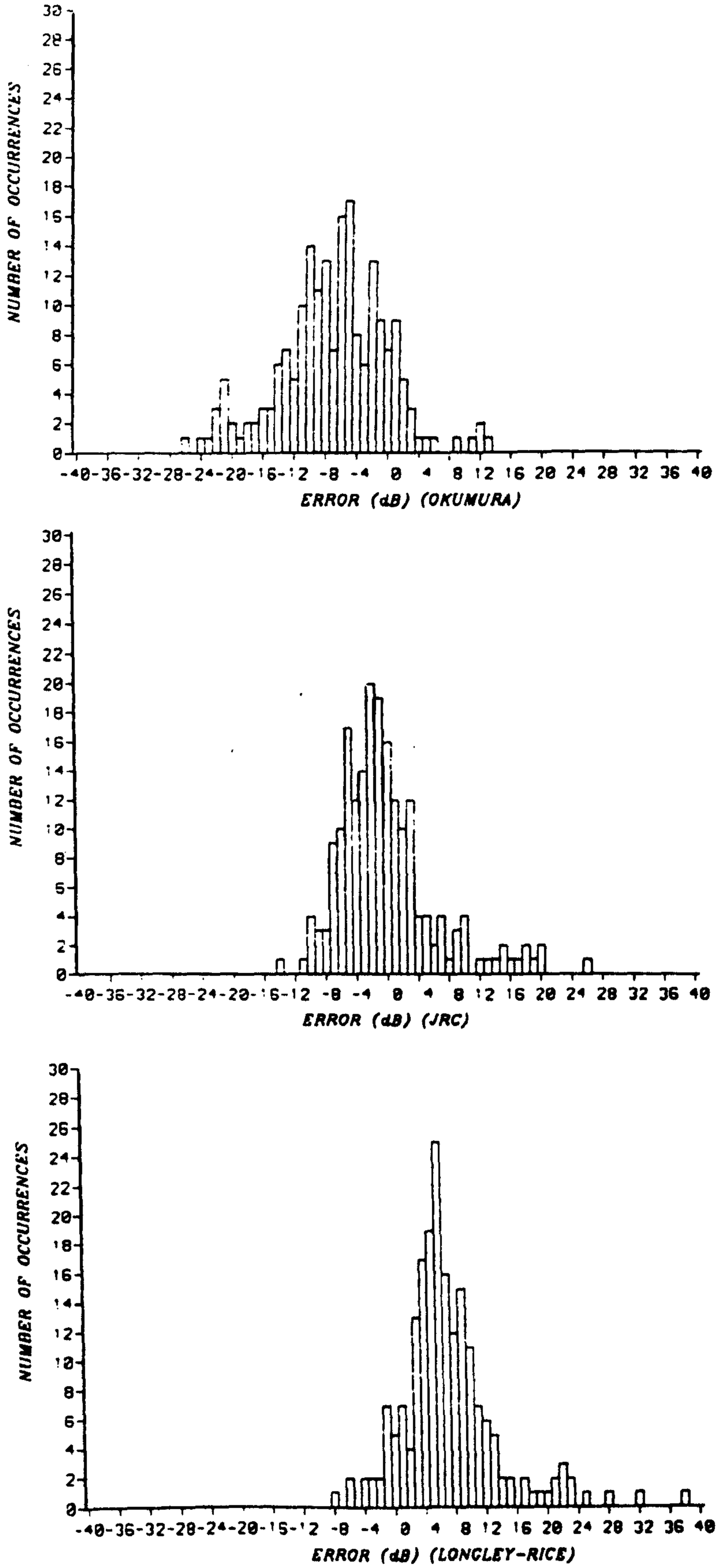

Fig. 5.8 Prediction Error Histograms (Newton Firs).

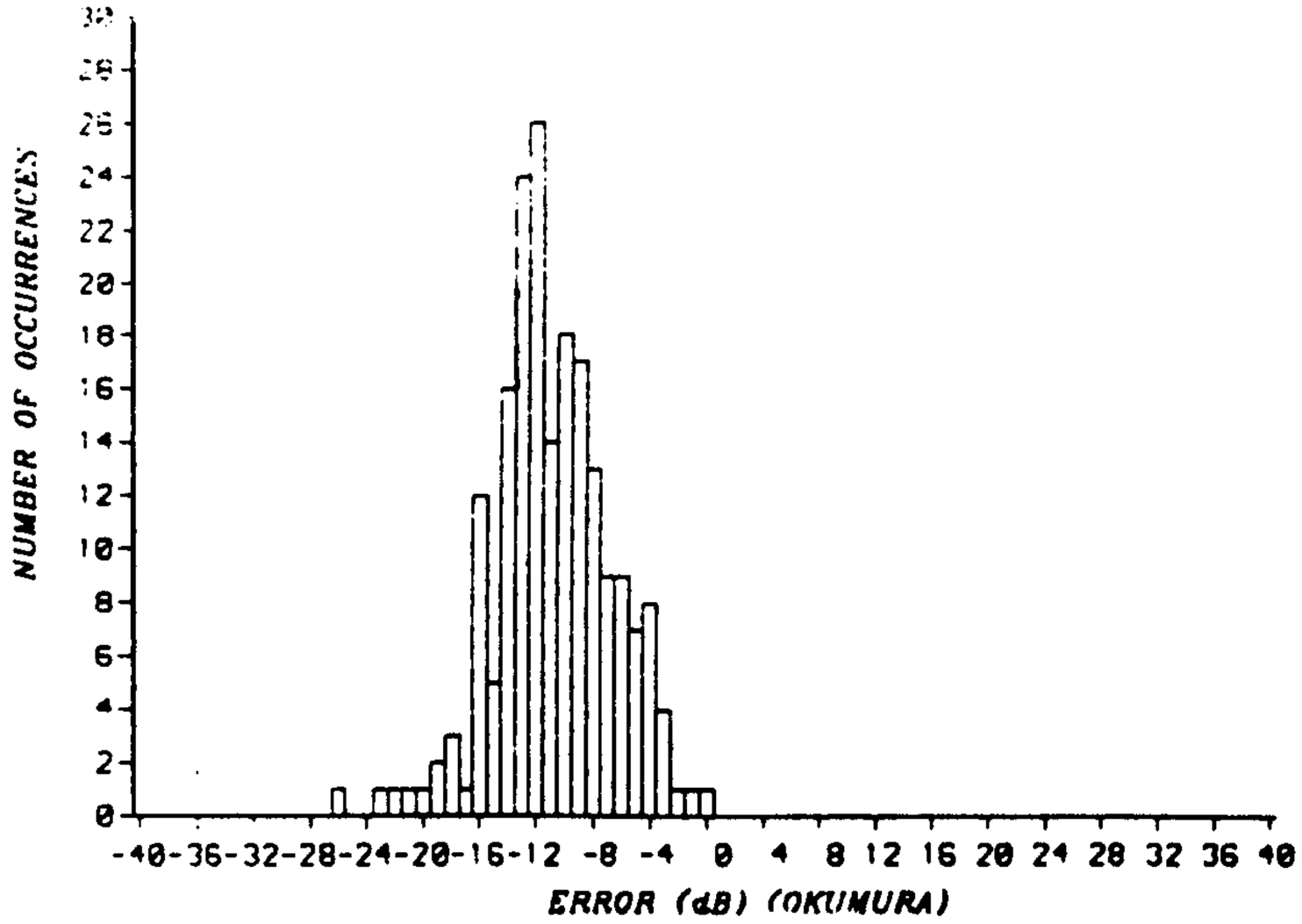

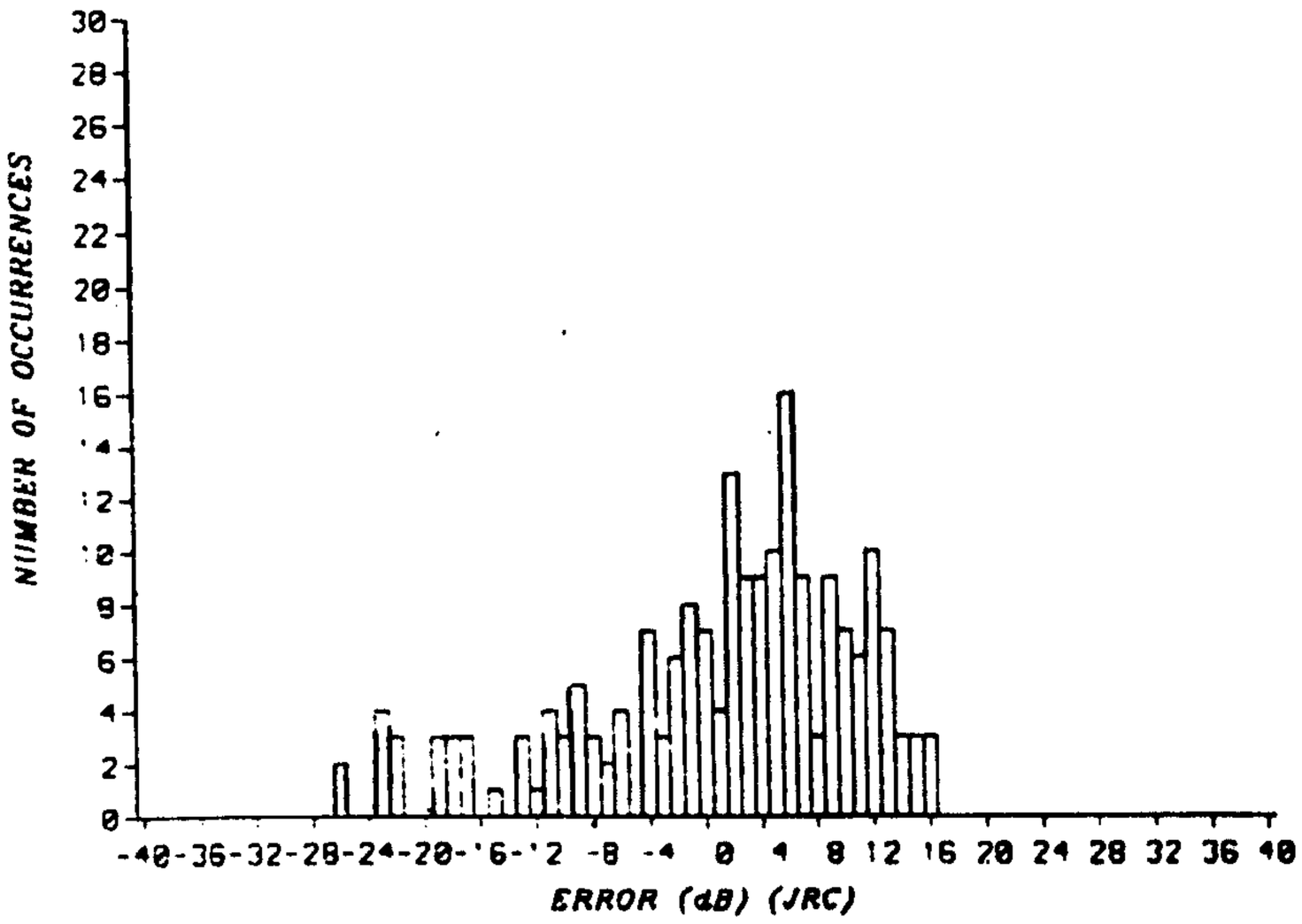

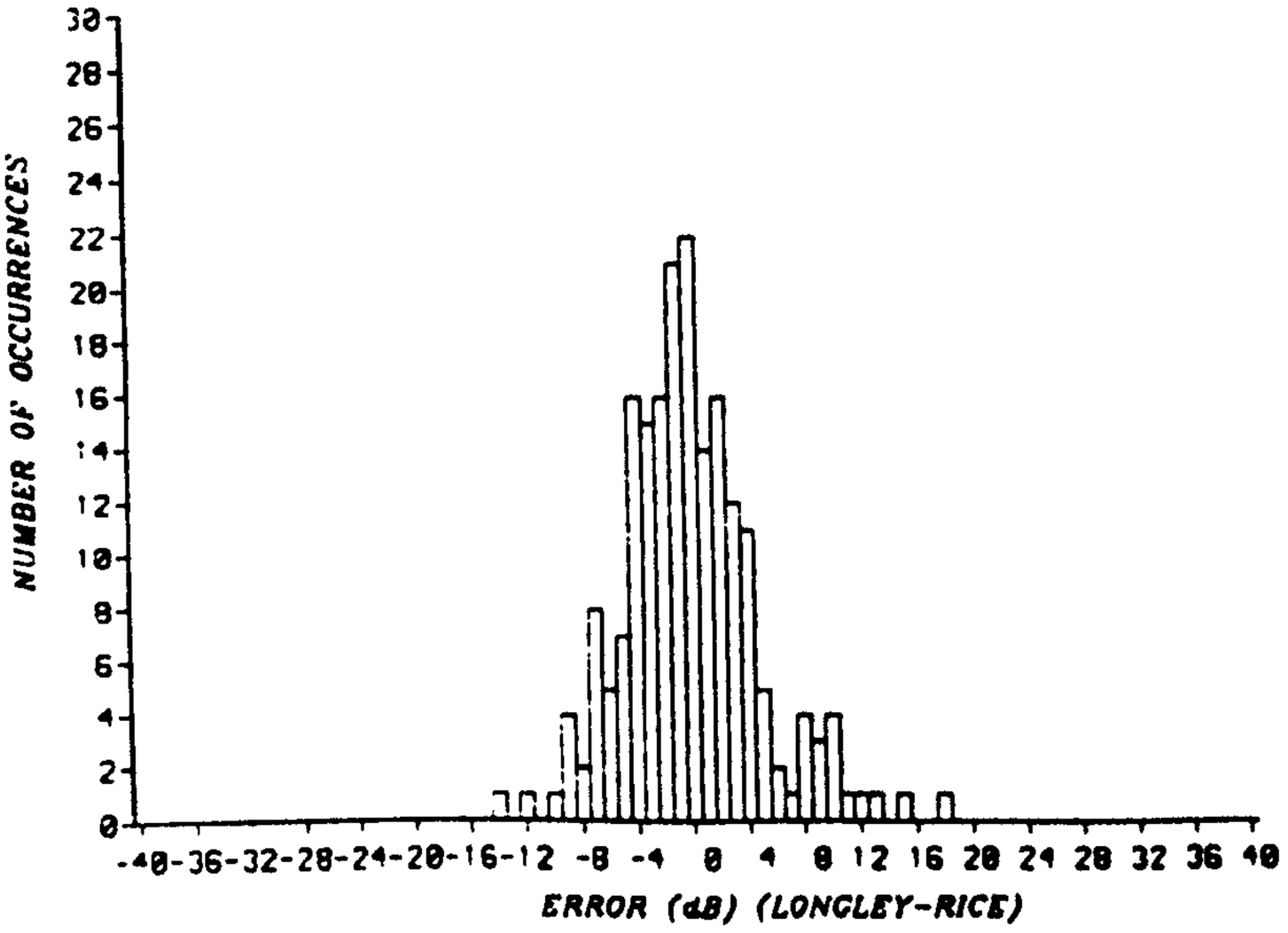

Fig. 5.9 Prediction Error Histograms (Altrincham).

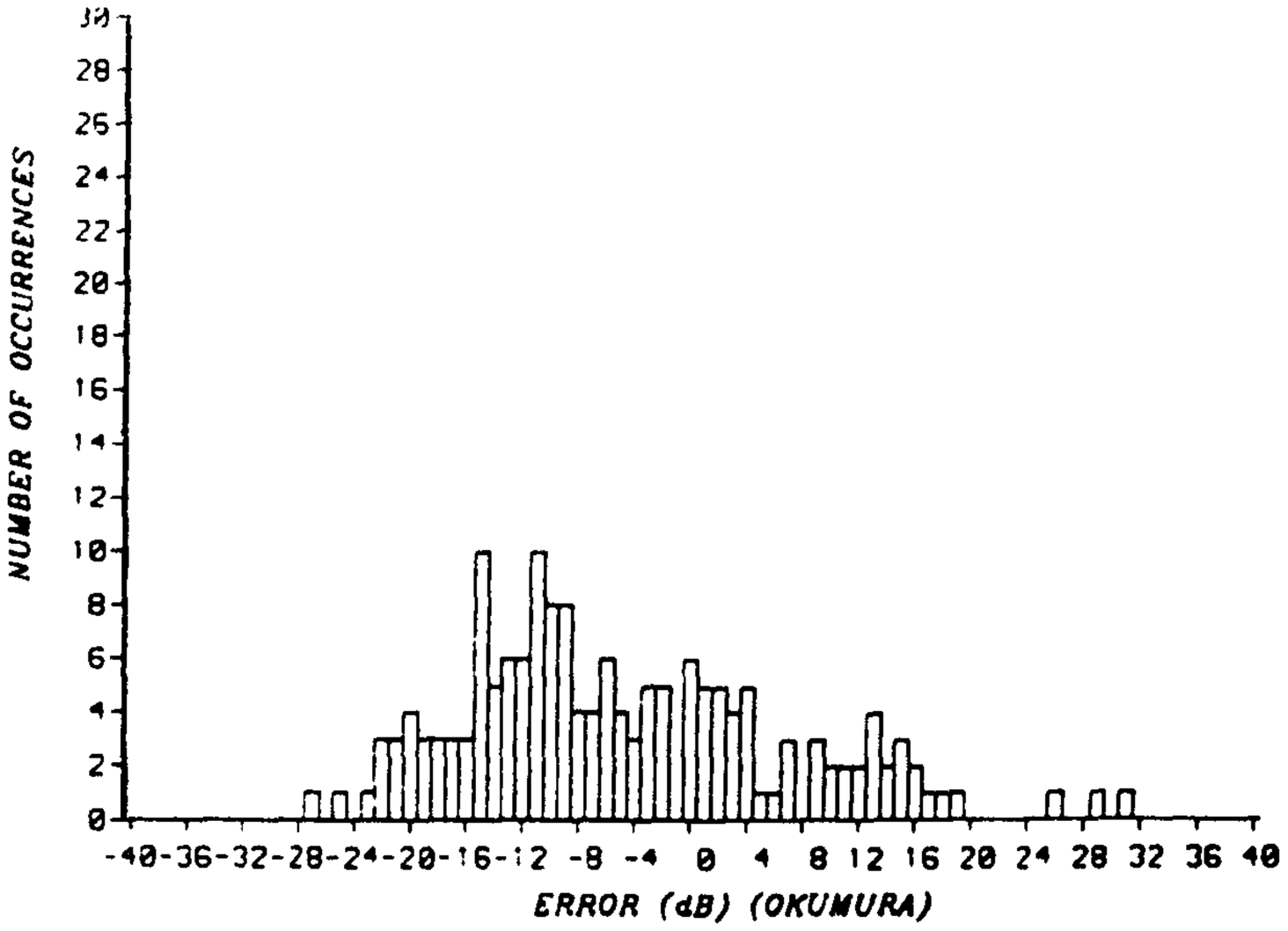

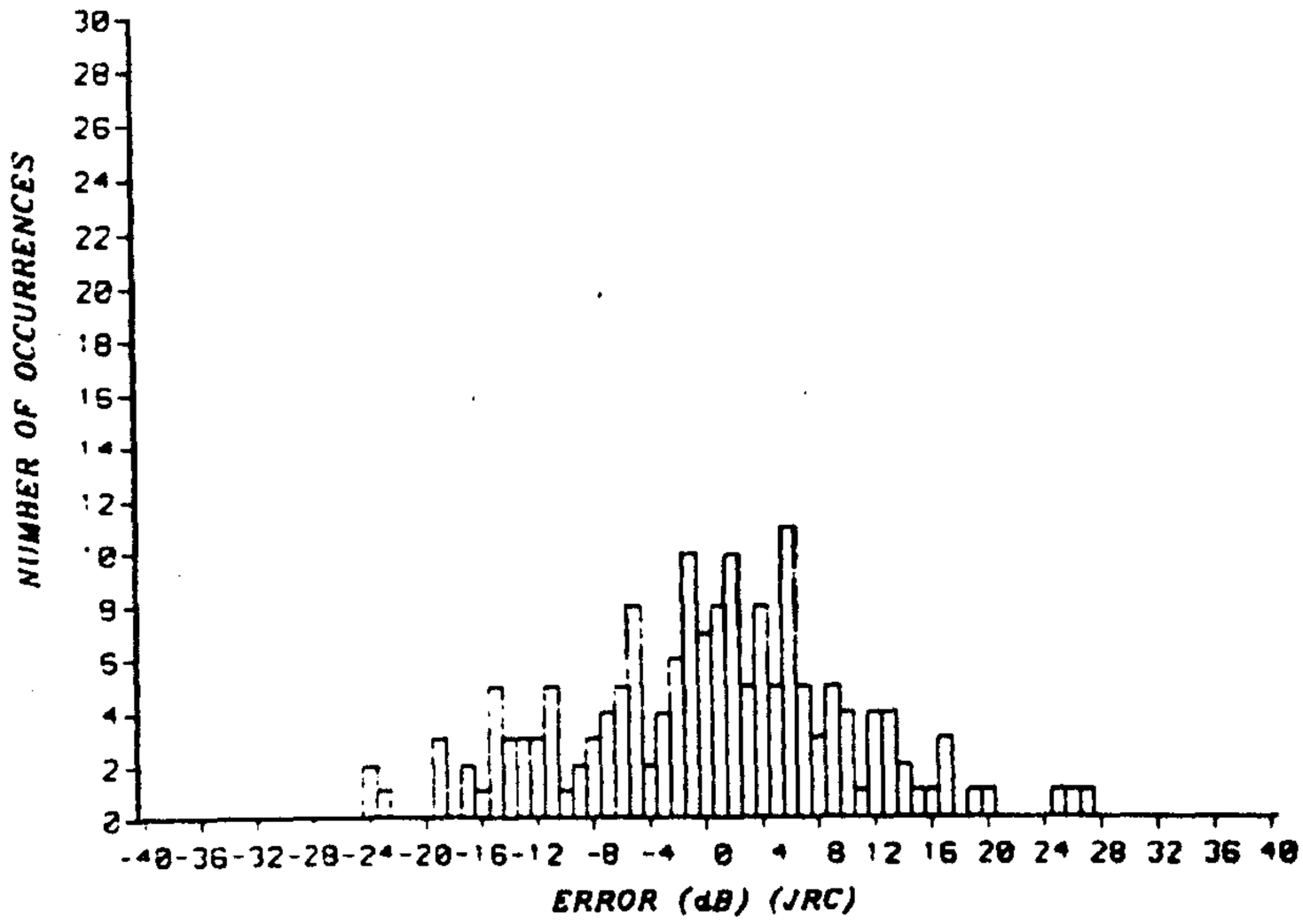

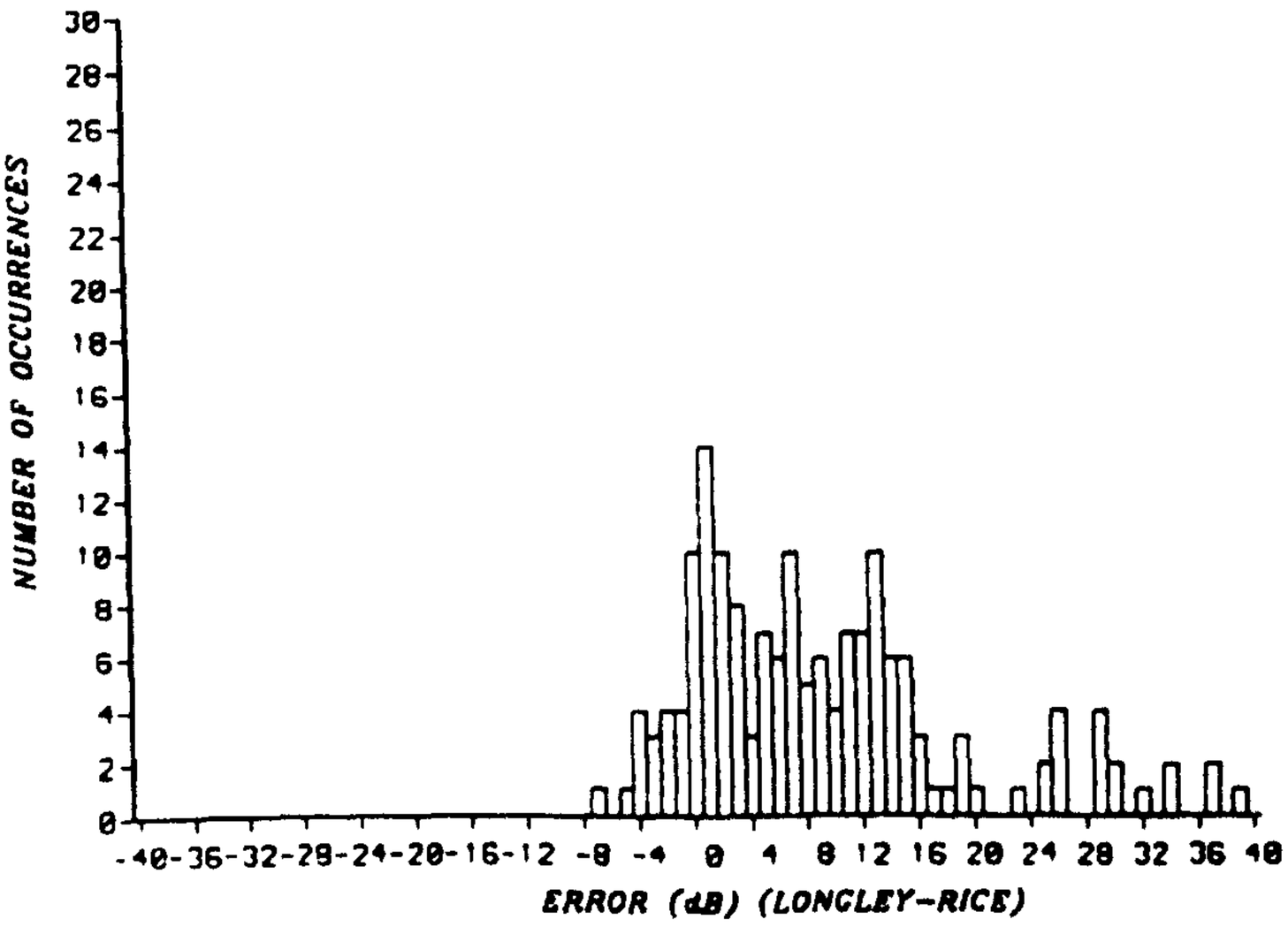

Fig. 5.10 Prediction Error Histograms (Wavertree).

Path profile from the Frodsham transmitter to square 136. The prediction does not respond to the increase in ground height near the receiver, hence leading to a pessimistic estimate of path loss.

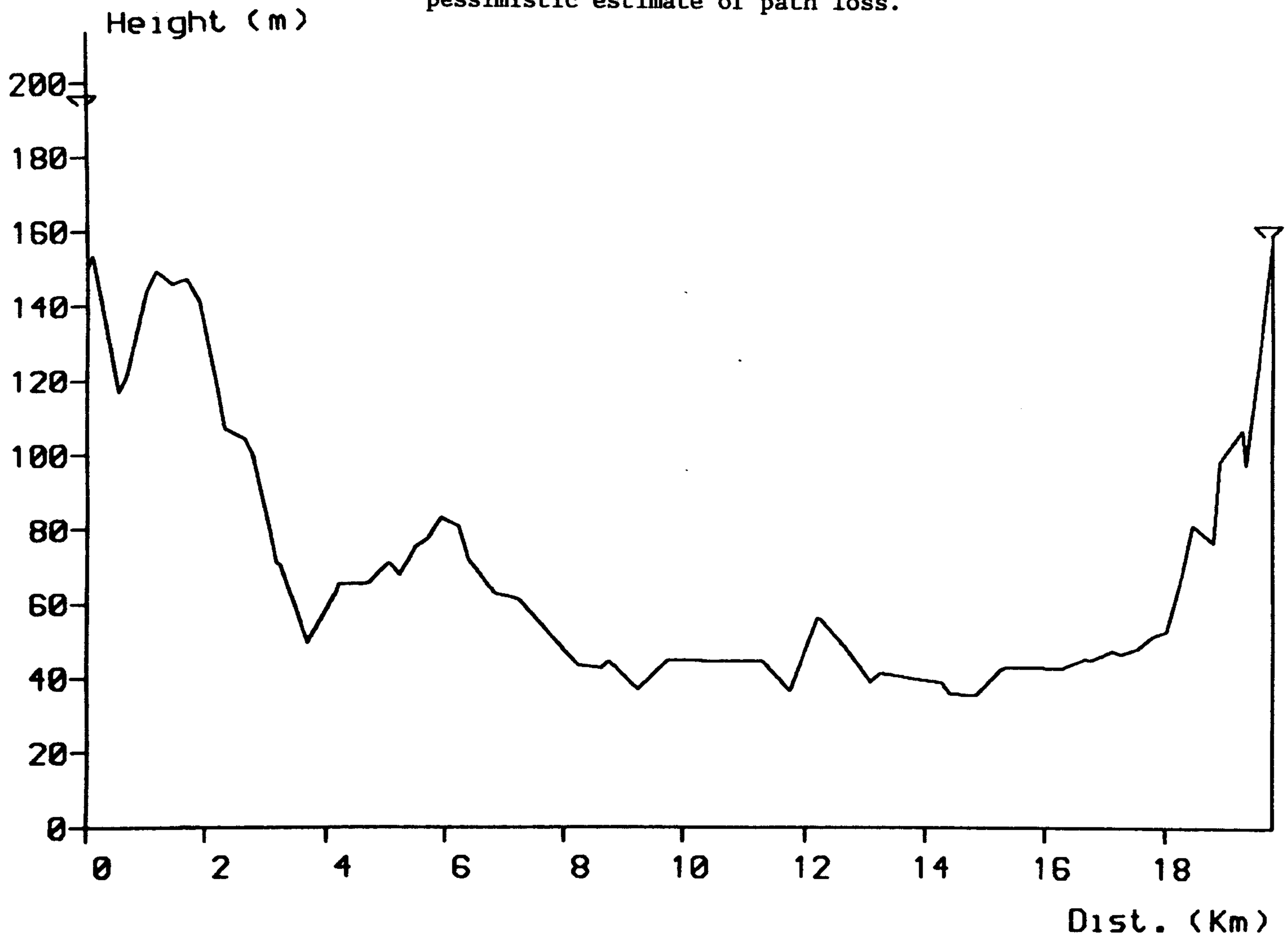

Fig. 5.11

Path profile from the Altrincham transmitter to square 36 showing how effective base station and mobile antenna heights are calculated.

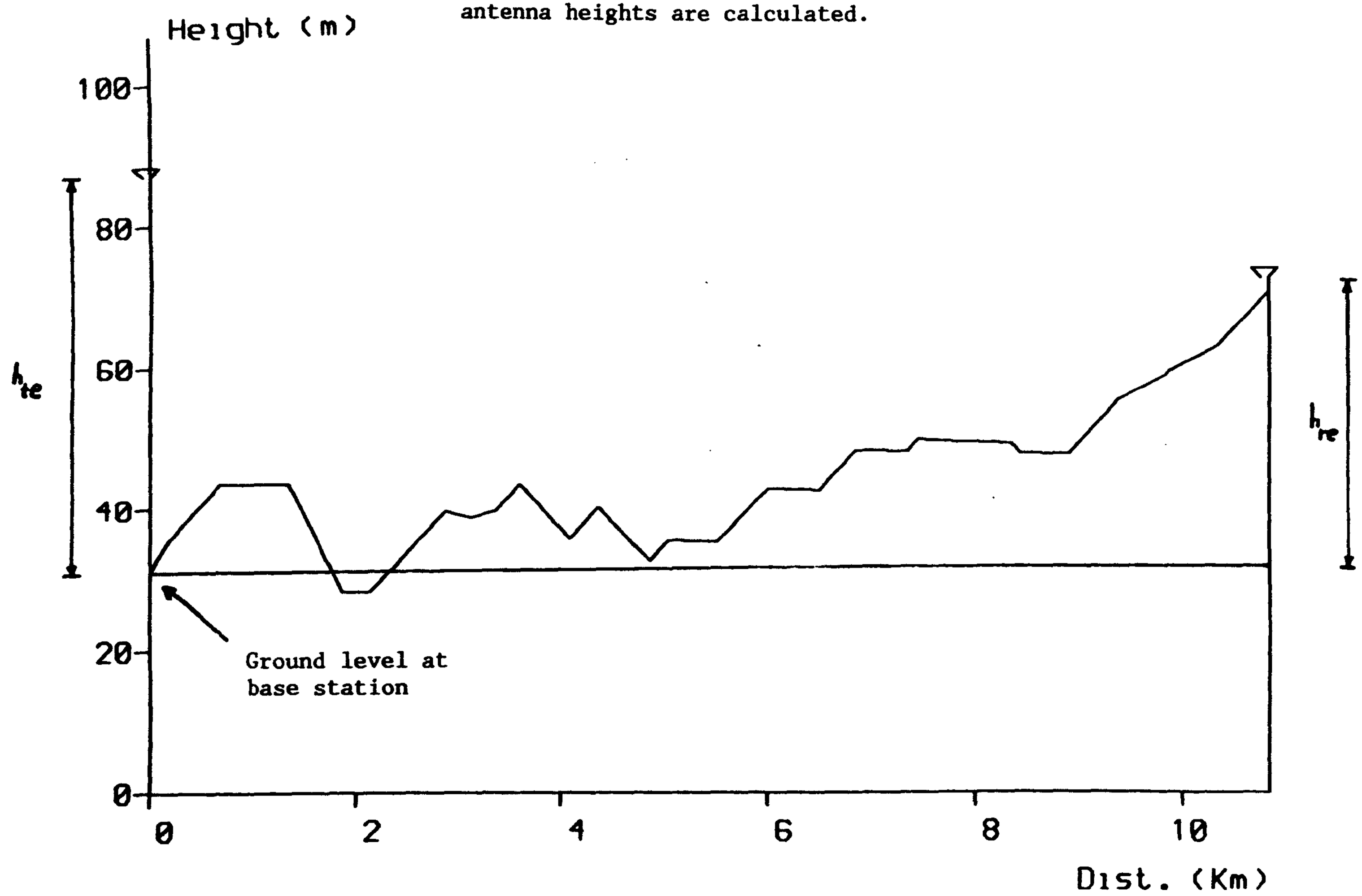

Fig. 5.12

Path profile from the Wavertree transmitter to square 80. It illustrates a situation where the mobile is located immediately behind an obstruction and where, consequently the Longley-Rice prediction produces a large error.

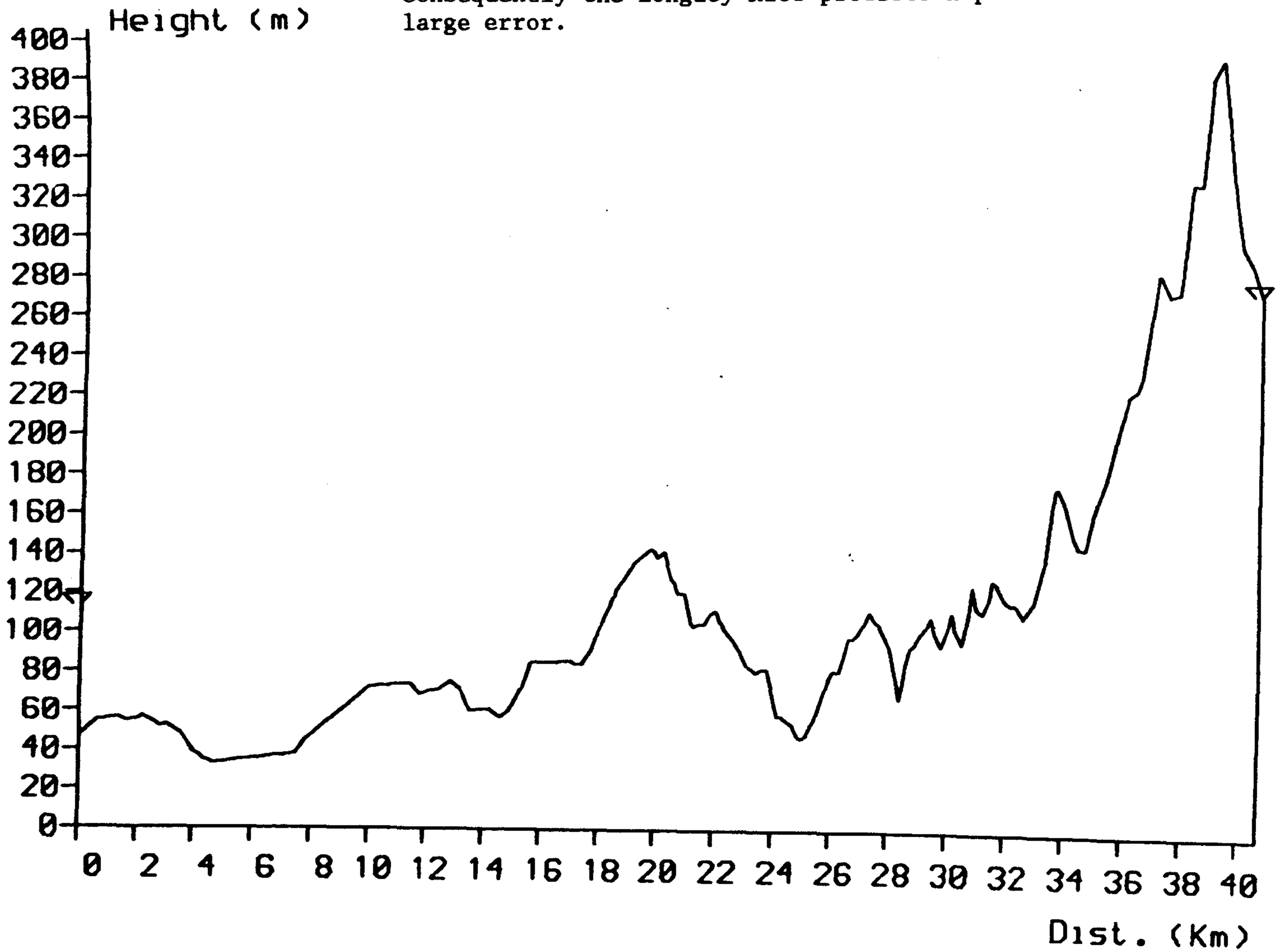

Fig. 5.13

Path profile from the Wavertree transmitter to square 63. The different path losses predicted for this typical square by the various models are shown in Table 5.4 (p.67).

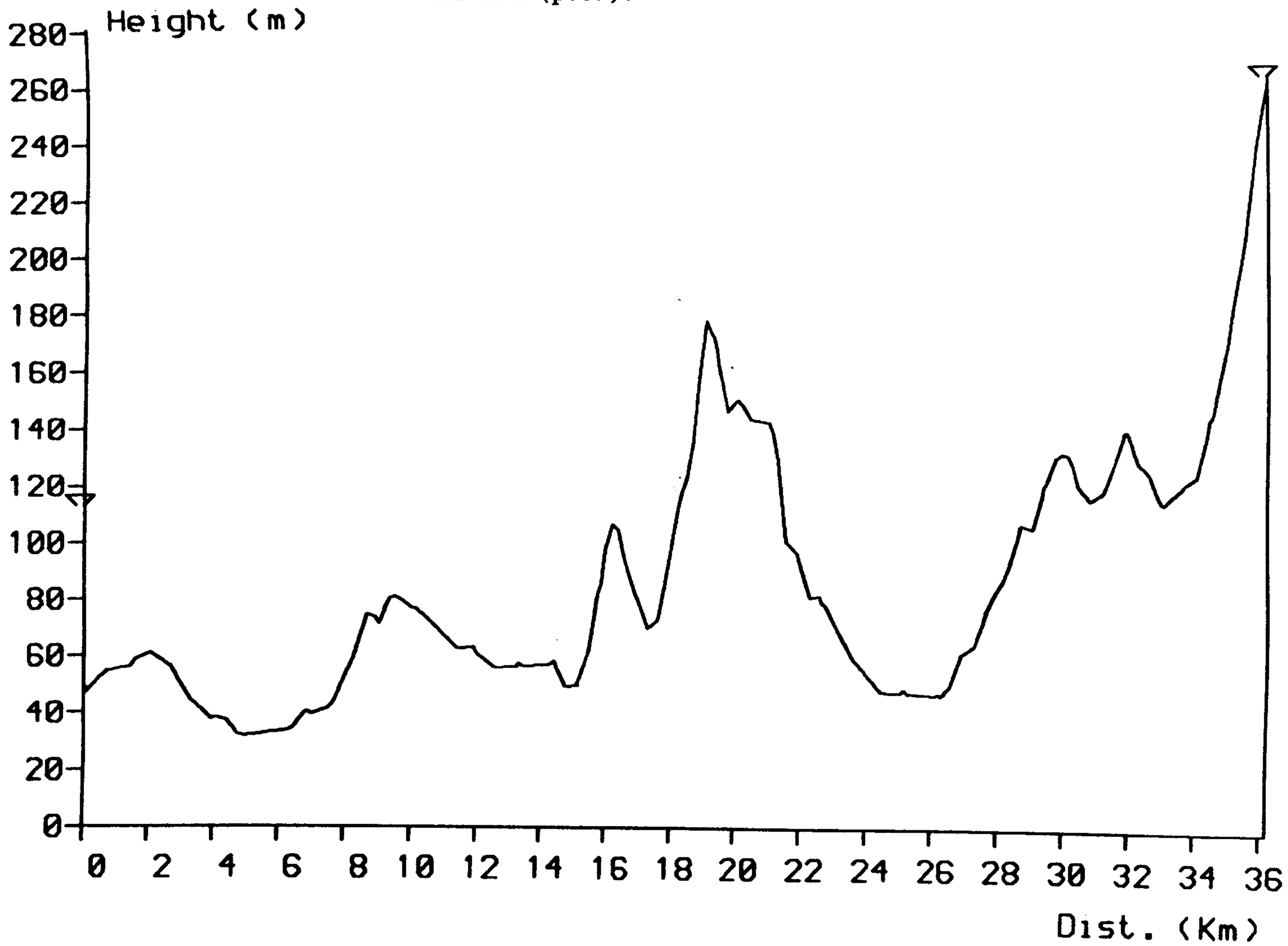

Fig. 5.14

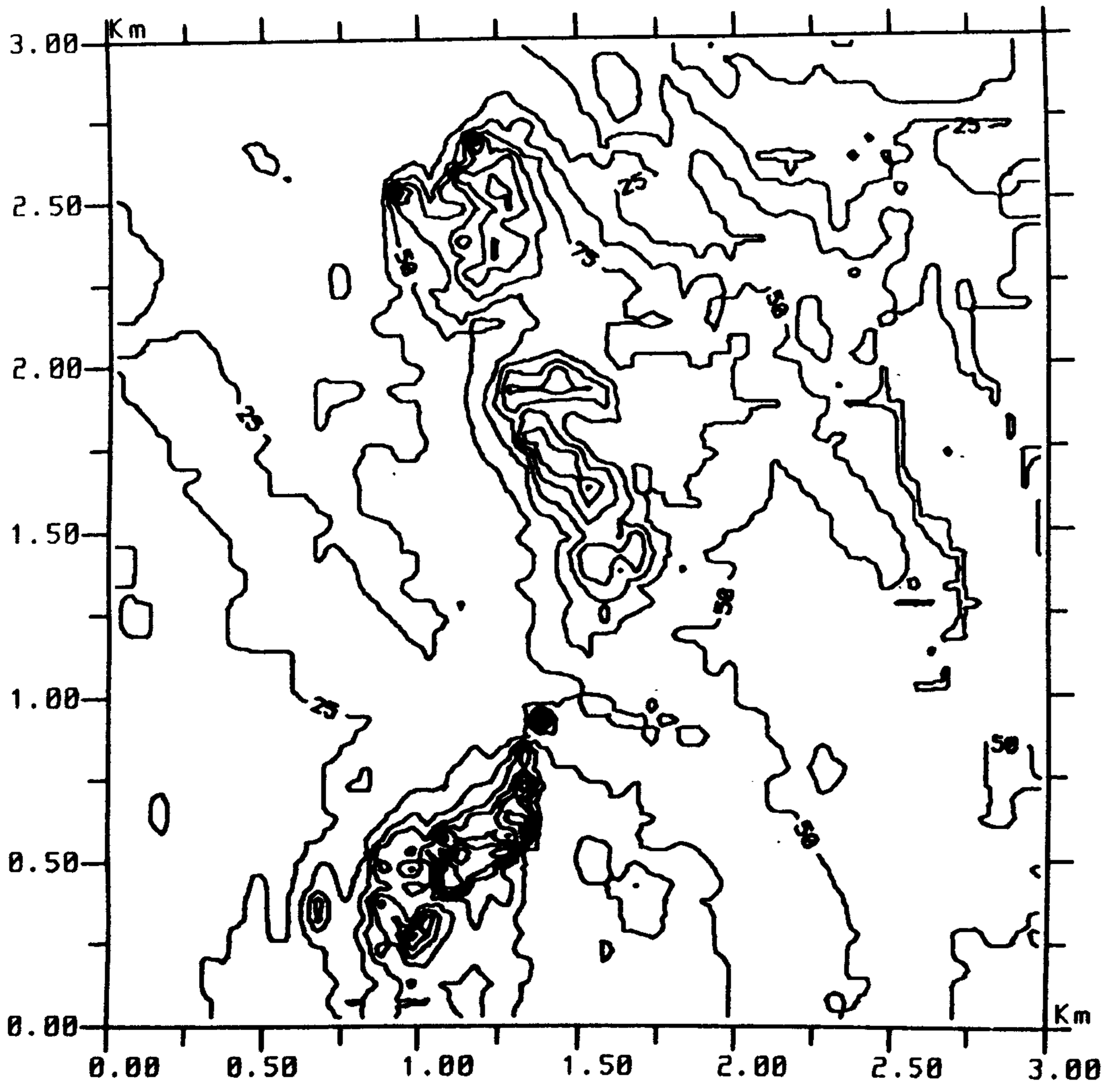

N

SD31	SD41	SD51	SD61	SD71
SD30	SD40	SD50	SD60	SD70
SJ39	SJ49	SJ59	SJ69	SJ79
SJ38	SJ48	SJ58	SJ68	SJ78
SJ37				SJ77
SJ36				SJ76
SJ35				SJ75

O.S. GRID
SQUARES; 10X10 Km

Fig. 5.15 Contour Heights in metres.

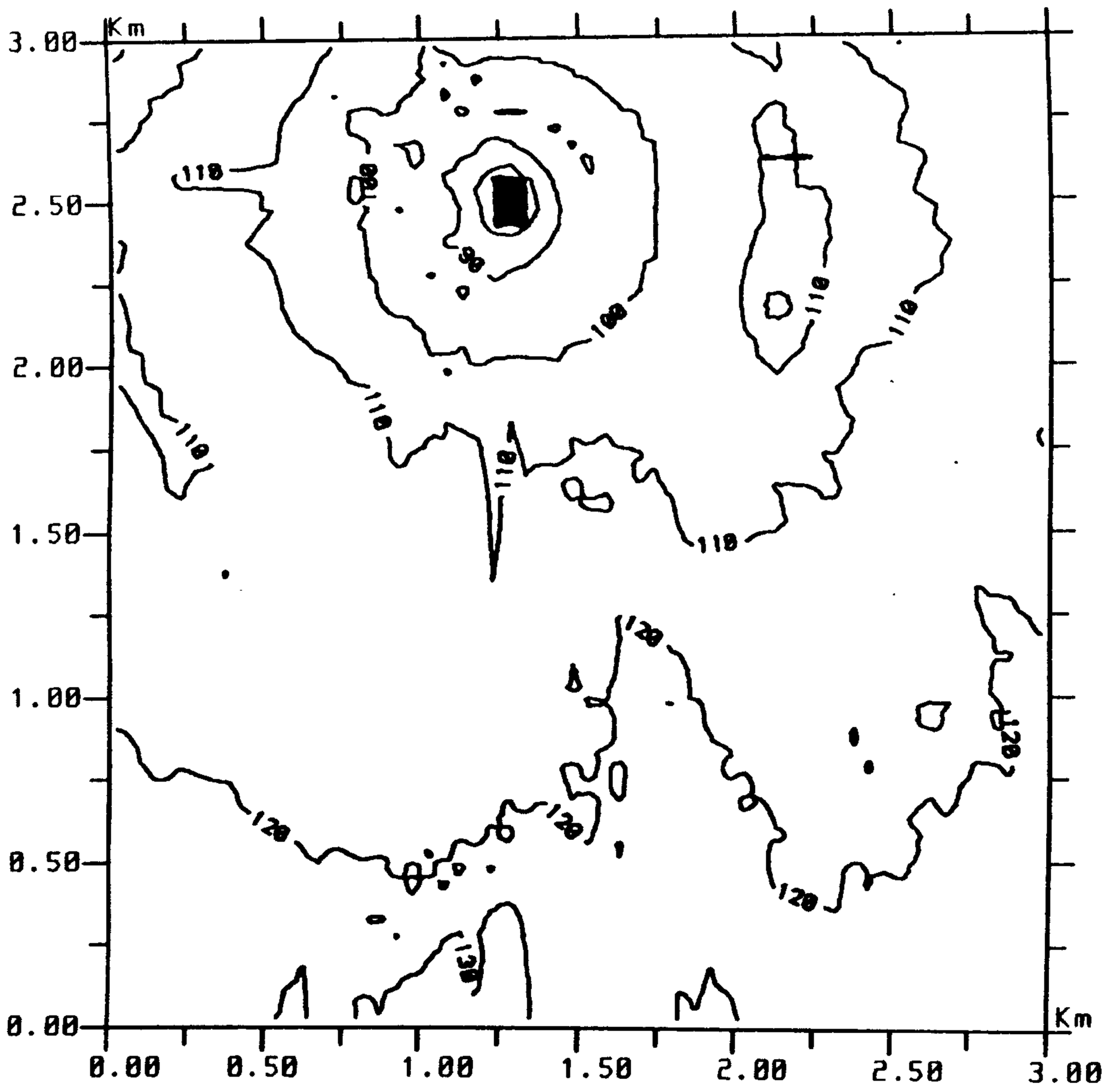

N

SD31	SD41	SD51	SD61	SD71
SD30	SD40	SD50	SD60	SD70
SJ39	SJ49	SJ59	SJ69	SJ79
SJ38	SJ48	SJ58	SJ68	SJ78
SJ37				SJ77
SJ36				SJ76
SJ35				SJ75

O.S. GRID
SQUARES; 10X10 Km

Fig. 5.16 Okumura Predicted Loss in dB.

CHAPTER 6

DEVELOPMENT OF THE MEDIAN PATH LOSS PREDICTION MODEL

The comparative study in Chapter 5 emphasised the problems which are associated with some of the available prediction models in estimating the median propagation loss over transmission paths in irregular terrain.

In general, the models are based to a varying degree on measured sets of signal strength data and the theory of radiowave propagation. The empirical approach takes into consideration the effects of many influencing factors implicit in the measured data, which cannot be accounted for in the theoretical approach. For example, measured data obtained in an urban area differs substantially from that obtained in an open area, even if the communication system parameters and terrain situation are similar and this reflects the influence of the environmental factors on the signal strength. In many situations theory can most reliably be used qualitatively to explain the spread in the measured data in terms of phenomena such as reflection and diffraction due to environmental features. An appropriate empirical model provides various statistical measures in relation to these features, which are associated with different areas. However, theory is used in derivation of the basic transmission loss such as free-space or plane-earth loss, which apply over a broad range of circumstances and are generally dependent on communication system parameters. The use of theory is also important in establishing appropriate relationships between various system or terrain related parameters, which are considered to be influencing the propagation of the transmitted signal. Measured data often

validates the theoretical considerations in these situations.

The aim of research in this field is to develop a more accurate method for the prediction of median path loss and at the same time, make the prediction task simpler and more efficient. Obviously the type and extent of the available measured data influences the propagation analysis and limits the number of factors which can be incorporated in any particular case. For example, data obtained over a fairly flat area is not suitable for a study of the effect of terrain features on propagation, and measured data collected in mainly rural areas cannot be used for the analysis of environmental clutter such as buildings. The use of a constant terrain loss factor in conjunction with the free-space or the plane-earth path loss, is quite inadequate for paths containing large irregularities, such as hills and mountain peaks, which have to be considered on their own merits in terms of the diffraction loss in their shadow regions. The approach adopted was to investigate the applicability of the theoretical treatments of free-space, plane-earth and the diffraction loss, and ways of incorporating them into the prediction model, and to look for a practical means of defining the required parameters in relation to the intervening terrain features in the transmission path separating the two terminals.

For the relatively long transmission paths considered in the present work, a value of $K = 4/3$ was assumed to allow for the earth's curvature, which also implies normal atmospheric conditions.

6.1 COMPARISON OF DIFFRACTION TECHNIQUES

Having the terrain data profiles as input, a computer routine locates edges which obstruct the line-of-sight path and also checks for first Fresnel zone clearance. At the operating frequency of 139 MHz, none of the line-of-sight paths considered were found to have adequate clearance. The diffraction techniques due to Bullington, Epstein-Peterson, Japanese Atlas and Deygout (section 2.3.10) were implemented on the computer and the various estimates of diffraction loss caused by the intervening obstacles in the path were subsequently compared.

The treatment of obstacles in the path as a series of knife-edges may seem oversimplified, since it ignores the contributions due to roundedness of the existing hills, with large radius of curvature compared to the wavelength. However, the roughness of the ground and the relatively greater diffraction losses, in many cases, reduce the effect of curvature of the obstacles and the idealisation of typical ground profiles over irregular terrain situations by knife-edges, offers a suitable method for rapid and repeated use.

The computer operates on the path profile matrix and identifies the points on the path which are not clear of the direct line drawn from one terminal (or a previously located point) to another. In many cases, it would be unrealistic to assume each one of these points constituted a knife-edge, one such situation is illustrated in Fig. 6.1a, in which a large number of points indicated by vertical lines in the path profile have been identified as obstructions by the computer routine. If each of these obstructions was treated as a knife-edge, an unrealistic value of estimated

diffraction loss would result. However, using a virtual edge construction approach for paths containing more than three edges, as suggested by the JRC method (section 3.2), was found to be a good approximation and resulted in largely improved results. Table 6.1 lists the values of diffraction loss estimated by the diffraction techniques for the path profile ALT165 considering all the edges which are located by the computer (case a) and when the three edges approach is used (case b).

Table 6.1

Path Profile ATL165	Estimated Diffraction Loss (dB)			
	Bullington	Epstein-Peterson	Japanese	Deygout
a	9.3	110.0	110.8	137.8
b	9.3	20.6	20.7	42.8

In order to make a comparison with the measured value of path loss, predicted values of path loss were calculated for each method by adding the diffraction loss and a basic transmission loss, as outlined in Table 6.2, where the basic loss is assumed to be either the theoretical free-space loss (case I) or the plane-earth loss (case II) using the value of antenna heights above local ground.

Table 6.2

Path Profile ALT165	Free-Space Loss (dB)	Plane-Earth Loss (dB)	Measured Path Loss (dB)	Predicted Path Loss (dB)							
				Bullington		Epstein-Peterson		Japanese		Deygout	
				I	II	I	II	I	II	I	II
a	106.5	141.5	141.0	115.8	150.8	216.5	251.5	217.3	252.3	244.3	279.3
b	106.5	141.5	141.0	115.9	150.8	127.1	162.1	127.2	162.2	149.3	184.3

Fig. 6.1b shows, for the same profile, the position of the virtual

edge, whose summit is the intersection point of two lines, each line joining the top of the two nearest edges of each terminal. Most radial path profiles from the transmitter to the centre of measurement squares in the Cheshire field trails contain up to three edges. However, a number of profiles have more edges obstructing the direct line-of-sight and in these cases the number of edges is reduced to three before calculating the diffraction loss. Figs. 6.2 to 6.4 show the loss estimated by the diffraction techniques, versus square number, for the three sites in the Cheshire area. The squares with zero diffraction loss indicate line-of-sight transmission and for this situation, only the Deygout method accounts for edges below the line-of-sight which are not clear of the first Fresnel zone. Generally, all the models estimate higher diffraction losses for transmission paths in the Wavertree test area, emphasising that terrain is more hilly in this region. The predicted path loss values obtained by adding the free-space loss to the estimated diffraction loss, as suggested by the models, have been compared against the measured data for the three test areas and the results are listed in Tables 6.3 and 6.4

The highest correlation coefficients between the predicted and measured path loss are obtained for all the models in the Newton Firs (Frodsham) test and the lowest in the Altrincham test, incidating that in the Newton Firs test, the prediction follows the measurement trend more closely. One reason for this could be due to the existence of more path profiles with similar terrain situations within this area. The path profiles in the Altrincham test vary more in terms of obstructing terrain features in the path which results in a larger variation in the values of estimated diffraction loss and

Table 6.3

Base Station Location	Correlation Coefficient				Mean Error (Pred.-Meas.) (dB)			
	Bullington	Epstein-Peterson	Japanese	Deygout	Bullington	Epstein-Peterson	Japanese	Deygout
Newton Firs	0.74	0.78	0.78	0.81	-20.3	-18.5	-18.3	-11.7
Altrincham	0.71	0.53	0.52	0.47	-29.1	-24.9	-24.6	-12.3
Wavertree	0.68	0.70	0.69	0.71	-21.0	-18.7	-17.8	- 6.7

Table 6.4

Base Station Location	Standard Error (dB)				Standard Deviation of Error (dB)			
	Bullington	Epstein-Peterson	Japanese	Deygout	Bullington	Epstein-Peterson	Japanese	Deygout
Newton Firs	21.0	19.4	19.3	14.3	5.3	5.7	5.9	8.2
Altrincham	29.4	25.9	25.7	17.3	4.4	7.2	7.4	12.2
Wavertree	21.9	19.9	19.3	13.1	6.1	6.8	7.6	11.3

hence the values of prediction error.

It is not difficult to see on general grounds that the Bullington method produces optimistic results, and by using the method, the lowest values of diffraction loss were predicted. The Deygout method produced the highest values of diffraction loss and the lowest standard errors. However, it has the largest values of the standard deviation of error, indicating large prediction errors for many path profiles.

The comparison of various statistical measures to assess the models' capabilities resulted in the Epstein-Peterson and Japanese models being considered as most reliable for the estimation of diffraction loss. The Epstein-Peterson and Japanese models produce similar results, with the r.m.s. difference value being about 0.6 dB for the Newton Firs and Altrincham tests, and 2 dB for the Wavertree test. However, as the obstructing knife-edges become closer to each other, the difference between the two models increases. Fig. 6.5 shows a typical path profile where the obstructing knife-edges lie very close to each other near the mobile receiver. The diffraction loss estimated by each model is listed in Table 6.5, the difference in the values obtained by the Epstein-Peterson and Japanese methods being 7 dB.

Table 6.5

Path Profile	Estimated Diffraction Loss (dB)			
	Bullington	Epstein-Peterson	Japanese	Deygout
WAV 78	21.8	25.9	32.9	48.7

It would seem most appropriate to treat these close edges as one effective knife-edge, and the Bullington method constructs such a single knife-edge in between these edges for its calculation of diffraction loss. However, for these situations, the Epstein-Peterson method produced closer results to those of Bullington and overall it was found to be more accurate for the terrain profiles considered. The fact that using the Epstein-Peterson method consumed less computing time, is another advantage in the deployment of the method for the computerised prediction model.

For line-of-sight transmission paths with inadequate first Fresnel zone clearance, the diffraction loss is calculated as that caused by the dominant edge.

6.2 VARIATION OF MEDIAN PATH LOSS WITH RANGE

One component of propagation analysis between a transmitter and a mobile receiver is the determination of the dependence of the transmission loss on range from the base station. In general, the median path loss increases with the distance between the terminals. To observe the range dependence of the measured path loss, they were plotted as shown in Figs. 6.6 to 6.8, and the best fit straight lines through these points were calculated by minimising the r.m.s. error. In the Frodsham test, the slope of this line was found to be 20.6 dB/decade which is very close to the square law function with range (20 dB/decade) of the theoretical free-space loss. A clutter factor can now be determined by finding the difference between the best square law fit and a line calculated using the free-space equation. This factor was found to be 25 dB for the Frodsham test.

The slopes of the best fit lines through the measured median

path loss versus range were found to be 31 dB/decade and 30.7 dB/decade for the Altrincham and Wavertree tests respectively. For the Altrincham test, the slope and the clutter factor (which was calculated to be about 35 dB) are much higher than those of Frodsham. This could be due to the fact that the Altrincham transmitter is situated in an urban area and its height is less than that of the Frodsham site. However, the slope values for both Altrincham and Wavertree tests are halfway in between the value of the square law function and the value given by the fourth law function with range (40 dB/decade) of the plane-earth loss.

6.3 DEFINITION OF EFFECTIVE ANTENNA HEIGHT

The comparative study of the prediction models revealed the importance of the way in which the position of the effective reflecting plane is defined in relation to the calculation of the effective antenna height of the terminals. In particular, the value of the base station effective antenna height affects the propagation calculations significantly, since in practice, as the antenna is mounted higher above the surrounding terrain features and other obstacles, the propagation area coverage is increased and the effect of multipath on the transmitted signal is reduced, resulting in an effective gain.

Following Okumura's definition (section 3.4), the base station effective antenna height becomes negative when the antenna height above local ground is less than the average ground level in the 3-15 Km range in the transmission path, and for these situations, the structural height of the antenna was used in the calculations. In the JRC method the effective reflecting plane is defined as the

horizontal plane drawn through the foot of the terminal which has the lowest local ground level, and this resulted in large errors in the calculation of the path loss. The Longley-Rice prediction model considers the terrain between each terminal and its radio horizon obstacle, to determine the position of the effective reflecting plane for that terminal. It is defined in this range as the smooth curve fitted by the least squares method to terrain elevations. Although the Longley-Rice model takes into account the effect of the terrain irregularity in parts of the transmission path for the calculation of the effective reflecting plane, it often ignores a large section of the radial path profile. An attempt was made to derive a correction factor which could be added to the transmitter antenna height above ground and to relate it to the terrain variations in the path. The terrain irregularity parameter, Δh, as defined by the Okumura and Longley-Rice models, was used for this purpose, but no viable conclusions could be drawn from the results.

An alternative method which takes into account the terrain variations along the whole path will be discussed. Initially the line joining the bases of the transmitter and the receiver is fitted and the median value of the deviations of terrain heights from this line, at all points along the path, is then obtained. If the median value is negative, i.e. on average the ground lies below the drawn line, the absolute value of the median deviation is added to the transmitter structural height. The mobile antenna height is small with respect to local terrain variations and therefore to make the local reflections more relevant in these situations, the height of the mobile antenna above ground is considered for calculating the transmission loss.

6.4 A PROPOSED IRREGULAR TERRAIN PREDICTION MODEL

Any prediction model depends on a number of input parameters relevant to the particular propagation mode. Certain input parameters have more significant effects than others on the accuracy of predicting the median path loss. However, in deriving a method for predicting the transmission loss, each input parameter should be considered as to the availability of input data and the extent of its influence on the results. Apart from the basic input parameters of transmission frequency, range and height of the terminals above ground, terrain data and information about environmental clutter such as buildings and foliage, particularly in the vicinity of the mobile, are required.

In order to make reliable predictions of radiowave propagation over irregular terrain, a proper treatment of the influencing terrain factors is required. However, it is not usually feasible to devise a detailed mathematical model of real terrain because of the complexity of the surface variations and because of the inevitably large amount of computer time which would be required to produce useful results. In addition, the lack of detailed knowledge about other features in the path, such as man-made obstacles and trees which could seriously modify the transmitted signal, causes the prediction work to resort to some form of approximation of the propagation medium. The use of a knife-edge approximation to calculate the diffraction losses caused by the intervening obstacles in the transmission path, provides a simple and efficient way of determining the terrain losses by the computerised prediction method. In the above, it was shown that the predicted median path loss, which was calculated as the sum of the free-space

loss and the diffraction loss, underestimated the measured loss. A further investigation revealed that when the plane-earth loss replaced the free-space loss, the prediction overestimated the measurement. The JRC model (section 3.2) calculates the median path loss as the sum of the diffraction loss and the greater of the free-space and the plane-earth loss.

The free-space path loss between isotropic antennas, with reference to Chapter 2, is given by:

$$L_F = 32.45 + 20 \log_{10} f_{MHz} + 20 \log_{10} d_{Km} \quad \text{dB}$$

and the plane-earth loss as:

$$L_P = 120 + 40 \log_{10} d_{Km} - 20 \log_{10} h_{te}\, h_{re} \quad \text{dB}$$

where the effective antenna heights, h_{te} and h_{re} are in metres. There is a difference of 20 dB/decade in the factor which determines the way in which these formulae predict the loss as a function of range. Following the JRC approach, it is often the case that for a given transmission frequency and antenna heights and over relatively smooth terrain, the free-space loss dominates at shorter distances, then as the distance increases, there will be a sudden change in the basic path loss slope with respect to range. It is however a common-sense requirement that the predicted path loss follows a smooth curve with changing transmission range when other propagation factors remain relatively constant. Therefore, the prediction model should incorporate the loss factors in an appropriate way and is also required to be capable of dealing with varying degrees of terrain irregularity in the transmission path. The approach adopted by Blomquist and Ladell (section 3.3) was found to be the most appropriate, as the median path loss is given by:

$$\text{Path Loss} = L_F + \left((L_p - L_F)^2 + L_D^2 \right)^{1/2} \quad \text{dB} \qquad (6.1)$$

where L_D is the diffraction loss in dB.

Although the above relationship does not appear to be based on any relevant radio propagation theory, it provides more realistic values of path loss for practical transmission paths over irregular terrain. It has also an appropriate theoretical structure for some particular propagation conditions. For example, when the ground in the transmission path is flat and the diffraction loss tends towards zero, the median path loss will be equal to the plane-earth loss, L_p. For highly irregular terrain, the value of L_D is more significant in the root squared term of (6.1) and the predicted path loss tends to be approximately equal to the sum of the free-space loss and the diffraction loss, $L_F + L_D$. Finally, the model provides a smooth transition in moving from one extreme propagation condition to another.

To summarise the above arguments, the following steps are proposed for the calculation of the median path loss in rural areas over irregular terrain:

1. Determine the transmission path terrain profile and use the value of K = 4/3 to correct the intervening terrain heights for the effective earth's curvature.

2. Calculate the median deviation of terrain heights along the path about the line joining the bases of the two terminals. If the median value is negative, add its magnitude to the base station transmitting antenna height above ground to derive the effective antenna height, otherwise take the structural antenna height.

3. Use the Epstein-Peterson method to compute the knife-edge diffraction loss, L_D, for up to three obstructing edges in the path. If a particular path profile has a greater number of edges, reduce the number to three, following the method suggested by the JRC and outlined in the preceding sections. For paths with line-of-sight transmission, if there is not adequate first Fresnel zone clearance, the loss is calculated as that due to the dominant obstacle causing the inadequacy, otherwise it will be taken as zero.

4. Calculate the free-space loss, L_F, and the plane-earth loss, L_P, and use relation (6.1) to derive the total median path loss.

6.5 PERFORMANCE OF THE PROPOSED MODEL AGAINST CHESHIRE DATA

A comparative study of path loss predictions using the proposed irregular terrain model and the corresponding measured median loss obtained as a result of Cheshire field trials, has been performed. In the analysis, various statistical measures were considered, similar to those previously calculated for other prediction models, so that they could be compared with each other. Table 6.6 lists the comparative results for each test area and also when all the transmission paths from the three tests are considered.

Table 6.6

Base Station Location	Correlation Coefficient	Mean Error (dB)	Standard Error (dB)	Standard Deviation of Error (dB)	Slope of Regression Line
Newton Firs	0.78	2.6	5.4	4.7	0.98
Altrincham	0.83	-1.4	4.1	3.9	0.76
Wavertree	0.69	0.7	5.7	5.7	0.82
All	0.83	0.6	5.1	5.0	0.98

As can be realised from the above table, the proposed model

produces much better results against Cheshire data than other prediction models studied in Chapter 5. The value of correlation coefficient between the predicted and measured values is higher in each case, a fact which can be observed by examining the plots of measured and predicted path loss values shown in Figs. 6.9 to 6.11 for the three tests. The prediction errors produced by the proposed model are much less than those of the other models which have been considered in the present work, as is indicated by the values listed in the standard error column of Table 6.6.

Although there are a small number of test squares with a relatively large prediction error, a significant improvement has been achieved in prediction of path loss for the test squares where other propagation models had produced very large errors. For example, the assumption of large values for the effective antenna height of the mobile receiver by the JRC model, which produced very optimistic results, does not exist in the proposed model. Also, the model copes much better with situations where the mobile lies very close behind an obstructing edge in the transmission path, which caused the Longley-Rice model to produce a large prediction errror in these situations. The regression lines fitted through the measured versus predicted path loss values, are generally closer to the ideal line of unity slope, as shown in Figs. 6.12 to 6.14 for the three tests. The values of mean error are quite small and the prediction errors spread more closely about the mean value, compared to the prediction error distributions obtained for other models in the previous chapter. This is indicated by the small values of standard deviation of error listed in Table 6.6 and the plots in Figs. 6.15 to 6.17 which show the error histograms produced by the proposed model.

Of all the 559 radial path profiles in the Cheshire test area, 156 test squares have line-of-sight transmission and the other 403 squares include at least one obstructing edge in the transmission path. The proposed prediction model copes equally well in both cases, producing values of correlation coefficients between prediction and measurement of 0.85 and 0.75 for the line-of-sight and obstructed paths respectively. The value of mean prediction error for the line-of-sight paths was found to be 2.7 dB and for the obstructed paths about -0.1 dB. The calculations showed values of around 5 dB for the standard error and the standard deviation of error for path loss prediction in both types of transmission path situation.

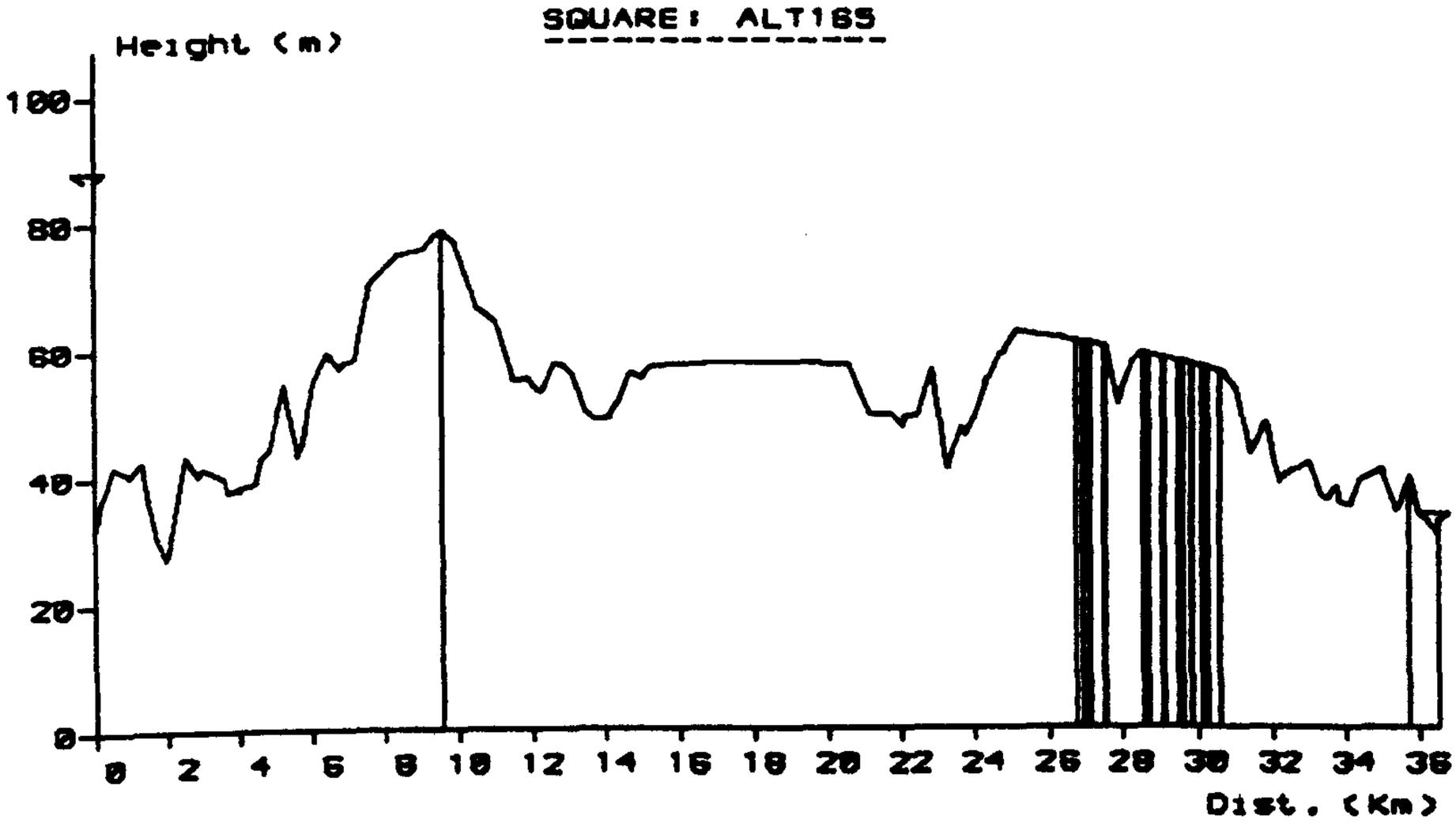

(a)

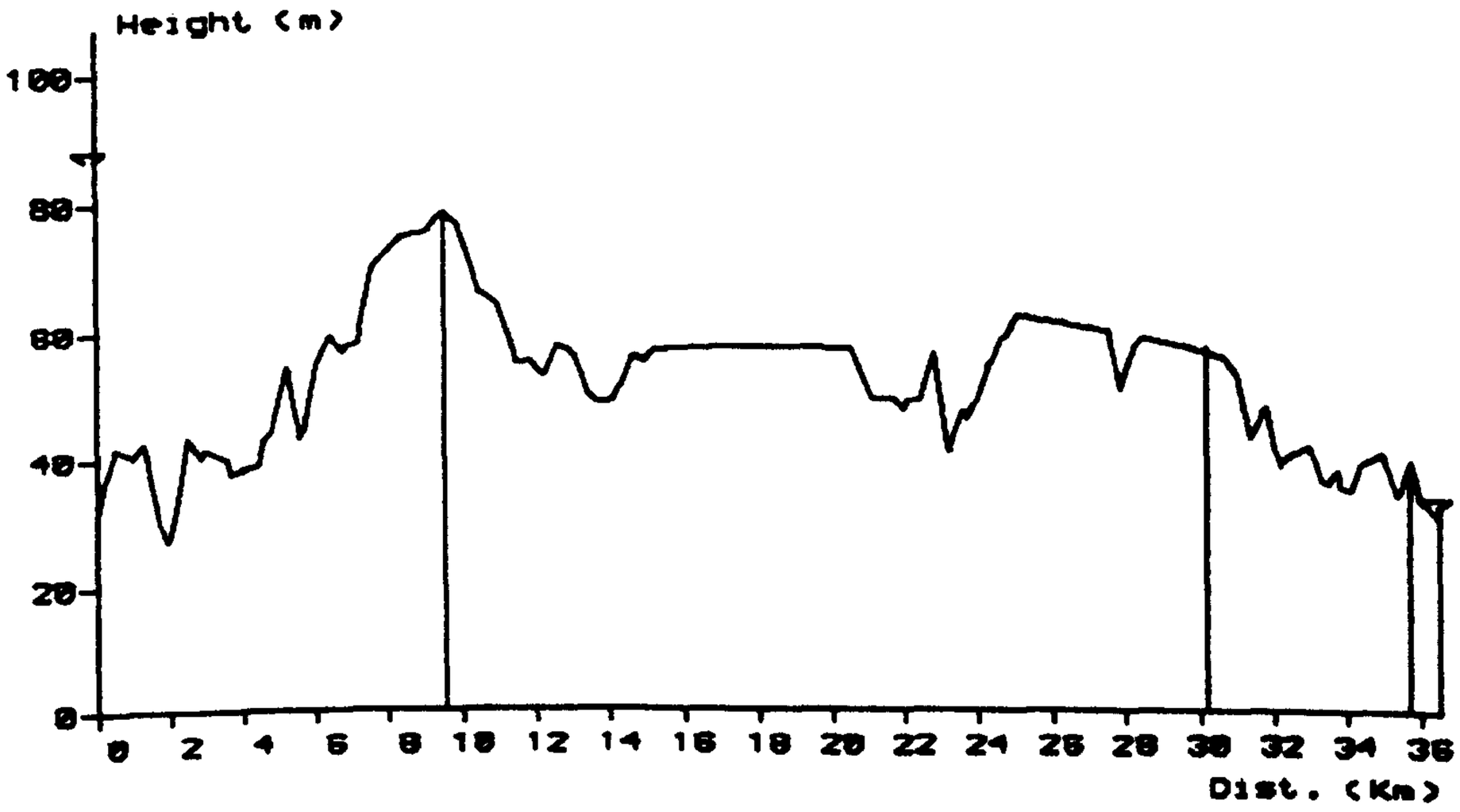

(b)

Fig. 6.1 A Computer Generated Path Profile,
(a) normal edge location
(b) three edges approach.

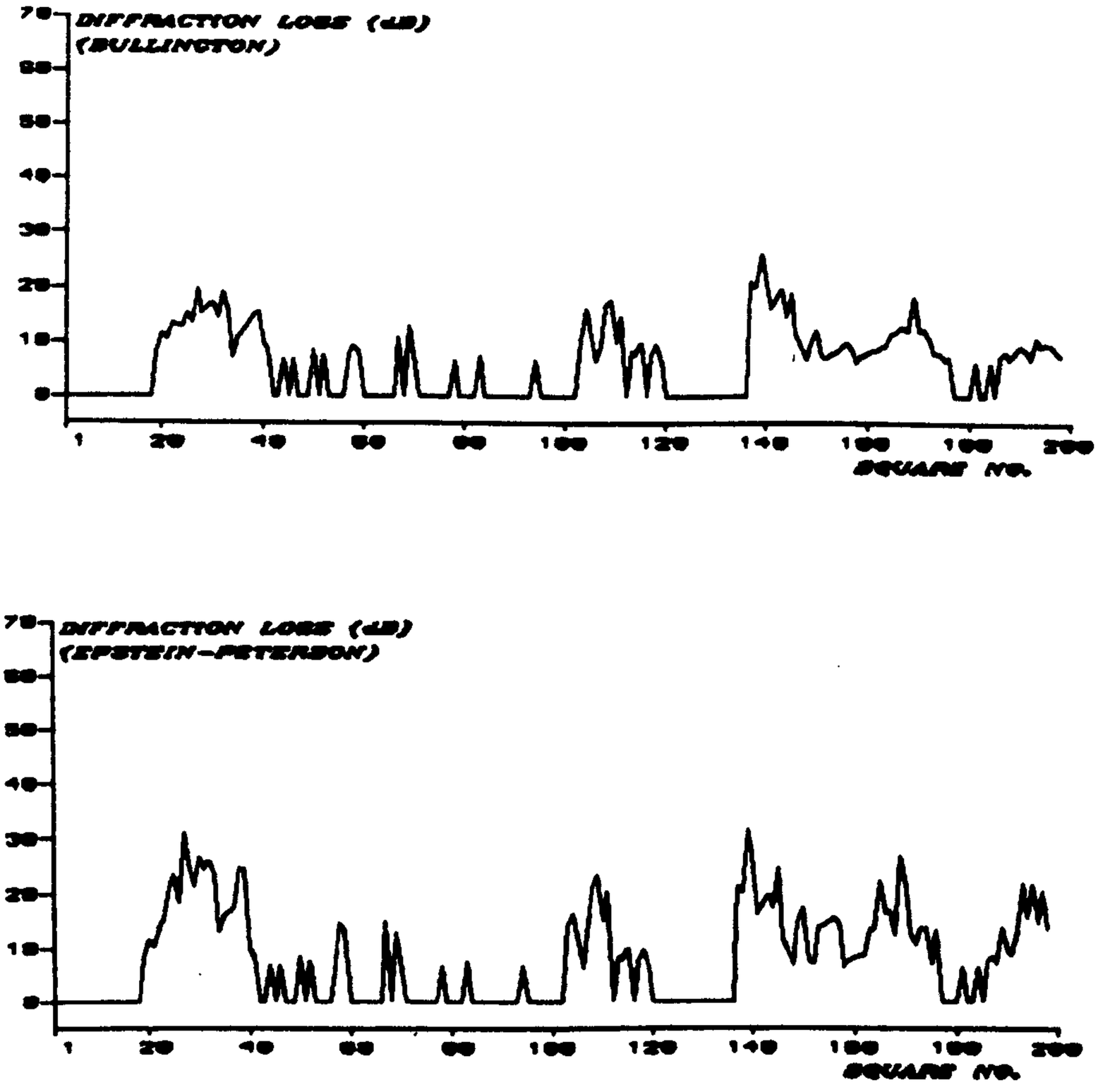

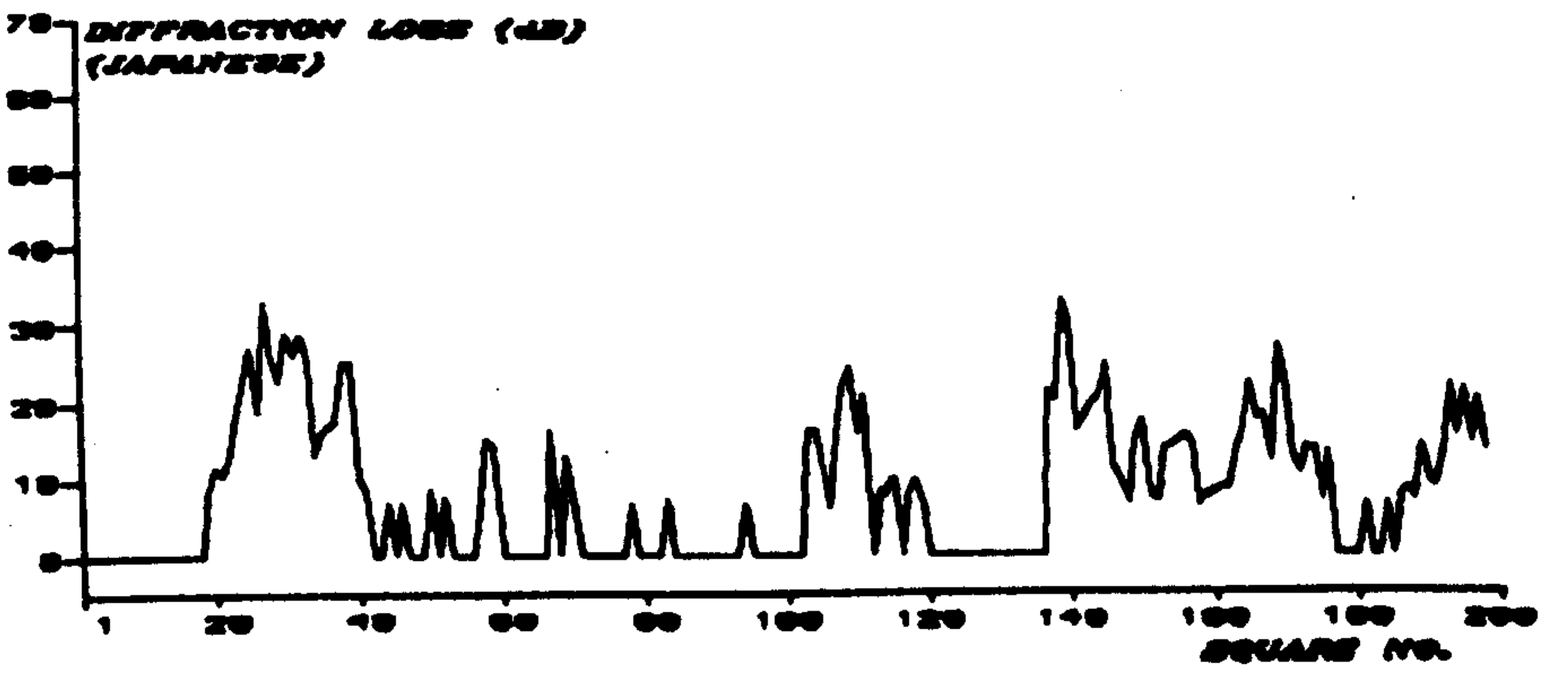

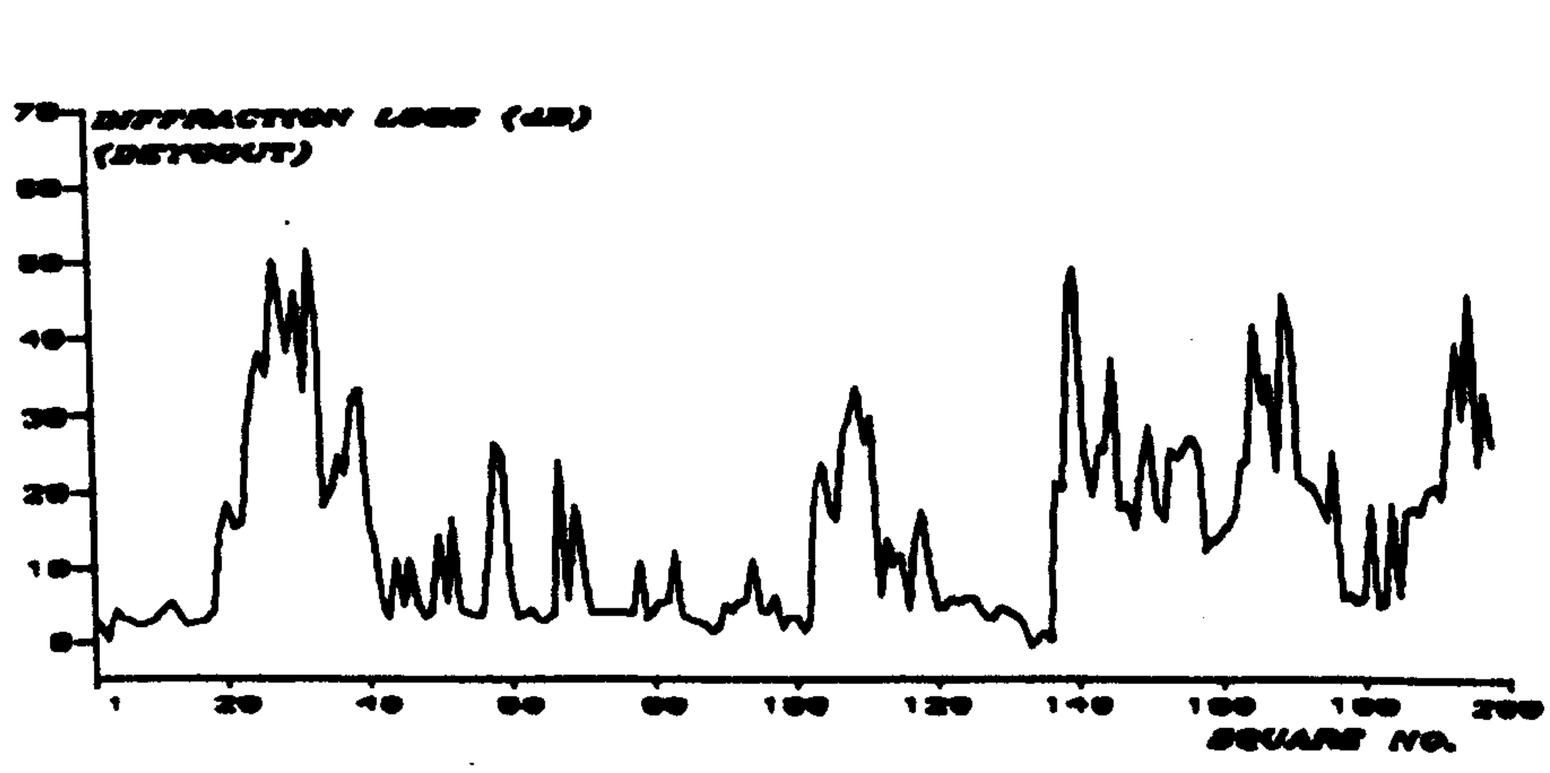

Fig. 6.2 Estimated Diffraction Loss (Newton Firs).

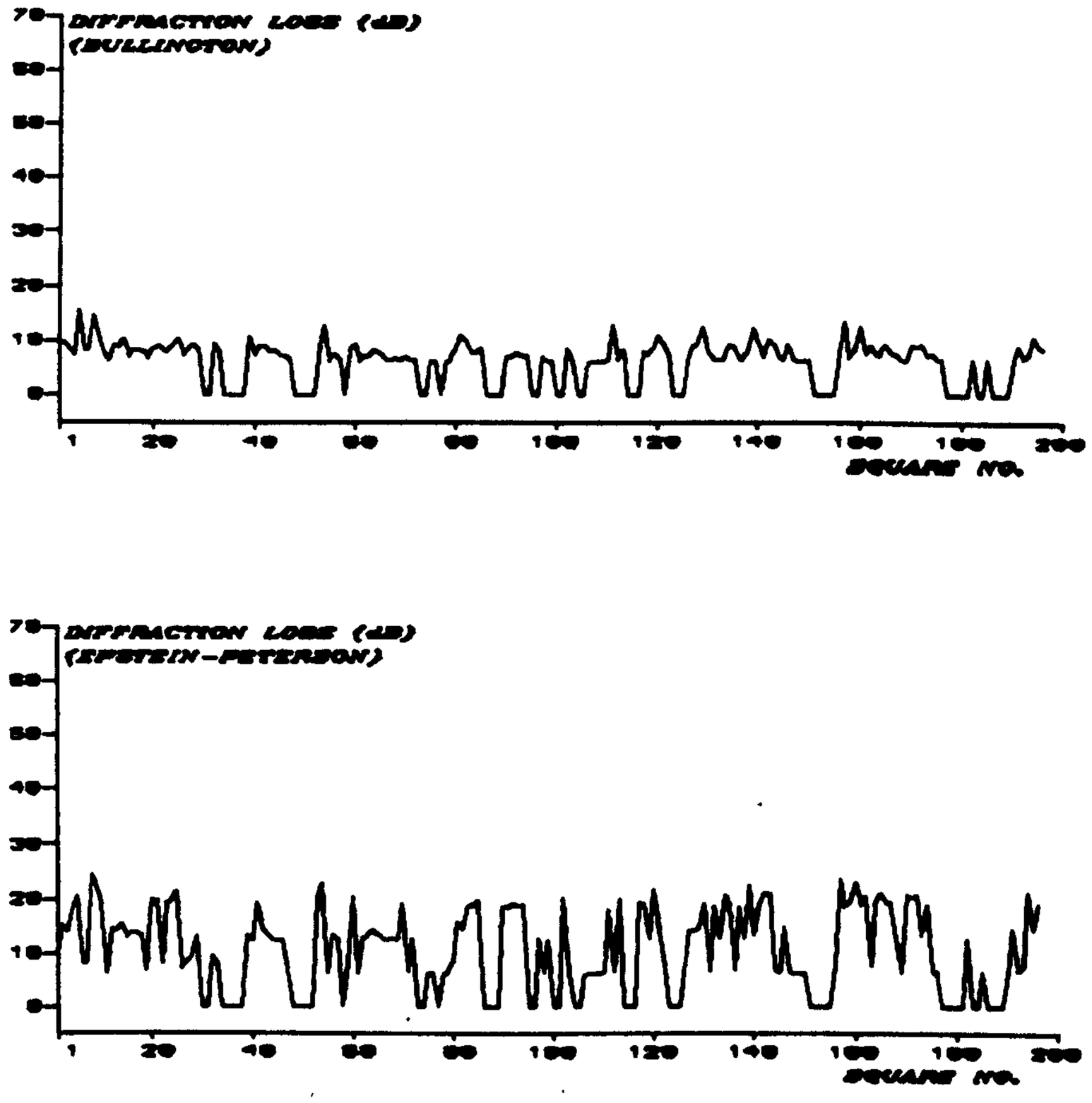

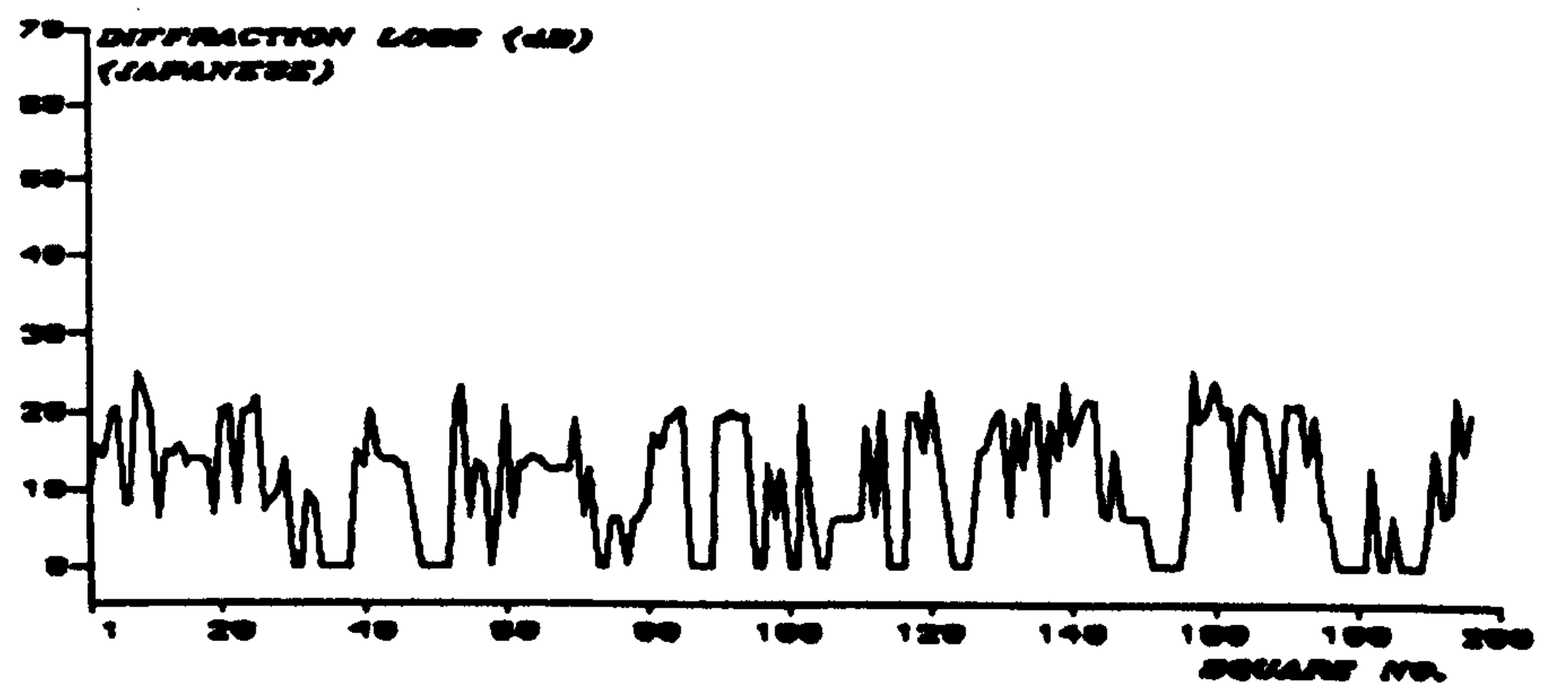

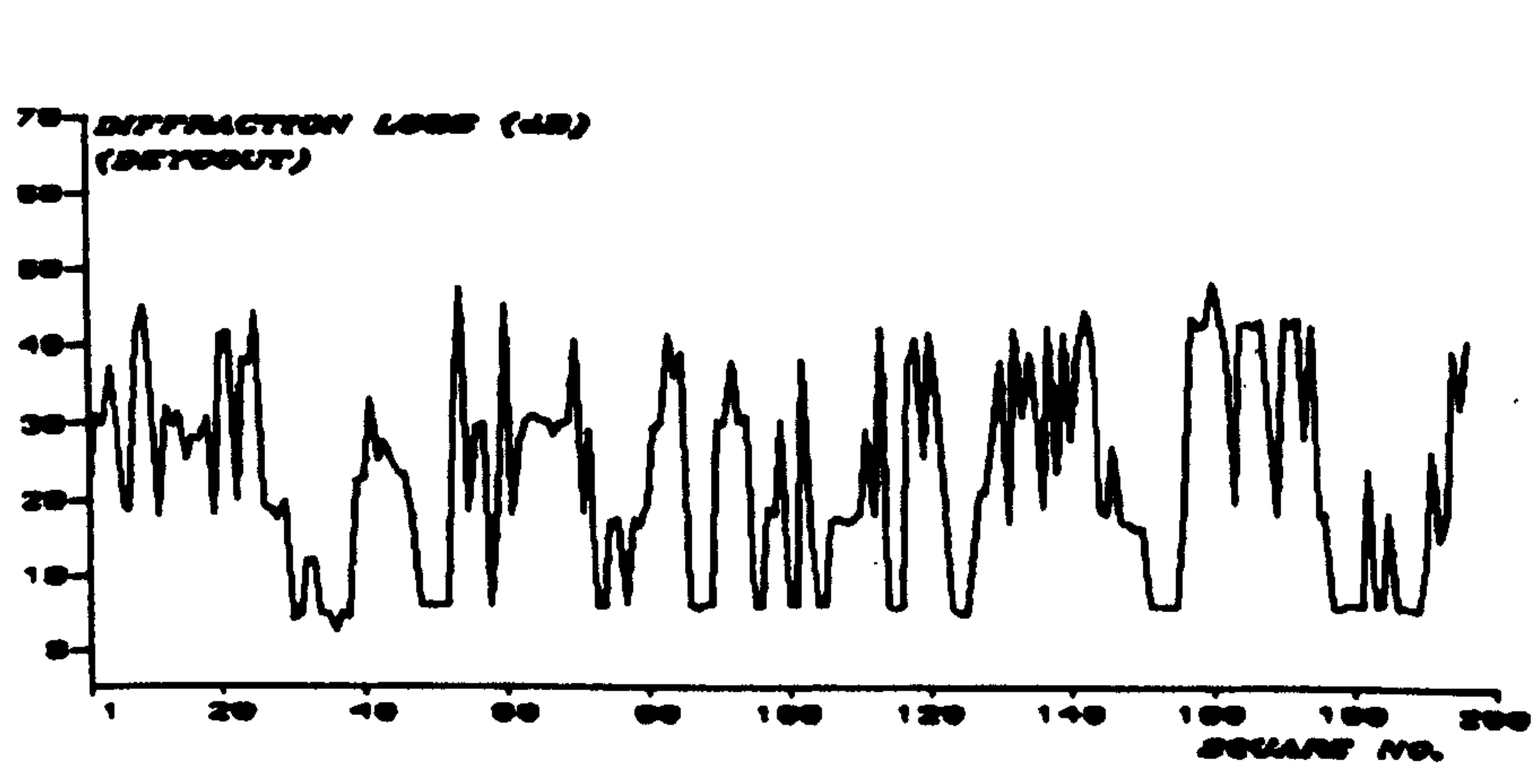

Fig. 6.3 Estimated Diffraction Loss (Altrincham).

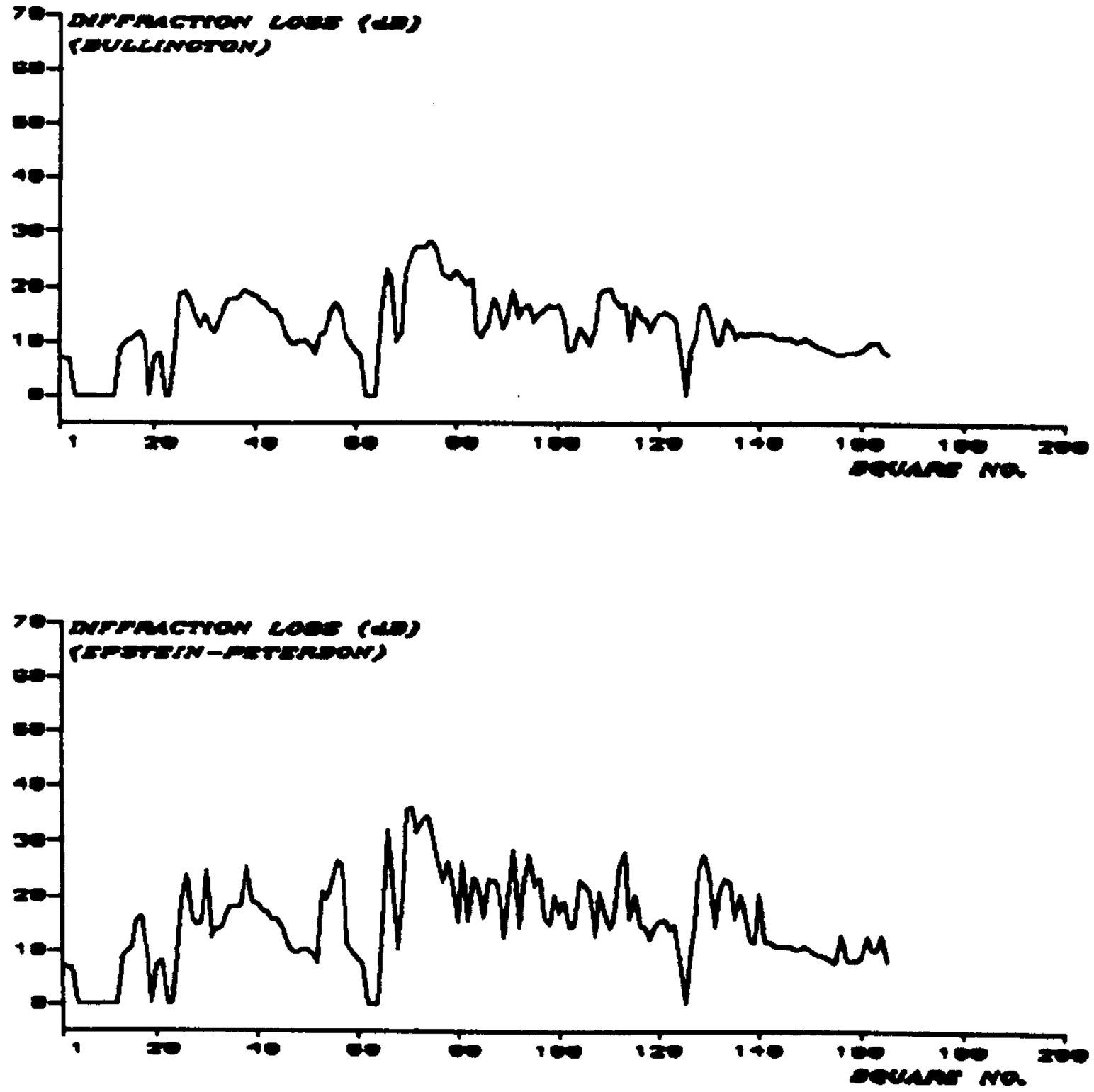

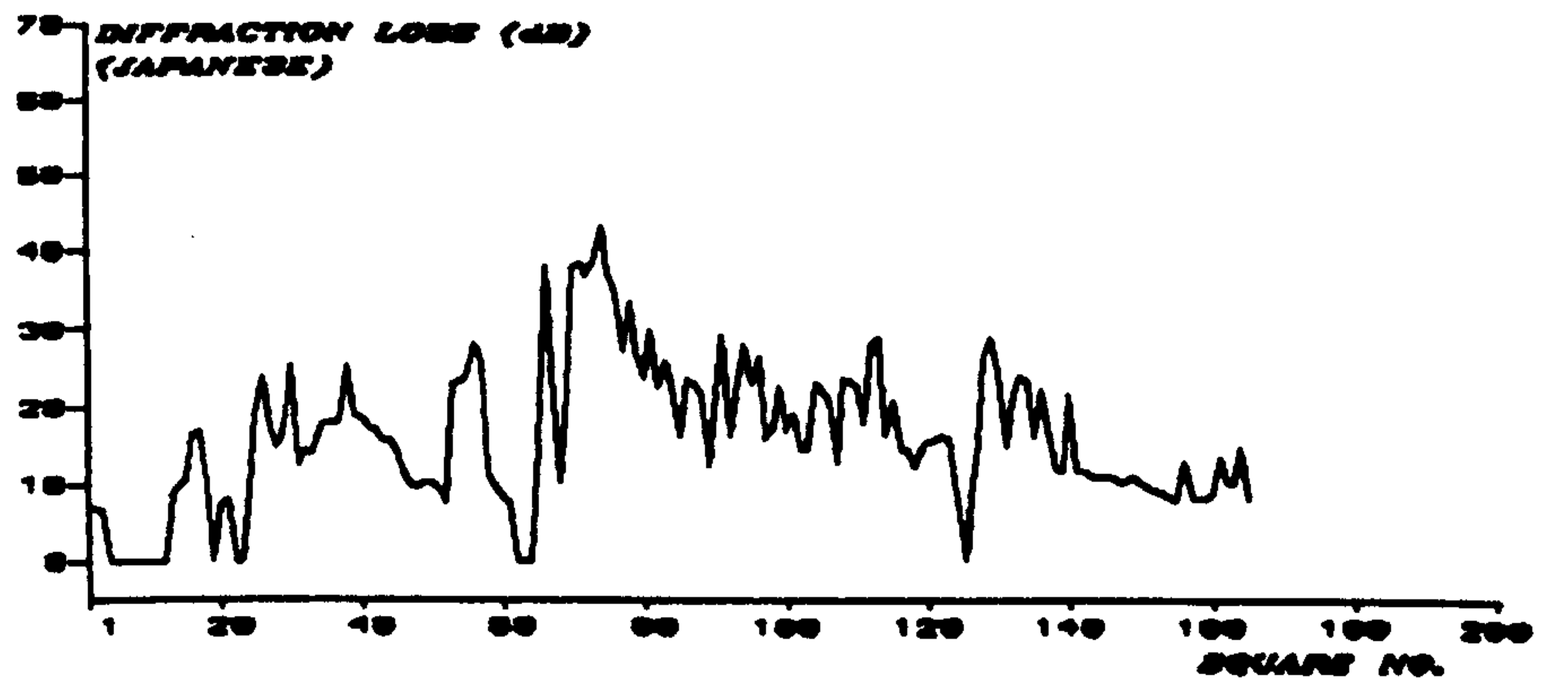

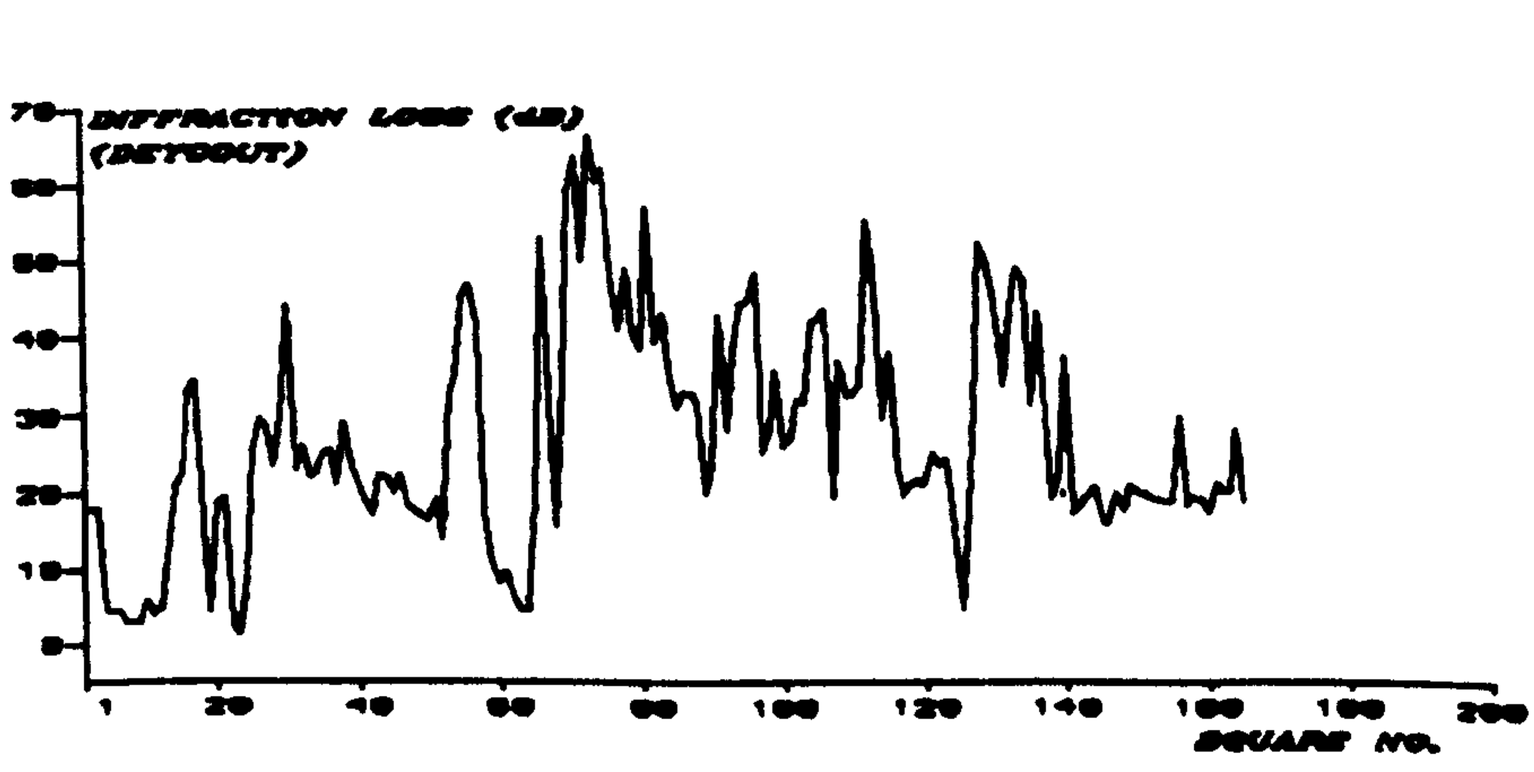

Fig. 6.4 Estimated Diffraction Loss (Wavertree).

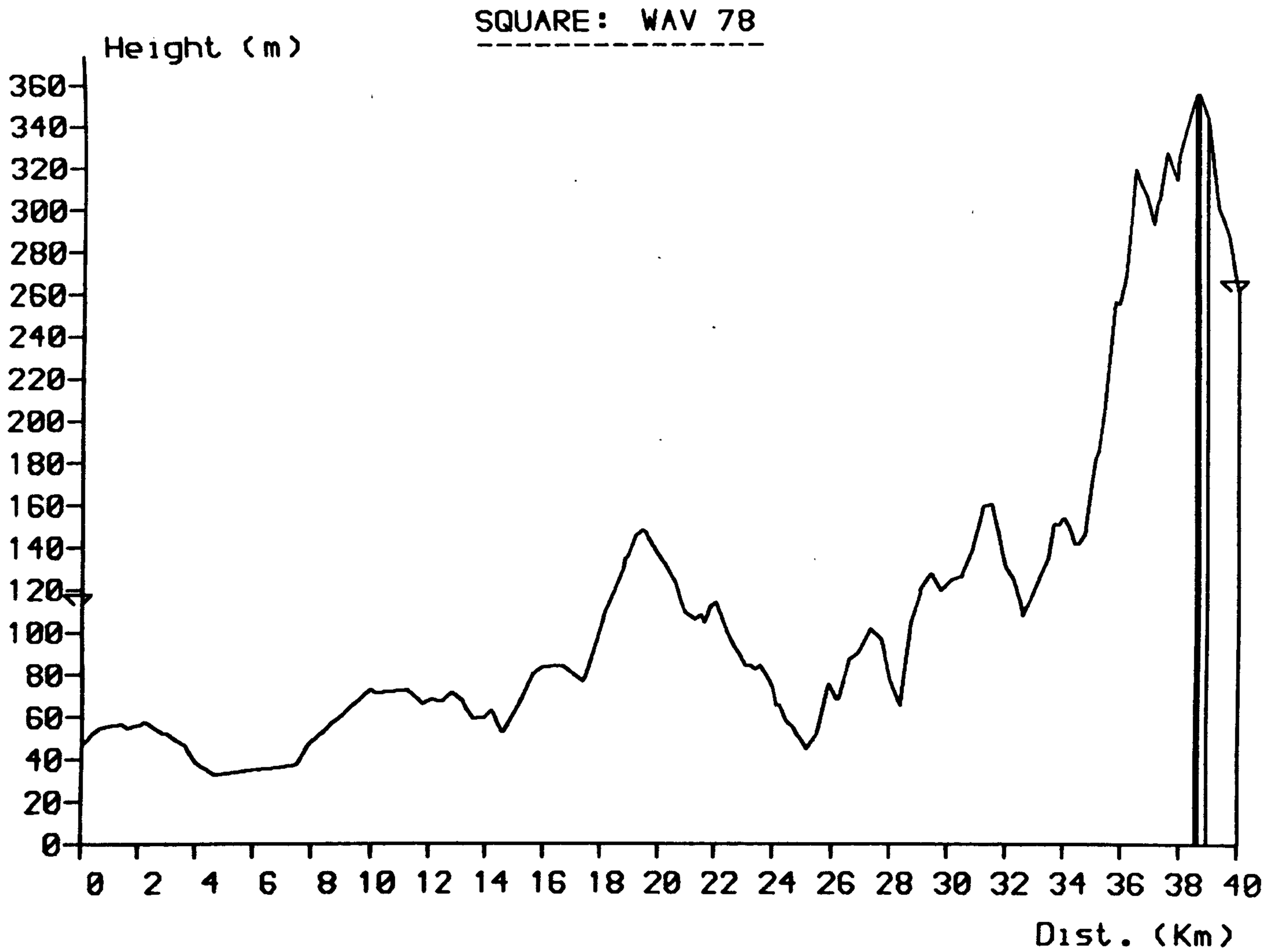

Fig. 6.5 A Typical Path Profile with Close Obstructing Edges.

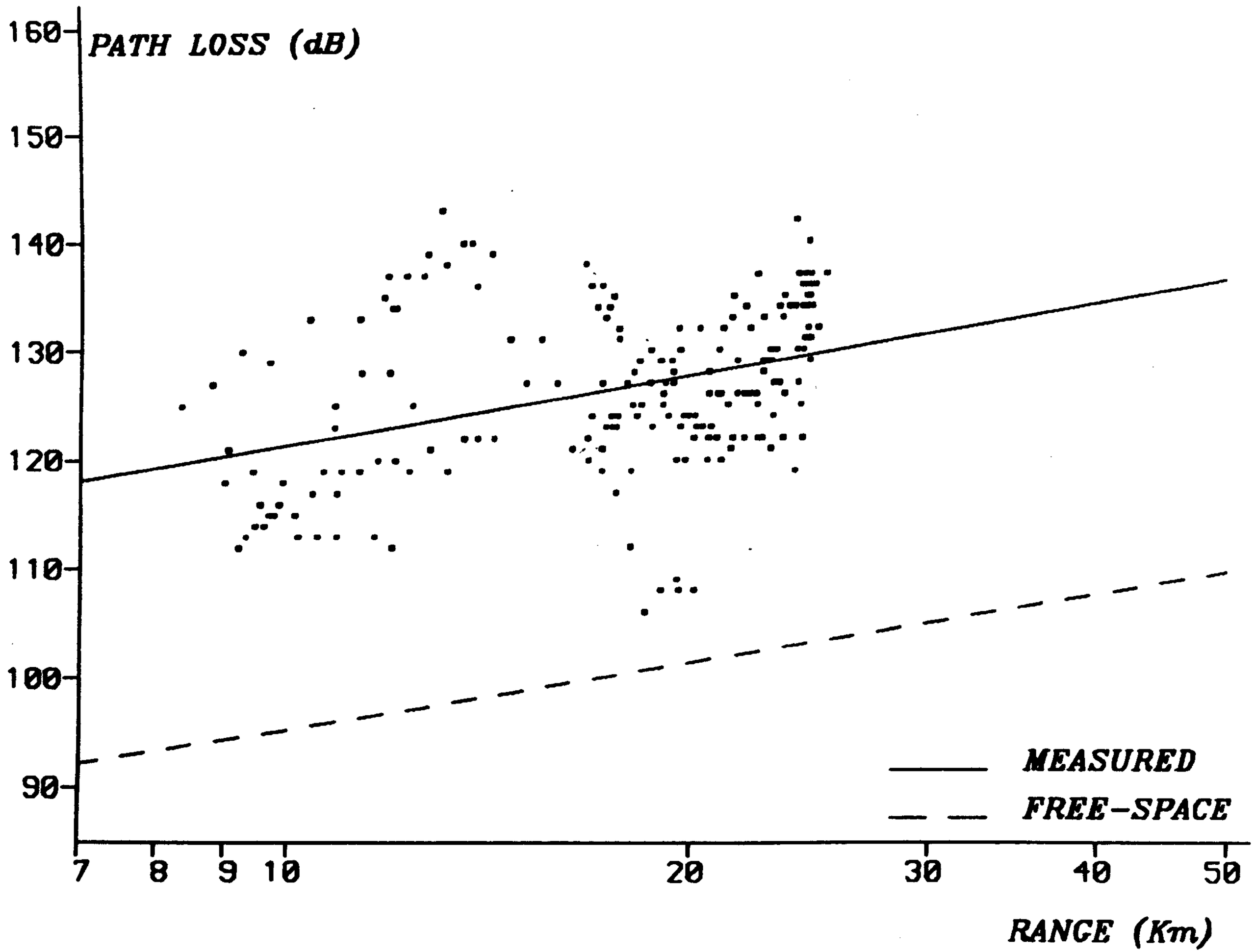

Fig. 6.6 Measured Median Path Loss Between Isotropic Aerials Versus Range (Newton Firs).

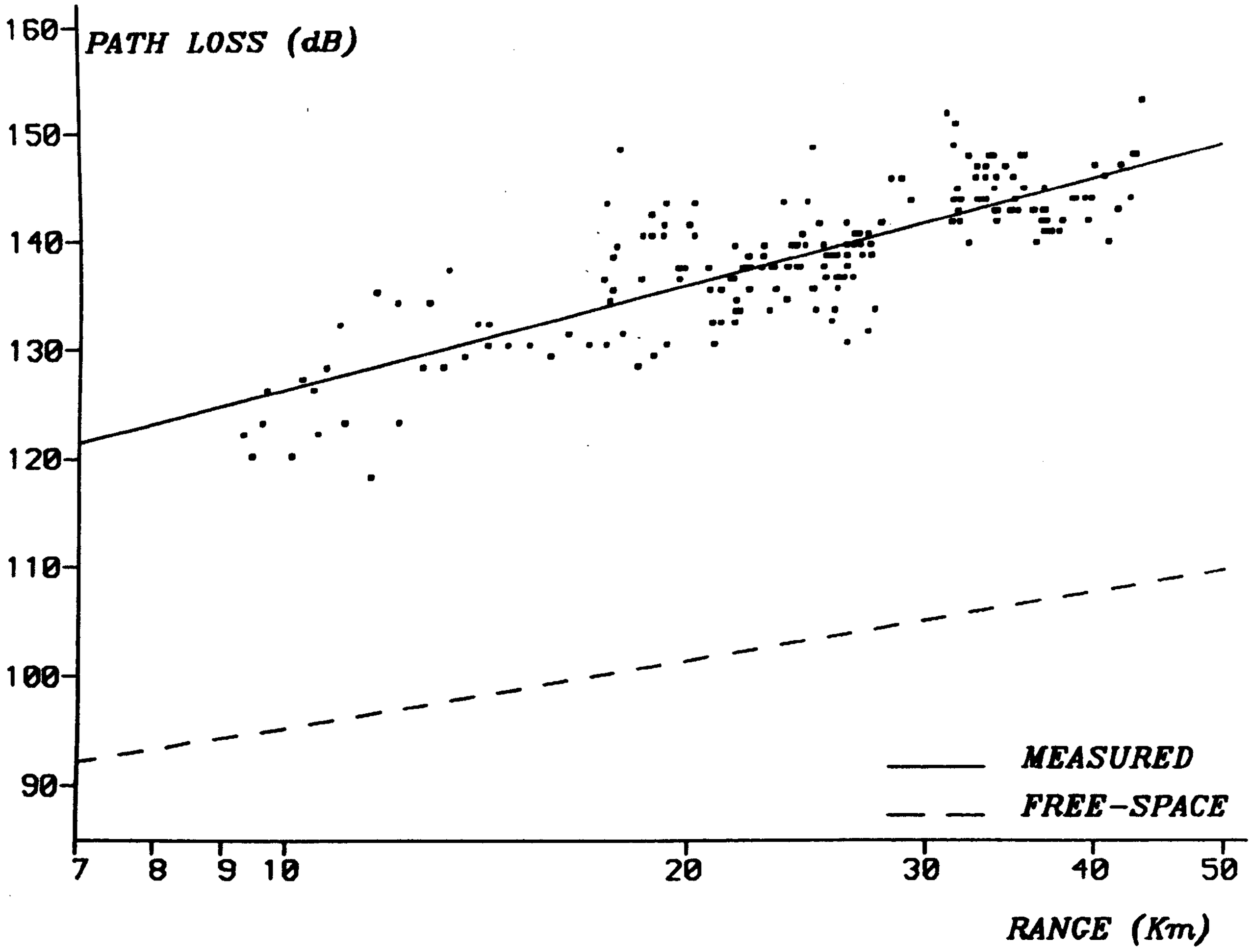

Fig. 6.7 Measured Median Path Loss Between Isotropic Aerials Versus Range (Altrincham).

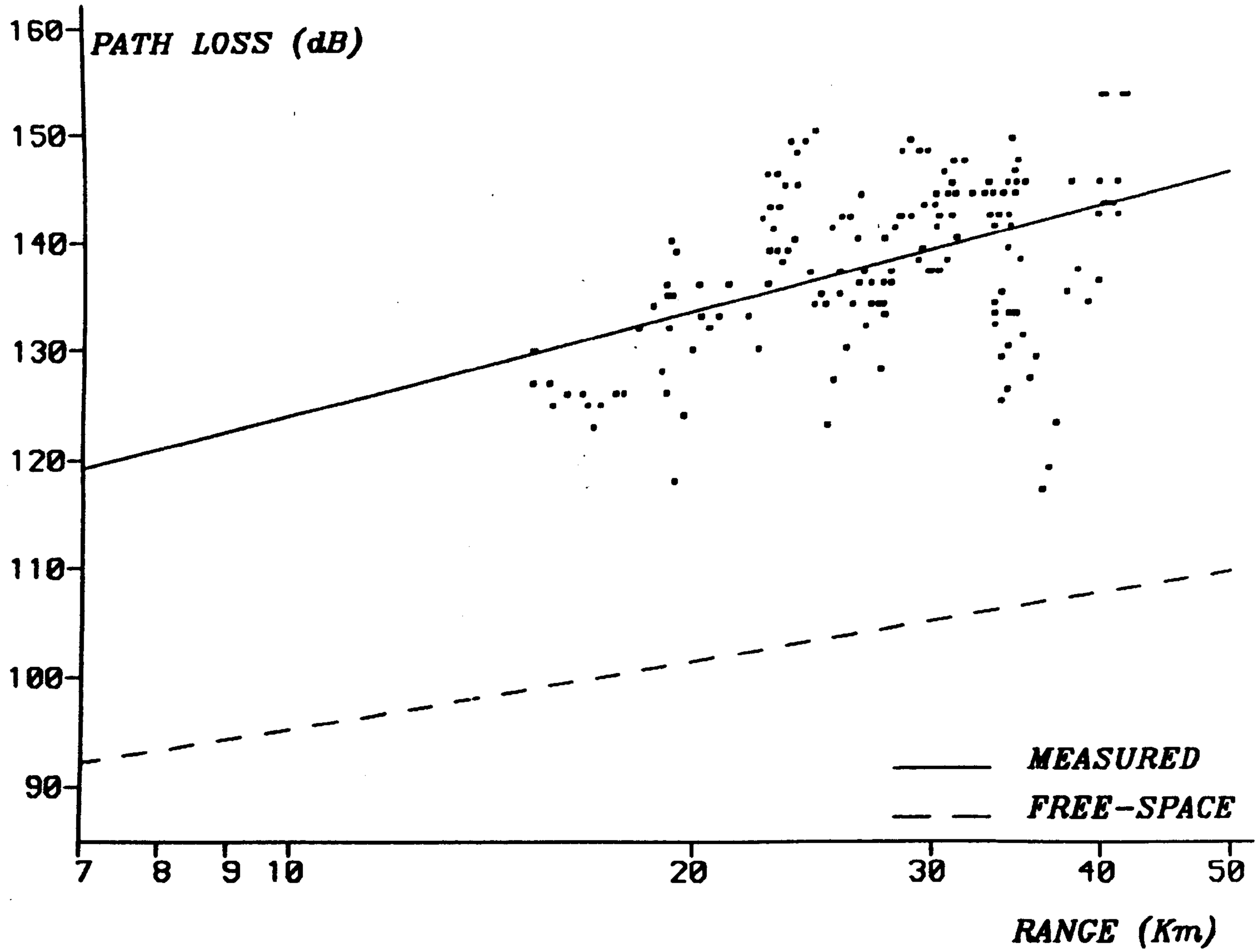

Fig. 6.8 Measured Median Path Loss Between Isotropic Aerials Versus Range (Wavertree).

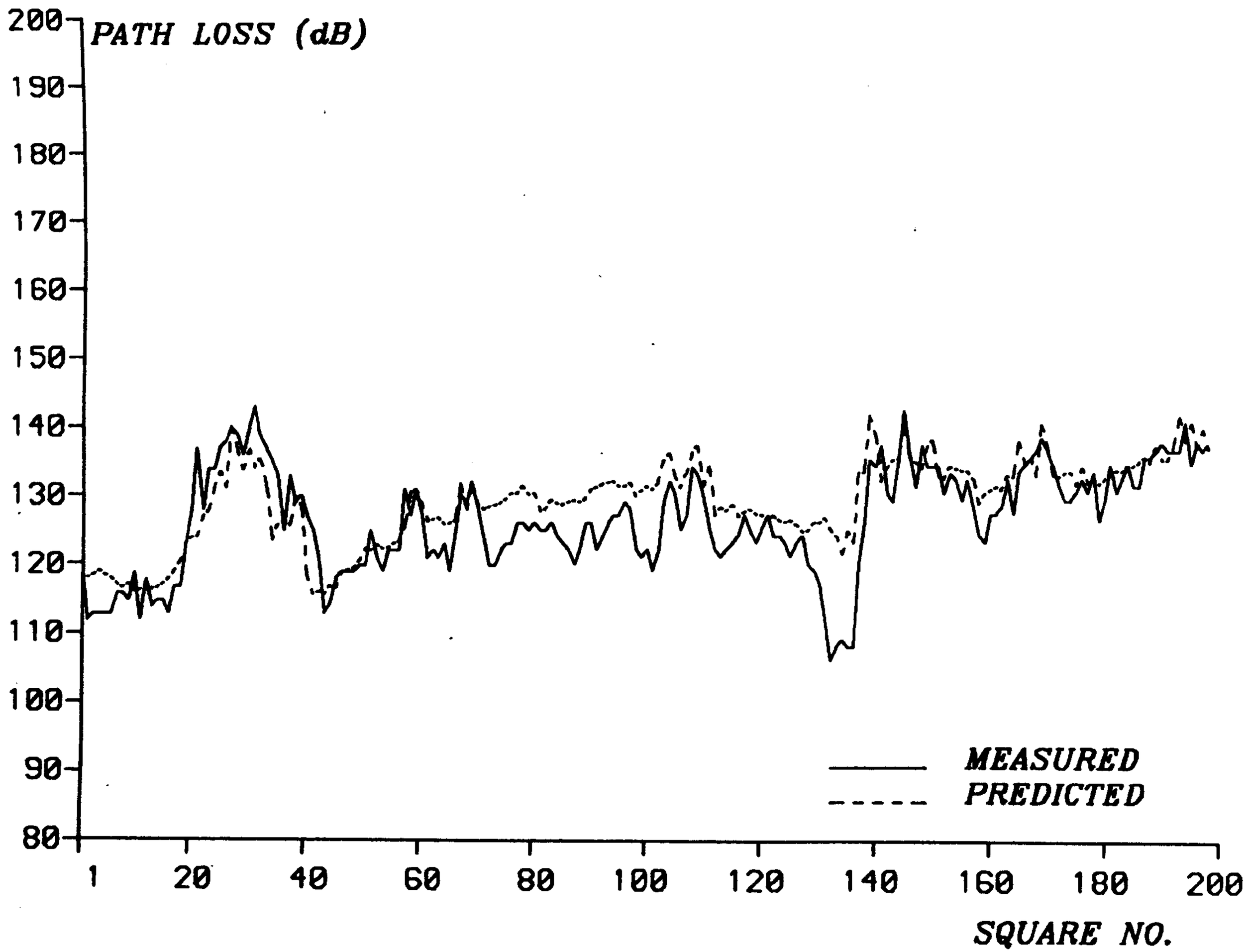

Fig. 6.9 Predicted and Measured Median Path Loss (Newton Firs).

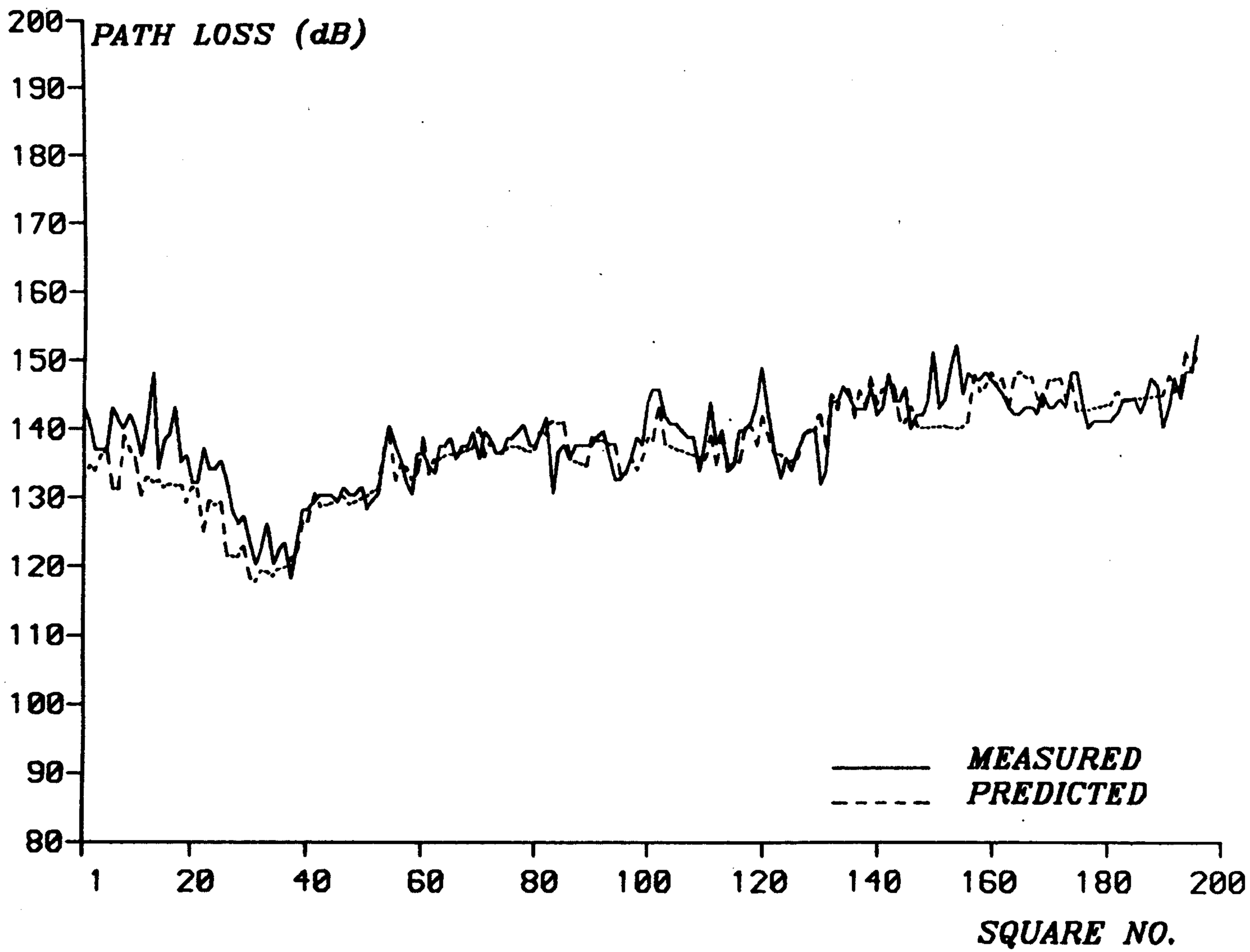

Fig. 6.10 Predicted and Measured Median Path Loss (Altrincham).

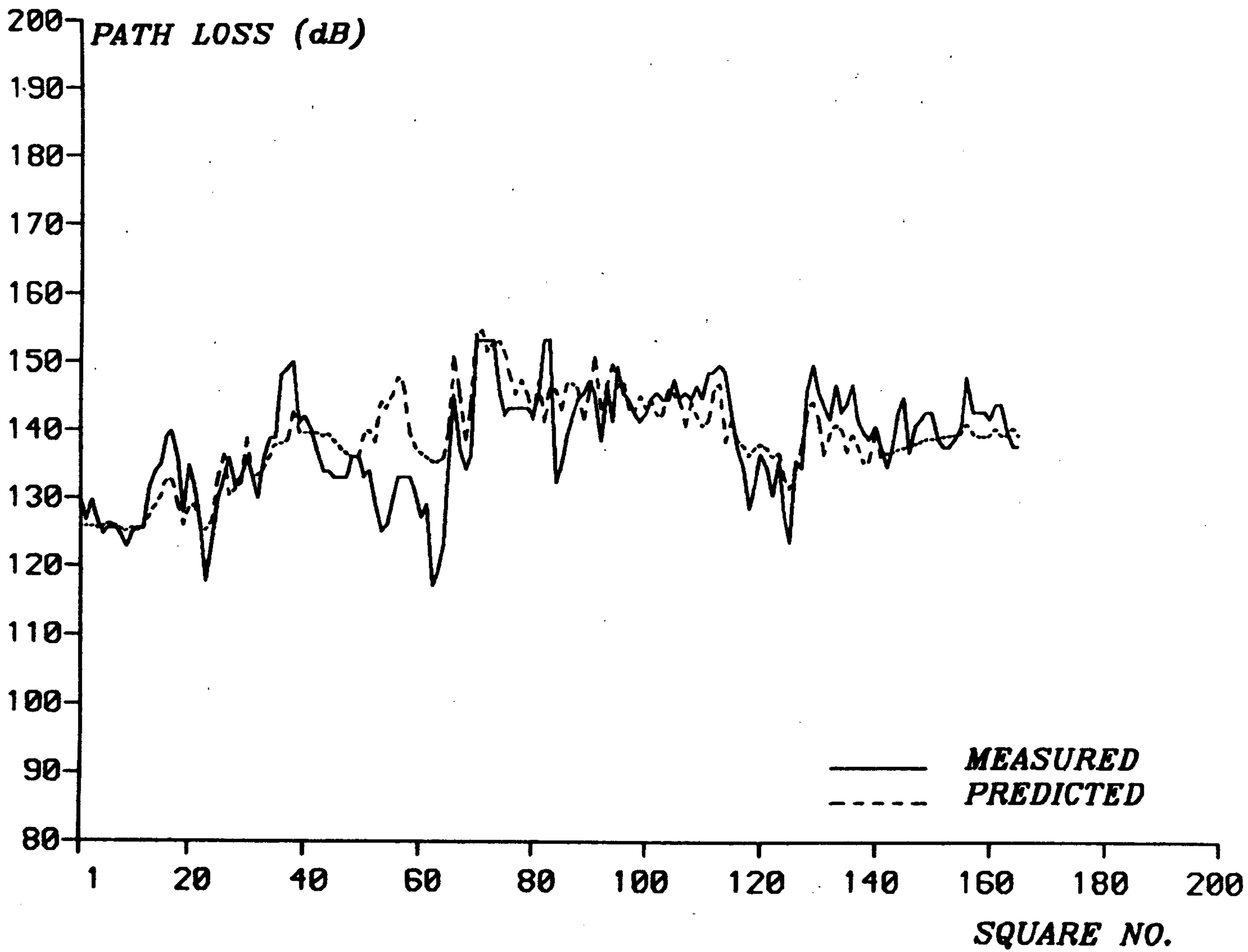

Fig. 6.11 Predicted and Measured Median Path Loss (Wavertree).

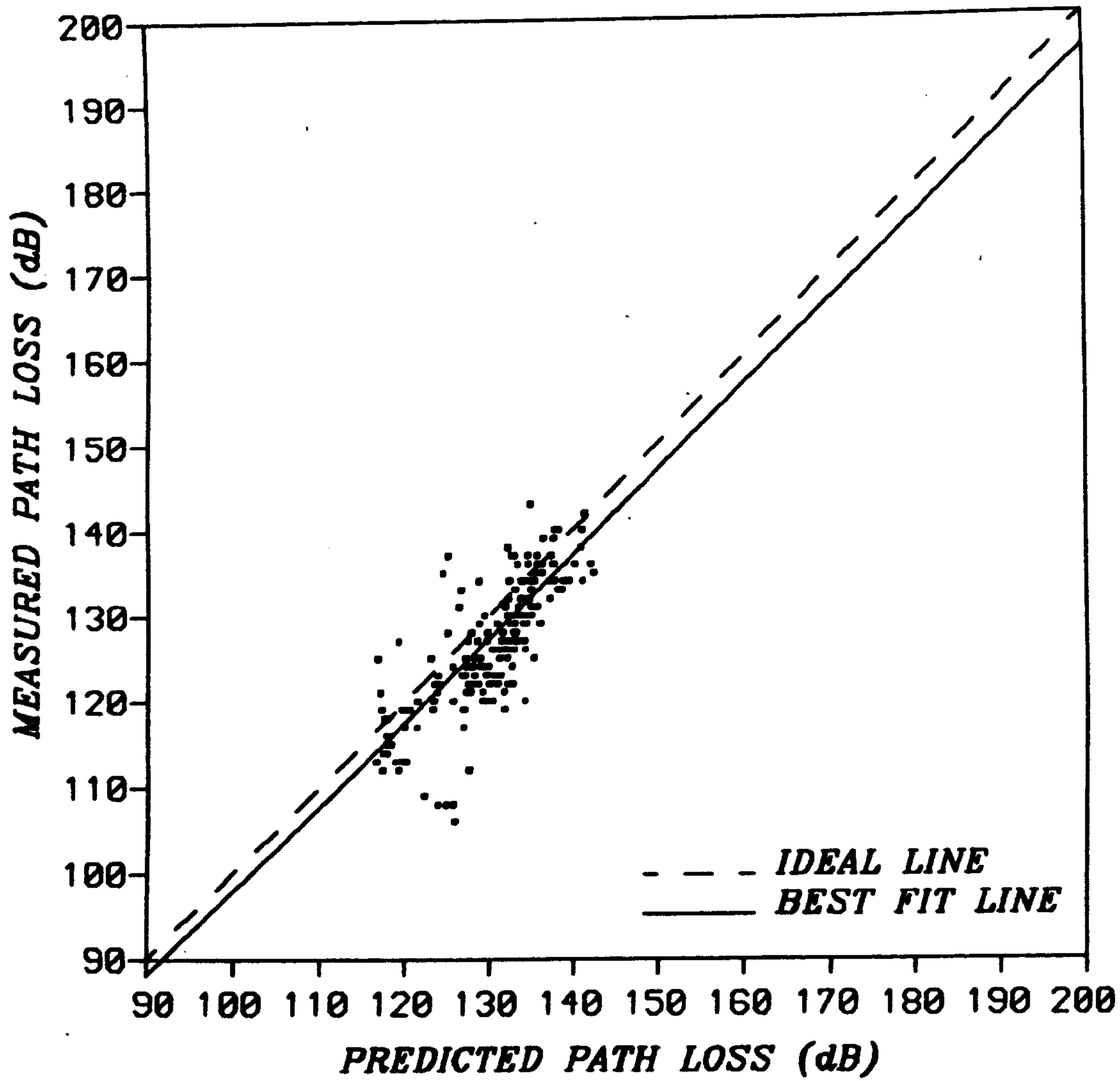

Fig. 6.12 Regression Line (Newton Firs).

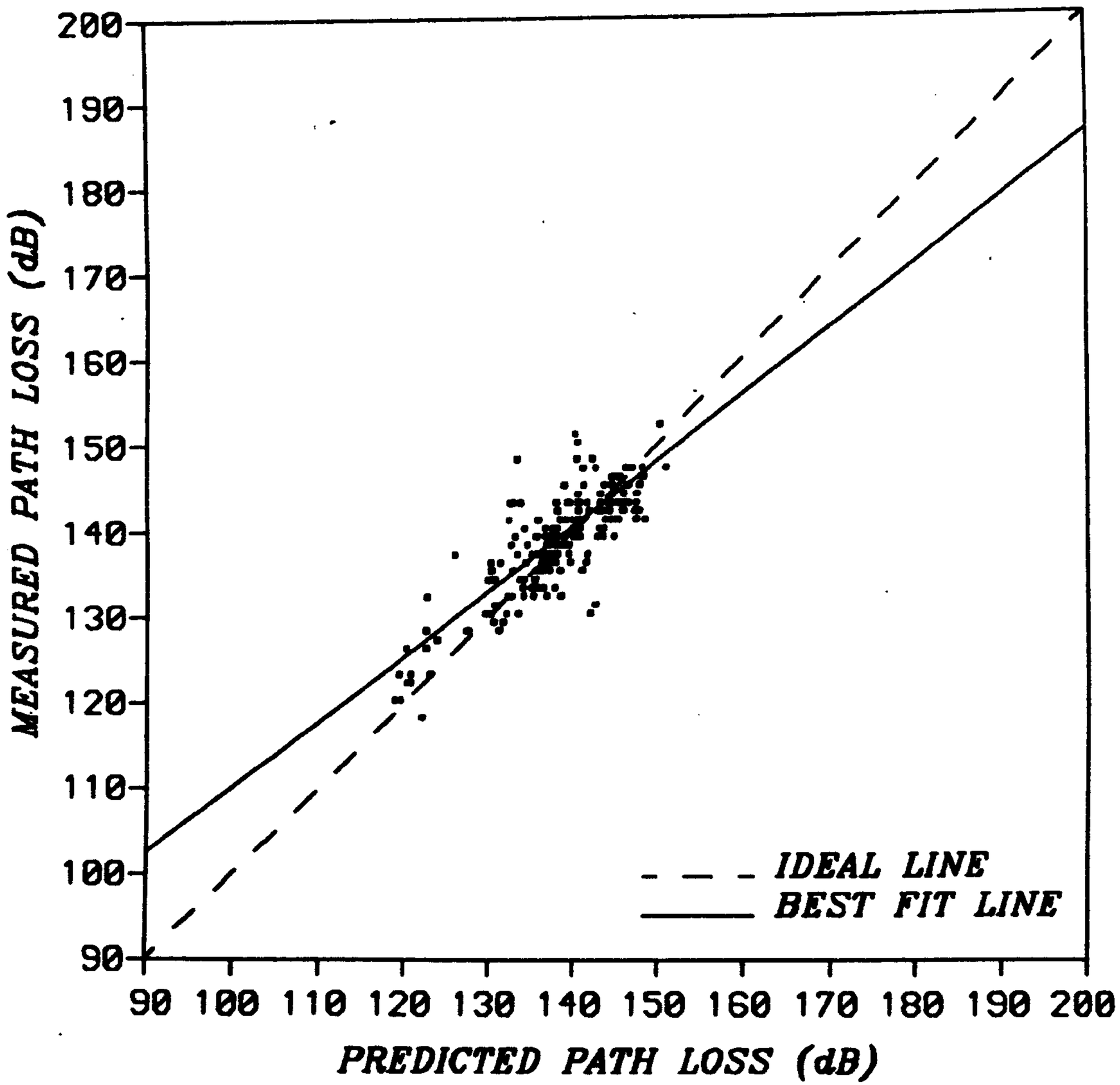

Fig. 6.13 Regression Line (Altrincham).

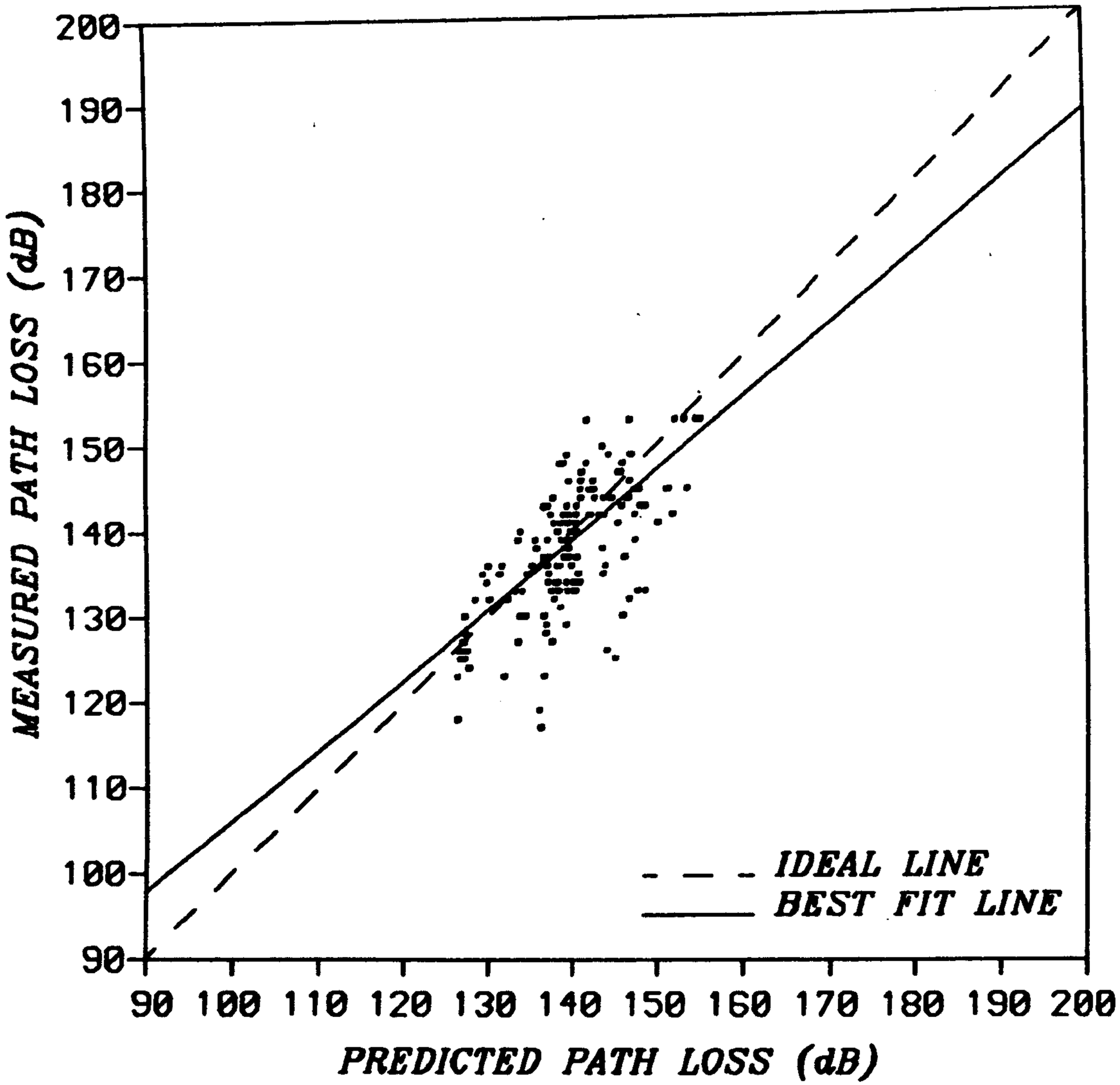

Fig. 6.14 Regression Line (Wavertree).

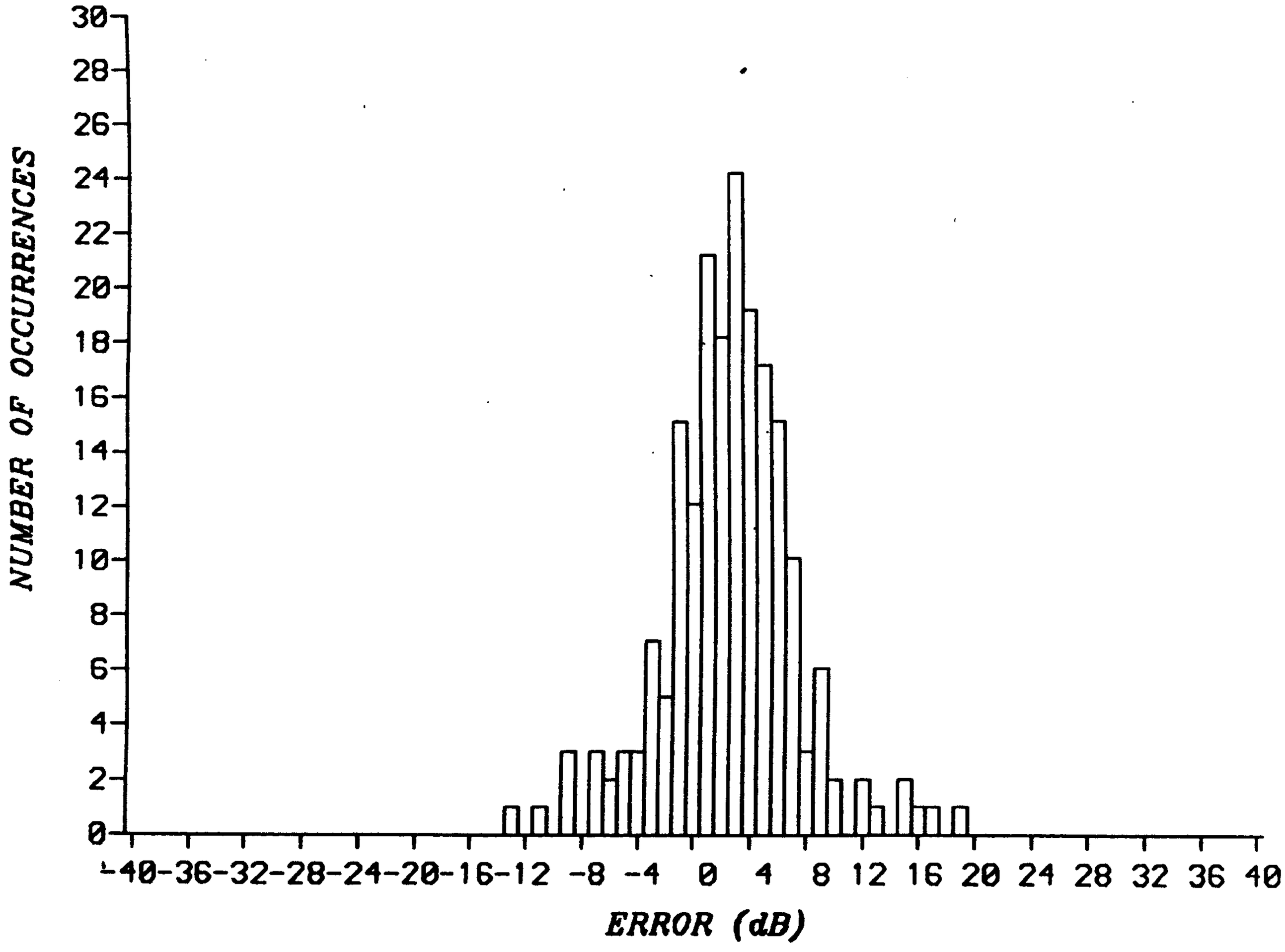

Fig. 6.15 Prediction Error Histogram (Newton Firs).

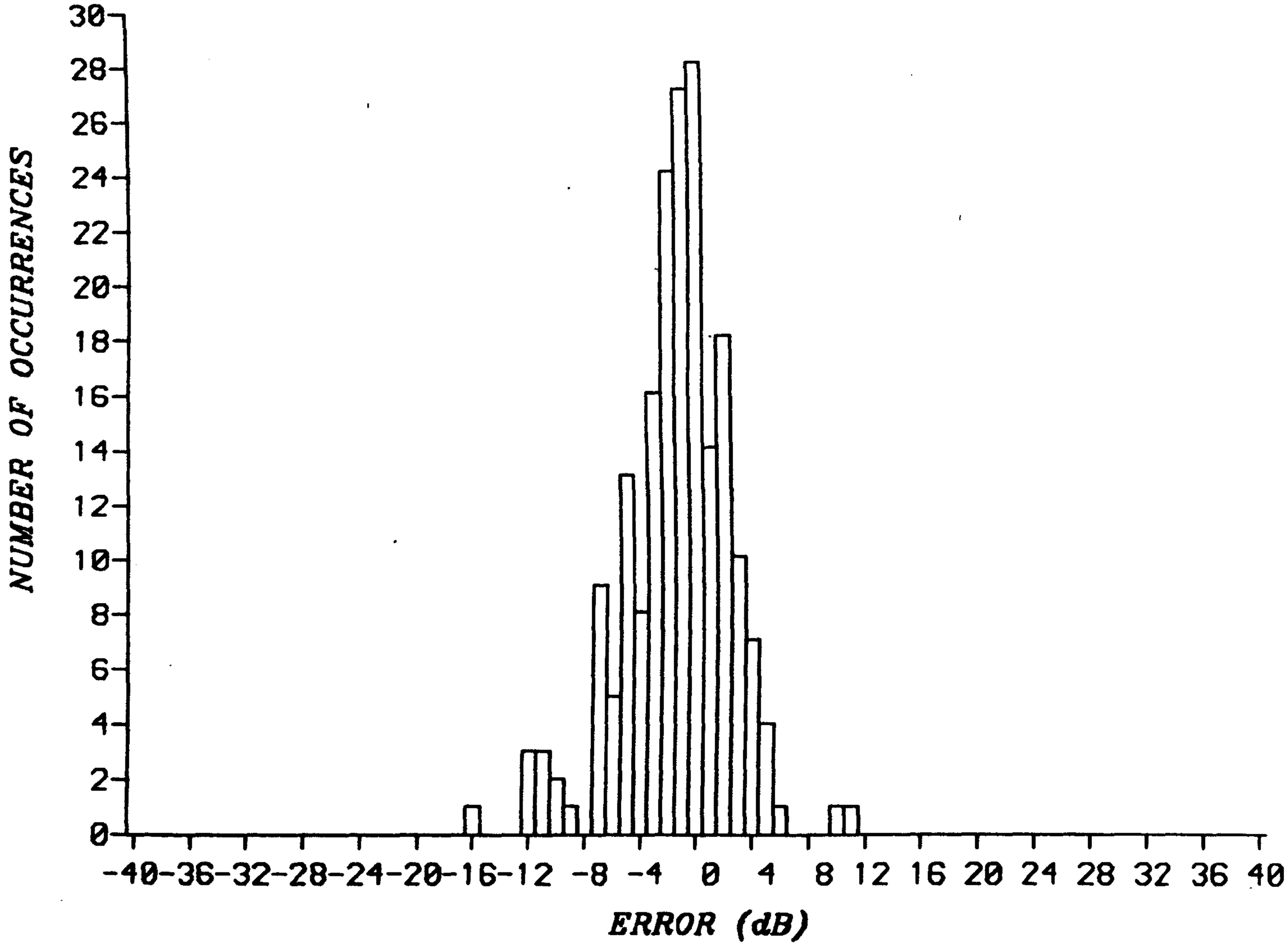

Fig. 6.16 Prediction Error Histogram (Altrincham).

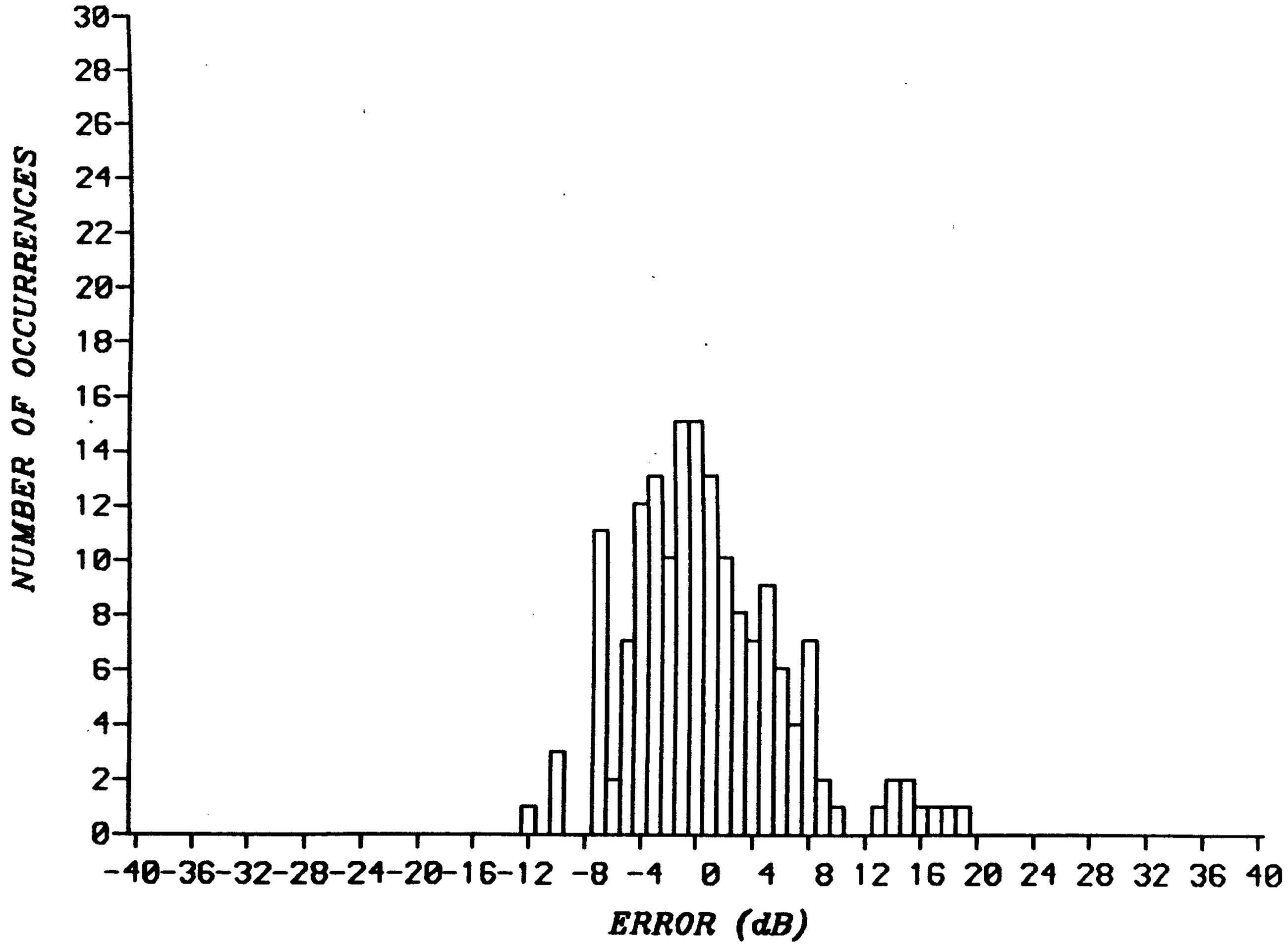

Fig. 6.17 Prediction Error Histogram (Wavertree).

CHAPTER 7

EVALUATION OF THE PROPOSED MODEL

The prediction model proposed in the last chapter calculates the median path loss using theoretical rules and a set of empirical definitions of the required parameters based on detailed terrain path profiles. However, it might be argued that the measured data obtained as a result of Cheshire field trials have partly influenced the model's structure. In order to evaluate the prediction model further, it is therefore necessary to test its performance against independent measured data. The data which was available for this purpose had been obtained as a result of field trials carried out by British Telecom at 160 and 900 MHz in Ipswich [7.1].

The proposed prediction model, as developed, has been intended for use over irregular terrain situations in rural areas and it does not take into account the effect of environmental structures such as buildings. However, since the measured data have been obtained in a built-up area (Ipswich), an attempt is made to introduce an urban clutter loss factor into the model. Comparisons are also made between the prediction models considered in the present work and the suggested model, with the measured data.

7.1 FEATURES RELATING TO THE MEASUREMENT RESULTS

The measured data had been collected in Ipswich using transmitters located at British Telecom Research Laboratories and receiving equipment placed in a mobile test vehicle. The signal strength was sampled every 3.2 cm as the mobile travelled through the streets and the mean signal strength was calculated for each square

of 500 m x 500 m over a survey area of approximately 5 Km x 7 Km. Two transmitting antennas were used both at 80 m above sea level (55 m above the surrounding ground), and the receiving aerials were on the roof of the vehicle, 2 m above local ground. The effective radiated power at 160 MHz was 64 W and about 10 W at 900 MHz.

The position of the measurement area is shown in Fig. 7.1 with reference to the Ordnance Survey map, together with the transmitting site location. There are 124 squares of ½ Km side as numbered in the figure and a contour map of the area marked by crosses is shown in Fig. 7.2. This has been derived by the Rutherford Appleton Laboratory (RAL), [7.2]. As can be noted, the measurements were performed mainly in urban areas where the height variations of the ground signify the irregular nature of the terrain. The terrain data map of the area was not available, however, RAL provided the transmission path profile terrain data matrices of the measurement squares, which were subsequently used by the appropriate computer routines to derive the required terrain parameters. The transmission range lies between 5.3 and 12.1 Km and the radial profiles to the squares include smooth to irregular terrain situations. Fig. 7.3 shows two typical terrain profiles encountered in the area.

By examining the path profiles and disregarding the buildings, half of the squares were found to have a line-of-sight transmission, none with adequate Fresnel zone clearance, at either frequency, due to the small mobile antenna height above ground. The signal transmission to some of the squares, particularly those on the east of the area, is mainly over rural areas, but these squares lie close to building sites and the whole survey area is interpreted as being urban for prediction purposes.

7.2 URBAN CLUTTER LOSS

In predicting the median path loss in urban areas, some prediction models calculate first the propagation loss to be expected if the buildings and other environmental clutter were not present, and then account for the additional loss caused by the features in the urban or suburban area of interest.

In order to add an allowance for the additional attenuation due to urban clutter to the computerised prediction model, a comparison is made with the values given by the empirically-derived prediction curves of the Okumura model. These prediction curves are widely used, however, it is more practical to use Hata's formulation of the Okumura model over the applicable range. Over quasi-smooth terrain, and in the frequency range of 150 to 1500 MHz and separation distance of 1 to 20 Km, the path loss in an urban area is given by (section 3.5):

$$P_{LH} = 69.55 + 26.16 \log_{10} f - 13.82 \log_{10} h_t - a(h_r) + (44.9 - 6.55 \log_{10} h_t) \log_{10} d \quad \text{dB}$$

where for a medium sized city:

$$a(h_r) = (1.1 \log_{10} f - 0.7)h_r - (1.56 \log_{10} f - 0.8) \quad \text{dB}$$

Using the values of h_t = 200 m and h_r = 3 m, which are assumed as standard, in the basic attenuation curves given by the Okumura model, the above relation reduces to:

$$P_{LH} = 39.05 + 24.42 \log_{10} f + 29.83 \log_{10} d \quad \text{dB} \qquad (7.1)$$

The computerised prediction model, as outlined in the previous chapter, calculates the path loss over the rural area as:

$$P_{LP} = L_F + [(L_P - L_F)^2 + L_D^2]^{1/2} \quad \text{dB}$$

Assuming a smooth terrain by equating the diffraction loss, L_D to zero, the path loss will be that of the plane-earth loss, L_p, given by:

$$P_{LP} = 120 + 40 \log_{10} d - 20 \log_{10} (h_t\ h_r) \quad \text{dB}$$

where by taking the antenna heights assumed in the above, the following will result:

$$P_{LP} = 64.44 + 40 \log_{10} d \quad \text{dB} \qquad (7.2)$$

The difference between the two models, as represented by (7.1) and (7.2), may be considered as providing the additional loss in an urban area,

$$UL = P_{LH} - P_{LP}$$

This urban loss factor is given in the following for frequency f in MHz and distance d in Km by:

$$UL = -25.39 + 24.42 \log_{10} f - 10.17 \log_{10} d \quad \text{dB} \qquad (7.3)$$

As can be realised from (7.3), the urban loss increases with frequency and at a given frequency the effect of urban loss diminishes with increasing distance from the transmitter. The urban loss factor is more applicable to the environment surrounding the mobile unit, as this is the mode considered in the Okumura's model.

7.3 PERFORMANCE OF THE MODEL AGAINST MEASURED DATA

The terrain data were used to calculate the diffraction loss along the transmission path and derive the transmitter effective antenna height. The median predicted path loss was then obtained by combining the appropriate loss factors including the urban loss given by (7.3). For a given transmission range, the calculated urban loss

differs by 18 dB at the two frequencies. The mean value of the measured path loss, obtained by averaging over all the measurement squares, was found to be 130.5 dB at 160 MHz, increasing by almost 24 dB to 154 dB at 900 MHz. The range of variation in the value of measured path loss also increases, indicated by the value of standard variation of 6.2 dB at 160 MHz, rising to 10.6 dB at 900 MHz.

The values of measured and predicted path loss obtained at the two frequencies are shown in Fig. 7.4 and Fig. 7.5 versus the square number. The sharp transitions of the curves indicated in the figures are due to the way by which the squares are numbered. However, the figures are useful in emphasising the difference between the measured and predicted results. The prediction seems to follow closely the trend of the measurement, however for most parts, the predictions overestimate the path losses, particularly at 160 MHz. This fact is emphasised further by Figs. 7.6 to 7.9 which illustrate the regression lines of measured versus predicted results and the prediction error histograms for both frequencies. There is a high correlation between measurement and the prediction (correlation coefficient of 0.81) and the regression lines have a slope value close to unity. The prediction error is more widely spread for the 900 MHz case with a mean value of 6.3 dB, whereas at 160 MHz it seems to be approximately normally distributed about the mean value of 3.6 dB.

Table 7.1 lists the quantitative results obtained by comparing the measured and predicted values of path loss.

Table 7.1

Frequency (MHz)	Correlation Coefficient	Standard Error (dB)	Standard Dev. of Error (dB)	Slope of Regression Line
160 900	0.81 0.81	7.9 8.2	3.6 6.3	1.11 1.11

It was realised from the results that the large prediction errors occurred mainly in the case of squares located on the eastern part of the survey area which lie closest to the transmitter. The main reason for these errors is the rather large values of calculated urban loss factor, which result in pessimistic values of predicted path loss.

7.4 COMPARISON WITH OTHER PREDICTION MODELS

The availability of the computer implementation of the prediction models which have been studied previously, facilitated a comparative analysis of these models and the proposed model with each other and with measurements.

The Okumura model is expected to show good performance against the measured data since the model is mainly intended for use in urban areas. Since the terrain is considered to be irregular over the survey area, the appropriate routines for the irregular terrain determine the required path parameters from an examination of the path profiles. Similarly, for the Longley-Rice prediction model, individual path profiles are processed to derive the appropriate values of the terrain irregularity parameter and other required input parameters. The Longley-Rice model includes an urban factor which is a function of frequency and range and hence the addition of the urban

loss factor to the proposed model is similar in approach to this model. The urban factor in the Longley-Rice prediction model was developed by comparing results from the model's computer method with Okumura's prediction curves. All comparisons utilised smooth earth and the factor is intended to provide the model with a means to adequately predict the median attenuation for moderately large cities in rather smooth terrain. The JRC prediction model is based purely on terrain data and does not take into consideration the influence of buildings on the median path loss. Obviously the JRC model is expected to produce the largest prediction errors. However, its inclusion in the comparative analysis with the measured Ipswich data, will provide further insight into the model's overall performance and its position for the introduction of an appropriate urban loss factor. Since the JRC's own predicted values of median path loss were not available, the implemented version of the model was used. This has been devised according to the general perception of the JRC model, as outlined in the published literature.

Similar statistical analyses were carried out on these prediction models and all except the Okumura model were found to have a high correlation coefficient of the same order as those for the proposed model. Also, apart from the JRC prediction model, the models overestimate the median path loss. However, the Okumura model produced the lowest values of mean prediction errors and standard error. Table 7.2 lists the values of standard error obtained for each model, where those of the proposed model are repeated for comparison.

Table 7.2

Frequency (MHz)	Standard Error (dB)			
	Okumura	JRC	Longley-Rice	Proposed
160	6.4	18.8	9.6	7.9
900	8.2	33.4	10.0	8.2

When the urban loss is not considered, the proposed model produces large values of standard error, similar to the JRC model, though by an order of 6 dB less. The Longley-Rice model performs much better and has the smallest values of standard deviation of error, 3.2 dB and 5.8 dB at 160 MHz and 900 MHz respectively. The standard error value produced by the Okumura model is equal to that of the proposed model, at 900 MHz and 1.5 dB lower at 160 MHz.

One interesting situation arose when considering the path profiles from the transmitter to the centre of the square numbered 49. There are twelve measurement squares whose centres lie on this radial profile, and the situation is illustrated at the top of Fig. 7.10, where the vertical lines drawn along the path profile indicate the location of the squares whose numbers are shown above the profile. A path loss analysis along this radial would demonstrate how the prediction models can cope under various conditions. The diagrams below the terrain profile in the figure show the measured and predicted path loss values against the range at the two frequencies. The scales on the distance axes are the same, which provide a simpler means of comparing the results on the square-by-square basis. As can be seen, the JRC model underestimates the loss by a large margin, this however follows the trend of measurement, indicating its ability to calculate the terrain diffraction losses.

The Longley-Rice model produces closer values to the measured data and abrupt changes in the predicted values rarely happen. The Okumura and the proposed models predict the nearest values to the measurements, with the Okumura model performing slightly better for the line-of-sight path situations. However, the Okumura model is not capable of following closely the measurements in the case of obstructed transmission paths, indicating its lack of consideration of the diffraction loss caused by terrain features. The statistical measures listed in Table 7.3 have been obtained by comparing the Okumura model with the measured data.

Table 7.3

Frequency (MHz)	Correlation Coefficient	Standard Dev. of Error (dB)	Slope of Regression Line
160	0.69	4.5	0.81
900	0.67	8.1	1.34

The comparative results indicate that, although the Okumura prediction model produces a lower value of the standard error at 160 MHz, it has a lower correlation coefficient, higher values of standard deviation of error and worst values of the slope of regression lines at both frequencies, compared to the proposed prediction model.

As a further evaluation of the models, an investigation on the models' performance versus transmission range was carried out. Measured data were drawn as points against the logarithmic axis of the range, and a best fit line was drawn through the points using the

least square method. In addition, best fit lines were drawn for the predicted path loss values due to the theoretical plane earth loss (using the antennas' structural heights), for the Okumura model and for the proposed prediction model. These are shown in Figs. 7.11 and 7.12 for the frequencies of 160 and 900 MHz respectively. Table 7.4 lists the calculated slope values of the best fit lines.

Table 7.4

Frequency (MHz)	Range Dependence Coefficient (dB/decade)		
	Measured	Okumura	Proposed
160	45.2	51.3	38.1
900	73.1	51.1	52.3

As can be noted from the table, the slope values for the measured data and the predicted results due to the proposed model are closer to the value of 40 dB/decade of the plane-earth loss at 160 MHz, whereas for the 900 MHz, the slope due to the measured data is much higher (by 20 dB) than those of the prediction models. The value of clutter loss defined as the difference between the best fit line and the line calculated using the plane-earth equation, is much larger at 900 MHz.

REFERENCES

7.1 Rose, D.J., "160 and 900 MHz Prediction Survey in Ipswich January 1982", British Telecom Memorandum No. R6/003/82.

7.2 Davies, P.G. and Bowman, M.R., "Comparison of Measured and Predicted Propagation Path Losses at 160 and 900 MHz in Ipswich Utilizing the UK Terrain Data Base", DURPP Research Note No. 60, October 1985.

7.3 Longley, A.G., "Radio Propagation in Urban Areas", OT Report 78-144, Boulder, Colorado, April 1978.

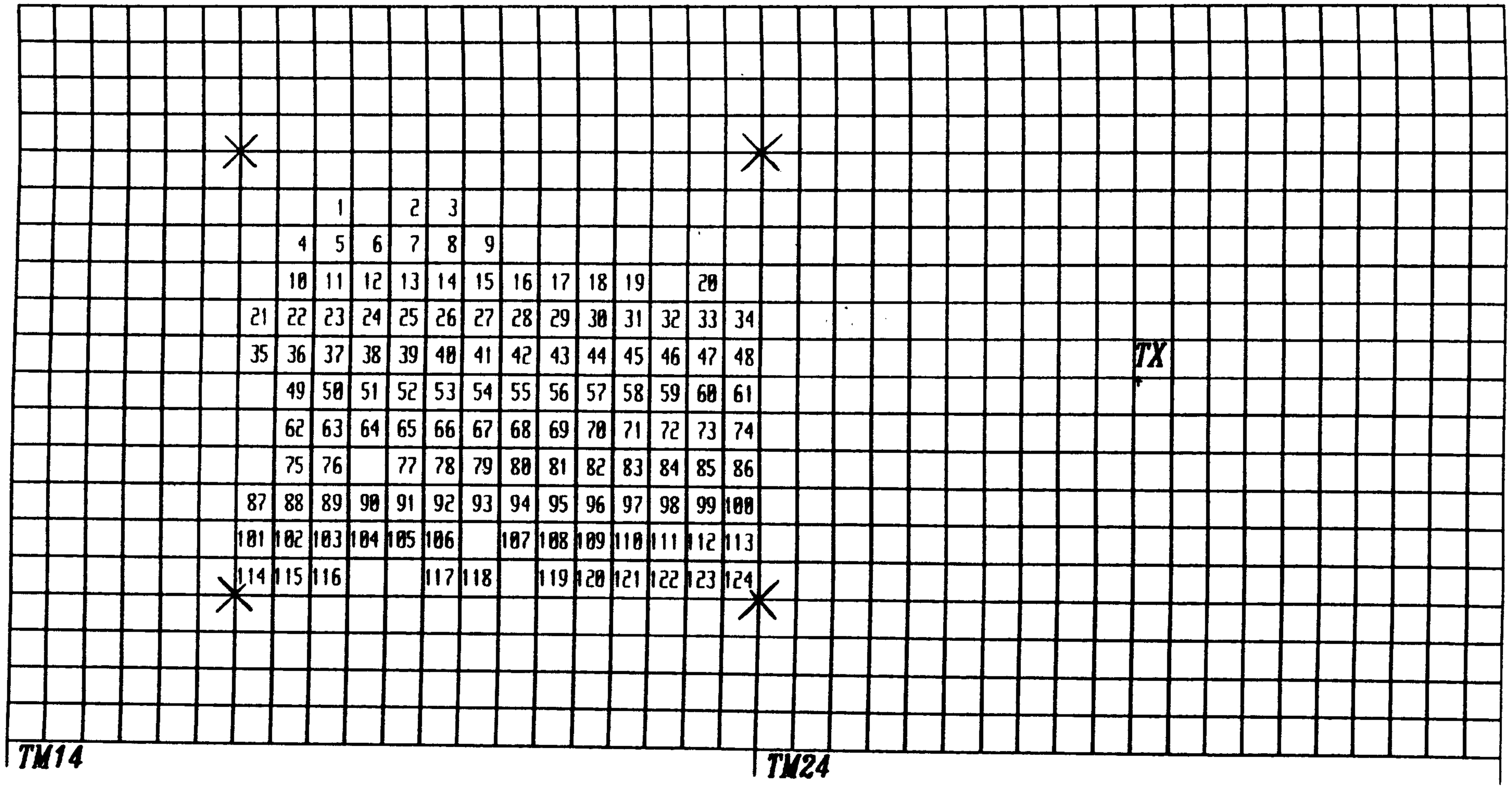

Fig. 7.1 The Survey Area in Ipswich.

Contour Key

Contour number	Height (m)
1	0
2	5
3	10
.	.
.	.
etc.	

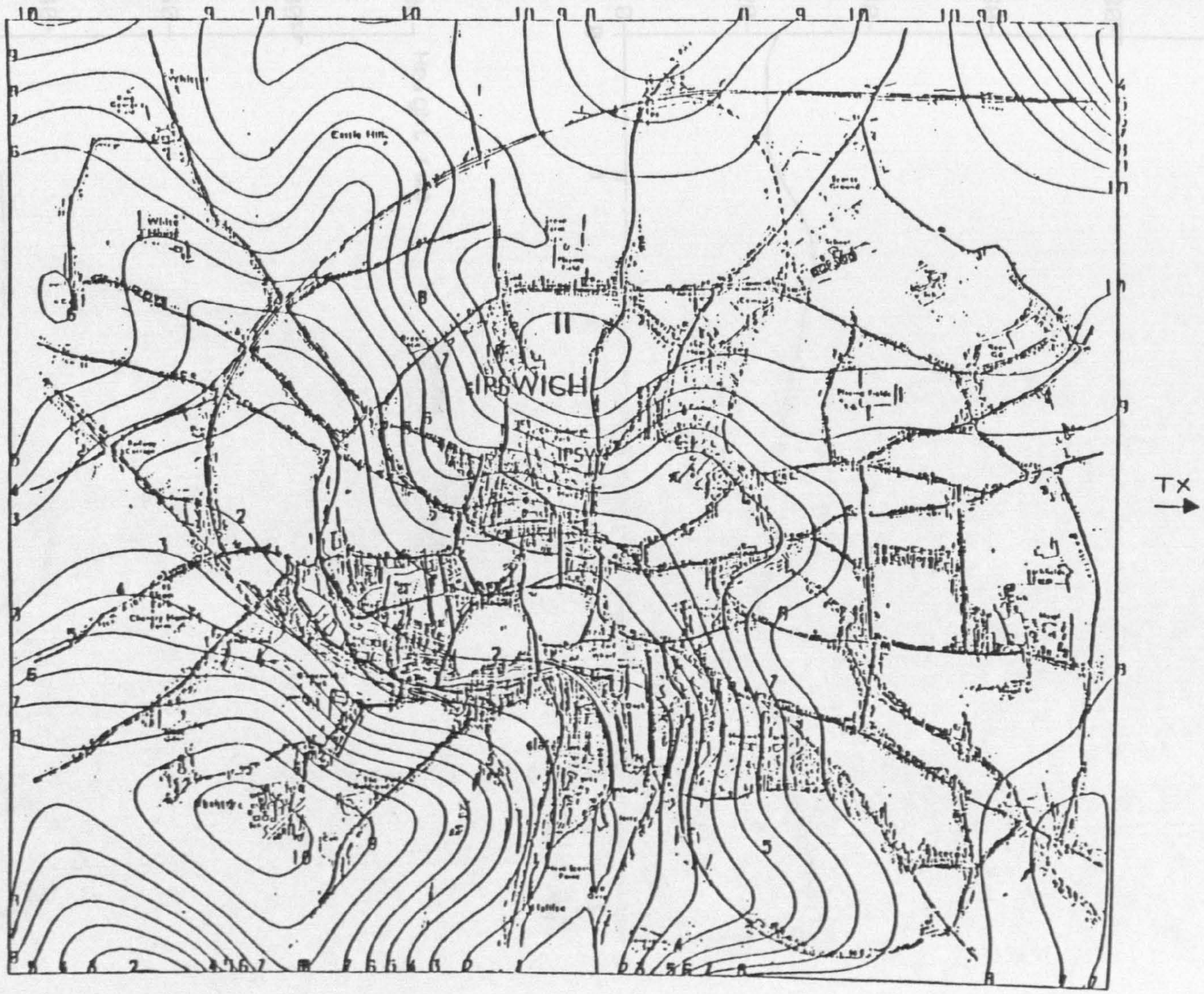

Fig. 7.2 Contour Map of the Measurement Area.

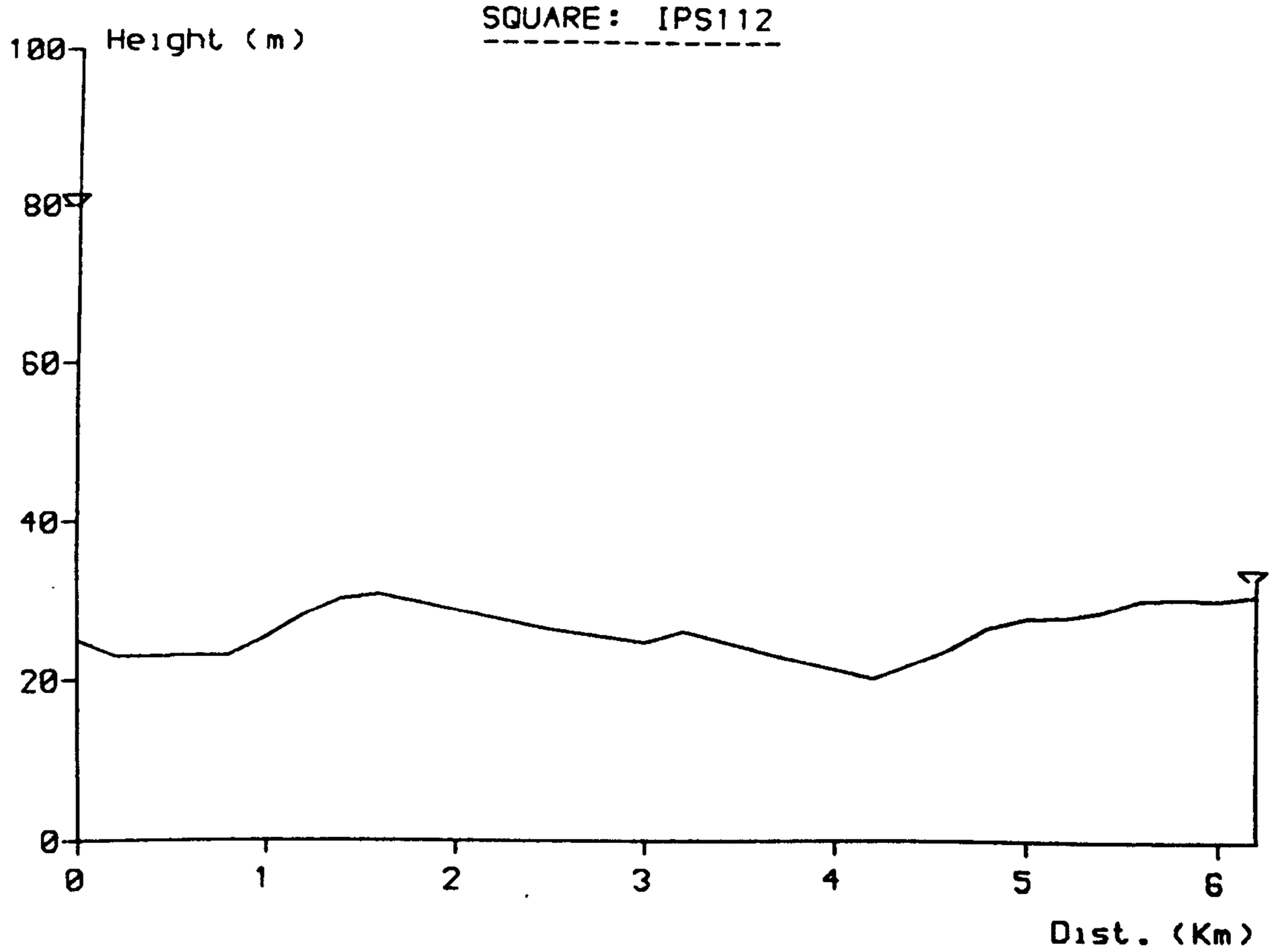

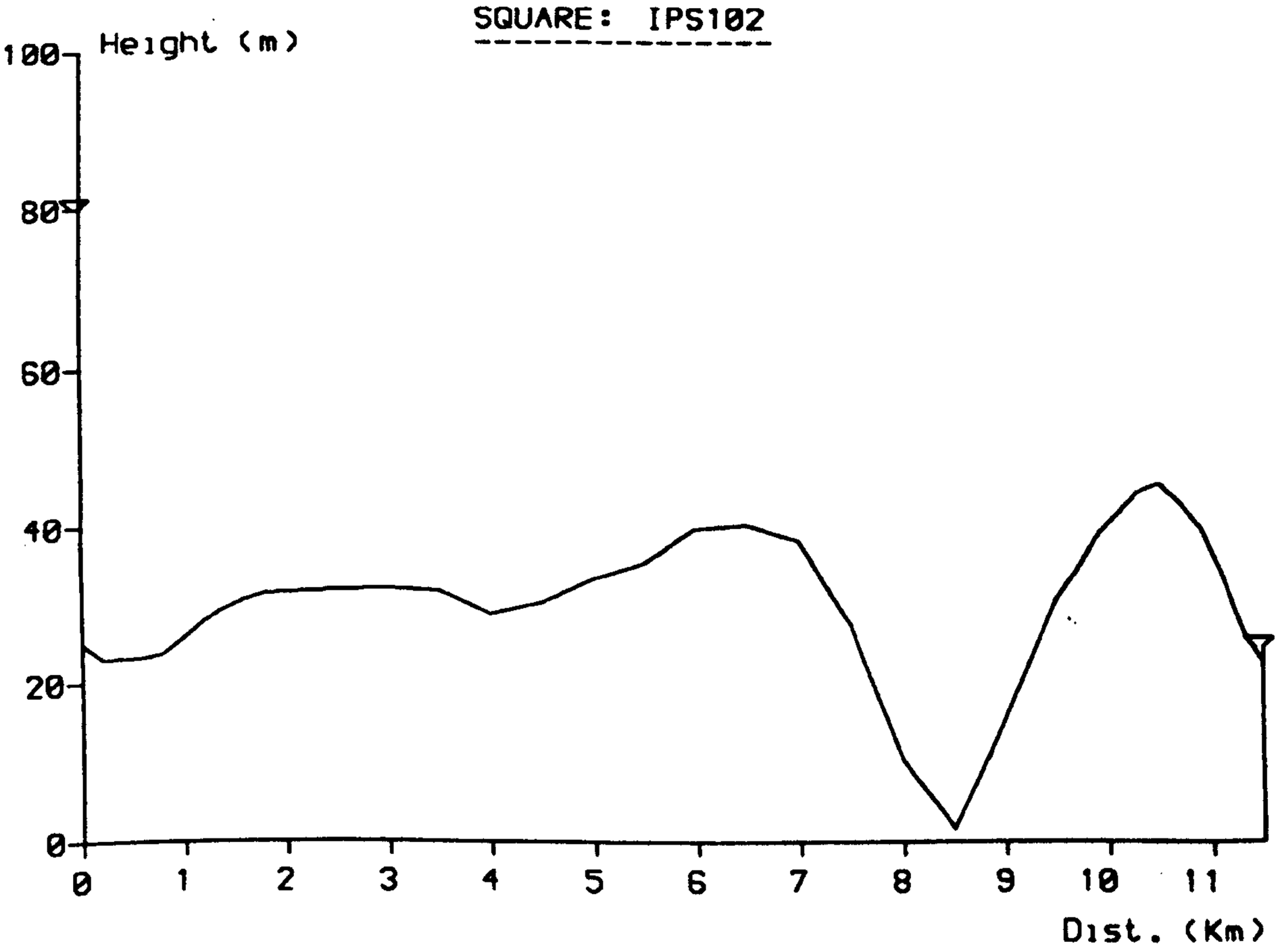

Fig. 7.3 Typical Path Profiles.

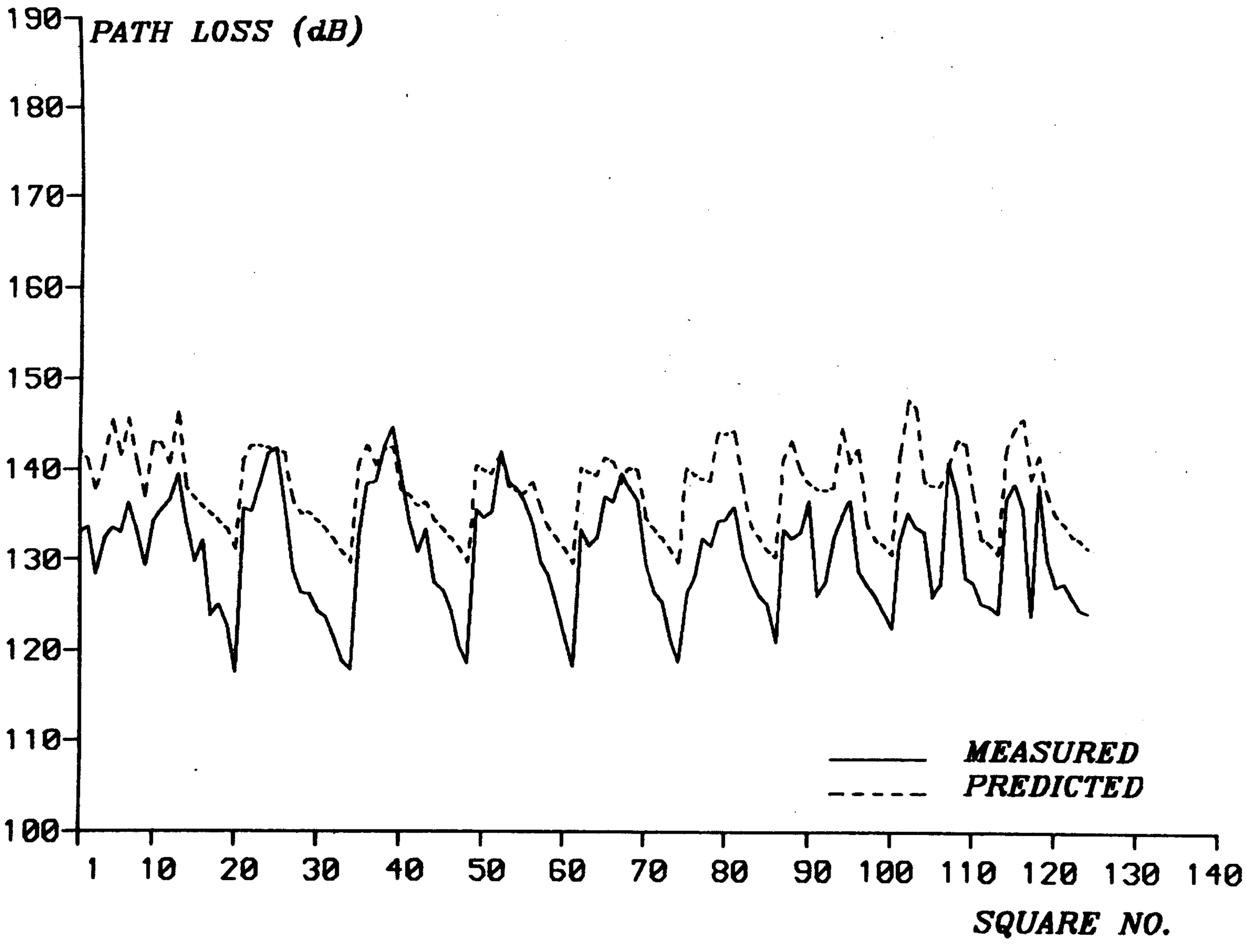

Fig. 7.4 Predicted and Measured Path Loss (Ipswich f = 160 MHz).

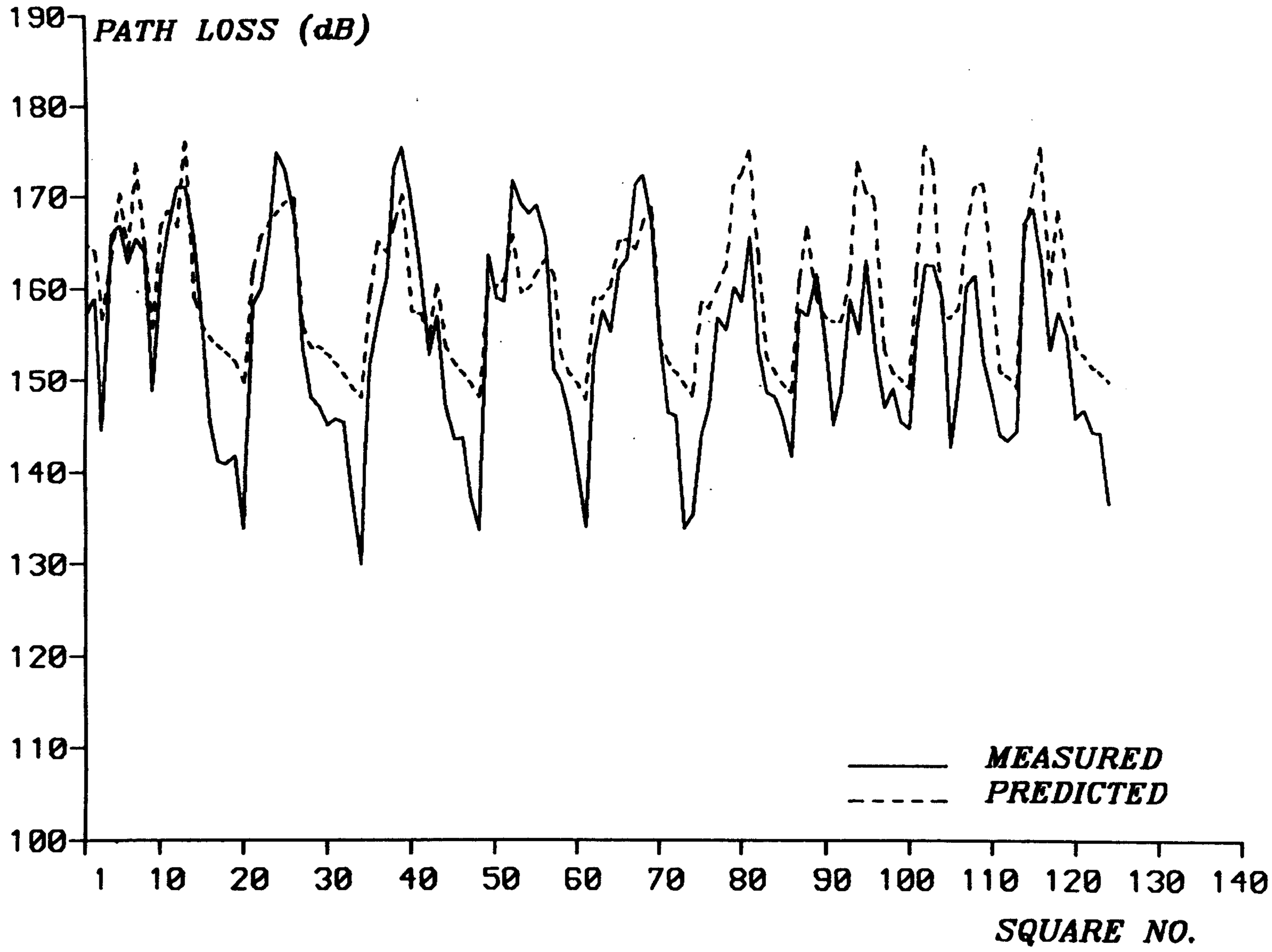

Fig. 7.5 Predicted and Measured Path Loss (Ipswich f = 900 MHz).

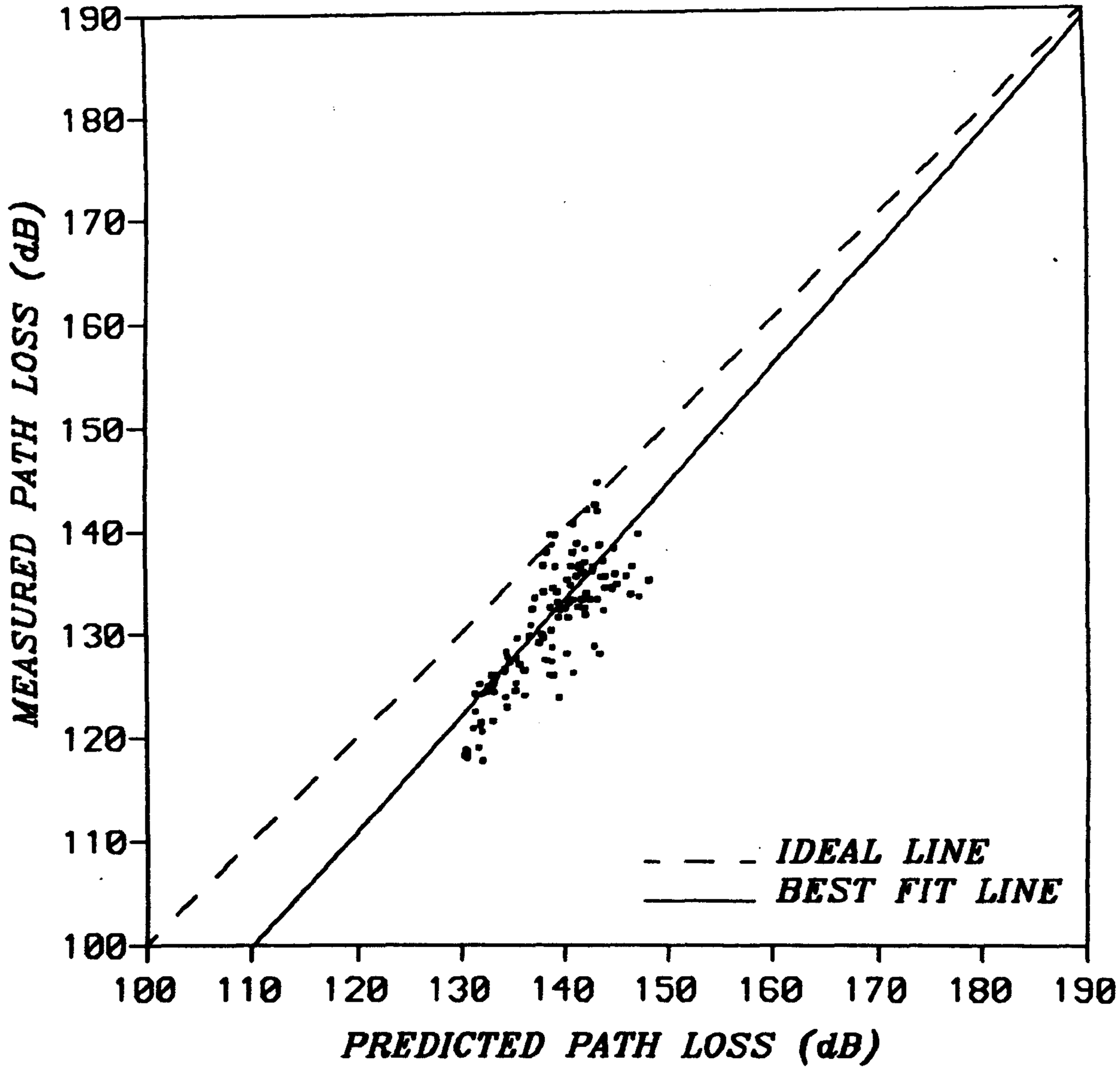

Fig. 7.6 Regression Line (Ipswich f = 160 MHz).

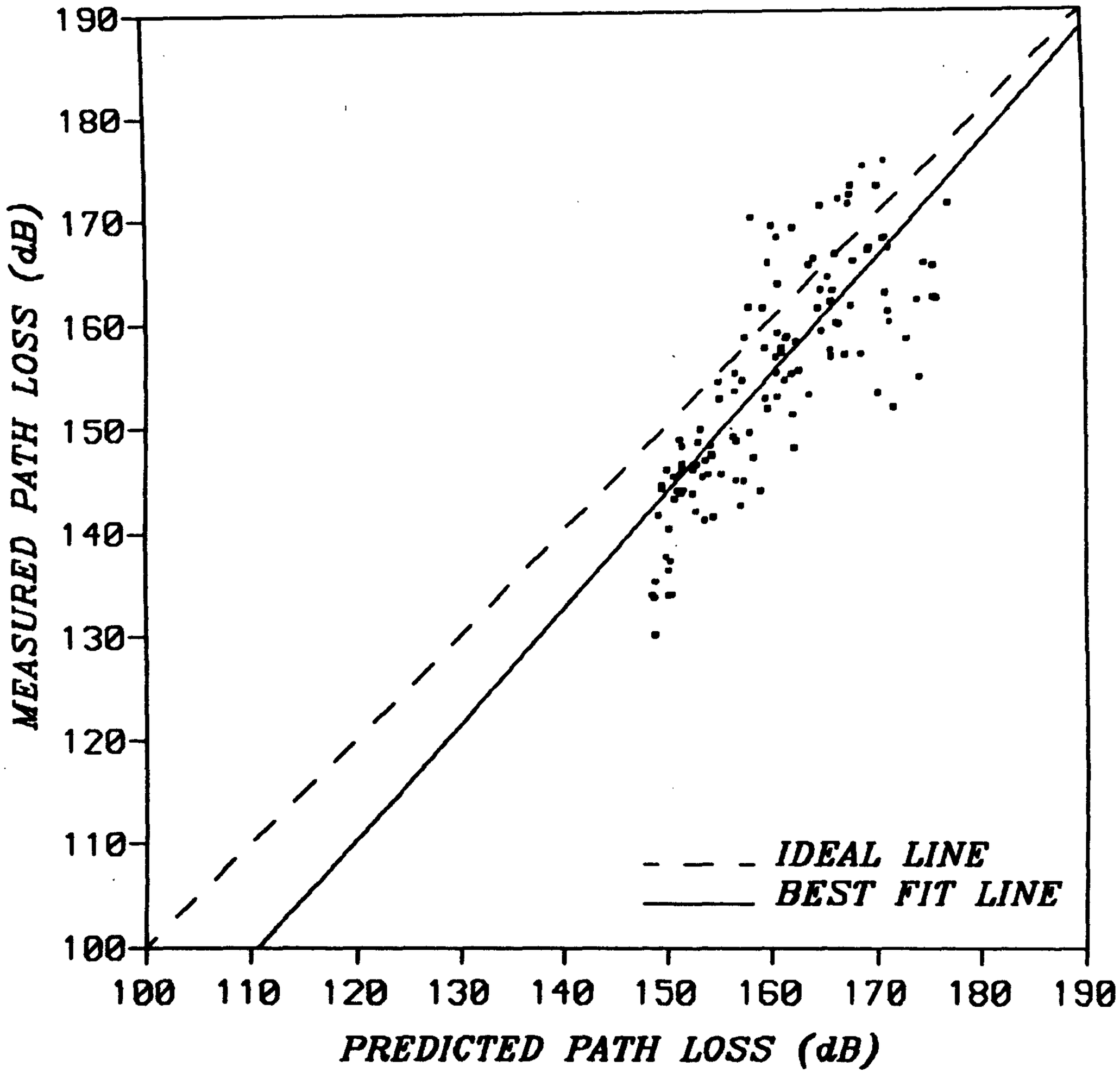

Fig. 7.7 Regression Line (Ipswich f = 900 MHz).

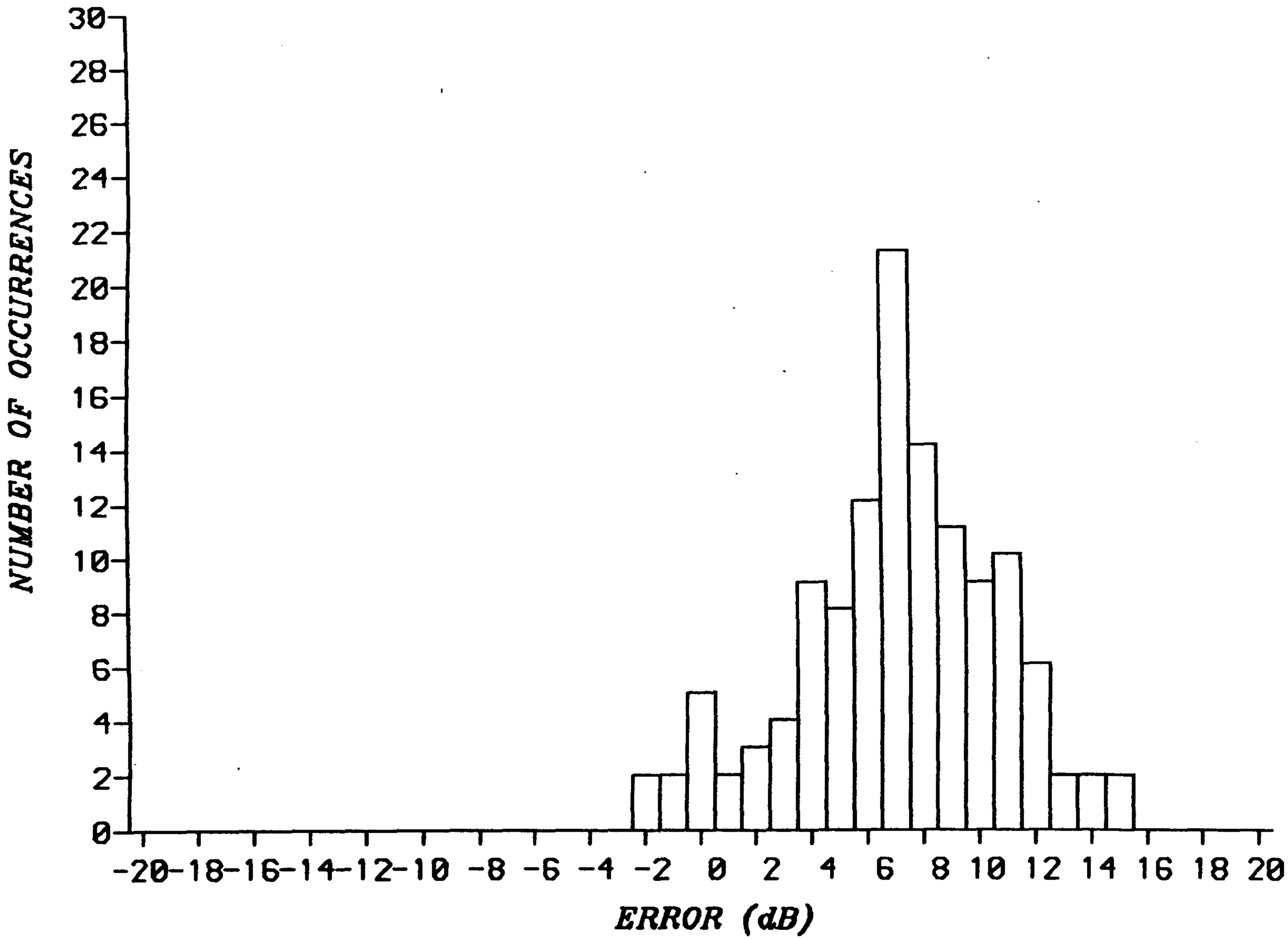

Fig. 7.8 Prediction Error Histogram (Ipswich f = 160 MHz).

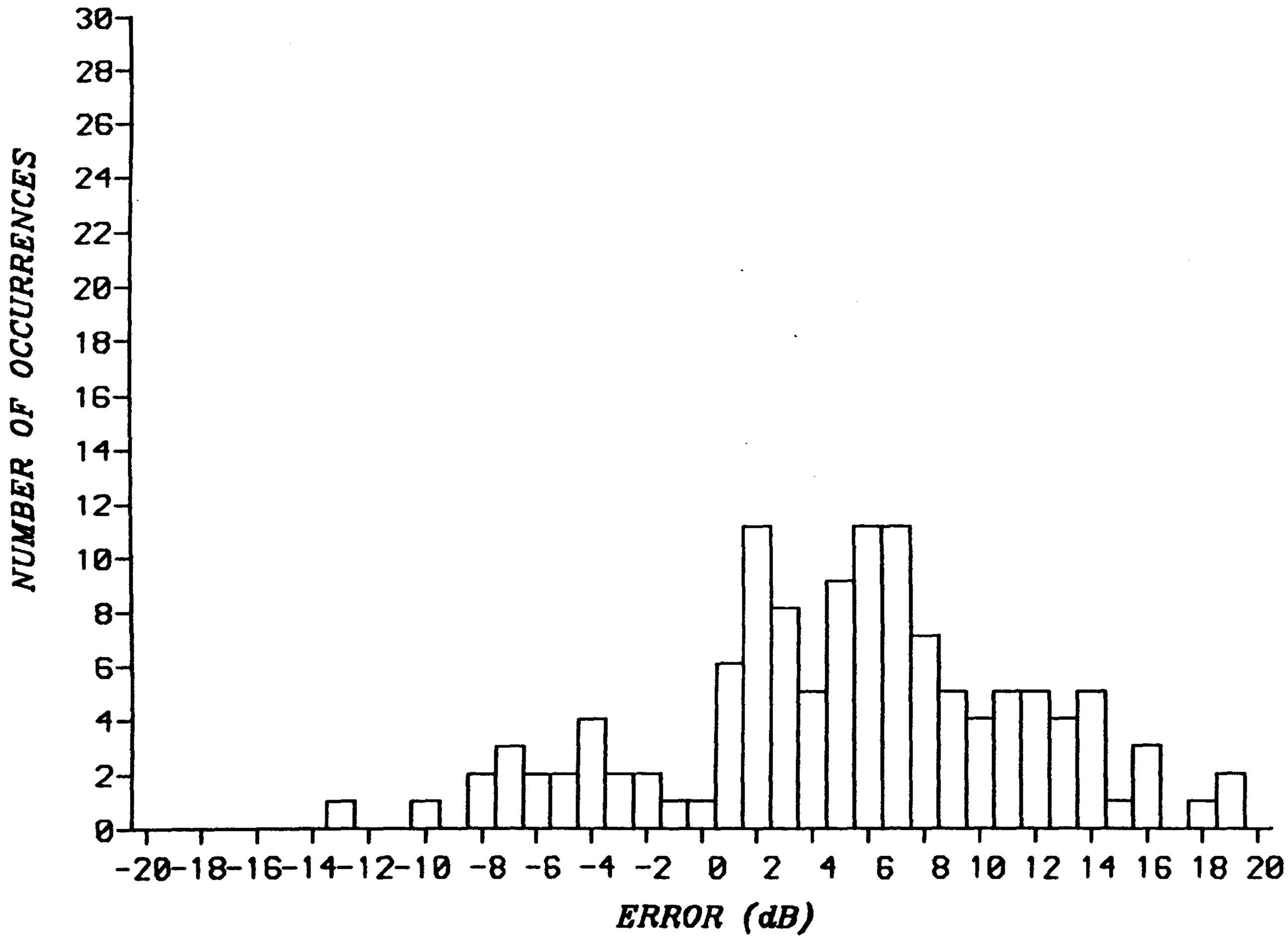

Fig. 7.9 Prediction Error Histogram (Ipswich f = 900 MHz).

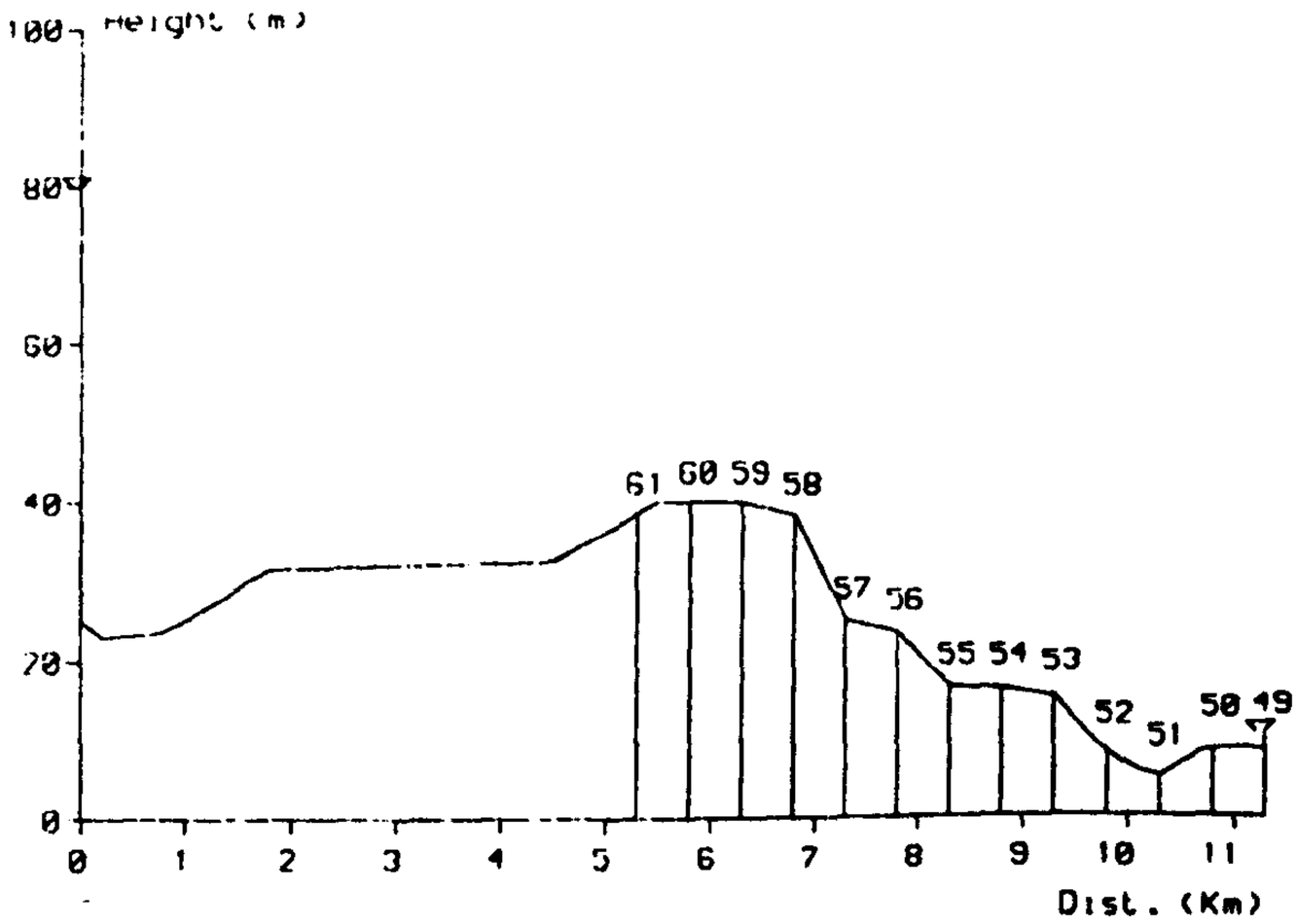

(a)

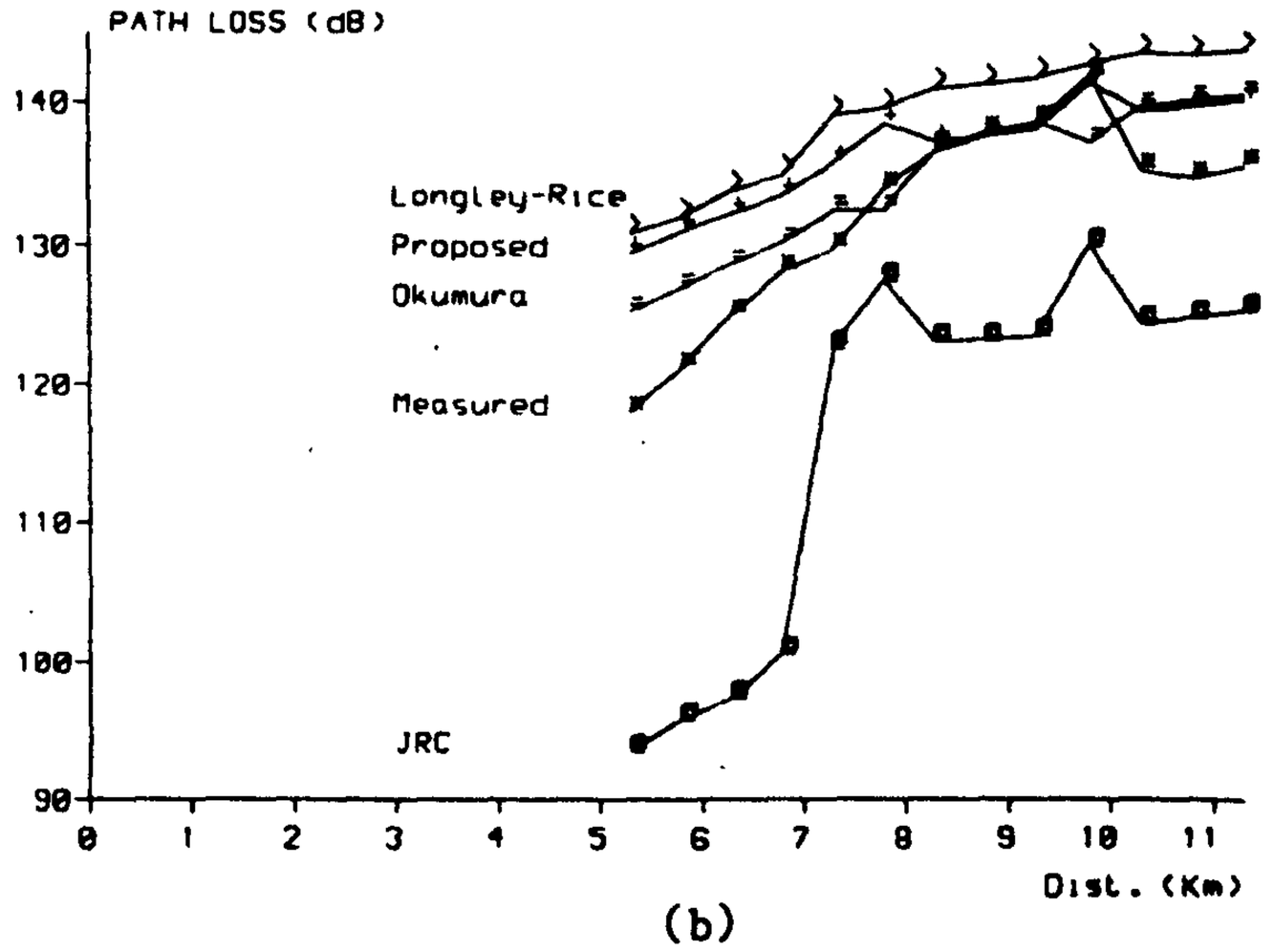

(b)

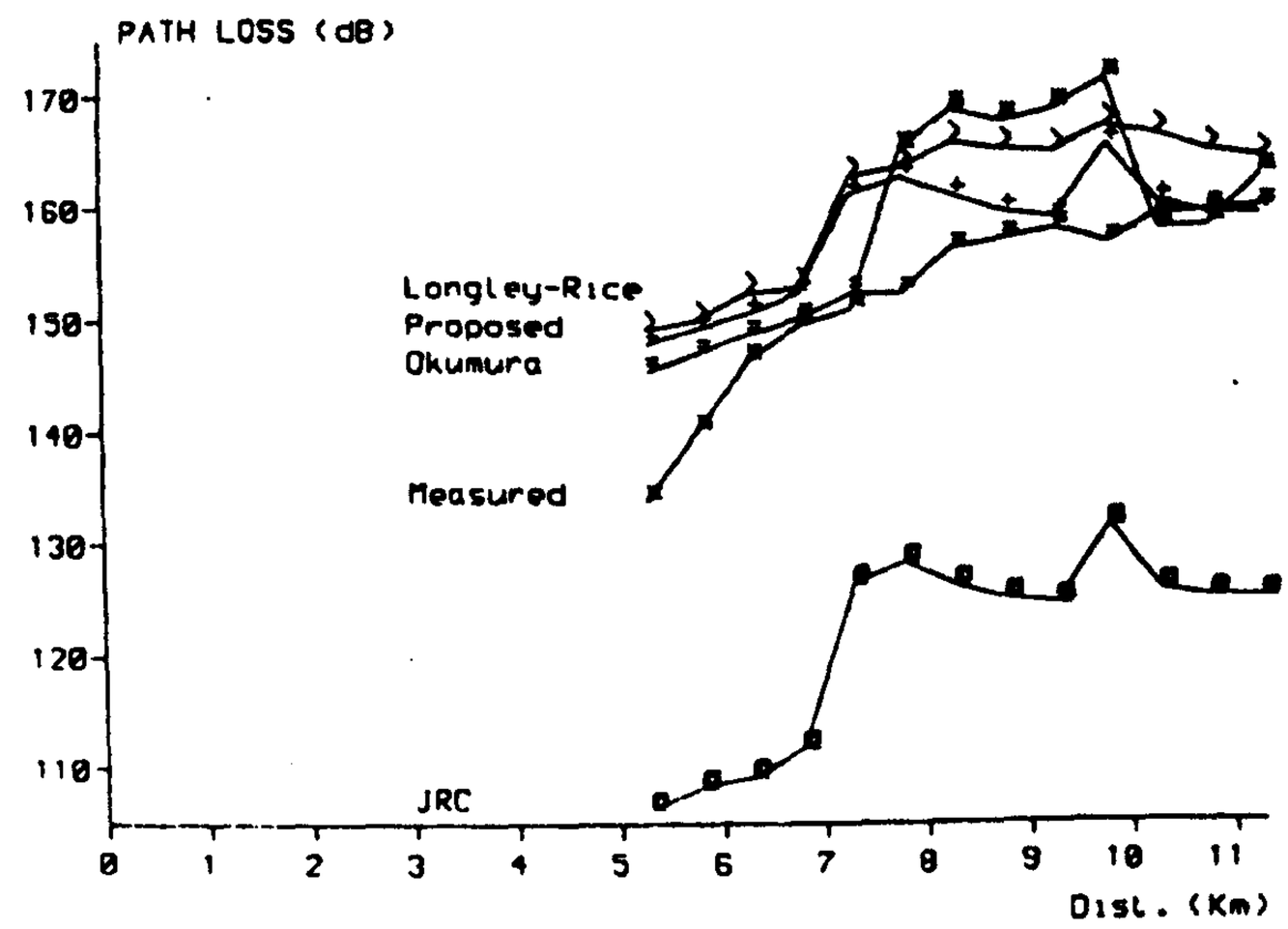

(c)

Fig. 7.10 A Radial Route (a) path profile
(b) path loss versus distance (160 MHz)
(c) path loss versus distance (900 MHz)

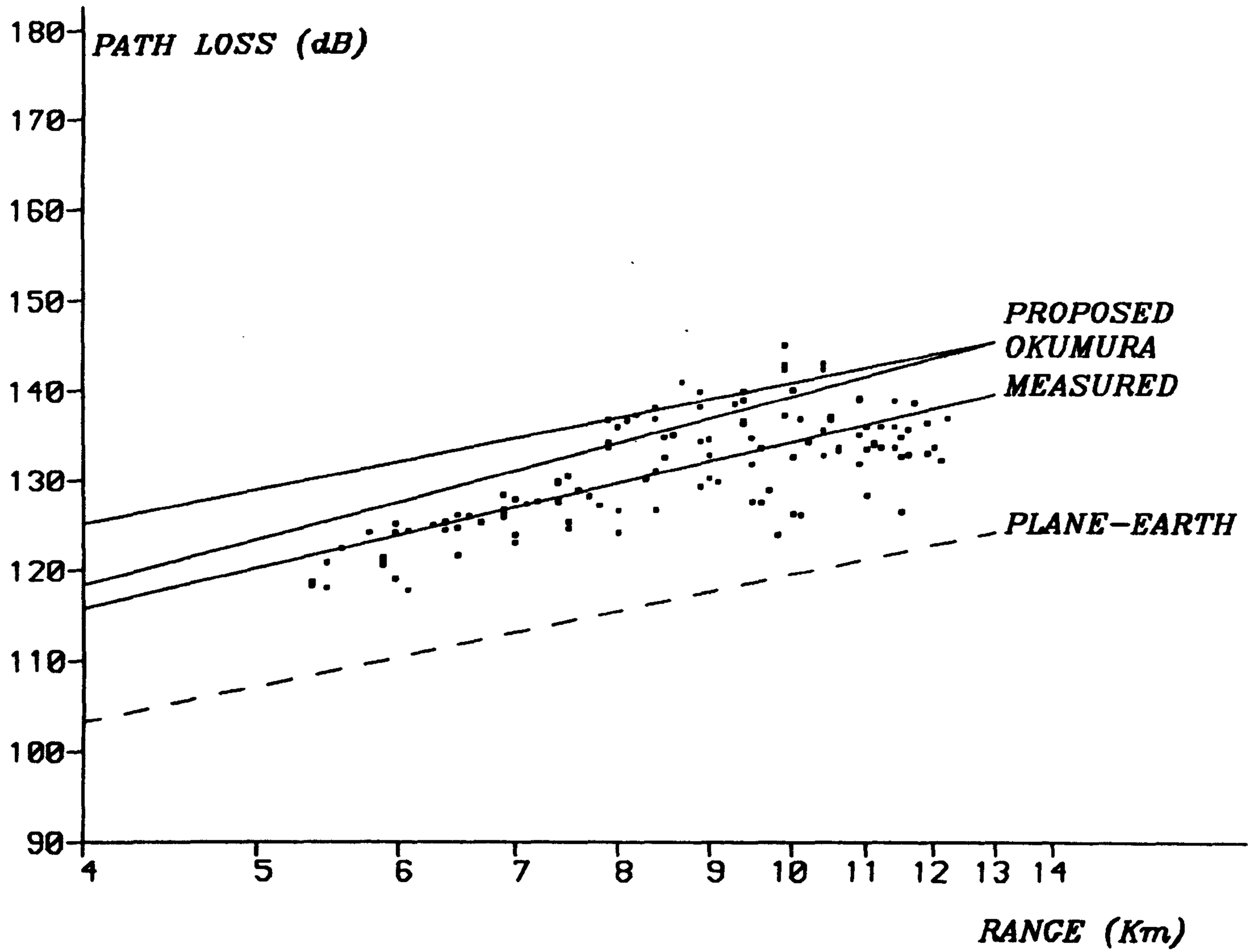

Fig. 7.11 Path Loss versus Logarithmic Range (Ipswich f = 160 MHz).

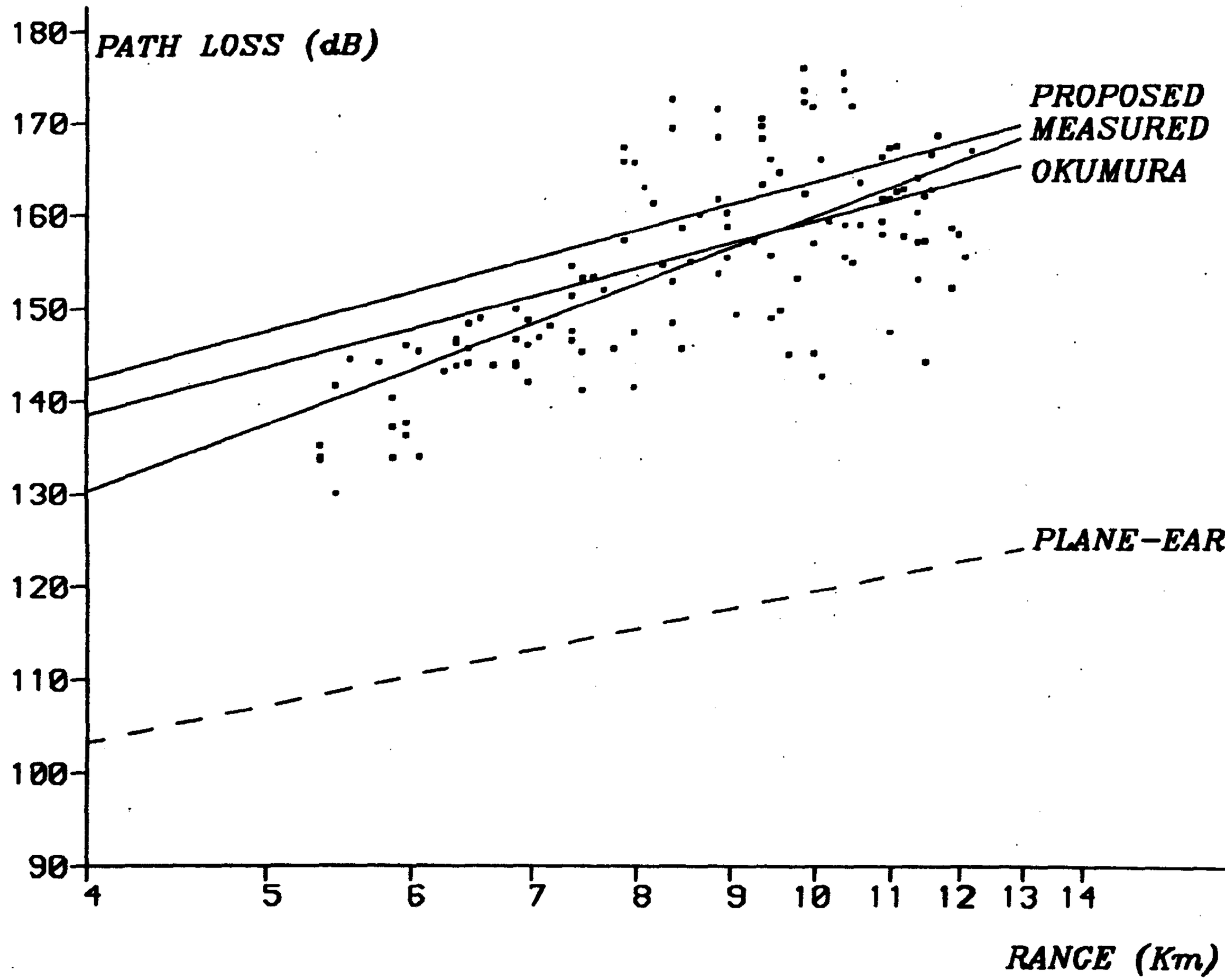

Fig. 7.12 Path Loss versus Logarithmic Range (Ipswich f = 900 MHz).

CHAPTER 8

CONCLUSIONS

A comparative study of several prediction models has identified the situations where each model is more applicable and where it is likely to produce large errors. In general, the prediction accuracy of a model depends on the similarity of the terrain and the environment of the area under investigation with that of the area for which the prediction model was designed.

The values of median path loss predicted by the propagation models have been compared with each other and with measurements for various propagation paths. Certain input parameters have a significant influence on the accuracy with which a given model can predict median transmission loss. In particular, information about terrain, buildings and foliage play an important role in making accurate predictions. The Okumura model and Hata's formulation produced the best results in urban areas. However, despite its treatment of terrain related propagation factors, the model was found to be most erroneous for prediction over rural areas in irregular terrain. The JRC model showed the best performance in predicting the propagation loss for hilly transmission paths, but produced large prediction errors in urban areas due to its lack of consideration of the building loss. However, the Longley-Rice prediction model can be judged to lie in between the above two extreme cases, although in some situations it produced the most accurate results.

The statistical analysis of the prediction errors showed that there is no obvious relationship between the errors and the transmission range. This is particularly the case for radio

propagation over irregular terrain, which further indicates that the dominant factors affecting the propagation are terrain related. One important factor in the calculation of path loss is the diffraction loss caused by the obstructing terrain features in the transmission path. The various approaches used to estimate the diffraction losses over different types of terrain vary widely in complexity depending upon the information available to make the required computations. A number of diffraction techniques have been examined which use the path profile terrain data to estimate the diffraction loss by considering the terrain obstacles as a series of knife-edges. The path profiles were constructed by a computer using a digital terrain data map of the particular area.

The profiles were also used for calculating the various terrain parameters which are required by the prediction models. The type of input parameters required by a prediction model, partly determines the model's complexity which is an important factor in the deployment of the model. A computerised prediction model has been developed which makes the prediction task simpler and more efficient. The proposed model uses the terrain data of the intervening path between the terminals in its calculation of median path loss and is best suited for prediction work over irregular terrain situations at VHF and UHF. It is based on the approach suggested by Blomquist and Ladell, which takes into account the contributing losses due to free-space plane-earth and diffraction by the terrain obstacles.

In the comparative study of the diffraction techniques, the Bullington method underestimated the diffraction loss while the Deygout method, apart from being complicated to use and more time consuming, produced large errors. The Japanese Atlas method and the

Epstein-Peterson method produced similar results, although the latter was found to be most appropriate for use in the prediction model for the calculation of the terrain diffraction loss. The JRC approach to reduce the number of intervening knife-edges in the path to three is applied to radial paths with a greater number of edges. For line-of-sight transmission paths, the diffraction loss is due to the dominant edge which does not clear the first Fresnel zone.

The transmitter effective antenna height influences the value of predicted loss and using the JRC definition, large prediction errors resulted. The proposed prediction model defines the ground reference level to be below the line joining the bases of the transmitting and the receiving terminals by a value equal to the median deviation of terrain heights along the path about this line. If the median value is positive, the line joining the terminals will be taken as the reference level. The mobile antenna height above local ground is usually small and its actual value is used in the plane-earth loss formula, which makes the effect of the surrounding features more relevant.

An urban loss factor has been derived by comparing the proposed model with Hata's formulae assuming Okumura's standard situation of quasi-smooth terrain with h_{te} = 200 m and h_{re} = 3 m. It is a function of frequency and range and should be added to the value of median path loss when the mobile lies in an urban area.

The proposed model showed a better performance against the available measured data than the existing prediction models, producing more accurate results particularly for situations where other models produced large prediction errors. The best results were obtained for Cheshire field trials which had been conducted at a

frequency of 139 MHz over mainly rural areas, and which constituted the main part of the measured data. Considering all the propagation paths, the proposed model improves the value of the standard error by more than 3 dB to 5.1 dB compared to the JRC's error of 8.8 dB, which is the best result among the prediction models studied. In the case of measurement results in Ipswich urban area, the proposed model produced a standard error value of 8.2 dB at 900 MHz, the same as that due to Okumura, whereas at 160 MHz, the Okumura model had a lower error value of 6.4 dB compared to the proposed model's value of 7.9 dB. However, the proposed model performed better in terms of other statistical measures, one example being the value of coefficient of correlation between the prediction and measurement.

The prediction model, as developed, does not take into account propagation losses due to foliage, and its treatment of the urban loss is limited. In urban areas there are a number of significant factors including the street orientation and other building-related factors which must be studied in detail so that a viable prediction method, specifically for use in urban environments, can be derived. Therefore, the proposed urban loss factor which is applicable over the same ranges as in Hata's formulae, cannot be expected to produce very accurate results when predicting in highly built-up areas. Further, the urban loss factor is related to the Okumura prediction curves facing the same question as that which has been raised about the applicability of the Okumura method to cities other than those which were examined in Japan during the development of the original model. In order to make reliable predictions of the transmission loss over irregular terrain, the propagation model depends on terrain data maps of the areas of interest. Digital terrain data bases do not

provide accurate elevations at all points; rather they provide accurate elevations only at discrete data points and interpolation procedures have to be used to determine elevations at other points. Thus ground elevations at other than the actual discrete data points are subject to error. In mobile radio environments, the receiver antenna is low so that any small change in the surrounding terrain can affect the calculation of terrain losses and consequently the median path loss. Inaccurate terrain data can result in the apparent presence of an obstructing edge in a particular reconstructed transmission path, even though the edge might not physically exist. The proposed prediction model depends also on terrain data to derive the transmitting antenna effective height and the accuracy of terrain data is of great influence on the reliability of the results.

Any radio propagation model has its own limitations in terms of the required input data, the propagation factors treated and the output parameters it provides. It is only realistic to accept that a certain degree of prediction error results when a prediction model is applied to a particular situation. Often, an attempt to increase the accuracy of a certain input parameter or the calculation of a particular propagation factor would result in undesired complications which do not necessarily produce the required performance. However, prediction work is increasingly required as demand for communication systems rises. The proposed propagation model is intended to increase the efficiency and the reliability of the median path loss prediction required for determining the area coverage over irregular terrain. However, as in the case of any other prediction model, further studies are needed to determine the applicability and usefulness of the proposed model to specific propagation conditions.

APPENDIX A

COMPUTER PROGRAMS

```
* MEDIAN PATH LOSS PREDICTION PROGRAM

      COMMON /ALL/F,HTG,HRG,RM,XT,YT,XR,YR,IT,JT,IR,JR,GHT,CS,H
      COMMON /PATH/TD,TH,U,Z,N
      DIMENSION H(100,140),TD(1000),TH(1000),U(1000),Z(1000),HC(1000)
     *,DE(100),HE(100),DE1(100),HE1(100),DE2(100),HE2(100)
     *,DEZ(100),HEZ(100),DEZ1(100),HEZ1(100),DEZ2(100),HEZ2(100)
     *,LE(100),LE1(100),LE2(100),IDED(100),IDEDZ(100)
     *,DVH(1000),XE(3),YE(3)
      PI=4.*ATAN(1.)

* SIZE OF THE TERRAIN DATA AND MEASUREMENT SQUARE SIDES
      CS=500.

* READ THE INPUT PARAMETERS (HEIGHTS AND DISTANCES IN METRES)
* F; FREQUENCY  HTG; TRANSMITTING ANTENNA HEIGHT ABOVE LOCAL GROUND
* GHT; HEIGHT OF THE LOCAL GROUND ABOVE SEA-LEVEL
* HRG; RECEIVING ANTENNA HEIGHT ABOVE LOCAL GROUND
* XT; X CO-ORDINATE OF THE TRANSMITTER IN METRES (ORIGIN AT SW CORNER
* OF THE TERRAIN DATA MAP)  YT; Y CO-ORDINATE OF THE TX IN METRE
* IR AND JR; HORIZONTAL AND VERTICAL POSITION OF THE RECEIVER SQUARE
* WITH RESPECT TO SW CORNER
      READ (1,*) F,HTG,GHT,HRG,XT,YT,IR,JR

* READ THE TERRAIN DATA
* THE ARRAY IS ARRANGED SUCH THAT H(1,1) REFERS TO THE SW CORNER OF THE
* MAP AND H(100,140) REFERS TO THE 100TH SQUARE TO THE EAST AND 140TH
* SQUARE TO THE NORTH
      DO 100 J=1,140
      DO 100 I=1,100
      READ (2,*) H(I,J)
100   CONTINUE

      PLTER=0.
      IT=INT(XT/CS)+1
      JT=INT(YT/CS)+1
      XR=REAL(IR*INT(CS))-(CS/2.)
      YR=REAL(JR*INT(CS))-(CS/2.)
      RM=SQRT(((XR-XT)**2)+((YR-YT)**2))
      R=RM/1000.

* DERIVE THE PATH PROFILE TERRAIN DATA (HEIGHTS AND DISTANCES IN METRES)
      CALL TPATH (TD,TH,U,Z,N)

* ADJUST THE HEIGHTS FOR THE EARTH CURVATURE
      CFK=4./3.
      DYY=2.*CFK*6370.E03
      DD2=(TD(N)-TD(1))/2.
      HMX=(DD2**2)/DYY
      DO 200 I=1,N
      HC(I)=HMX-(((TD(I)-DD2)**2)/DYY)
      TH(I)=TH(I)+HC(I)
200   CONTINUE

* FREE-SPACE LOSS
      FSL = 20.*ALOG10(40.*PI*R*F/3.)

* LINE JOINING THE BASES OF THE TERMINALS
      SL=(TH(N)-TH(1))/TD(N)
```

```
* DEVIATIONS OF TERRAIN HEIGHTS ABOUT THIS LINE
      DO 300 I=1,N
      DVH(I)=TH(I)-(TH(1)+(SL*TD(I)))
300   CONTINUE

* MEDIAN DEVIATION
      DVHM = CUM(50.,DVH,N)

* TRANSMITTER EFFECTIVE ANTENNA HEIGHT
      HTE=HTG+ABS(MIN(0.,DVHM))

* PLANE-EARTH LOSS
      PEL = 120.+(40.*ALOG10(R))-(20.*ALOG10(HTE*HRG))

*** DIFFRACTION LOSS

      CALL EDGES (TD,TH,N,LE,DE,HE,NE,LE1,DE1,HE1,NE1
     *           ,LE2,DE2,HE2,NE2,IDED)

      DLOSS=0.

      IF (NE1.EQ.0) THEN
* NO TYPE I EDGES (LINE-OF-SIGHT)

      IF (NE2.EQ.1) THEN
* LINE-OF-SIGHT WITH INADEQUATE FRESNEL-ZONE CLEARANCE
      DO 400 I=1,3
      XE(I)=DE(I)
      YE(I)=HE(I)
400   CONTINUE
      DLOSS = -DLKN(XE,YE)
      END IF

      ELSE
* NON LINE-OF-SIGHT

* ARRANGE THE EDGES DATA FOR THE EPSTEIN-PETERSON METHOD, REDUCING
* EDGES OF TYPE I INTO 3 FOR PATHS WITH GREATER NUMBER OF EDGES

      CALL PREDG (1,F,TD,TH,N,DE,HE,NE,IDED,DEZ,HEZ,NEZ
     *           ,DEZ1,HEZ1,NEZ1,DEZ2,HEZ2,NEZ2,IDEDZ)

      CALL EPS (DEZ1,HEZ1,NEZ1,DLS)
      DLOSS=DLS

      END IF
***

* PREDICTION MEDIAN PATH LOSS
      PLP = FSL+SQRT(((PEL-FSL)**2)+(DLOSS*DLOSS))

      STOP
      END

* EPSTEIN-PETERSON ESTIMATED DIFFRACTION LOSS
      SUBROUTINE EPS (XD,YD,ND,DIFL)
      DIMENSION XD(ND),YD(ND),XE(3),YE(3)

      DIFL=0.
      DO 200 I=1,ND-2
      DO 100 J=1,3
      K=I+J-1
      XE(J)=XD(K)
      YE(J)=YD(K)
100   CONTINUE
```

```
      DL=DLKN(XE,YE)

      DIFL = DIFL-DL
  200 CONTINUE

      RETURN
      END

* KNIFE-EDGE DIFFRACTION LOSS
      FUNCTION DLKN (XX,YY)
      COMMON /ALL/F
      REAL LAMBDA,XX(3),YY(3)
      DIST(I,J)=SQRT(((XX(I)-XX(J))**2)+((YY(I)-YY(J))**2))
      LAMBDA=300./F

      DD=DIST(1,3)
      D1=DIST(1,2)
      D2=DIST(2,3)
      SL=(YY(3)-YY(1))/(XX(3)-XX(1))
      C=YY(1)-(SL*XX(1))
      YP=(SL*XX(2))+C
      HP=YY(2)-YP
      YY(2)=YP
      R1=DIST(1,2)
      R2=DIST(2,3)
      A=(2.*((1./R1)+(1./R2)))/LAMBDA
      V=-HP*SQRT(A)
      Q=1.
      IF (V.LE.1..AND.V.GE.0.) Q=.5+(.625*V)
      IF (V.LT.0..AND.V.GE.-1.) Q=.5*EXP(.95*V)
      IF (V.LT.-1..AND.V.GE.-2.4) Q=.4-SQRT(.1184-(((.1*V)+.38)**2))
      IF (V.LT.-2.4) Q=-.225/V
      DLKN = 20.*ALOG10(Q)
      RETURN
      END

* QUANTILES
      FUNCTION CUM (PER,A,N)
      DIMENSION A(N)
   10 CONTINUE
      DO 100 L=1,N-1
      IF (A(L).GT.A(L+1)) THEN
      AA=A(L)
      A(L)=A(L+1)
      A(L+1)=AA
      GO TO 10
      END IF
  100 CONTINUE
      P=PER/100.
      R=1.+(P*(N-1))
      I1=INT(R)
      I2=I1+1
      D=R-REAL(I1)
      CUM=(D*A(I2))+((1.-D)*A(I1))
      RETURN
      END
```

```
* DETERMINES THE PATH PROFILE. TD; DISTANCE OF THE POINTS FROM TX. TH;
* CORRESPONDING HEIGHT ABOVE SEA LEVEL. U; POINT X CO-ORD. Z; Y CO-ORD.
* (THE ORIGIN OF THE U AND Z CO-ORDS. IS THE SAME AS THAT OF XT, ETC.)
* N; NUMBER OF PATH DATA POINTS.
* IF GHT(GROUND HEIGHT AT THE TX SITE) IS < 0 , HEIGHT OF SQUARE INCLUDI
* NG THE TX WILL BE TAKEN FOR TH(1).
* THE PARAMETER 'IM' CAN BE SET FOR DIFFERENT COMBINATION OF INTERPOLATI
* ON MODES FOR DERIVATION OF THE PATH PROFILE TERRAIN HEIGHTS.
*
      SUBROUTINE TPATH (TD,TH,U,Z,N)
      COMMON /ALL/F,HTG,HRG,D,XT,YT,XR,YR,IT,JT,IR,JR,GHT,CS,H
      REAL H(100,140),TDR(1000),THR(1000),UR(1000),ZR(1000)
     *,TDC(1000),THC(1000),UC(1000),ZC(1000)
     *,TDD(1000),THD(1000),UD(1000),ZD(1000)
     *,TD(1000),TH(1000),HD(1000),U(1000),Z(1000)

      ICS=INT(CS)

C   INTERPOLATION,IM, 1;RAW 2;COLUMN 3;DIAGONAL 4;R&C 5;R&D 6;C&D 7;R,C&D
      IM=7

      IF (XT.EQ.XR) THEN
      IF (YT.LT.YR) INC=1
      IF (YT.GT.YR) INC=-1
      JL=JT
      CD=REAL(INC)*(YT-REAL((JT*ICS)-(ICS/2)))
      IF (CD.GE.0.) JL=JT+INC
      N=1
      DO 200 L=JL,JR-INC,INC
      N=N+1
      TD(N)=ABS(YT-REAL((L*ICS)-(ICS/2)))
      TH(N)=H(IT,L)
      U(N)=XR
      Z(N)=REAL((L*ICS)-(ICS/2))
  200 CONTINUE
      N=N+1
      GO TO 5000
      END IF

      IF (YT.EQ.YR) THEN
      IF (XT.LT.XR) INC=1
      IF (XT.GT.XR) INC=-1
      IL=IT
      CD=REAL(INC)*(XT-REAL((IT*ICS)-(ICS/2)))
      IF (CD.GE.0.) IL=IT+INC
      N=1
      DO 300 L=IL,IR-INC,INC
      N=N+1
      TD(N)=ABS(XT-REAL((L*ICS)-(ICS/2)))
      TH(N)=H(L,JT)
      U(N)=REAL((L*ICS)-(ICS/2))
      Z(N)=YR
  300 CONTINUE
      N=N+1
      GO TO 5000
      END IF

      CALL ROW (TDR,THR,UR,ZR,NR)
      CALL COLUMN (TDC,THC,UC,ZC,NC)
      CALL DGNAL (TDD,THD,UD,ZD,ND)
```

```
      IF (IM.EQ.1) THEN
      N=NR+2
      DO 400 K=N-1,2,-1
      TD(K)=TDR(K-1)
      TH(K)=THR(K-1)
      U(K)=UR(K-1)
      Z(K)=ZR(K-1)
  400 CONTINUE
      GO TO 5000
      END IF

      IF (IM.EQ.2) THEN
      N=NC+2
      DO 500 K=N-1,2,-1
      TD(K)=TDC(K-1)
      TH(K)=THC(K-1)
      U(K)=UC(K-1)
      Z(K)=ZC(K-1)
  500 CONTINUE
      GO TO 5000
      END IF

      IF (IM.EQ.3) THEN
      N=ND+2
      DO 600 K=N-1,2,-1
      TD(K)=TDD(K-1)
      TH(K)=THD(K-1)
      U(K)=UD(K-1)
      Z(K)=ZD(K-1)
  600 CONTINUE
      GO TO 5000
      END IF

      IF (IM.EQ.4) THEN
      NN=NR+NC
      DO 700 K=1,NN
      IF (K.LE.NR) THEN
      TD(K)=TDR(K)
      TH(K)=THR(K)
      U(K)=UR(K)
      Z(K)=ZR(K)
      ELSE
      TD(K)=TDC(K-NR)
      TH(K)=THC(K-NR)
      U(K)=UC(K-NR)
      Z(K)=ZC(K-NR)
      END IF
  700 CONTINUE
  750 CONTINUE
      DO 800 K=1,NN-1
      IF (TD(K).GE.TD(K+1)) THEN
      IF (TD(K).EQ.TD(K+1)) THEN
      NN=NN-1
      DO 775 L=K+1,NN
      TD(L)=TD(L+1)
      TH(L)=TH(L+1)
      U(L)=U(L+1)
      Z(L)=Z(L+1)
  775 CONTINUE
```

```
      ELSE
      DD=TD(K)
      HH=TH(K)
      UU=U(K)
      ZZ=Z(K)
      TD(K)=TD(K+1)
      TH(K)=TH(K+1)
      U(K)=U(K+1)
      Z(K)=Z(K+1)
      TD(K+1)=DD
      TH(K+1)=HH
      U(K+1)=UU
      Z(K+1)=ZZ
      END IF
      GO TO 750
      END IF
  800 CONTINUE
      N=NN+2
      DO 900 K=N-1,2,-1
      TD(K)=TD(K-1)
      TH(K)=TH(K-1)
      U(K)=U(K-1)
      Z(K)=Z(K-1)
  900 CONTINUE
      GO TO 5000
      END IF

      IF (IM.EQ.5) THEN
      NN=NR+ND
      DO 1000 K=1,NN
      IF (K.LE.NR) THEN
      TD(K)=TDR(K)
      TH(K)=THR(K)
      U(K)=UR(K)
      Z(K)=ZR(K)
      ELSE
      TD(K)=TDD(K-NR)
      TH(K)=THD(K-NR)
      U(K)=UD(K-NR)
      Z(K)=ZD(K-NR)
      END IF
 1000 CONTINUE
 1050 CONTINUE
      DO 1100 K=1,NN-1
      IF (TD(K).GE.TD(K+1)) THEN
      IF (TD(K).EQ.TD(K+1)) THEN
      NN=NN-1
      DO 1075 L=K+1,NN
      TD(L)=TD(L+1)
      TH(L)=TH(L+1)
      U(L)=U(L+1)
      Z(L)=Z(L+1)
 1075 CONTINUE
      ELSE
      DD=TD(K)
      HH=TH(K)
      UU=U(K)
      ZZ=Z(K)
      TD(K)=TD(K+1)
      TH(K)=TH(K+1)
```

```
      U(K)=U(K+1)
      Z(K)=Z(K+1)
      TD(K+1)=DD
      TH(K+1)=HH
      U(K+1)=UU
      Z(K+1)=ZZ
      END IF
      GO TO 1050
      END IF
1100  CONTINUE
      N=NN+2
      DO 1200 K=N-1,2,-1
      TD(K)=TD(K-1)
      TH(K)=TH(K-1)
      U(K)=U(K-1)
      Z(K)=Z(K-1)
1200  CONTINUE
      GO TO 5000
      END IF

      IF (IM.EQ.6) THEN
      NN=NC+ND
      DO 1300 K=1,NN
      IF (K.LE.NC) THEN
      TD(K)=TDC(K)
      TH(K)=THC(K)
      U(K)=UC(K)
      Z(K)=ZC(K)
      ELSE
      TD(K)=TDD(K-NC)
      TH(K)=THD(K-NC)
      U(K)=UD(K-NC)
      Z(K)=ZD(K-NC)
      END IF
1300  CONTINUE
1350  CONTINUE
      DO 1400 K=1,NN-1
      IF (TD(K).GE.TD(K+1)) THEN
      IF (TD(K).EQ.TD(K+1)) THEN
      NN=NN-1
      DO 1375 L=K+1,NN
      TD(L)=TD(L+1)
      TH(L)=TH(L+1)
      U(L)=U(L+1)
      Z(L)=Z(L+1)
1375  CONTINUE
      ELSE
      DD=TD(K)
      HH=TH(K)
      UU=U(K)
      ZZ=Z(K)
      TD(K)=TD(K+1)
      TH(K)=TH(K+1)
      U(K)=U(K+1)
      Z(K)=Z(K+1)
      TD(K+1)=DD
      TH(K+1)=HH
      U(K+1)=UU
      Z(K+1)=ZZ
      END IF
```

```
      GO TO 1350
      END IF
1400  CONTINUE
      N=NN+2
      DO 1500 K=N-1,2,-1
      TD(K)=TD(K-1)
      TH(K)=TH(K-1)
      U(K)=U(K-1)
      Z(K)=Z(K-1)
1500  CONTINUE
      GO TO 5000
      END IF

      IF (IM.EQ.7) THEN
      NN=NR+NC+ND
      DO 1600 K=1,NN
      IF (K.LE.NR) THEN
      TD(K)=TDR(K)
      TH(K)=THR(K)
      U(K)=UR(K)
      Z(K)=ZR(K)
      END IF
      IF(K.GT.NR.AND.K.LE.(NR+NC)) THEN
      TD(K)=TDC(K-NR)
      TH(K)=THC(K-NR)
      U(K)=UC(K-NR)
      Z(K)=ZC(K-NR)
      END IF
      IF(K.GT.(NR+NC)) THEN
      TD(K)=TDD(K-NR-NC)
      TH(K)=THD(K-NR-NC)
      U(K)=UD(K-NR-NC)
      Z(K)=ZD(K-NR-NC)
      END IF
1600  CONTINUE
1650  CONTINUE
      DO 1700 K=1,NN-1
      IF (TD(K).GE.TD(K+1)) THEN
      IF (TD(K).EQ.TD(K+1)) THEN
      NN=NN-1
      DO 1675 L=K+1,NN
      TD(L)=TD(L+1)
      TH(L)=TH(L+1)
      U(L)=U(L+1)
      Z(L)=Z(L+1)
1675  CONTINUE
      ELSE
      DD=TD(K)
      HH=TH(K)
      UU=U(K)
      ZZ=Z(K)
      TD(K)=TD(K+1)
      TH(K)=TH(K+1)
      U(K)=U(K+1)
      Z(K)=Z(K+1)
      TD(K+1)=DD
      TH(K+1)=HH
      U(K+1)=UU
      Z(K+1)=ZZ
      END IF
```

```
      GO TO 1650
      END IF
1700  CONTINUE
      N=NN+2
      DO 1800 K=N-1,2,-1
      TD(K)=TD(K-1)
      TH(K)=TH(K-1)
      U(K)=U(K-1)
      Z(K)=Z(K-1)
1800  CONTINUE
      GO TO 5000
      END IF
5000  TD(1)=0.
      TH(1)=GHT
      IF (GHT.LT.0.) TH(1)=H(IT,JT)
      U(1)=XT
      Z(1)=YT
      TD(N)=SQRT(((XR-XT)**2)+((YR-YT)**2))
      TH(N)=H(IR,JR)
      U(N)=XR
      Z(N)=YR
      RETURN
      END

      SUBROUTINE ROW (TD,TH,U,Z,N)
      COMMON /ALL/F,HTG,HRG,D,XT,YT,XR,YR,IT,JT,IR,JR,GHT,CS,H
      REAL H(100,140),TD(1000),TH(1000),U(1000),Z(1000)
      INTEGER II(1000),JJ(1000)
      ICS=INT(CS)
      JL=JT
      IF (YT.LT.YR) THEN
      IF (REAL((JT*ICS)-(ICS/2)).LE.YT) JL=JL+1
      JU=JR-1
      INC=1
      END IF
      IF (YT.GT.YR) THEN
      IF (REAL((JT*ICS)-(ICS/2)).GE.YT) JL=JL-1
      JU=JR+1
      INC=-1
      END IF
      N=0
      DO 100 J=JL,JU,INC
      N=N+1
      Y=REAL((J*ICS)-(ICS/2))
      X=XR+((Y-YR)*(XR-XT)/(YR-YT))
      IX=X/500.
      XX=REAL(IX*ICS)+(CS/2.)
      I1=IX
      IF (XX.LT.X) I1=1+IX
      I2=1+I1
      H1=H(I1,J)
      H2=H(I2,J)
      DX=X-REAL((I1*ICS)-(ICS/2))
      TD(N)=SQRT(((Y-YT)**2)+((X-XT)**2))
      U(N)=X
      Z(N)=Y
      TH(N)=H1+((H2-H1)*DX/CS)
      II(N)=I1
      JJ(N)=J
100   CONTINUE
      RETURN
      END
```

```
      SUBROUTINE COLUMN (TD,TH,U,Z,N)
      COMMON /ALL/F,HTG,HRG,D,XT,YT,XR,YR,IT,JT,IR,JR,GHT,CS,H
      REAL H(100,140),TD(1000),TH(1000),U(1000),Z(1000)
      INTEGER II(1000),JJ(1000)
      ICS=INT(CS)
      IL=IT
      IF (XT.LT.XR) THEN
      IF (REAL((IT*ICS)-(ICS/2)).LE.XT) IL=IL+1
      IU=IR-1
      INC=1
      END IF
      IF (XT.GT.XR) THEN
      IF (REAL((IT*ICS)-(ICS/2)).GE.XT) IL=IL-1
      IU=IR+1
      INC=-1
      END IF
      N=0
      DO 100 I=IL,IU,INC
      N=N+1
      X=REAL((I*ICS)-(ICS/2))
      Y=YR+((X-XR)*(YR-YT)/(XR-XT))
      JY=Y/500.
      YY=REAL(JY*ICS)+(CS/2.)
      J1=JY
      IF (YY.LT.Y) J1=1+JY
      J2=1+J1
      H1=H(I,J1)
      H2=H(I,J2)
      DY=Y-REAL((J1*ICS)-(ICS/2))
      TD(N)=SQRT(((Y-YT)**2)+((X-XT)**2))
      U(N)=X
      Z(N)=Y
      TH(N)=H1+((H2-H1)*DY/CS)
      JJ(N)=J1
      II(N)=I
  100 CONTINUE
      RETURN
      END

      SUBROUTINE DGNAL (TD,TH,U,Z,N)
      COMMON /ALL/F,HTG,HRG,D,XT,YT,XR,YR,IT,JT,IR,JR,GHT,CS,H
      REAL H(100,140),TD(1000),TH(1000),U(1000),Z(1000)
      INTEGER II(1000,2),JJ(1000,2)
      REAL M
      ICS=INT(CS)
      XTD=XT
      YTD=YT
      XRD=XR
      YRD=YR
      ITD=IT
      JTD=JT
      IRD=IR
      JRD=JR
      M=(YRD-YTD)/(XRD-XTD)
      C=YTD-(M*XTD)
      L=0
      IF (M.LT.0.) THEN
      L=1
      XTD=((ITD-1)*ICS)+((ITD*ICS)-XTD)
      IRD=(2*ITD)-IRD
      XRD=REAL((IRD*ICS)-(ICS/2))
      END IF
```

```
      M=(YRD-YTD)/(XRD-XTD)
      C=YTD-(M*XTD)
      KL=ITD+JTD-1
*     Y=MX+C
      Y=(KL*ICS)-XTD
      IF (Y.LE.YTD) KL=ITD+JTD
      KU=IRD+JRD-2
      INC=1
      IF (XRD.LT.XTD) THEN
      KL=KL-1
      IF (Y.EQ.YTD) KL=KL-1
      KU=IRD+JRD
      INC=-1
      END IF
      N=0
      DO 100 K=KL,KU,INC
      N=N+1
      X=(REAL(ICS*K)-C)/(M+1)
      Y=REAL(ICS*K)-X
      IX=X/CS
      JY=Y/CS
      I1=IX+1
      J1=JY+1
      IF (Y.EQ.REAL(JY*ICS).OR.X.EQ.REAL(IX*ICS)) THEN
      I1=I1+1
      J1=J1-1
      END IF
      X1=REAL((I1*ICS)-(ICS/2))
      Y1=REAL((J1*ICS)-(ICS/2))
      IF (X.LT.X1) THEN
      I2=I1-1
      J2=J1+1
      ELSE
      I2=I1+1
      J2=J1-1
      END IF
      IF (L.EQ.1) THEN
      I1=(2*ITD)-I1
      I2=(2*ITD)-I2
      END IF
      H1=H(I1,J1)
      H2=H(I2,J2)
      DXY=SQRT(((Y-Y1)**2)+((X-X1)**2))
      TD(N)=SQRT(((Y-YTD)**2)+((X-XTD)**2))
      U(N)=X
      IF (L.EQ.1) U(N)=(2.*REAL((ITD*ICS)-(ICS/2)))-X
      Z(N)=Y
      TH(N)=H1+((H2-H1)*DXY/(CS*SQRT(2.)))
      II(N,1)=I1
      II(N,2)=I2
      JJ(N,1)=J1
      JJ(N,2)=J2
  100 CONTINUE
      RETURN
      END
```

```
* FINDS THE EDGES OBSTRUCTING THE DIRECT LINE-OF-SITE
* AND WITHIN THE FIRST FRESNEL ZONE.

      SUBROUTINE EDGES (DP,HP,NP,LE,DE,HE,NE,LE1,DE1,HE1,NE1
     *                  ,LE2,DE2,HE2,NE2,IDED)
      COMMON X,Y,N,LAMBDA
      COMMON /ALL/F,HTG,HRG
      DIMENSION DP(1000),HP(1000),X(1000),Y(1000),DE(100),HE(100)
     *,LLE1(100),LE(100),LE1(100),DE1(100),HE1(100)
     *,LE2(100),DE2(100),HE2(100),IDED(100)
      REAL LAMBDA
      LAMBDA=300./F
      PI=4.*ATAN(1.)

      N=NP
      DO 100 I=1,N
      X(I)=DP(I)
      Y(I)=HP(I)
100   CONTINUE
      Y(1)=Y(1)+HTG
      Y(N)=Y(N)+HRG
      D=X(N)-X(1)

* FIND THE EDGES OBSTRUCTING THE LINE-OF-SIGHT
* MM1 = NUMBER (INC. TX. & RX.),LLE1; THEIR POSITION IN THE TERRAIN DATA

      CALL EDG1 (LLE1,MM1)

      NE1=MM1-2
      DO 200 I=1,NE1
      LE1(I)=LLE1(I+1)
      DE1(I)=X(LE1(I))
      HE1(I)=Y(LE1(I))
200   CONTINUE

* FIND THE ADDITIONAL EDGES WHICH LIE IN THE FIRST FRESNEL ZONE
* THE MOST SIGNIFICANT ONE IS TAKEN BETWEEN TWO OF THE ABOVE EDGES
* (I.E. MINIMUM V ,AS V=HP.SQRT(2.)/RADIUS1(HP TAKEN AS POSITIVE).

      CALL EDG2 (LLE1,MM1,LE,NE)

      NE2=0
      DO 400 I=2,NE-1
      IDED(I)=1
      ID=0
      DO 300 J=1,MM1
      IF (LE(I).EQ.LLE1(J)) ID=1
300   CONTINUE
      IF (ID.EQ.0) THEN
      IDED(I)=2
      NE2=NE2+1
      LE2(NE2)=LE(I)
      DE2(NE2)=X(LE(I))
      HE2(NE2)=Y(LE(I))
      END IF
400   CONTINUE

      IDED(1)=0
      IDED(NE)=0
```

```
      DO 500 I=1,NE
      DE(I)=X(LE(I))
      HE(I)=Y(LE(I))
500   CONTINUE

      RETURN
      END

      SUBROUTINE EDG1 (LLE1,MM1)
      COMMON X,Y,N
      DIMENSION X(1000),Y(1000),LLE1(100)
      LLE1(1)=1
      JJ=1
      L=1
100   CONTINUE
      K=0
      J=JJ
      SL=(Y(N)-Y(J))/(X(N)-X(J))
      DO 200 I=J+1,N-1,1
      SL1=(Y(I)-Y(J))/(X(I)-X(J))
*  FIRST CONDITION IS FOR THE CASE OF GRAZING INCIDENCE.
      IF ((K.EQ.0.AND.SL1.GE.SL).OR.(SL1.GT.SL)) THEN
      K=K+1
      JJ=I
      SL=SL1
      END IF
200   CONTINUE
      IF (K.EQ.0) JJ=N
      L=L+1
      LLE1(L)=JJ
      IF (JJ.LT.N) GOTO 100
      MM1=L
      RETURN
      END

      SUBROUTINE EDG2 (LLE1,MM1,LE,NE)
      COMMON X,Y,N,LAMBDA
      DIMENSION X(1000),Y(1000),LLE1(MM1),LE(100)
      REAL LAMBDA
      L=0
      DO 200 I=1,MM1-1
      L=L+1
      JL=LLE1(I)
      JU=LLE1(I+1)
      LE(L)=JL
      SL=(Y(JL)-Y(JU))/(X(JL)-X(JU))
      K=0
*  TO FIND THE SMALLEST V LATER,LET VMIN=2.(SINCE VMAX=SQRT(2.) WHEN THE
*  CONDITION OF HP <= RAD1 IS APPLIED).
      VMIN=2.
      DO 100 J=JL+1,JU-1
*  POINT OF INTERSECTION (XP,YP) WITH THE BASE LINE.
      XP=X(J)
      YP=Y(JL)+(SL*(XP-X(JL)))
*  FIND THE RADIUS OF THE FIRST FRESNEL ZONE FOR THIS POINT,RAD1.
      D1=SQRT(((YP-Y(JL))**2)+((XP-X(JL))**2))
      D2=SQRT(((YP-Y(JU))**2)+((XP-X(JU))**2))
      RAD1=SQRT(LAMBDA*D1*D2/(D1+D2))
*  FIND THE HEIGHT TO THE BASE LINE,HP.
      HP=YP-Y(J)
      IF (HP.LE.RAD1) THEN
      K=K+1
```

```
*  FIND THE V PARAMETER.
        V=(HP*SQRT(2.))/RAD1
        IF (V.LT.VMIN) THEN
        VMIN=V
        JJ=J
        END IF
        END IF
  100   CONTINUE
        IF (K.NE.0) THEN
        L=L+1
        LE(L)=JJ
        END IF
  200   CONTINUE
        NE=L+1
        LE(NE)=LLE1(MM1)
        RETURN
        END
```

```
* PREPARES THE EDGES DATA FOR THE DIFFRACTION MODELS, AND IF REQUIRED
* REDUCES EDGES OF TYPE I INTO 3 FOR PATHS WITH GREATER NUMBER THAN THIS

      SUBROUTINE PREDG (IND,F,TD,TH,N,DE,HE,NE,IDED,DEZ,HEZ,NEZ
     *                 ,DEZ1,HEZ1,NEZ1,DEZ2,HEZ2,NEZ2,IDEDZ)
      DIMENSION TD(1000),TH(1000),DE(100),HE(100),IDED(100)
     *,DEZ(100),HEZ(100),DEZ1(100),HEZ1(100)
     *,DEZ2(100),HEZ2(100),IDEDZ(100)
      REAL LAMBDA
      CC(X1,Y1,X2,Y2)=((X2*Y1)-(X1*Y2))/(X2-X1)
      PI=4.*ATAN(1.)
      LAMBDA=300./F

      NEZ1=0
      NEZ2=0
      NEZ=NE
      DO 100 I=1,NEZ
      IDEDZ(I)=IDED(I)
      DEZ(I)=DE(I)
      HEZ(I)=HE(I)
      IF (IDEDZ(I).EQ.0.OR.IDEDZ(I).EQ.1) THEN
     .NEZ1=NEZ1+1
      DEZ1(NEZ1)=DEZ(I)
      HEZ1(NEZ1)=HEZ(I)
      ELSE
      NEZ2=NEZ2+1
      DEZ2(NEZ2)=DEZ(I)
      HEZ2(NEZ2)=HEZ(I)
      END IF
100   CONTINUE

      IF (IND.EQ.1) THEN
*****
* REDUCE THE TYPE I EDGES TO THREE.
      IF (NEZ1.GT.5) THEN
      SL1=(HEZ1(3)-HEZ1(2))/(DEZ1(3)-DEZ1(2))
      C1=CC(DEZ1(2),HEZ1(2),DEZ1(3),HEZ1(3))
      SL2=(HEZ1(NEZ1-2)-HEZ1(NEZ1-1))/(DEZ1(NEZ1-2)-DEZ1(NEZ1-1))
      C2=CC(DEZ1(NEZ1-1),HEZ1(NEZ1-1),DEZ1(NEZ1-2),HEZ1(NEZ1-2))

      IF (SL1.EQ.SL2) THEN
* TO ACCOUNT FOR THE GRAZING INCIDENCE,(SL1=SL2).
      DEZ1(3)=(DEZ1(NEZ1-1)-DEZ1(2))/2.
      HEZ1(3)=(SL1*DEZ1(3))+C1

      ELSE
      DEZ1(3)=(C2-C1)/(SL1-SL2)
      HEZ1(3)=((SL1*C2)-(SL2*C1))/(SL1-SL2)
      END IF

      DO 200 I=4,5
      DEZ1(I)=DEZ1(NEZ1+I-5)
      HEZ1(I)=HEZ1(NEZ1+I-5)
200   CONTINUE
```

```
      NEZ1=5
* FIND THE TYPE II EDGES
      NEZ2=0
      NEZ=0
      DO 400 I=1,NEZ1-1
      NEZ=NEZ+1
      DEZ(NEZ)=DEZ1(I)
      HEZ(NEZ)=HEZ1(I)
      IDEDZ(NEZ)=1
      SL=(HEZ1(I)-HEZ1(I+1))/(DEZ1(I)-DEZ1(I+1))
      K=0
* TO FIND THE SMALLEST V LATER,LET VMIN=2.(SINCE VMAX=SQRT(2.) WHEN THE
* CONDITION OF HP <= RAD1 IS APPLIED).
      VMIN=2.
      DO 300 J=1,N
      IF (TD(J).GT.DEZ1(I).AND.TD(J).LT.DEZ1(I+1)) THEN
* POINT OF INTERSECTION (XP,YP) WITH THE BASE LINE.
      XP=TD(J)
      YP=HEZ1(I)+(SL*(XP-DEZ1(I)))
* FIND THE RADIUS OF THE FIRST FRESNEL ZONE FOR THIS POINT,RAD1.
      D1=SQRT(((YP-HEZ1(I))**2)+((XP-DEZ1(I))**2))
      D2=SQRT(((YP-HEZ1(I+1))**2)+((XP-DEZ1(I+1))**2))
      RAD1=SQRT(LAMBDA*D1*D2/(D1+D2))
* FIND THE HEIGHT TO THE BASE LINE,HP.
      HP=YP-TH(J)
      IF (HP.LE.RAD1) THEN
      K=K+1
* FIND THE V PARAMETER.
      V=(HP*SQRT(2.))/RAD1
      IF (V.LT.VMIN) THEN
      VMIN=V
      JJ=J
      END IF
      END IF
      END IF
300   CONTINUE
      IF (K.NE.0) THEN
      NEZ2=NEZ2+1
      DEZ2(NEZ2)=TD(JJ)
      HEZ2(NEZ2)=TH(JJ)
      NEZ=NEZ+1
      DEZ(NEZ)=TD(JJ)
      HEZ(NEZ)=TH(JJ)
      IDEDZ(NEZ)=2
      END IF
400   CONTINUE
      NEZ=NEZ+1
      DEZ(NEZ)=DEZ1(NEZ1)
      HEZ(NEZ)=HEZ1(NEZ1)
      IDEDZ(1)=0
      IDEDZ(NEZ)=0
      END IF
*****
      END IF

      RETURN
      END
```

APPENDIX B

"Comparison of Prediction Models for VHF Mobile Radio"

by

A. Fouladpouri
Professor J.D. Parsons

IERE Fourth International Conference on Land Mobile Radio,
University of Warwick, December 1987.

COMPARISON OF PROPAGATION PREDICTION MODELS FOR VHF MOBILE RADIO

A. Fouladpouri and Professor J.D. Parsons*

Summary

A comparative study has been undertaken to assess some of the available propagation prediction models under various circumstances in irregular terrain. The measured data used for comparison was collected during field trials carried out in rural areas of Cheshire using three transmitter sites operating at 139 MHz. The median signal strength was measured in 0.5 km squares along a number of test routes using receiving equipment mounted in a vehicle. A terrain data map was used to construct path profiles between the transmitter and the receiver location and predictions were made using computer routines. The results reveal where each of the models is applicable and where relatively large errors are likely to occur.

1. Introduction

The propagation models available for the prediction of transmission path loss over irregular terrain differ in the approaches used to calculate the attenuation caused by various factors. Different models produce different results when applied to a given situation. However the models can be assessed for their accuracy, over their range of applicability, by comparing the predictions with measured data. The data used for comparison in the tests described in this paper has been collected as a result of measurement programmes carried out in rural areas of Cheshire. Three different transmitter sites were used and the received signals were recorded in a mobile unit at distances of up to 40 km from the base station. The median signal strength has been obtained in over 550 test squares, each of side 0.5 km, at a transmitting frequency of 139 MHz. Since the terrain features over these long transmission paths have a substantial influence on the signal strength a proper understanding of their effects is necessary for prediction purposes. Three well-known models, those due to Okumura [1], J.R.C. [2] and Longley-Rice [3] have been examined to assess their applicability under various circumstances over irregular terrain and a quantitative comparison of their accuracy has been derived. The models have been implemented on a computer, together with routines by means of which a ground profile between the base station and mobile, or other appropriate terrain parameters, can be derived from a computerised terrain data map of the area.

*University of Liverpool

2. Propagation Models

When the terrain is highly irregular obstacles in the signal path introduce a diffraction loss before the signal reaches the receiver, which is in the shadow region. Furthermore, irregularities in the ground surface cause part of the incident energy to be diffused in all directions. It is almost impossible to take all the various different irregularities into account and the prediction models vary in their dependence upon different terrain-related parameters for the prediction of path loss. The basic approach however is first to construct the radial path profile from the transmitter to the receiver and use it to calculate terrain loss. While some models rely more on empirical relationships for this purpose, others include theoretically based techniques.

2.1 The Okumura Prediction Model

Following an extensive series of propagation measurements in and around Tokyo, Okumura [1] produced an analysis of the results and hence arrived at an empirical method for signal strength prediction. Essentially Okumura's method is based on determining the free-space path loss between the transmitter and the receiver and then adding or subtracting numerous correction factors to account for the nature of the terrain, the extent of urbanisation, the heights of the antennas, etc. The basic formulation of the prediction technique can be expressed as

$$\text{Path loss} = L_F + A_{mn} - H_{tn} - H_{rn} \text{ dB}$$

In this expression L_F is the free-space path loss and A_{mn} is the median attenuation relative to L_F in urban areas over what is defined as "quasi-smooth" terrain with a transmitter antenna height h_t of 200 m and a receiver antenna height h_r of 3 m. A_{mn} is a function of frequency and range and is expressed in graphical form. H_{tn} and H_{rn} are correction factors to account for antennas not at the reference heights of 200 m and 3 m; they are called the height-gain factors and are also functions of frequency and range.

Okumura's paper contains graphs from which the appropriate values for any specific situation can be extracted.

If the terrain cannot be treated as "quasi-smooth" or if the environment is not urban, then further corrections have to be made. In fact Okumura produced eight factors intended to correct for suburban and open areas, sloping terrain, hilly terrain, mixed land-sea paths, etc., all these factors being expressed in graphical form. Street orientation in urban areas can also be taken into account.

In the computerised version of the model the prediction curves are stored in the computer and can be accessed using an interpolation technique. The terrain undulation height Δh (the interdecile value) classifies surface irregularities and is defined as the difference between the 10% and 90% values of terrain height within a distance of 10 km of the receiver, in a direction towards the transmitter. Diffraction loss due to intervening obstacles is not explicitly calculated, however where there is an isolated ridge it is taken into account.

2.2 The JRC Method

The Joint Radio Committee of the Nationalised Power Industries of the U.K. have developed a computer-based prediction method which has been described, at different stages of its development, by Edwards and Durkin [2], and Dadson [4]. The method is used to predict the coverage area of a base station using a computer and a topographic data base, the output being presented in the form of a listing of the predicted field strengths and path losses at half-kilometre intervals over the service area. A transparency plot is also produced for overlaying on maps, giving a pictorial representation of the signal levels although not in the form of contours of equal signal strength. The topographic data base has been extracted from Ordnance Survey maps, providing 800,000 height reference points at 0.5 km intervals for Britain.

To calculate the received signal level, the computer reconstructs the ground path profile between the transmitter and the receiver, it then tests for the existence of a line of sight path and whether Fresnel-zone clearance is obtained over the path. If both tests are satisfied, both free space and plane earth losses are calculated and the higher value is chosen. If the tests fail, the programme evaluates the loss caused by obstructions, grading them into single or multiple diffraction edges. Calculations are made for up to three diffracting edges, and any greater number of obstructions is converted into three edges, using the method of Bullington [5].

The JRC method appears to be the most widely used prediction method in the U.K. and since its inception in 1971 several thousand propagation surveys have been carried out, on a commercial basis, for different users. The main shortcoming of the method is its inability to take into account the effects of buildings.

In view of the influence of the method on the mobile radio community in the U.K. and Europe, a close examination of its prediction accuracy against experimental data is highly desirable.

2.3 The Longley-Rice Prediction Model

This is a general purpose semi-empirical model in which statistical terrain parameters are used, together with some of the well-known rules of electromagnetic wave propagation. The model can be used even if the actual terrain profile in any given situation is not available since estimates of the various terrain parameters required are available. These have been obtained statistically from a large number of terrain profiles of various types. Apart from the required transmission parameters, including frequency, distance and the antenna heights above ground, the prediction model considers the effect of the atmosphere and the ground constants along the transmission path. Several geometric parameters related to the path are derived, one important parameter being Δh, the interdecile range of terrain elevations. The method by which this is evaluated differs from that used in the Okumura model and is related to a function $\Delta h(d)$ which varies with the path distance d. This function $\Delta h(d)$ is called the interdecile range of terrain heights above and below a straight line fitted to elevations above sea level and for long enough path lengths the asymptotic behaviour $\Delta h(d)$ is very close to Δh. In making calculations, the model uses theoretical treatments of reflection from rough ground, refraction through a standard atmosphere, diffraction around the earth and over sharp obstacles and tropospheric scatter. It combines these using empirical relations derived from the analysis of measured data. The diffraction loss is a weighted average of knife-edge and smooth earth diffraction calculations, the weighting factor being a function of frequency, terrain irregularity and antenna heights. For highly irregular terrain the horizon obstacles from the terminals are considered as sharp ridges and hence the diffraction loss is calculated over a double knife-edge path.

3. Comparison, Analysis and Results.

In calculating the predicted path loss value for each test square a computer routine initially determines the ground profile from the transmitter to the centre of the test square under consideration by using the terrain data map stored in the computer. The profile is then processed to derive the terrain-related parameters which are required

by the particular prediction model under consideration. To allow for the earth's curvature over these relatively long paths a value of k = 4/3 was assumed which also implies normal atmospheric conditions. At the operating frequency of 139 MHz it was found that none of the line-of-sight paths had adequate first Fresnel zone clearance. Predictions using the JRC method had previously been provided.

Figs. 1-3 show the relationships between the predicted and measured median path loss values in each test square for the three transmitter sites. The predicted path loss is also plotted against the measured values and the regression lines show the best fit.

The errors were calculated as the difference between the predicted and measured values and the standard error is calculated as the standard deviation of the difference. Table 1 lists the results of the data analysis for all the prediction models. Generally the Okumura model produced the largest prediction errors over all the transmitter sites, indicating its weakness for predictions over irregular terrain. It was also apparent that there were some constraints in deriving some of the terrain parameters. This was particularly so in the case of defining the base station effective antenna height; if the height of the transmitter above local ground was less than the average ground level in the 3-15 km range then a negative effective transmitter height resulted. Also for the isolated ridge situation, if the ridge is close to the receiver then the average height of the ground from the ridge to the transmitter may be greater than the ridge height above sea level, resulting in a negative value for the defined ridge height. Certain assumptions therefore had to be made in order that the computer implementation of the model could deal with such situations. The JRC prediction method includes a specific calculation of diffraction loss and hence produces a lower prediction error. However in certain situations the model produces large errors, for example using the Altrincham site and in the squares numbered 26-40. As shown in Fig. 2, the predicted path loss is very much lower than the measured values.

Fig. 4a shows the terrain profile for one such square, and as can be seen the effective receiving antenna height h_{re} as defined by the model and used in the plane earth formula is quite large. In this case the prediction is improved when the actual structural heights above the ground are used, thereby indicating the importance of the local ground surrounding the mobile receiver.

The error values indicated in Table 1 for the Longley-Rice model have been derived when individual values of Δh appropriate to the path under consideration have been used in the prediction procedure. However when the median value of Δh is used the error increases by approximately 1 dB for all three transmitter sites. One interesting aspect is a comparison of the value of Δh as derived according to the Okumura and Longley-Rice definitions. The Longley-Rice definition always produces a lower value even compared to those suggested by the model for the areas of interest. For some of the test squares with the Wavertree transmitter site the prediction path loss is much higher than the corresponding measured results. Fig. 4b shows the terrain profile of one such square and the reason for these large differences can be explained in terms of the receiver location with respect to the closest obstructing hill. This is the receiving terminal horizon obstacle, and as can be realised from the figure, it will result in a large horizon elevation angle which is defined as the angle between the line joining the top of the obstacle to the antenna and the horizon line. The value of this angle affects the weighting factor used for the calculation of diffraction loss. Generally the errors due to the prediction models are smallest when the transmitter is in the strictly rural area of Frodsham and its height is largest. The errors are greatest for the Wavertree site where the transmitter is within the City of Liverpool, surrounded by buildings, and the transmission ranges are longer. In the majority of cases the models seem to be optimistic, predicting a lower value for the path loss than that actually measured.

4. Conclusions

The prediction models have been compared with each other and against measured data which has been obtained in rural areas over irregular terrain. In order to improve the prediction accuracy it is necessary to investigate the factors which can be incorporated into the different models to make them more applicable to the different situations. For example the method of determining the position of the effective reflecting plane for the calculation of the plane-earth path loss and the way in which the terrain irregularity factor is defined with respect to the intervening path, plays an important part in the prediction procedure. Although the Longley-Rice prediction model has been found to compare well with the measured data in general, there is more scope within the JRC model to introduce improvements. This is not the case for the Okumura model since it is wholly dependent on empirical results and only empirical improvements can be added.

The non-availability of data about buildings and trees over the paths of interest affects the prediction accuracy. This is of more significance in situations where this type of clutter is dominantly close to the radio terminals.

During the comparison study, computerised routines have been devised which provide a

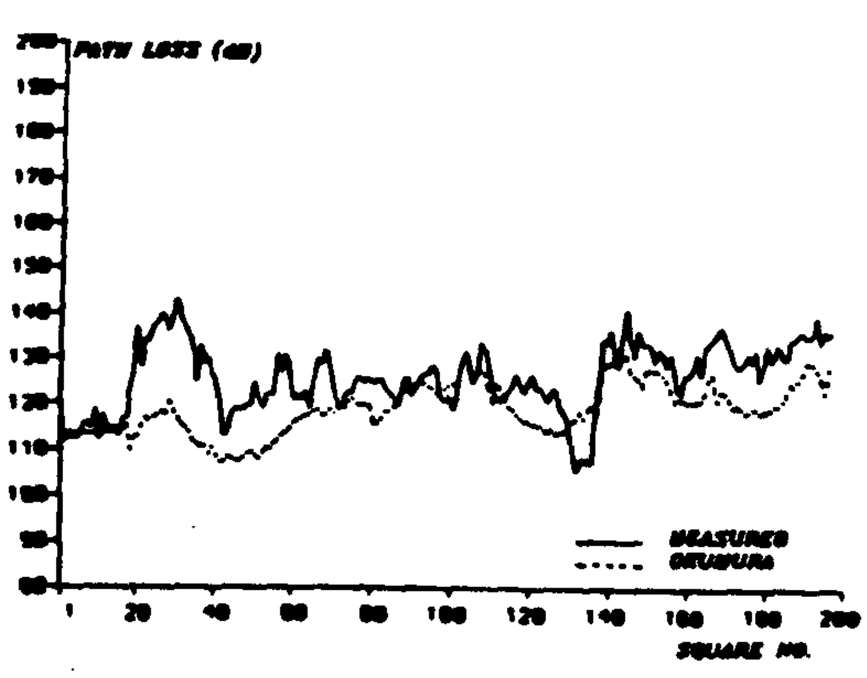

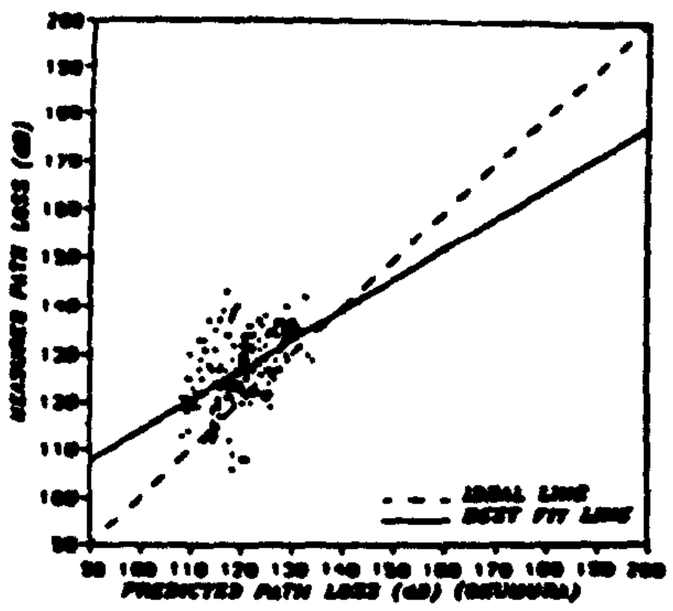

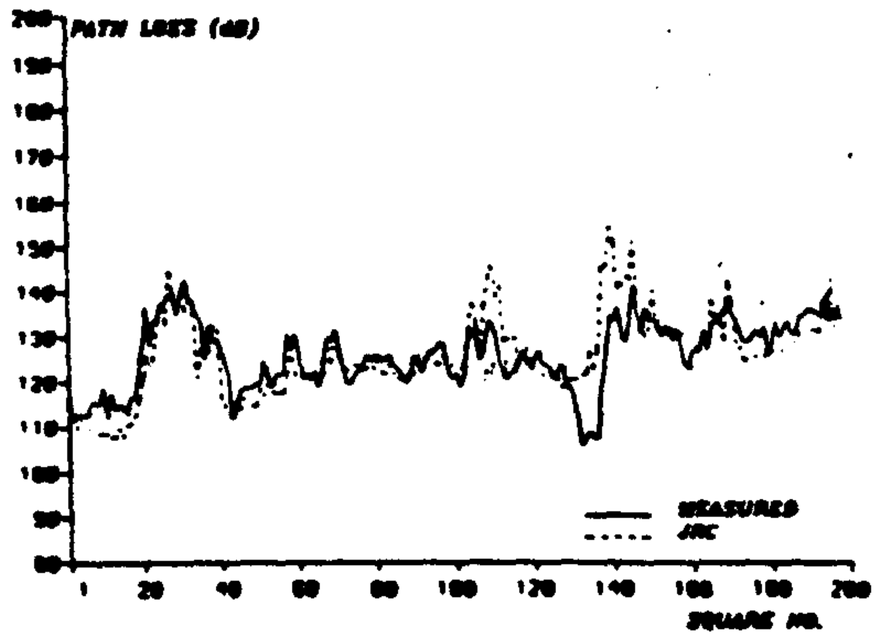

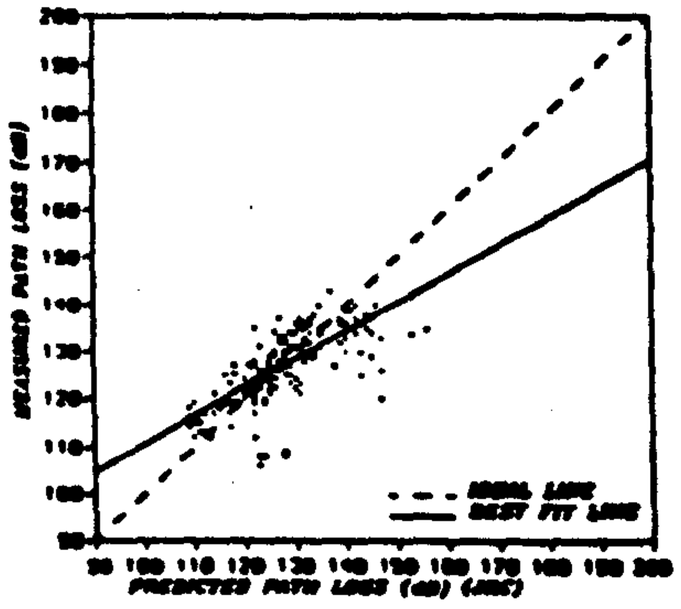

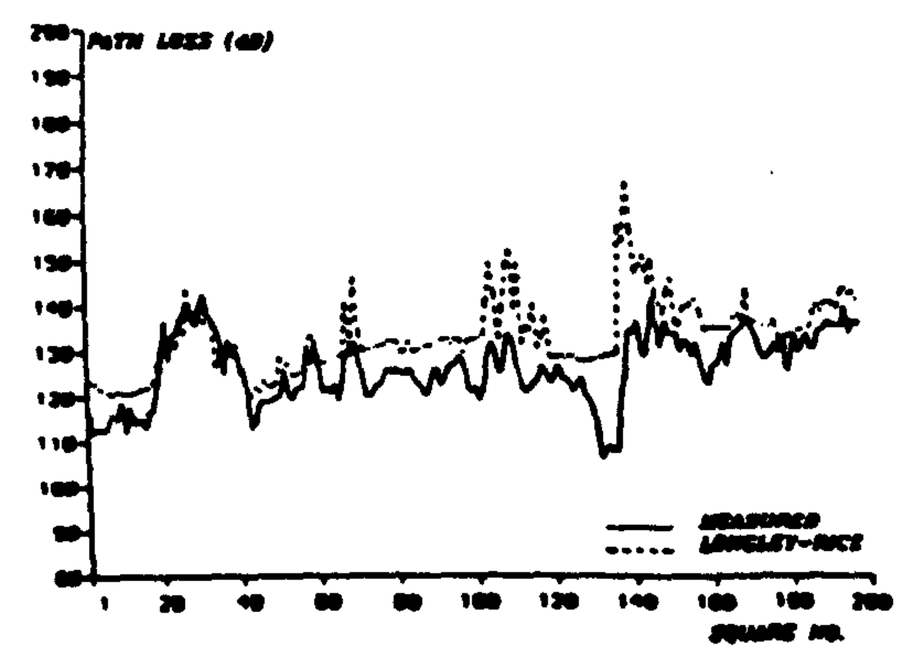

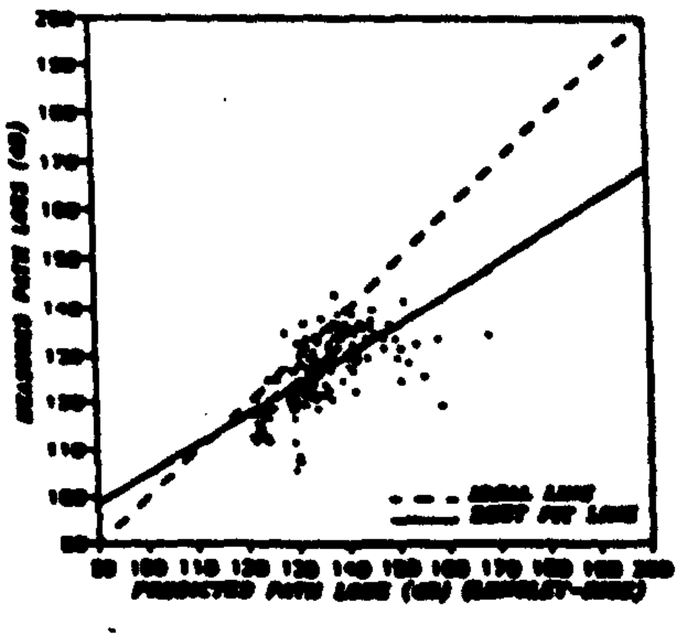

Fig. 1: Predicted and measured path loss (Frodsham).

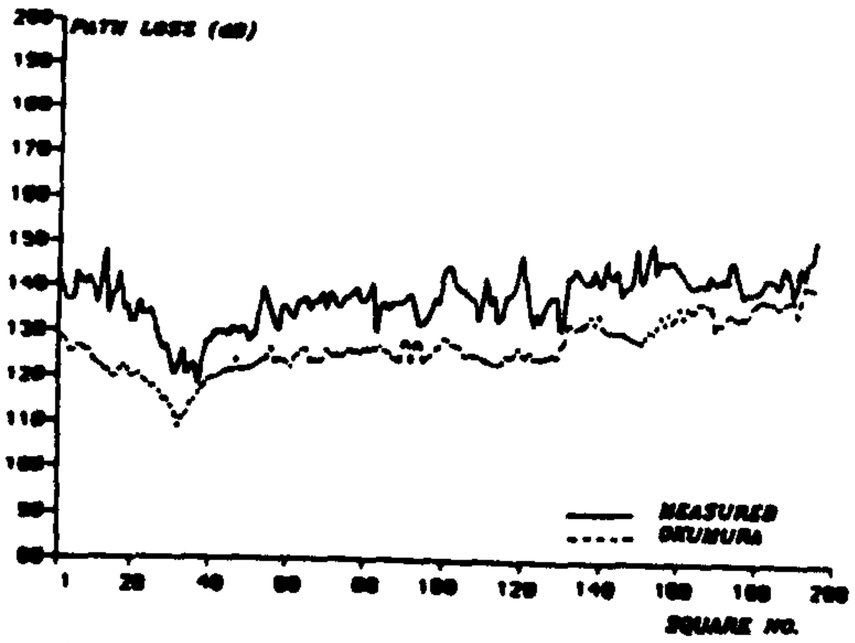

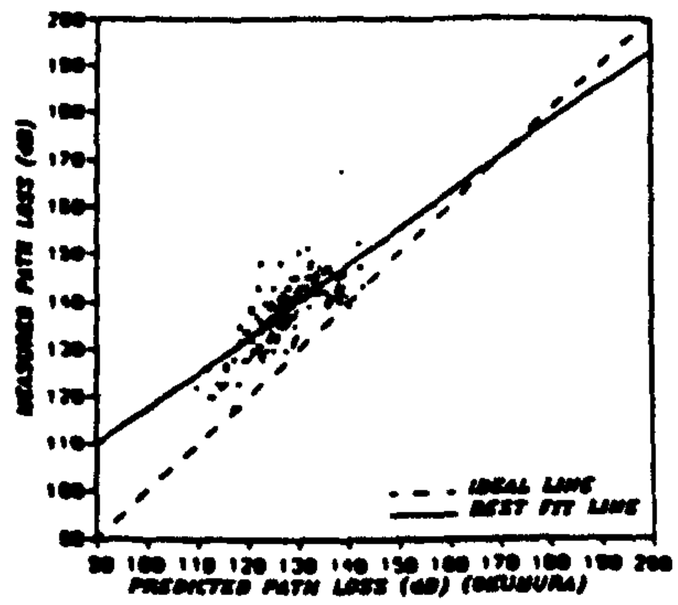

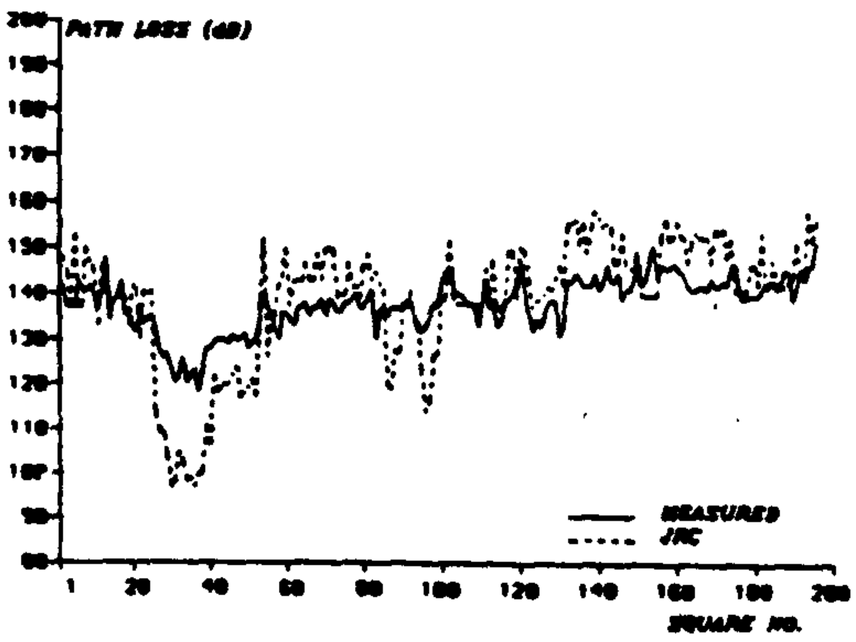

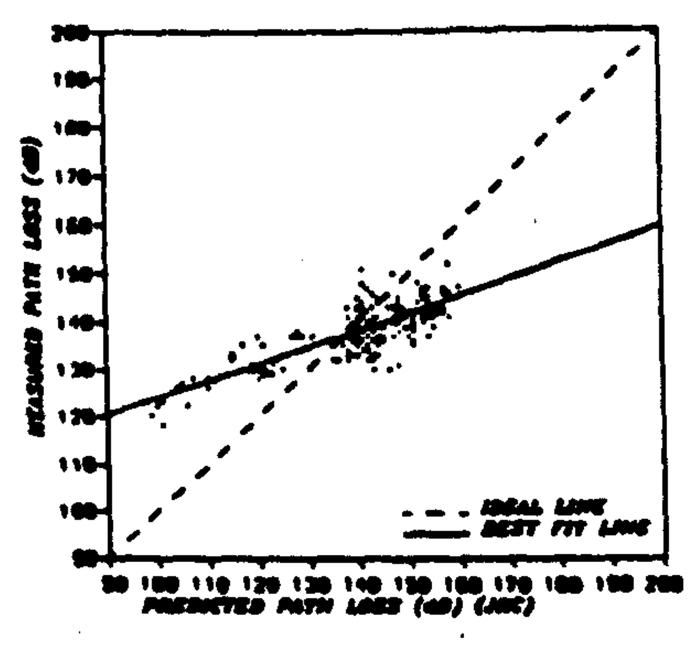

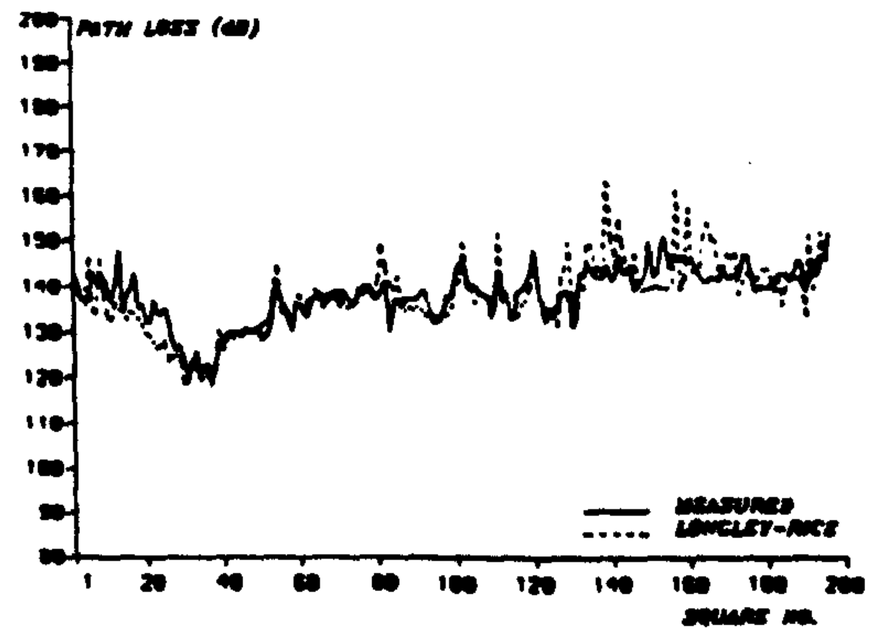

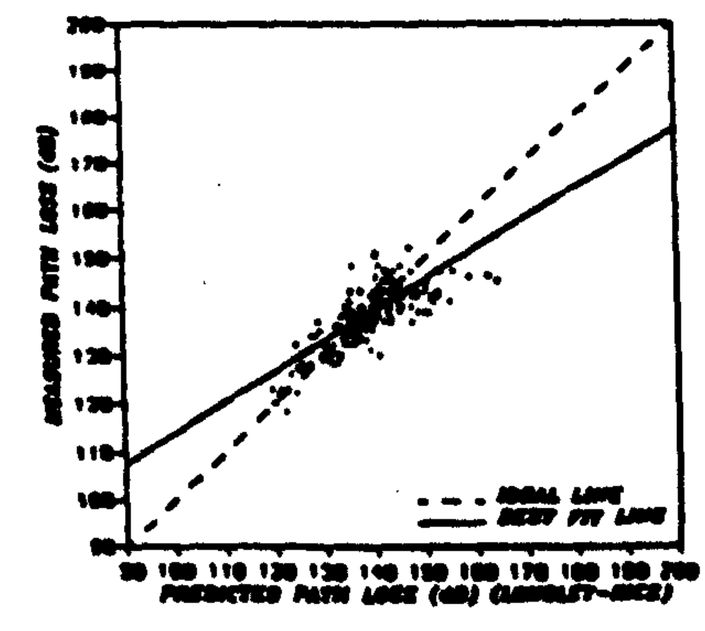

Fig. 2: Predicted and measured path loss (Altrincham).

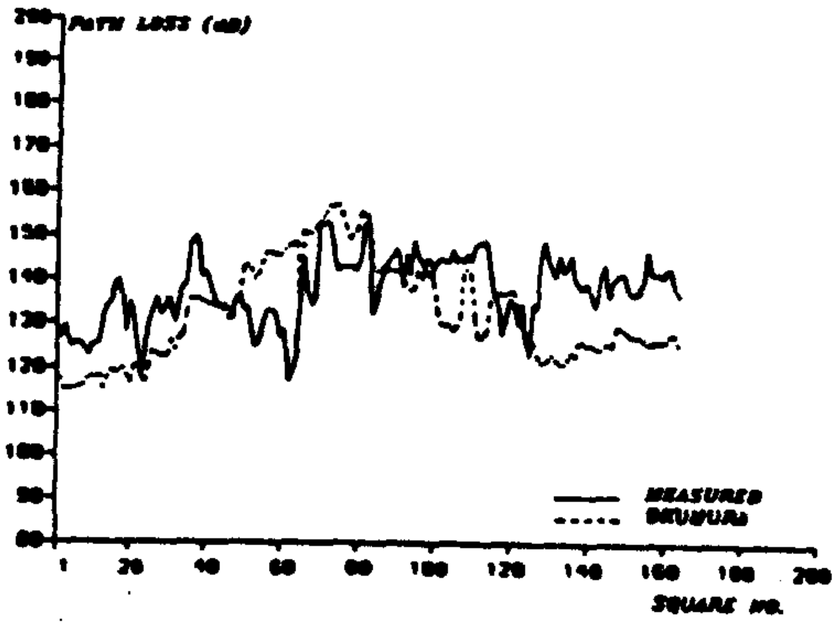

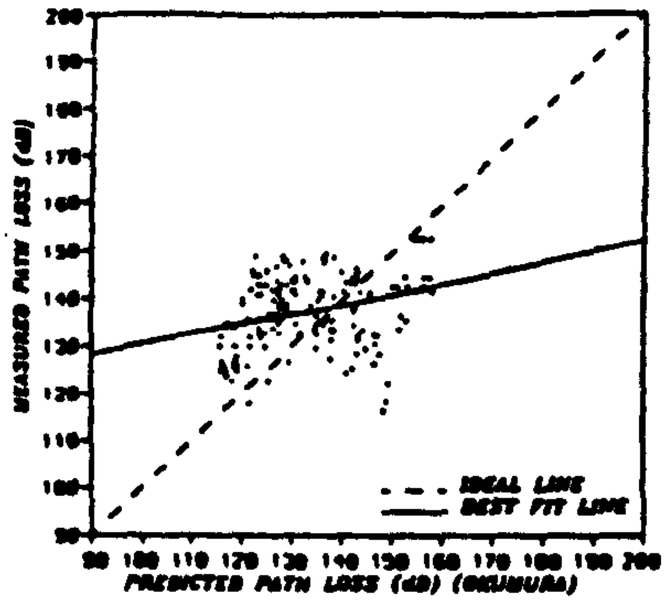

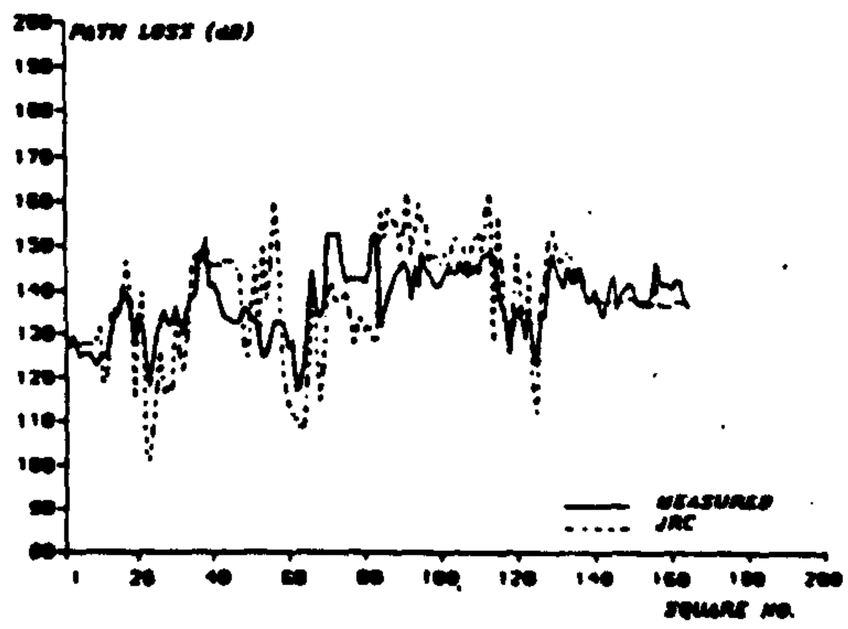

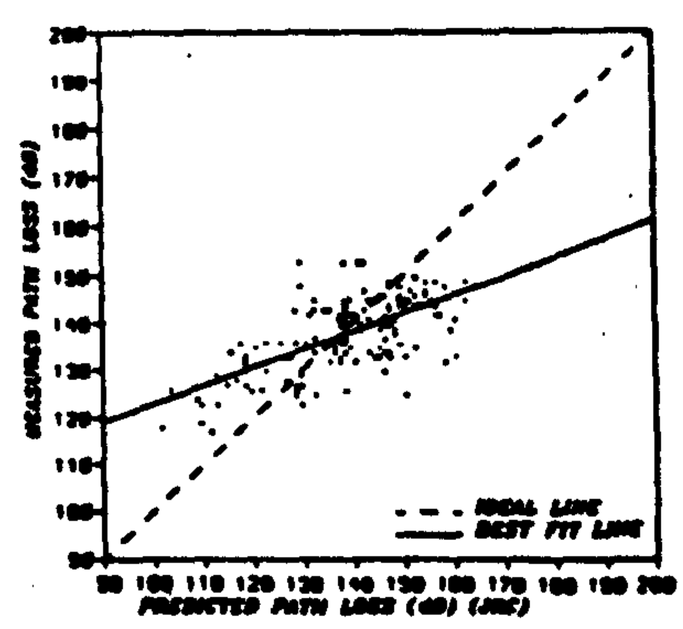

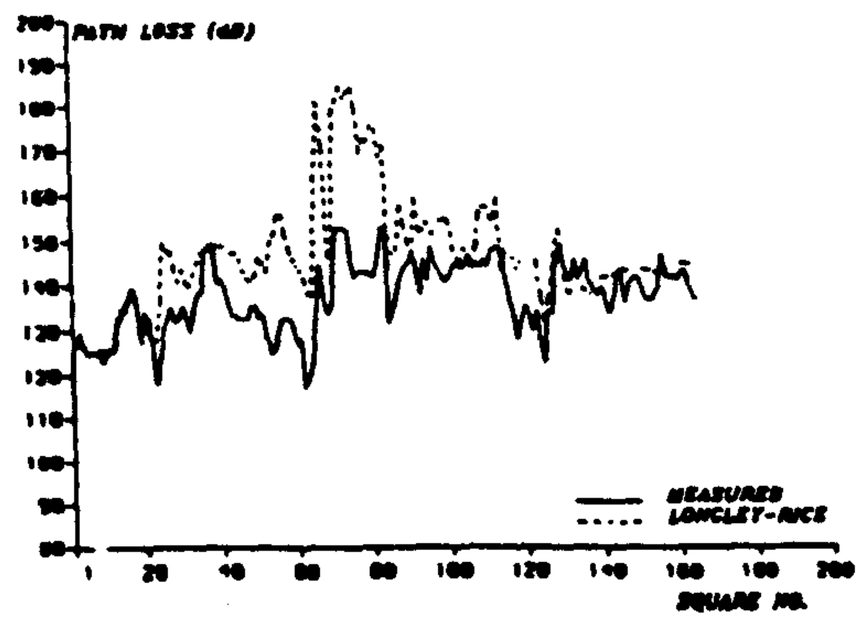

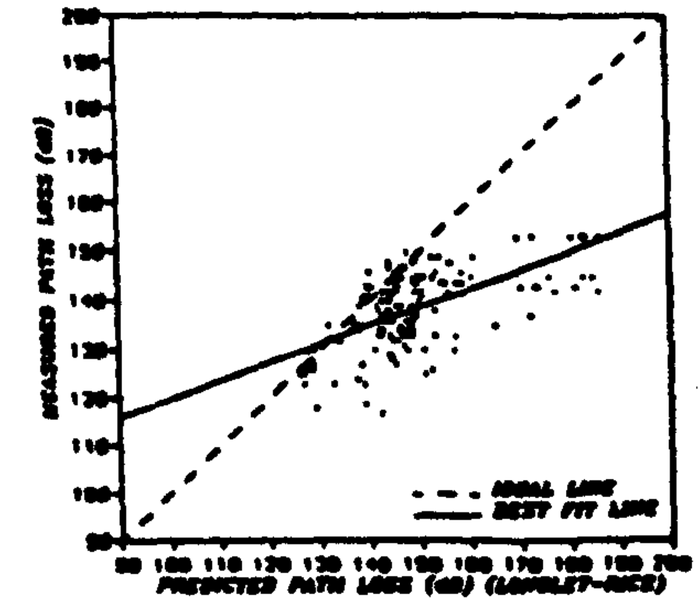

Fig.3: Predicted and measured path loss (Wavertree).

more efficient way for calculating the propagation losses. The routines are flexible and can accommodate changes in the size of the terrain data grid and also provide means by which the path can be examined for different transmission parameters. A contour analysis of the terrain heights and the predicted signal strength values provides a simpler way of determining the coverage area of a particular transmitter.

References

1. Okumura, Y., Ohmori, E., Kawano, T. and Fukuda, K. (1968), "Field strength and its variability in VHF and UHF land-mobile radio service", Rev. Elec. Commun. Lab., Vol. 16, pp. 825-873.

2. Edwards, R. and Durkin, J. (1969), "Computer prediction of service areas for v.h.f. mobile radio networks", Proc. IEE, Vol. 116, No. 9, pp. 1493-1500.

3. Longley, A.G. and Rice, P.L. (1968), "Prediction of tropospheric radio transmission loss over irregular terrain, a computer method, 1968", ESSA Tech. Report ERL 79-ITS 67.

4. Dadson, C.E., Durkin, J., Martin, R.E. (1975), "Computer prediction of field strength in the planning of radio systems", Trans. IEEE Vehicular technology, Vol. VT. 24, No. 1, pp. 1-8.

5. Bullington, K. (1947) "Radio propagation at frequencies above 30 MHz", Proc. IRE, Vol. 35, pp. 1122-1136.

6. Hufford, G.A., Longley, A.G. and Kissick, W.A. (1982), "A guide to the use of the ITS irregular terrain model in the area prediction mode", NTIA Report, 82-100.

f = 139 MHz

hm = 2.0 m

TX. LOCATION	Overall Antenna Height (m)	Standard Error (dB)			Standard Dev. of Error (dB)			Slope of Regression Line		
		OKUM.	JRC	L-R	OKUM.	JRC	L-R	OKUM.	JRC	L-R
Frodsham	194	9.8	6.4	9.5	7.0	6.4	6.4	0.64	0.60	0.64
Altrincham	87	11.6	9.9	4.8	4.2	9.8	4.8	0.75	0.36	0.63
Wavertree	113	12.4	9.8	13.6	11.4	9.8	10.0	0.21	0.38	0.37

Table 1 - Comparative results

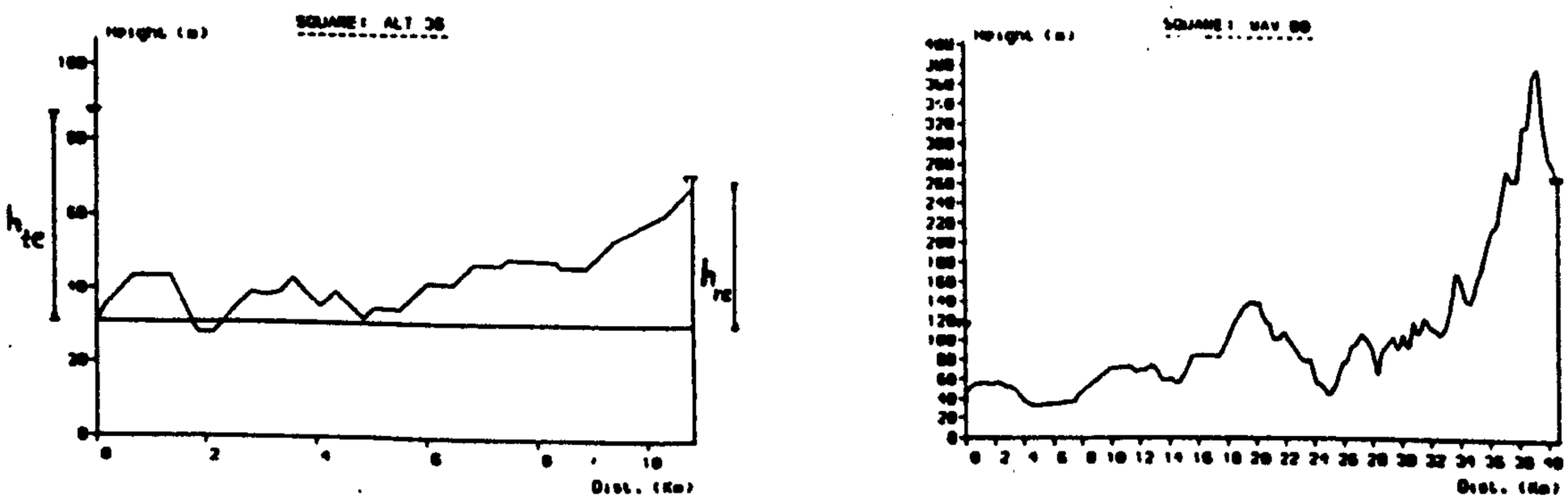

(a) (b)

Fig. 4: Terrain profiles.